LMSC-HEC TR F268592

FINAL REPORT

AERODYNAMIC FLIGHT EVALUATION ANALYSIS AND DATA BASE UPDATE

May 1989

Contract NAS8-33807

(NASA-CR-183654) AERODYNAMIC FLIGHT EVALUATION ANALYSIS AND DATA BASE UPDATE Final Report (Lockheed Missiles and Space Co.) 294 p CSCL 10C

N89-25276

Unclas

G3/20 0216755

NATIONAL AERONAUTICS AND SPACE ADMINISTRATION
MARSHALL SPACE FLIGHT CENTER, AL 35812

by

W. W. Boyle
M. S. Miller
G. O. Wilder
R. D. Reheuser
R. S. Sharp
G. I. Bridges

Lockheed
Missiles & Space Company, Inc.
Huntsville Engineering Center
4800 Bradford Blvd., Huntsville, AL 35807

293

FOREWORD

This final report presents the results of work performed by personnel of the Flight Technology Group of Lockheed's Huntsville Engineering Center for NASA-MSFC under Contract NAS8-33807. The NASA Contracting Officer's Representative and technical monitor for this contract was Mr. Charlie C. Dill, Jr., to whom the authors are grateful for his valuable assistance, direction, and contributions to the successful completion of this study.

CONTENTS

Section		Page
	FOREWORD	ii
	CONTENTS	iii
	NOMENCLATURE	x
1	INTRODUCTION	1
2	PHASE I LIQUID ROCKET BOOSTER (LRB) TEST DATA	2
	2.1 Test Configurations and Conditions	2
	2.2 Increment Development Methodology	5
	2.3 Verification of Interpolations Performed on LRB Phase I Data	12
	2.3.1 Angle of Attack Interpolation	12
	2.3.2 Mach Number Interpolation	12
	2.4 Evaluation of Plume Effect	22
	2.5 Data Analysis Review	38
	2.5.1 Data Analysis Review of Longitudinal Effects	38
	2.5.2 Data Analysis Review of Wing Loads	38
3	PHASE II LIQUID ROCKET BOOSTER TESTING	51
	3.1 Test Conditions and Configurations	51
	3.2 Test Results	51
	3.3 Phase I and Phase II Comparison	51
	3.3.1 Data Analysis	57
	3.3.2 Angle of Attack Trends	69
	3.3.3 Results of Data Comparison	69
4	LRB LATERAL/DIRECTIONAL WIND TUNNEL DATA	92
	5 PROTUBERANCE EFFECTS	113
	5.1 Protuberance Effects	113
	5.2 SRB Increment Data Base Summary	113
6	GAP AND AFT SKIRT EFFECTS	135
	6.1 Gap Effects Summary	135
	6.2 Aft Skirt Effects Summary	168

CONTENTS (Concluded)

Section			Page
7	LRB BASE DRAG STUDY		195
	7.1	Original Base Drag Estimates	195
	7.2	Base Drag Calculation Code	208
	7.3	STS Flights 2, 3, 5	208
	7.4	Martin Pump Fed (LRB1)	208
	7.5	Martin Pressure Fed (LRB2)	224
	7.6	General Dynamics 02/H2 Pump Fed (LRB3)	224
	7.7	General Dynamics 02/RP1 Pump Fed (LRB4)	224
	7.8	Concept Comparison/Conclusion	249
8	SUMMARY		254
A	APPENDIX A-1		

LIST OF FIGURES

Figure		Page
2-1	Phase-I LRB Test Configurations	3
2-2	Methodology Used to Generate Increments	7
2-3	Recommended Future Methodology To Generate Increments	8
2-4	Comparison of Increment Development Methods	10
2-5	CMF vs a (M = 0.6)	13
2-6	CAF vs a (M = 0.6)	14
2-7	CNF vs a (M = 0.6)	15
2-8	CNF vs a (M = 0.9)	16
2-9	CNF vs a (M = 1.11)	17
2-10	CNF vs a (M = 1.26)	18
2-11	CNF vs MACH (Mach = -4)	20
2-12	CAF vs Mach (Mach = -4)	21
2-13	W Normal Force Coefficient (TWT 675)	24
2-14	W Pitching Moment Coefficient (TWT 675)	25
2-15	W Normal Force Coefficient (TWT IA300)	26
2-16	W Pitching Moment Coefficient (TWT IA300)	27
2-17	W Normal Force Coefficient (TWT 675 & TWT IA300)	28
2-18	W Pitching Moment Coefficient (TWT 675 & TWT IA300)	29
2-19	Shuttle LRB Configurations Used in Study	30
2-20	Booster CPB vs Mach	33
2-21	ET CPB vs Mach	34
2-22	CD Increment vs Mach	35
2-23	CN Increment vs Mach	36
2-24	CM Increment vs Mach	37
2-25	CAF vs Mach (Length and Diameter Effects)	39
2-26	CNF vs Mach (Length and Diameter Effects)	40

LIST OF FIGURES (Continued)

Figure		Page
2-27	CMF vs Mach (Length and Diameter Effects)	41
2-28	X_{AC} vs Mach (Length and Diameter Effects)	42
2-29	C_{SR} vs Mach (Length and Diameter Effects)	46
2-30	C_{TR} vs Mach (Length and Diameter Effects)	47
2-31	C_{BR} vs Mach (Length and Diameter Effects)	48
2-32	CHEI vs Mach (Length and Diameter Effects)	49
2-33	CHEO vs Mach (Length and Diameter Effects)	50
3-1	Phase II Configurations	52
3-2	Phase I LRB Wind Tunnel Test Configurations	58
3-3	Phase I/Phase II Incremental Data, and D2L2/SD15 Configuration	60
3-4	Phase I/Phase II Total Data, Comparison and D2L2/SD15 Configuration	63
3-5	Phase I/Phase II Total Data, Comparison and D1L1/SD12L1 Configuration	66
3-6	Angle of Attack and Diameter Effects on Phase I/Phase II Data	71
3-7	LRB Diameter Effects	75
3-8	Data Increments Phase II	78
3-9	Data Increments vs Diameter	87
4-1	Scope of Test (TWT016)	93
4-2	Test Configurations (TWT016)	94
4-3	Launch Vehicle Sign Convention	95
4-4	CY_β vs Length	100
4-5	CY_β vs Diameter	101
4-6	CYM_β vs Length	102
4-7	CYM_β vs Diameter	103
4-8	CRM_β vs Length	104
4-9	CRM_β vs Diameter	105
4-10	ΔCSR vs Length	106
4-11	ΔCSR vs Diameter	107
4-12	ΔCTR vs Length	108
4-13	ΔCTR vs Diameter	109
4-14	ΔCBR vs Length	110
4-15	ΔCBR vs Diameter	111
5-1	SRB Protuberance Configurations	114
5-2	SRB Fairing Configurations	115
5-3	CNF (Protuberance Effects)	116
5-4	CMF (Protuberance Effects)	117
5-5	CSR (Protuberance Effects)	118
5-6	CTOR (Protuberance Effects)	119
5-7	CRBM (Protuberance Effects)	120
5-8	CHMIE (Protuberance Effects)	121
5-9	CHMOE (Protuberance Effects)	122
5-10	CAF (Fairing/Protuberance Effects)	123
5-11	CSR (Fairing/Protuberance Effects)	124

List of Figures (continued)

Figure		Page
5-12	CTOR (Fairing/Protuberance Effects)	125
5-13	CRBM (Fairing/Protuberance Effects)	126
5-14	CHMIE (Fairing/Protuberance Effects)	127
5-15	CHMOE (Fairing/Protuberance Effects)	128
5-16	CSR (Fairing/Protuberance Effects)	129
5-17	CTOR (Fairing/Protuberance Effects)	130
5-18	CRBM (Fairing/Protuberance Effects)	131
5-19	CHMIE (Fairing/Protuberance Effects)	132
5-20	CHMOE (Fairing/Protuberance Effects)	133
6-1	Gap Effect Configurations (D1L1)	136
6-2	Gap Effect Configurations (D1L2)	137
6-3	CAF vs Mach (D1L1)	138
6-4	CNF vs Mach (D1L1)	139
6-5	CSR vs Mach (D1L1)	140
6-6	CTR vs Mach (D1L1)	141
6-7	CBR vs Mach (D1L1)	142
6-8	CHEI vs Mach (D1L1)	143
6-9	CHEO vs Mach (D1L1)	144
6-10	CAF vs Gap (D1L1)	145
6-11	CNF vs Gap (D1L1)	146
6-12	CMF vs Gap (D1L1)	147
6-13	CSR vs Gap (D1L1)	148
6-14	CBR vs Gap (D1L1)	149
6-15	CTR vs Gap (D1L1)	150
6-16	CHEI vs Gap (D1L1)	151
6-17	CHEO vs Gap (D1L1)	152
6-18	CAF vs Mach (D2L2)	153
6-19	CNF vs Mach (D2L2)	154
6-20	CSR vs Mach (D2L2)	155
6-21	CTR vs Mach (D2L2)	156
6-22	CBR vs Mach (D2L2)	157
6-23	CHEI vs Mach (D2L2)	158
6-24	CHEO vs Mach (D2L2)	159
6-25	CAF vs Gap (D2L2)	160
6-26	CNF vs Gap (D2L2)	161
6-27	CMF vs Gap (D2L2)	162
6-28	CSR vs Gap (D2L2)	163
6-29	CTR vs Gap (D2L2)	164
6-30	CBR vs Gap (D2L2)	165
6-31	CHEI vs Gap (D2L2)	166
6-32	CHEO vs Gap (D2L2)	167
6-33	Aft Skirt Configurations (D1L1)	169
6-34	Aft Skirt Configurations (D2L2)	170
6-35	CNF vs Mach (D1L1)	171
6-36	CSR vs Mach (D1L1)	172

List of Figures (continued)

Figure		Page
6-37	CTR vs Mach (D1L1)	173
6-38	CBR vs Mach (D1L1)	174
6-39	CHEI vs Mach (D1L1)	175
6-40	CHEO vs Mach (D1L1)	176
6-41	CNF vs α (D1L1, M = 1.25)	177
6-42	CSR vs α (D1L1, M = 1.25)	178
6-43	CTR vs α (D1L1, M = 1.25)	179
6-44	CBR vs α (D1L1, M = 1.25)	180
6-45	CNF vs α (D1L1, M = 1.47)	181
6-46	CSR vs α (D1L1, M = 1.47)	182
6-47	CTR vs α (D1L1, M = 1.47)	183
6-48	CBR vs α (D1L1, M = 1.47)	184
6-49	CNF vs Mach (D2L2)	185
6-50	CSR vs Mach (D2L2)	186
6-51	CTR vs Mach (D2L2)	187
6-52	CBR vs Mach (D2L2)	188
6-53	CHEI vs Mach (D2L2)	189
6-54	CHEO vs Mach (D2L2)	190
6-55	CNF vs α (D2L2, M = 1.47)	191
6-56	CSR vs α (D2L2, M = 1.47)	192
6-57	CTR vs α (D2L2, M = 1.47)	193
6-58	CBR vs α (D2L2, M = 1.47)	194
7-1	Baseline Study LRB Configurations	196
7-2	Current SRB	197
7-3	Baseline Study LRB	198
7-4	Baseline Study Altitude vs Mach	199
7-5	Baseline Study Q vs Mach	200
7-6	Baseline Study Plume Angle vs Mach	201
7-7	Baseline Study SRB Total Base Drag	205
7-8	Baseline Study LRB Total Base Drag	206
7-9	Baseline Study LRB Delta Base Drag	207
7-10	Base Drag Calculation Code Flowchart	209
7-11	Base Drag Calculation Code Output	210
7-12	STS 2, 3, 5 Altitude vs Mach	211
7-13	STS 2, 3, 5 Q vs Mach	212
7-14	STS 2, 3, 5 Plume Angle vs Mach	213
7-15	STS 2, 3, 5 Total Base Drag	215
7-16	LRB1 (Martin Pump Fed)	216
7-17	LRB1 Altitude vs Mach	217
7-18	LRB1 Q vs Mach	218
7-19	LRB1 Plume Angle vs Mach	219
7-20	LRB1 Total Base Drag	222
7-21	LRB1 Delta Base Drag	223
7-22	LRB2 (Martin Pressure Fed)	225
7-23	LRB2 Altitude vs Mach	226

List of Figures (Concluded)

Figure		Page
7-24	LRB2 Q vs Mach	227
7-25	LRB2 Plume Angle vs Mach	228
7-26	LRB2 Total Base Drag	231
7-27	LRB2 Delta Base Drag	232
7-28	LRB3 (General Dynamics O2H2 Pump Fed)	233
7-29	LRB3 Altitude vs Mach	234
7-30	LRB3 Q vs Mach	235
7-31	LRB3 Plume Angle vs Mach	236
7-32	LRB3 Total Base Drag	239
7-33	LRB3 Delta Base Drag	240
7-34	LRB4 (General Dynamics O2RP1 Pump Fed)	241
7-35	LRB4 Altitude vs Mach	242
7-36	LRB4 Q vs Mach	243
7-37	LRB4 Plume Angle vs Mach	244
7-38	LRB4 Total Base Drag	247
7-39	LRB4 Delta Base Drag	248
7-40	Launch Vehicle Total Base Drag	250
7-41	Orbiter Base Total Drag	251
7-42	Booster Total Base Drag	252
7-43	External Tank Total Base Total	253

LIST OF TABLES

Table		Page
2-1	Phase I LRB Configurations	4
2-2	Matrix of Data Files used to Generate the Phase I LRB Incremental Data	6
2-3	Phase I LRB Dimensions	19
2-4	Analytical Uncertainties	31
2-5	Summary of Vehicle Longitudinal Effects	45
3-1	Matrix of Data Files Used to Generate Phase II Data	56
3-2	Matrix of Data Files Used to Generate Phase I LRB Incremental Data	59
3-3	Additional Test Runs Suggested to Redevelop Phase I Data Base	70
4-1	Diameter Effects of Phase II Configurations	112
7-1	Baseline Concept (SRB)	202
7-2	Baseline Concept (LRB)	203
7-3	Baseline Concept (LRB)	204
7-4	STS 2, 3, 5 (SRB)	214
7-5	Martin Pump Fed (LRB1)	220
7-6	Martin Pump Fed (LRB1)	221
7-7	Martin Pressure Fed (LRB2)	229

List of Tables (Concluded)

Table		Page
7-8	Martin Pressure Fed (LRB2)	230
7-9	General Dynamics O2H2 Pump Fed Total Base Drag	237
7-10	General Dynamics O2H2 Pump Fed Delta Base Drag	238
7-11	General Dynamics O2RP1 Pump Fed Total Base Drag	245
7-12	General Dynamics O2RP1 Pump Fed Delta Base Drag	246

NOMENCLATURE

α	angle of attack
β	yaw angle
C_{AF}	axial force coefficient
C_{BR}	wing bending moment coefficient
C_D	drag coefficient
CHEI	inner elevon moment coefficient
CHEO	outer elevon moment coefficient
C_{MF}	pitching moment coefficient
C_{NF}	normal force coefficient
C_P	pressure coefficient
C_{PB}	base pressure coefficient
C_{PBET}	base pressure coefficient external tank
C_{RM}	rolling moment coefficient
C_{SR}	wing shear force coefficient
C_T	thrust coefficient
C_{TR}	wing torque moment coefficient
C_Y	side force coefficient
C_{YM}	yawing moment coefficient
DSRB	base diameter (booster)
ε	nozzle area ratio
MRP (WING)	wing moment reference point
P_C	chamber pressure
P_I	ambient pressure
Q	dynamic pressure
T/A	thrust/base area
δei	inner elevon deflection
δeo	outer elevon deflection
X	nozzle extension past base
ϕ	roll angle

ORIGINAL PAGE IS
OF POOR QUALITY

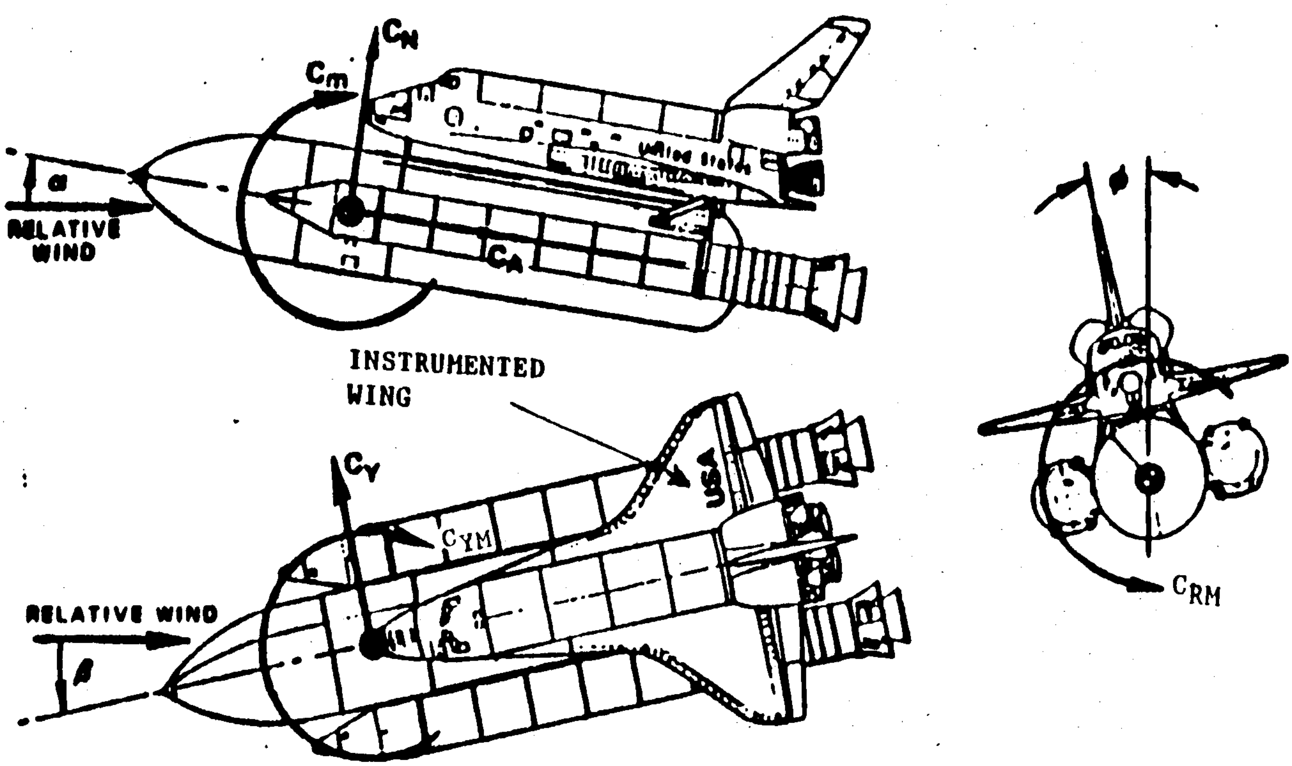

Launch Vehicle Sign Convention

ORIGINAL PAGE IS OF POOR QUALITY

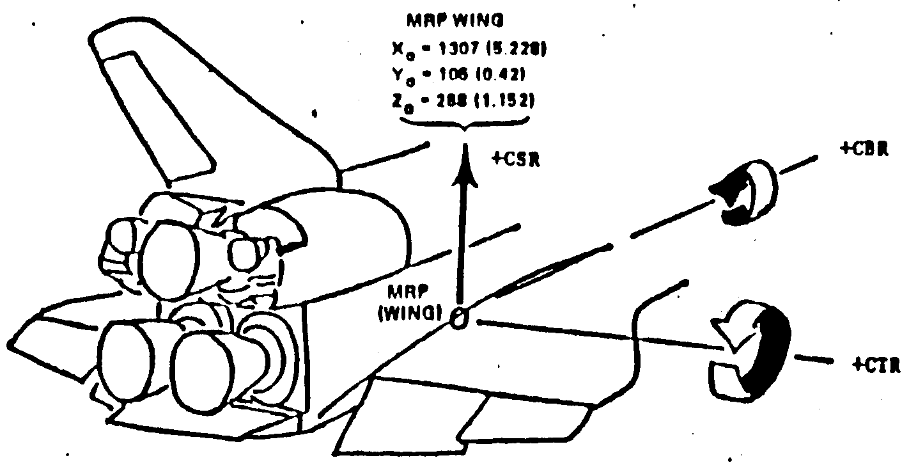

ALL DIMENSIONS IN INCHES
MODEL SCALE IN PARENTHESES

Wing Coordinate Axes
(Ref. Dimensions and Axes are the same for all Databases)

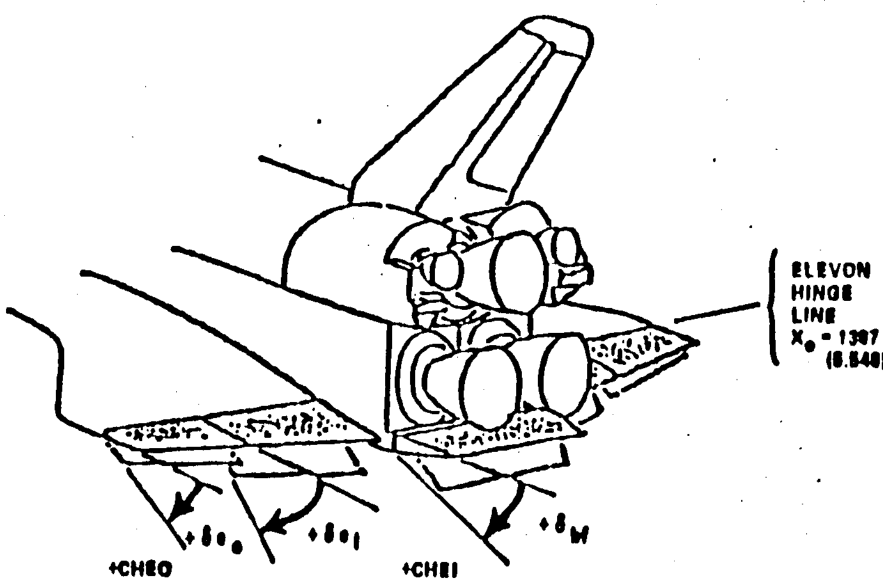

ALL DIMENSIONS IN INCHES
MODEL SCALE IN PARENTHESES

Elevon Coordinate Axes
(Ref. Dimensions and Axes are the same for all Databases)

Launch Vehicle Sign Convention

1. INTRODUCTION

Research was conducted to determine the feasibility of replacing the Solid Rocket Boosters on the existing Space Shuttle Launch Vehicle (SSLV) with Liquid Rocket Boosters (LRB). As a part of the LRB selection process, a series of wind tunnel tests was conducted along with aero studies to determine the effects of different LRB configurations on the SSLV. Final results were tabulated into increments and added to the existing SSLV data base.

The research conducted in this study was taken from a series of wind tunnel tests conducted at Marshall Space Flight Center's 14-inch Trisonic Wind Tunnel. The effects on CAF, CNF, CMF, CY, CSR, CTR, CBR were investigated for a number of candidate LRB configurations. The aero effects due to LRB protuberances, ET/LRB sep. distance, and aft skirts were also gathered from the tests. Analysis was also conducted to investigate the base pressure and plume effects due to the new booster geometries

Section 2 of this study discusses the test results found in Phase I of wind tunnel testing. Section 3 discusses the results in Phase II of testing, along with a comparison to Phase I tests. Section 4 gives preliminary LRB lateral/directional data results and trends. Section 5 discusses the protuberance effects and section 6 the gap/skirt effects. Section 7 discusses and gives results of the base pressure/plume effects study.

2. PHASE I LIQUID ROCKET BOOSTER (LRB) TEST DATA

This section delineates the methods and results of the Phase I (TWT0707) wind tunnel test. Section 2.1 presents the test configurations and conditions used during testing, and the methodology of determining the incremental data is discussed in Section 2.2. Section 2.3 presents the interpolations performed on the LRB data.

2.1 TEST CONFIGURATIONS AND CONDITIONS

Testing was conducted to determine the effects of length and diameter on aerodynamic coefficients. The configurations tested used diameters of 12.2 ft, 15 ft, 18 ft, and 21 ft. Three lengths were tested for each diameter configuration ranging from 144 ft to 190 ft. Figure 2-1 and Table 2-1 present the test configurations used in Phase I wind tunnel testing. Table 2-2 shows the test matrix for Phase I. The lengths were measured from nose tip to base, excluding the nozzle. The LRB/ET attach points were the same for all LRB configurations, and the base of the nose cones was not to extend aft of this point. The nose tip had a radius of 1.11 ft, and nose half angles were all 18 degrees. All LRB's were tested - without protuberances.

The angle of attack for the tests ranged from -10 degrees to +10 degrees in even increments. The Mach numbers used were 0.6, 0.8, 0.9, 0.95, 1.05, 1.15, 1.25 1.48, 1.96, 2.74, 3.48, and 4.96. The sideslip angle was zero. Nominal settings of 10 degrees/5 degrees were used for the inboard/outboard elevon settings.

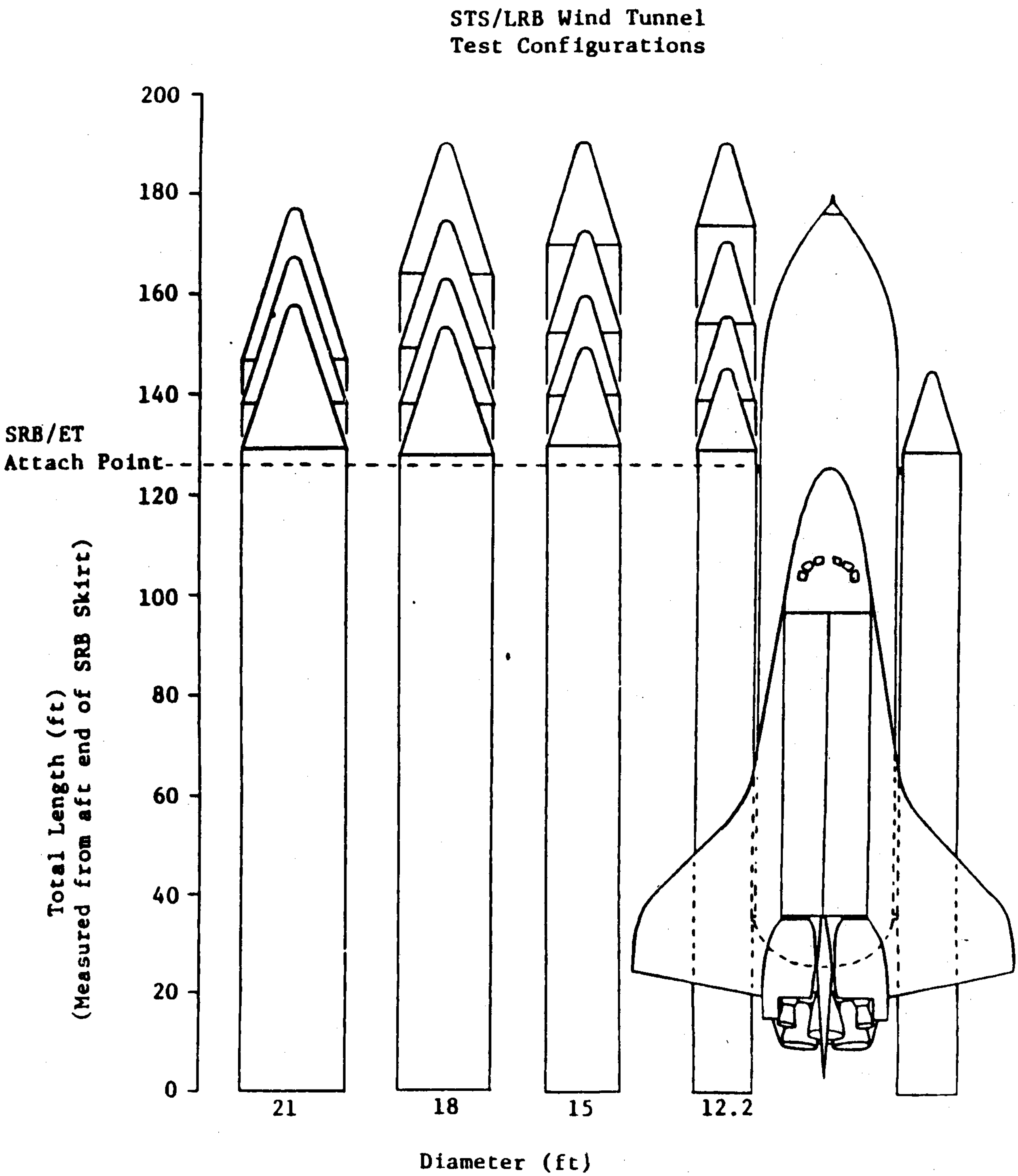

Fig. 2-1 Phase I LRB Test Configurations

Table 2-1 PHASE I LRB CONFIGURATIONS

Diameter (ft.) / Length (ft.)	D1 12.2*	D2 15	D3 18	D4 21
L1	144*	149	154	158
L2	150	159	163	167
L3	170	172	175	177
L4	190	190	190	-

*Represents Current SSLV Configuration

2.2 INCREMENT DEVELOPMENT METHODOLOGY

The development of the coefficient incremental data was initiated by the analysis of Phase I data obtained from wind tunnel testing. The data were compared to the current SSLV data and evaluated for validity. The increments were developed from the difference between a particular set of LRB data and that of the D1L1 configuration, the latter being equivalent to the current SRB less the aft skirtand protuberances. The resulting increments could then be added directly to the SSLV data base. Increments were developed for each LRB configuration and test point.

For the LRB Phase I effort, the test Mach numbers are shown in Table 2-2. Incremental data at Mach numbers corresponding to 0.95, 1.05, 1.15, and 3.48 were generated for the "D2", "D3", and "D4" configurations by subtracting experimental baseline (D1L1) data from data generated by linear interpolation using the method outlined in Fig. 2-2.

Analysis of the incremental data at the above transonic Mach numbers has shown that valid increments cannot be generated using this method. However, at higher Mach numbers where changes in the coefficient data with changes in Mach number are small, this method can be used with relatively good results.

Shown in Fig. 2-3 is a flowchart detailing the approach recommended for any future incremental data base development efforts. The new method differs from the old method only in that the interpolation for desired Mach numbers is not performed until after incremental data are generated. This new methodology for obtaining incremental data at desired Mach numbers (between Mach numbers for which experimental data are available) will assure that consistent increments will be generated.

Shown in Fig. 2-4 are several example plots which illustrate the differences between Phase I incremental data obtained using the previous interpolation method and the recommended future method. Figures 2-4 verifies

Table 2-2 MATRIX OF DATA FILES USED TO GENERATE THE PHASE I LRB INCREMENTAL DATA

TWT0707 LRB WIND TUNNEL DATA FILES

MACH # / CONFIG.	0.60	0.80	0.90	0.95	1.05	1.10	1.15	1.25	1.40	1.46	1.55	1.80	1.96	2.20	2.50	2.74	3.48	3.50	4.45
D1L1	TWT013	TWT017	TWT021	TWT025	TWT029	TWT033	TWT037	TWT041	*TWT197	TWT045	*TWT212	*TWT227	TWT049	*TWT242	*TWT257	TWT053	TWT057	*TWT283	TWT061
L2	TWT014	TWT018	TWT022	TWT026	TWT030	TWT034	TWT038	TWT042	*TWT198	TWT046	*TWT213	*TWT228	TWT050	*TWT243	*TWT258	TWT054	TWT058	*TWT284	TWT062
L3	TWT015	TWT019	TWT023	TWT027	TWT031	TWT035	TWT039	TWT043	*TWT199	TWT047	*TWT214	*TWT229	TWT051	*TWT244	*TWT259	TWT055	TWT059	*TWT285	TWT063
L4	TWT016	TWT020	TWT024	TWT028	TWT032	TWT036	TWT040	TWT044	*TWT200	TWT048	*TWT215	*TWT230	TWT052	*TWT245	*TWT260	TWT056	TWT060	*TWT286	TWT064
D2L1	TWT097	TWT093	TWT089	*TWT164	*TWT175	TWT085	*TWT186	TWT081	*TWT201	TWT077	*TWT216	*TWT231	TWT073	*TWT246	*TWT261	TWT069	*TWT272	*TWT287	TWT065
L2	TWT098	TWT094	TWT090	*TWT165	*TWT176	TWT086	*TWT187	TWT082	*TWT202	TWT078	*TWT217	*TWT232	TWT074	*TWT247	*TWT262	TWT070	*TWT273	*TWT288	TWT066
L3	TWT099	TWT095	TWT091	*TWT166	*TWT177	TWT087	*TWT188	TWT083	*TWT203	TWT079	*TWT218	*TWT233	TWT075	*TWT248	*TWT263	TWT071	*TWT274	*TWT289	TWT067
L4	TWT100	TWT096	TWT092	*TWT167	*TWT178	TWT088	*TWT189	TWT084	*TWT204	TWT080	*TWT219	*TWT234	TWT076	*TWT249	*TWT264	TWT072	*TWT275	*TWT290	TWT068
D3L1	TWT101	TWT105	TWT109	*TWT168	*TWT179	TWT113	*TWT190	TWT117	*TWT205	TWT121	*TWT220	*TWT235	TWT125	*TWT250	*TWT265	TWT129	*TWT276	*TWT291	TWT133
L2	TWT102	TWT106	TWT110	*TWT169	*TWT180	TWT114	*TWT191	TWT118	*TWT206	TWT122	*TWT221	*TWT236	TWT126	*TWT251	*TWT266	TWT130	*TWT277	*TWT292	TWT134
L3	TWT103	TWT107	TWT111	*TWT170	*TWT181	TWT115	*TWT192	TWT119	*TWT207	TWT123	*TWT222	*TWT237	TWT127	*TWT252	*TWT267	TWT131	*TWT278	*TWT293	TWT135
L4	TWT104	TWT108	TWT112	*TWT171	*TWT182	TWT116	*TWT193	TWT120	*TWT208	TWT124	*TWT223	*TWT238	TWT128	*TWT253	*TWT268	TWT132	*TWT279	*TWT294	TWT136
D4L1	TWT161	TWT158	TWT155	*TWT172	*TWT183	TWT152	*TWT194	TWT149	*TWT209	TWT146	*TWT224	*TWT239	TWT143	*TWT254	*TWT269	TWT140	*TWT280	*TWT295	TWT137
L2	TWT162	TWT159	TWT156	*TWT173	*TWT184	TWT153	*TWT195	TWT150	*TWT210	TWT147	*TWT225	*TWT240	TWT144	*TWT255	*TWT270	TWT141	*TWT281	*TWT296	TWT138
L3	TWT163	TWT160	TWT157	*TWT174	*TWT185	TWT154	*TWT196	TWT151	*TWT211	TWT148	*TWT226	*TWT241	TWT145	*TWT256	*TWT271	TWT142	*TWT282	*TWT297	TWT139

* - INTERPOLATED

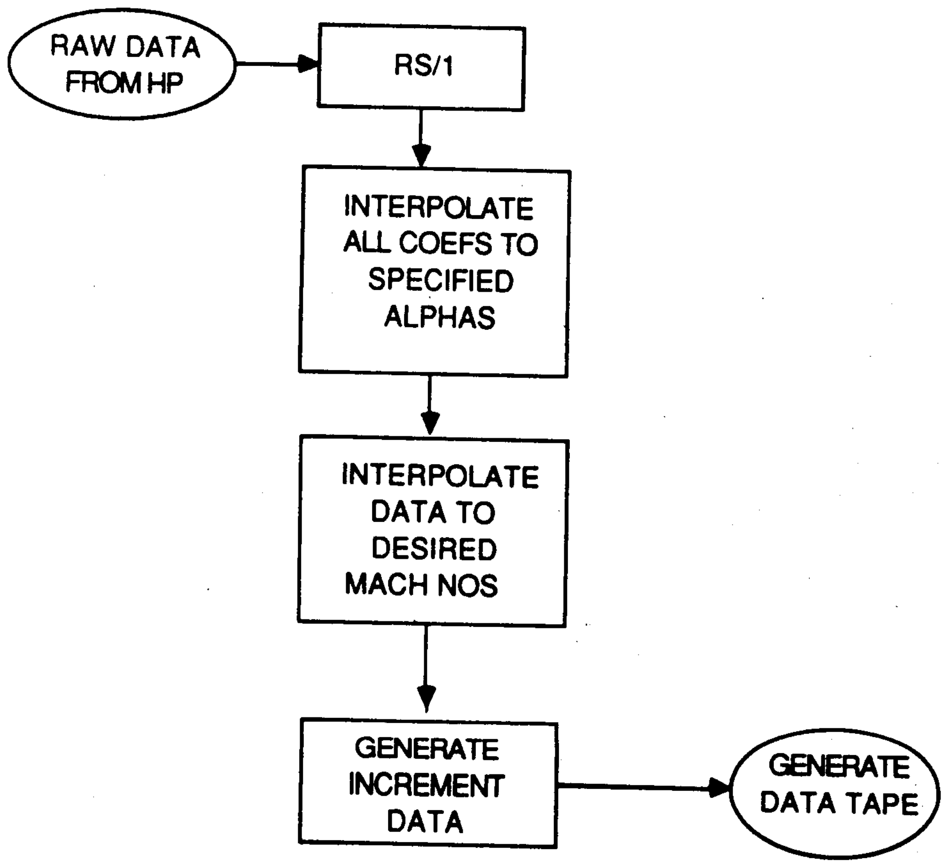

Fig. 2-2 Methodology used to Generate Incremental Data for the Phase I LRB Effort

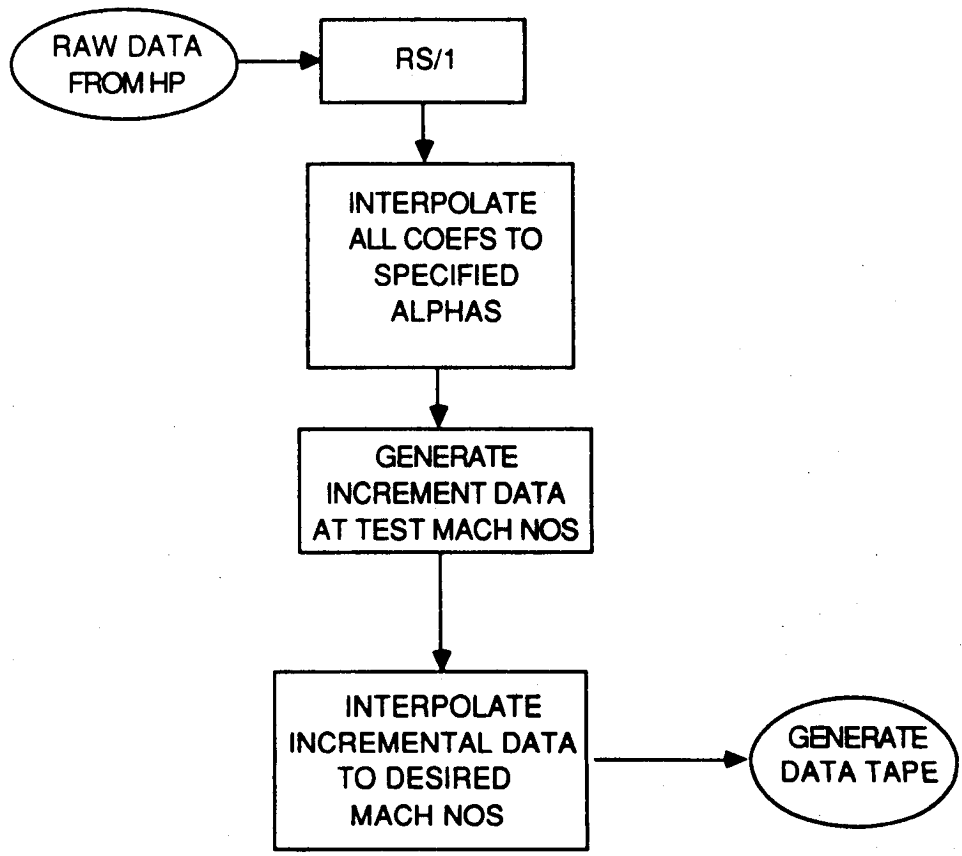

Fig. 2-3 Recommended Future Methodology that Should Be Used to Generate Incremental Data

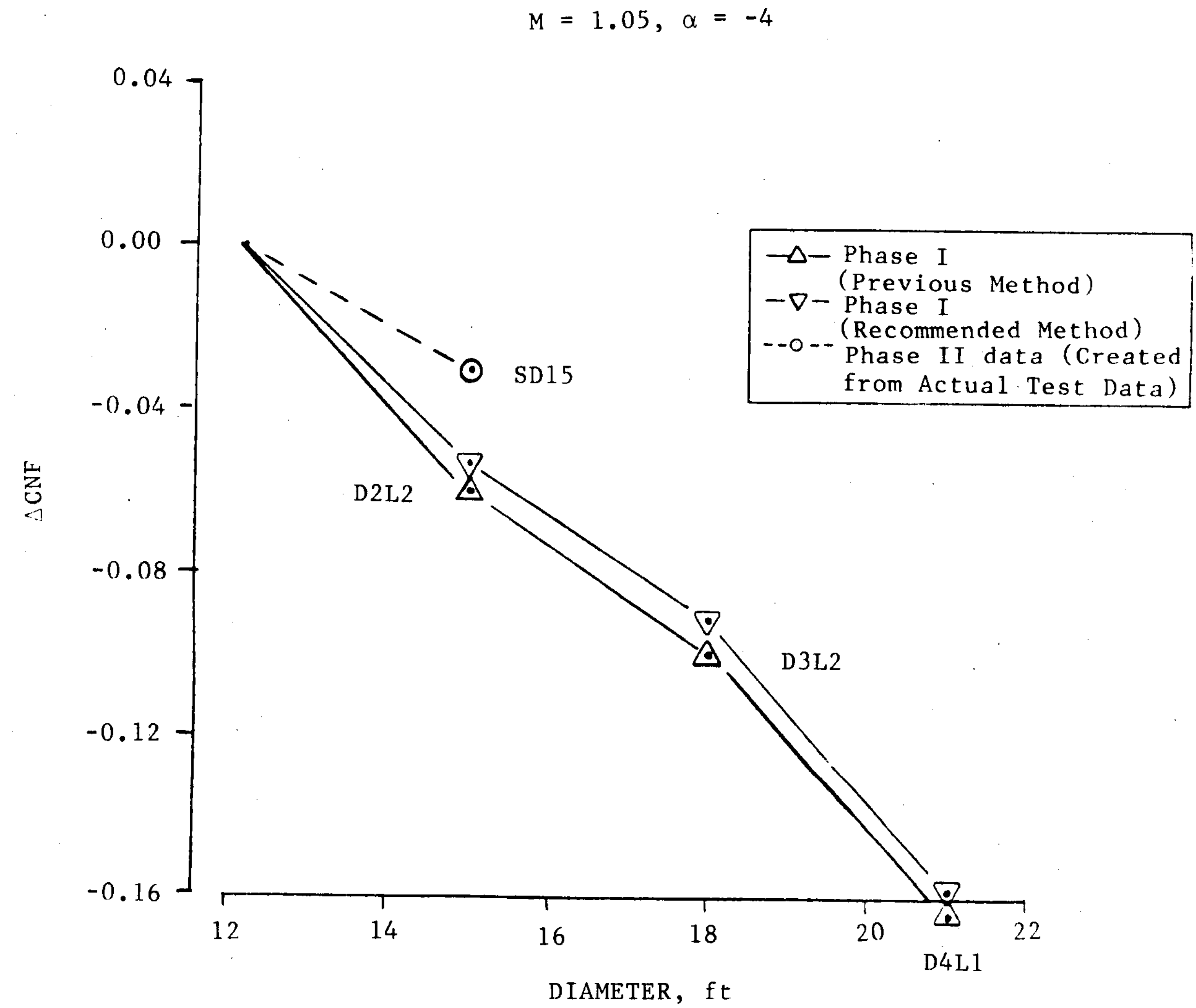

Fig. 2-4a Comparison of Increment Development Methods (ΔCNF)

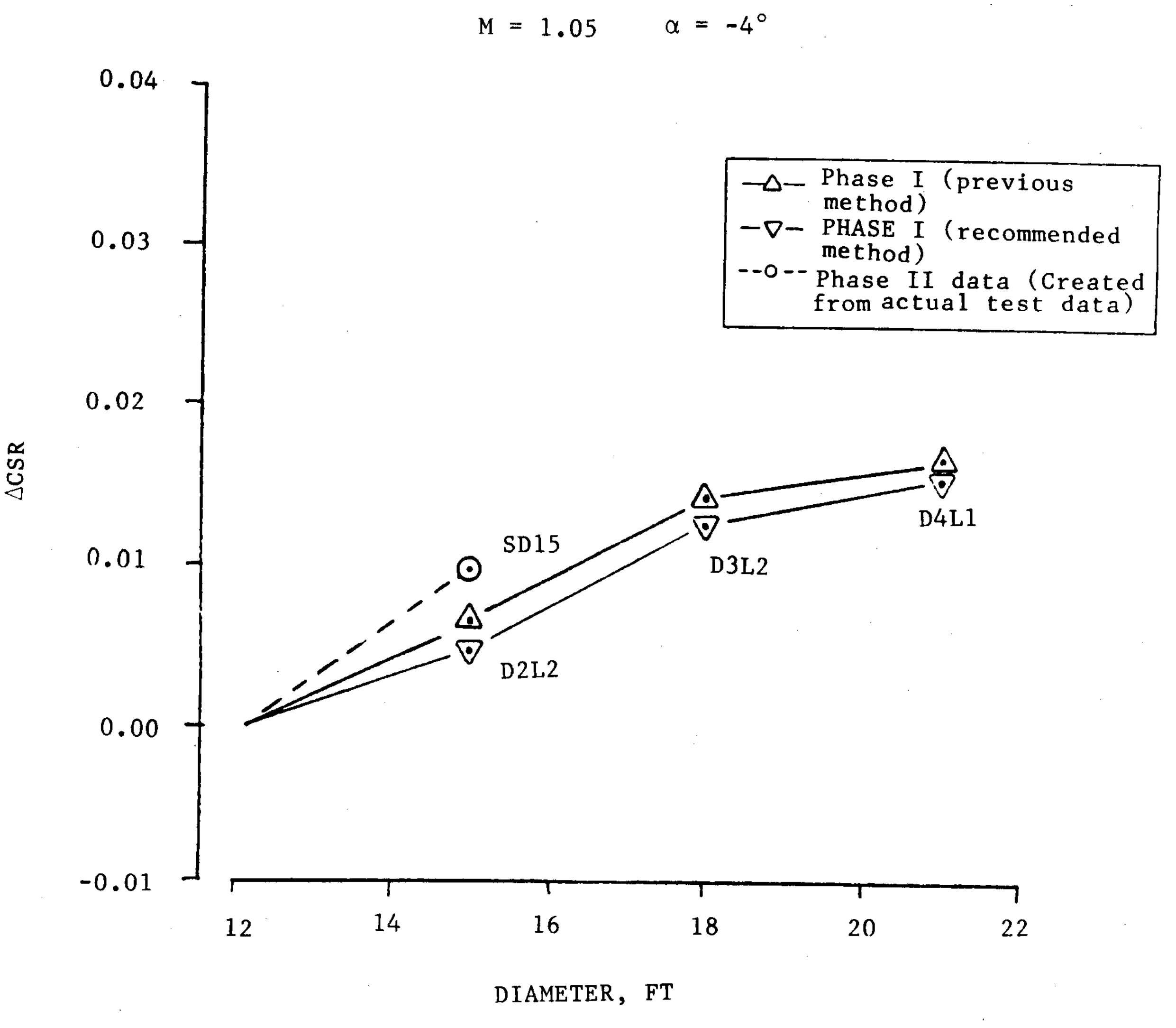

Fig. 2-4b Comparison of Increment Development Methods (ΔCSR)

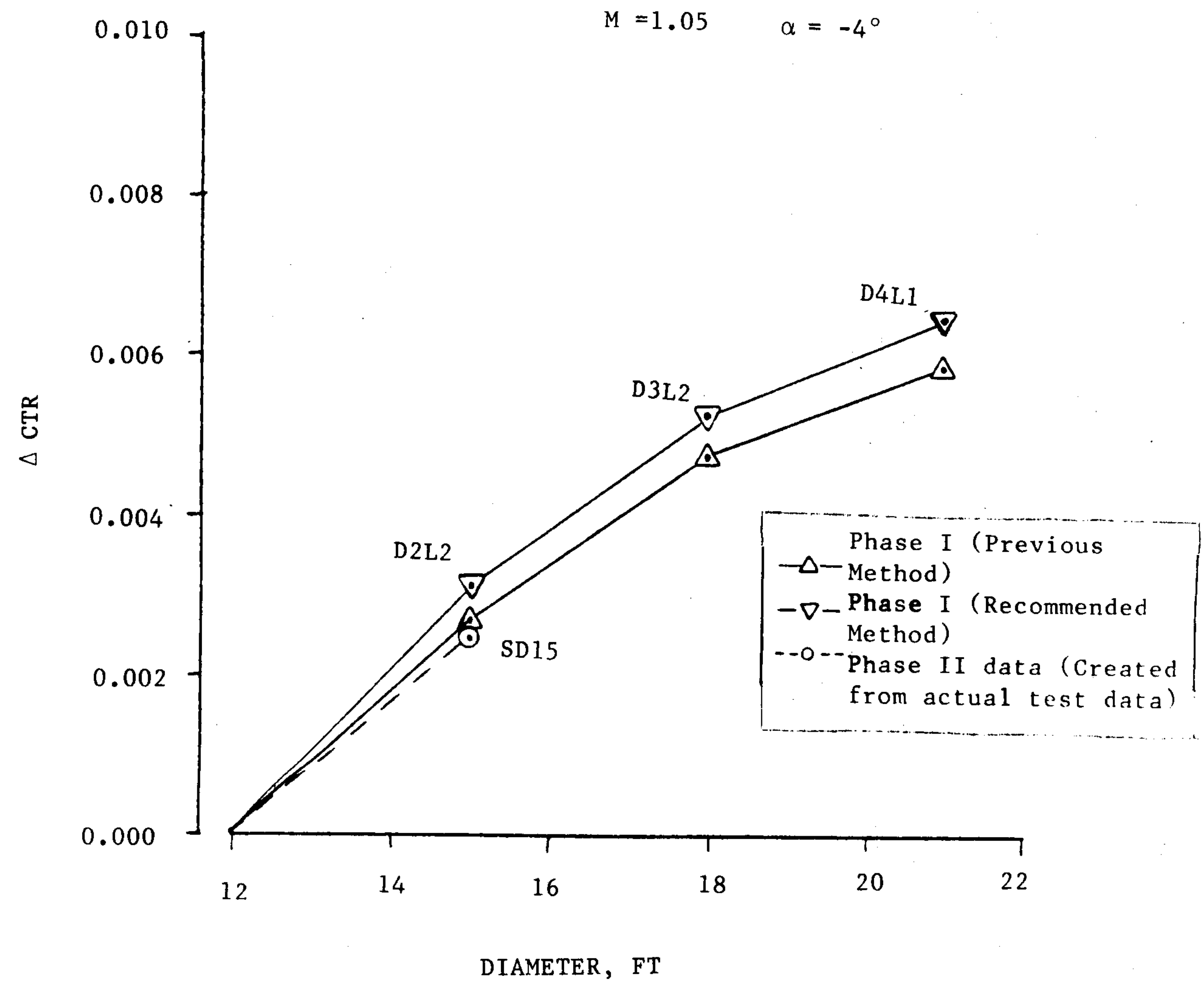

Fig. 2-4c Comparison of Increment Development Methods (ΔCTR)

that the previous increment development method used to generate the Phase I data is not responsible for the large differences that exist between the Phase I and the Phase II incremental data at transonic Mach numbers.

2.3 VERIFICATION OF INTERPOLATIONS PERFORMED ON LRB DATA

Once raw data were available and an incremental development chosen, the results were interpolated versus alpha and Mach and compared to existing SSLV data. Section 2.3.1 gives results for angle of attack interpolations, and section 2.3.2 gives results for Mach number interpolations.

2.3.1 Angle of Attack Interpolation

Phase I results were interpolated to even angles of attack ranging from -8 degrees to +8 degrees in 2 degree increments from the raw wind tunnel data. Attached are the plots of various coefficients as a function of attack (Figs. 2-5 to 2-10). As the plots show, the interpolated data overlay the raw data extremely well for relatively linear curves (CMF and CNF). For non-linear curves (CAF), there are some slight differences in the curves representing raw and interpolated data.

These differences are due to using a linear interpolation on a nonlinear curve and not to faulty interpolation. In all cases, the differences are quite small and are well within the accuracy range of the experimental data. In future efforts, higher order interpolation methods will be used in interpolating non-linear and/or critical data.

2.3.2 Mach Number Interpolation

The raw data from the wind tunnel testing were interpolated for Mach numbers within the LRB Phase I data base. Table 2-3 presents the LRB Phase I configurations represented in the data. The attached Mach numbers plots (Figs. 2-11 through 2-12) detail the data that were linearly interpolated from the raw data. The circled data points shown in the plots lie in a straight

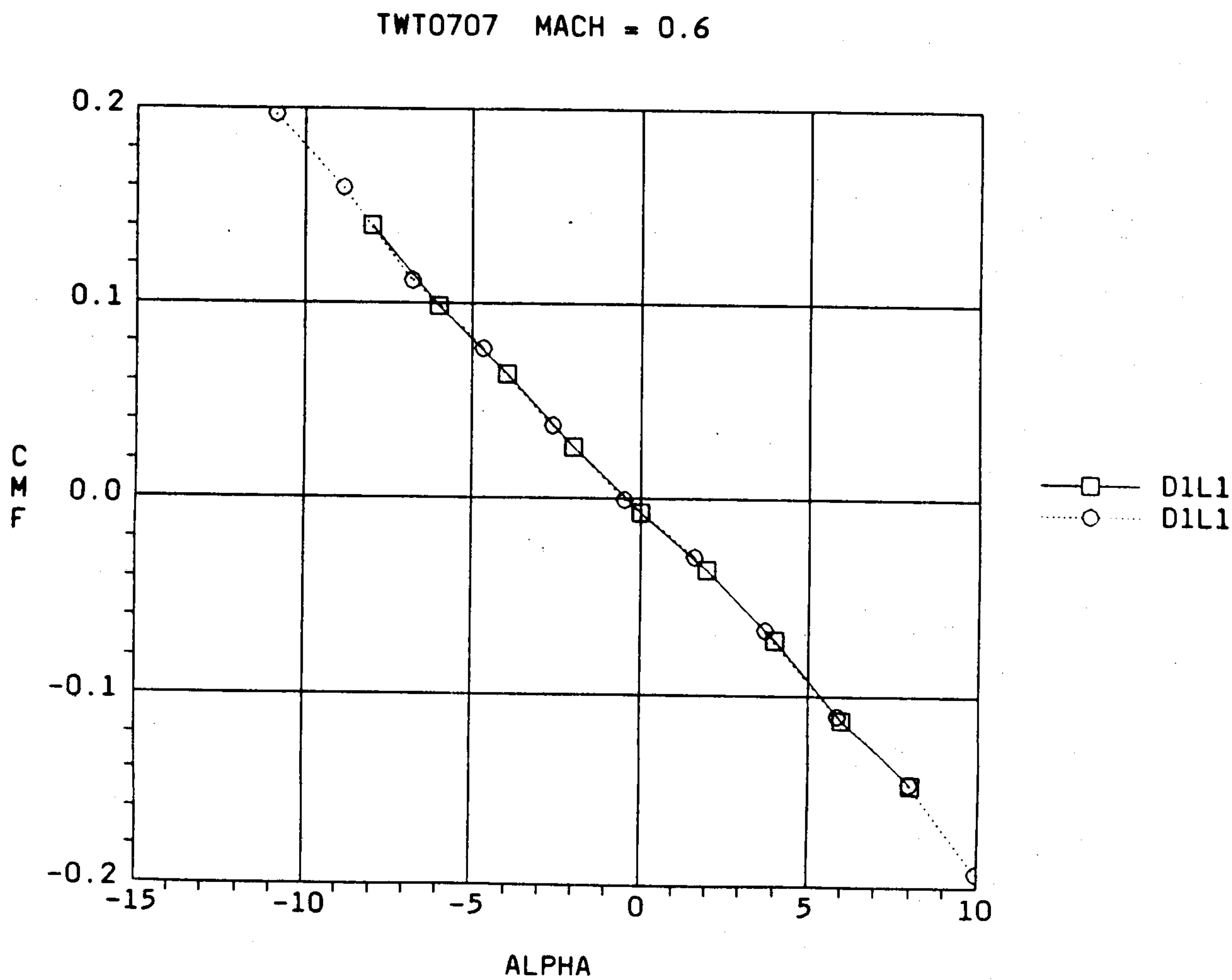

Fig. 2-5 CMF vs α

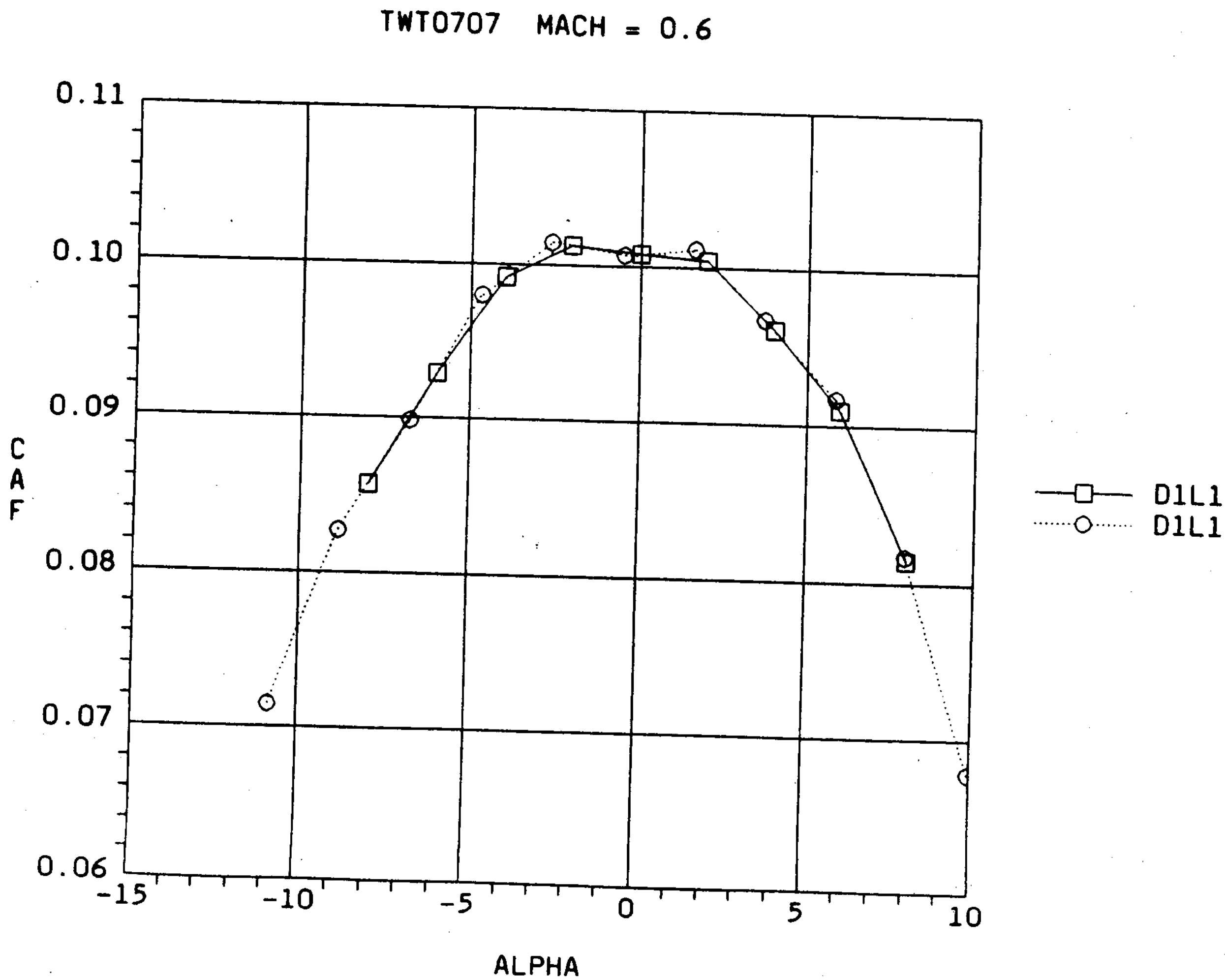

Fig. 2-6 CAF vs α

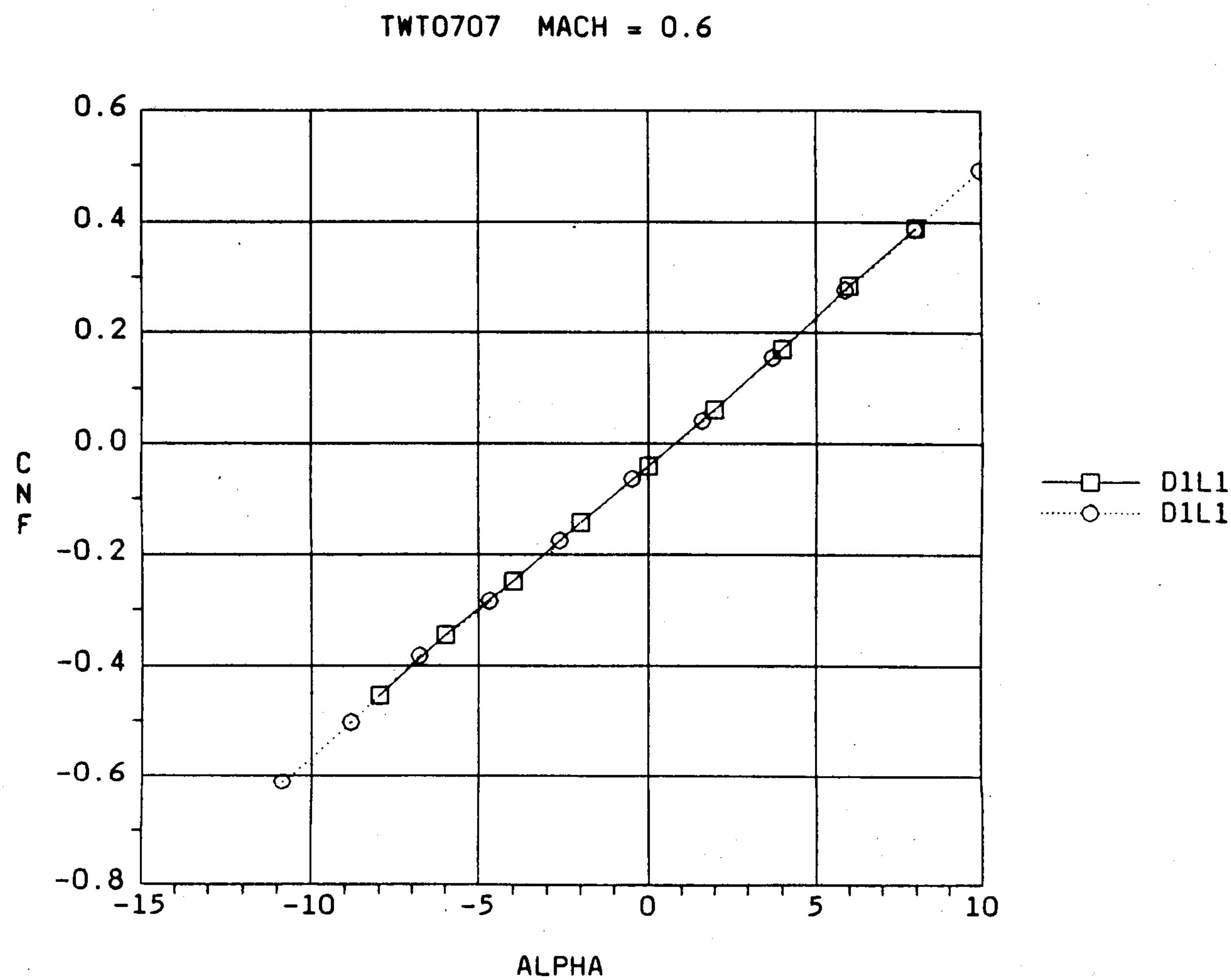

Fig. 2-7 CNF vs α

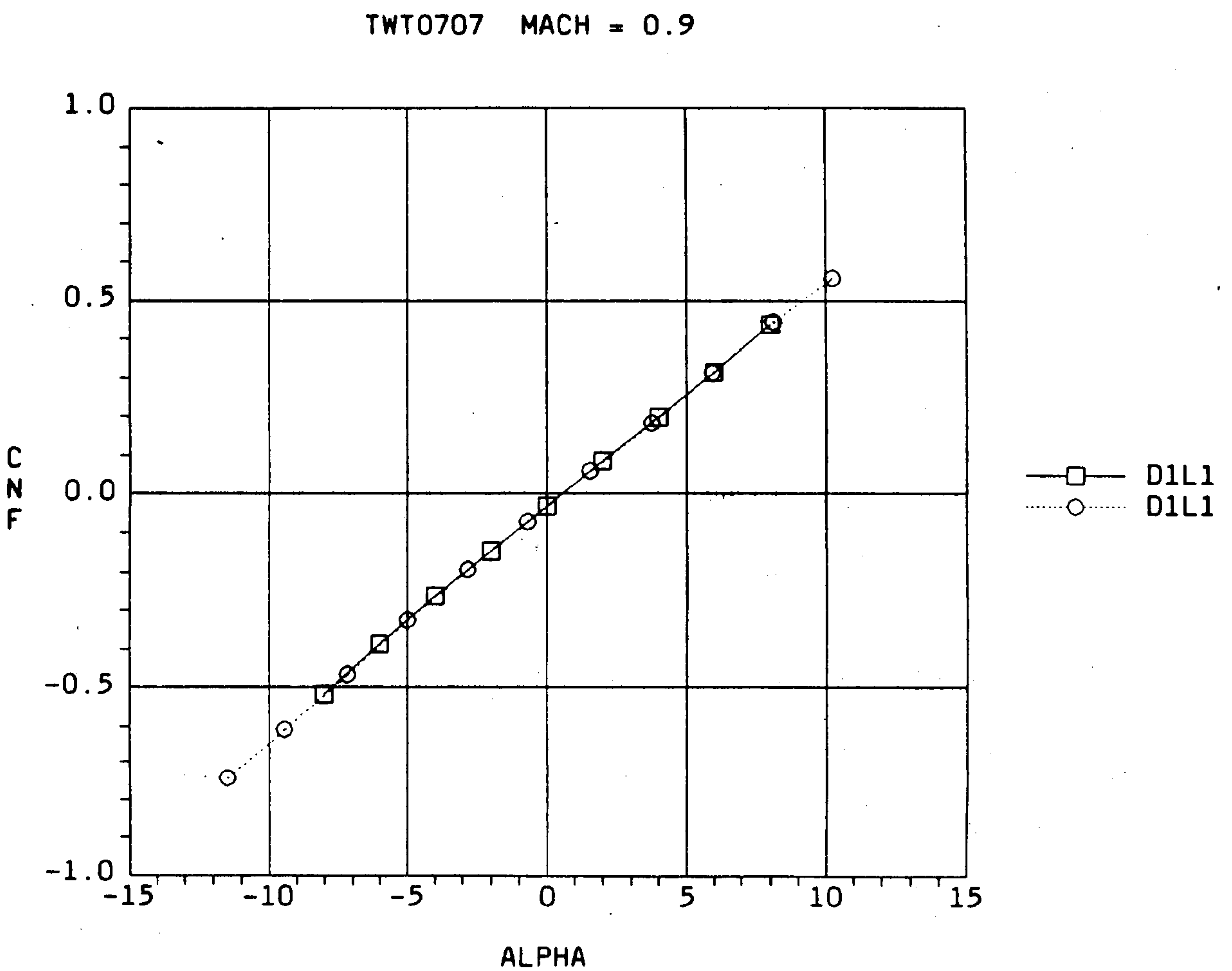

Fig. 2-8 CNF vs α

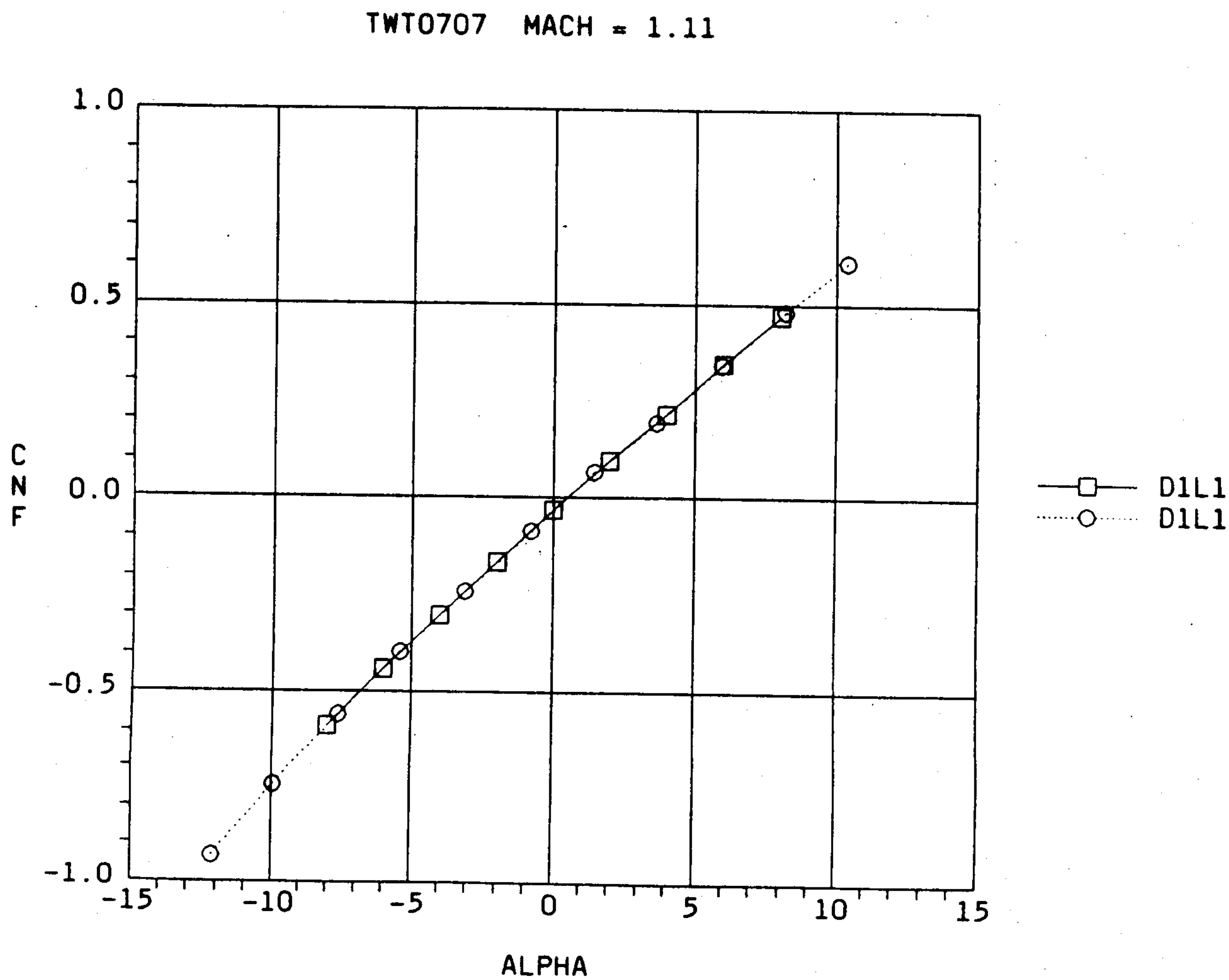

Fig. 2-9 CNF vs α

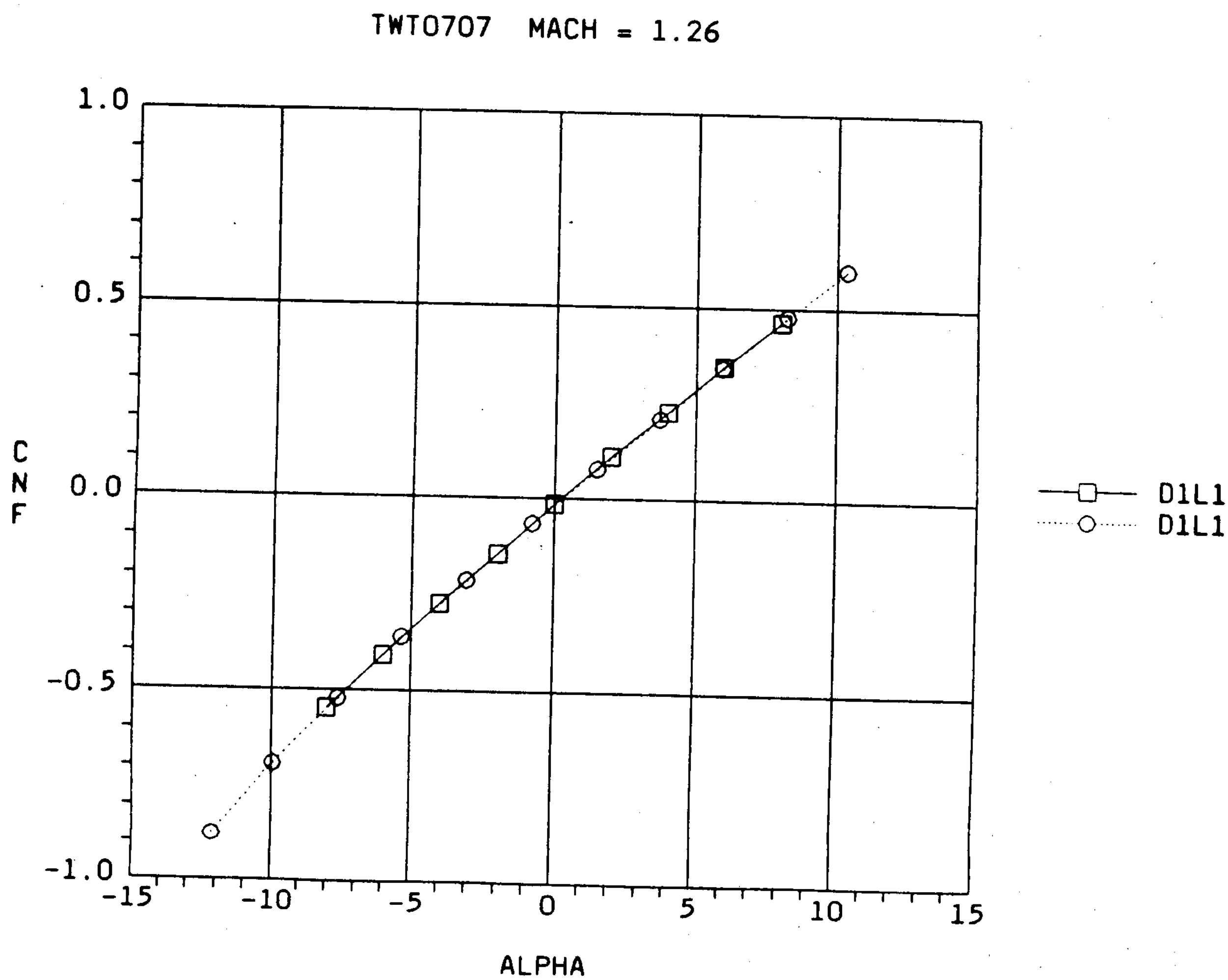

Fig. 2-10 CNF vs α

Table 2-3 PHASE I LRB DIMENSIONS

Length (ft) \ Diameter (ft)	D1	D2	D3	D4
	12.2*	15	18	21
L1	144*	149	154	158
L2	150	159	163	167
L3	170	172	175	177
L4	190	190	190	-

*Current SSLV configuration.

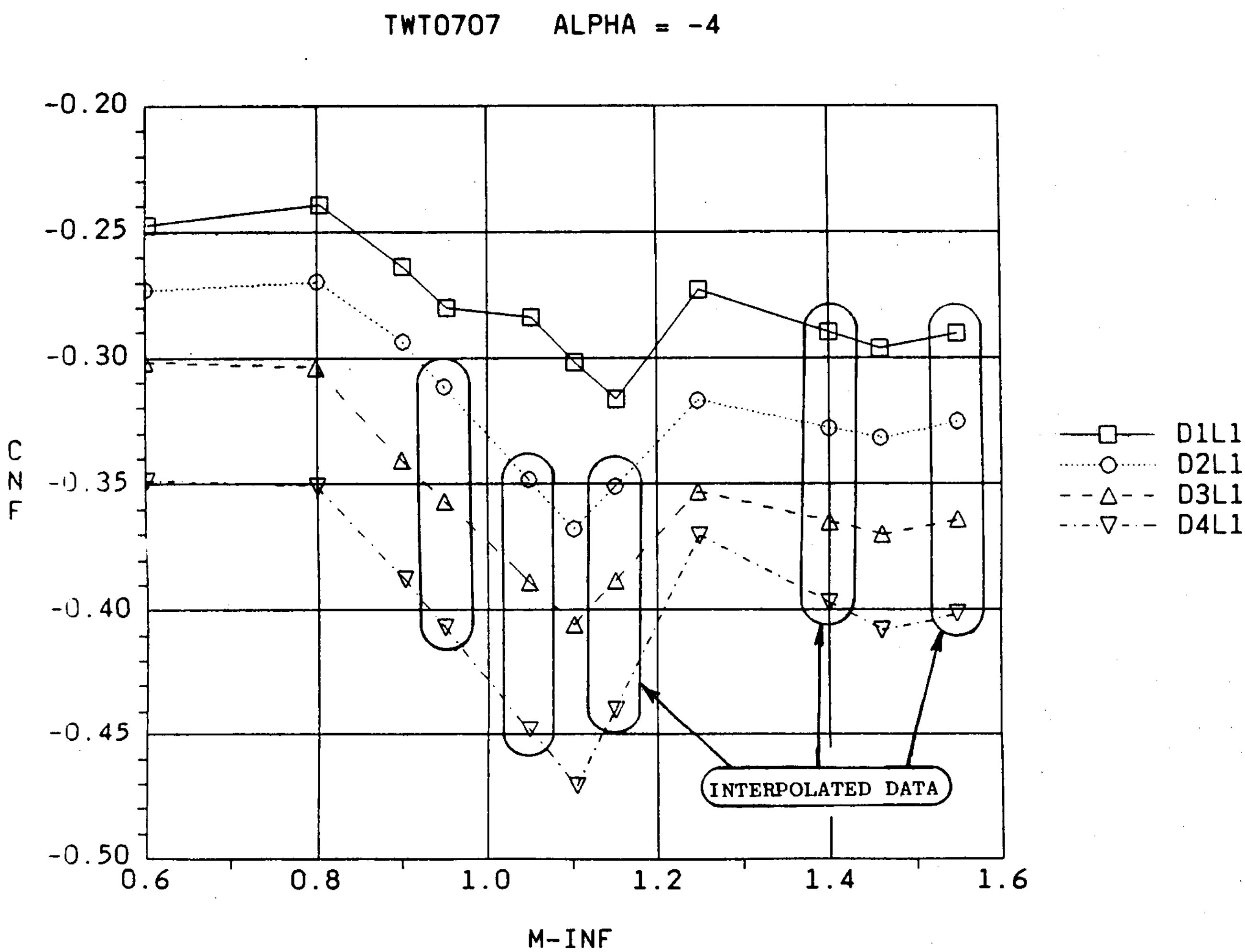

Fig. 2-11 CNF vs MACH (α = -4)

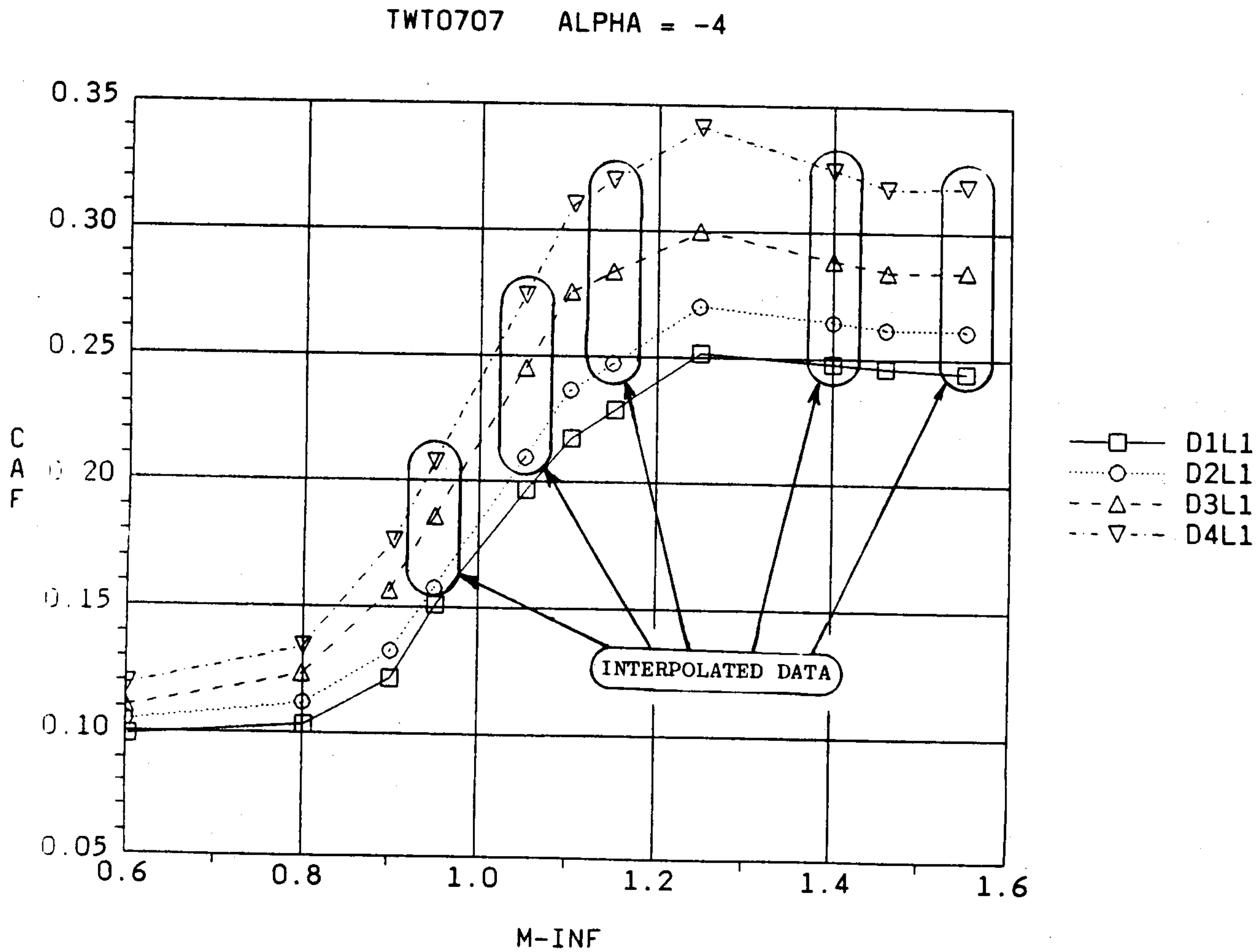

Fig. 2-12 CAF vs Mach (α = -4)

line between the actual data points. From the plots it is evident that the data base generated was compatible with the existing operational Shuttle aerodynamic data.

2.4 EVALUATION OF PLUME EFFECTS

An analysis was conducted to investigate plume effects on Shuttle LRB configuration aerodynamic characteristics. The analysis included prediction of the correlation between base pressure and various parameters such as the number of nozzles, thrust, area ratio, chamber pressure and base geometry. The plume effects were evaluated with regard to axial force, normal force and pitching moment.

The method used to predict the correlation between base pressure and the parameters was determined by a review of the <u>Compendium of Flight Vehicle and Base Pressure Techniques</u> (Lockheed Missiles & Space Co., Inc. August 1983). From this review, the base pressure technique used was developed. This technique is outlined as follows:

1. Define configuration, dimensions, etc.
2. Define trajectory and thrust history
3. Calculate thrust coefficient and thrust loading using base area
4. Determine generic base pressure
5. Determine correction for nozzle axial extension
6. Determine correction for flare
7. Determine correction for multiple nozzle plume effects
8. Calculate base pressure coefficient.

The base pressure technique was then applied to each LRB configuration to determine the base pressure coefficients. The resulting coefficients were compared to actual flight data for validation. The coefficients were then used to determine how a change in base configuration would affect aerodynamic characteristics and to predict base drag numbers and how base drag would affect vehicle performance. Section 7 discusses the effects of the base drag further.

The effect of a change in base configuration was analyzed with regard to normal force and pitching moment coefficient. The correlation between base pressure on the external tank base and pressure distribution on the oribiter's lower wing and fuselage was investigated. The investigation was based on previous analysis of solid and gaseous plume simulation test data. Figs. 2-13 through 2-18 present graphic representations of the analysis.

From the evaluation of the wind tunnel data the following relationships were derived for the LRB study:

$$\Delta C_N = 0.28\ \Delta C_{PB}$$

$$\Delta C_M = -0.27\ \Delta C_{PB_{ET}}$$

where ΔC_N, ΔC_M are increments relative to the current Shuttle. $\Delta C_{PB_{ET}}$ is the ET base pressure coefficient increment of the LRB configuration relative to the current Shuttle. $\frac{\Delta C_M}{\Delta C_N}$ is the value consistent with plume effects acting in the aft region of the vehicle. It was concluded that the mated vehicle normal force and pitching moment effects can be predicted if the ET base pressure effects can be predicted.

The LRB plume effects study utilized five different booster configurations. These configuration are presented in Fig. 2-19. The lack of a definite configurations necessitated the estimation of certain parameters. These uncertainties are outlined in Table 2-4.

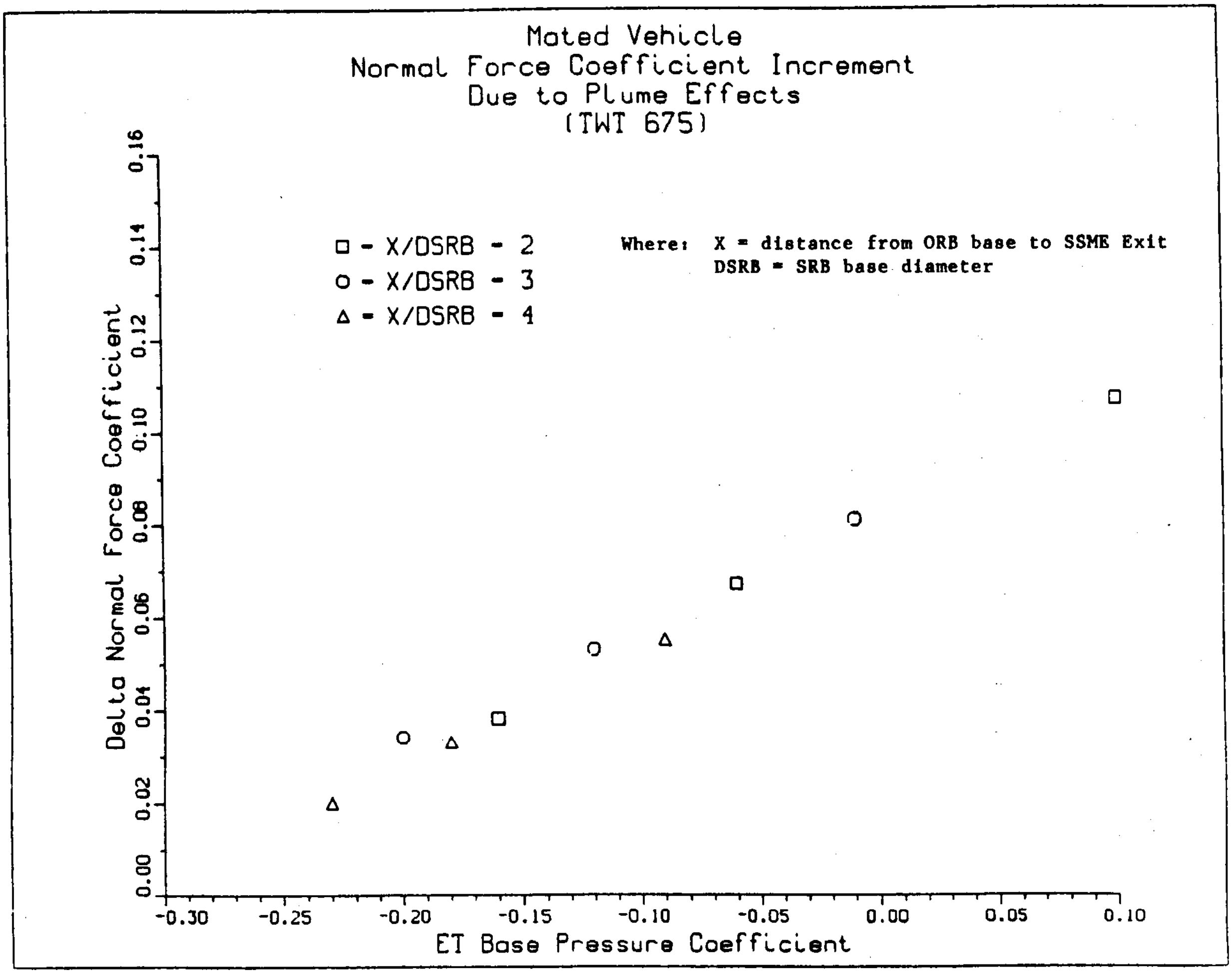

Fig. 2-13 Δ Normal Force Coefficient (TWT 675)

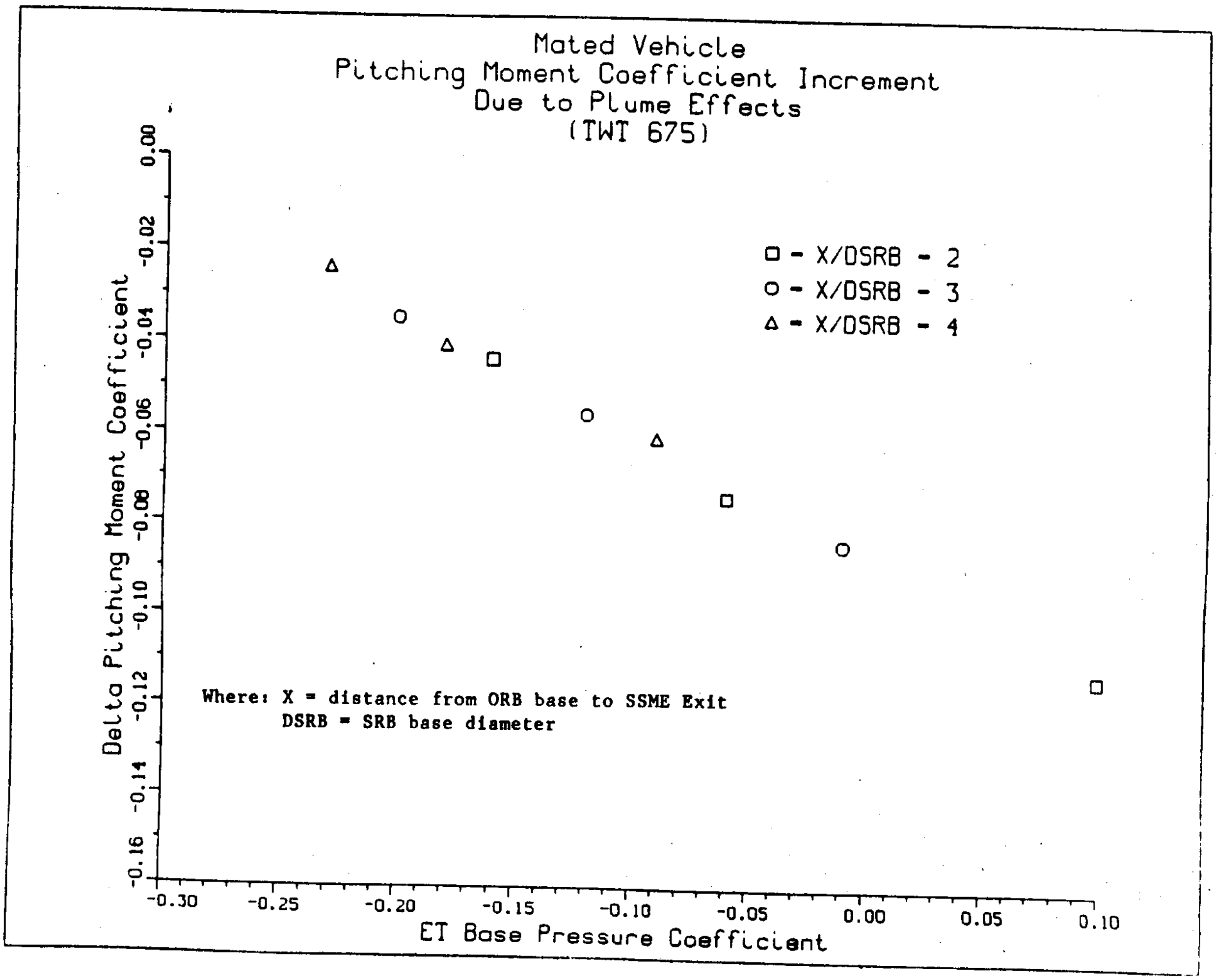

Fig. 2-14 Δ Pitching Moment Coefficient (TWT 675)

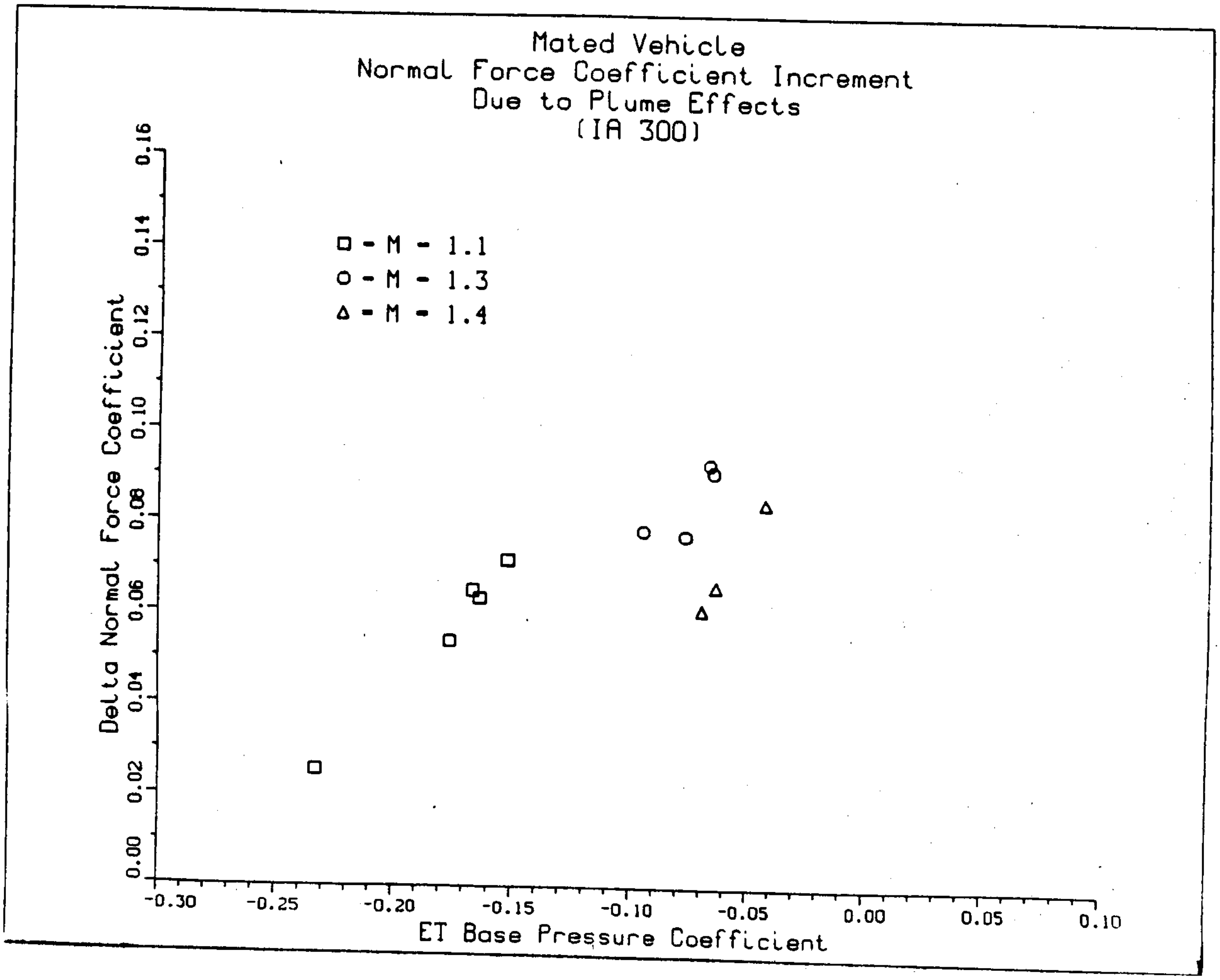

Fig. 2-15 Δ Normal Force Coefficient (IA300)

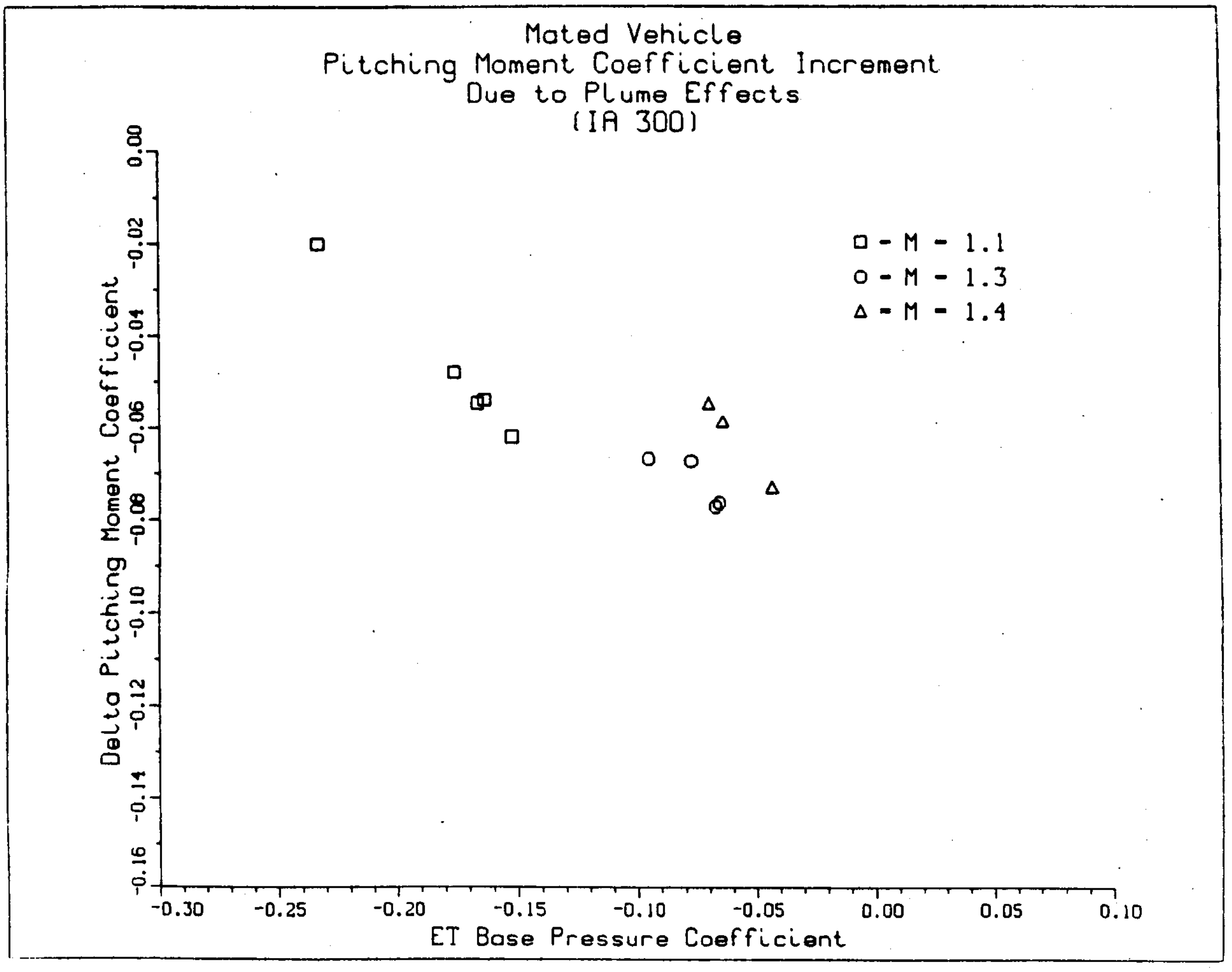

Fig. 2-16 Δ Pitching Moment Coefficient (IA300)

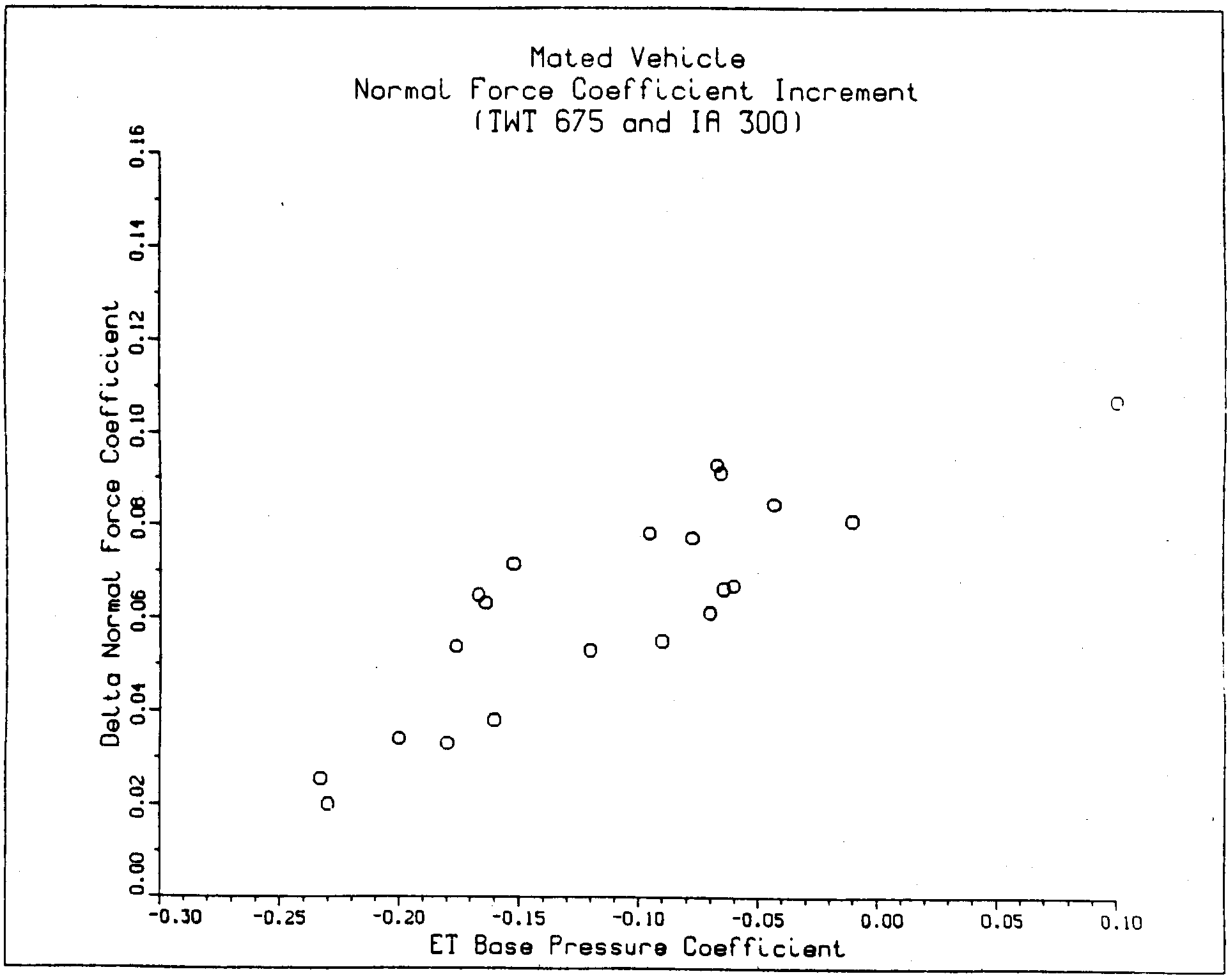

Fig. 2-17 Δ Normal Force Coefficient (TWT 675 & IA300)

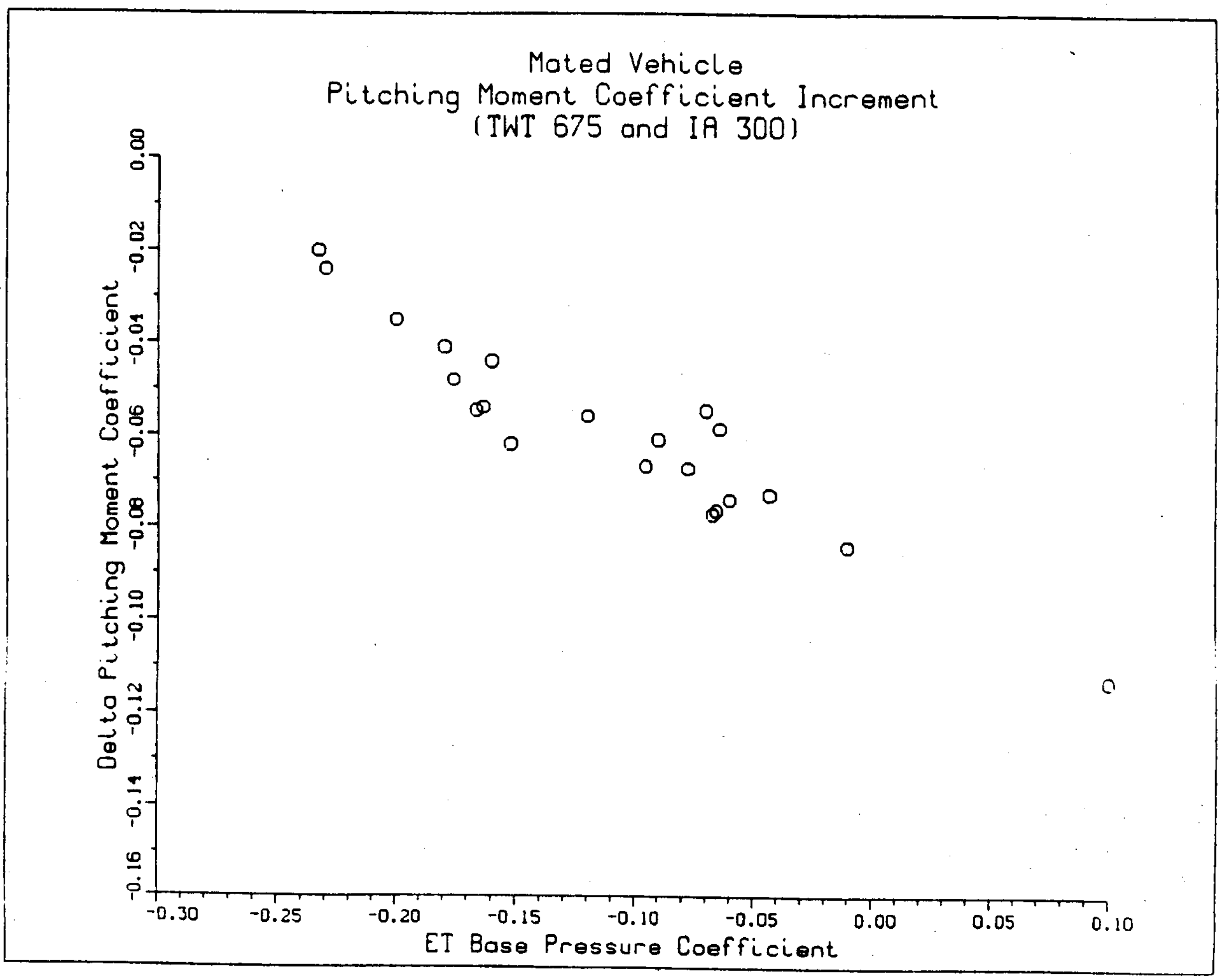

Fig. 2-18 Δ Pitching Moment Coefficient (TWT 675 & IA300)

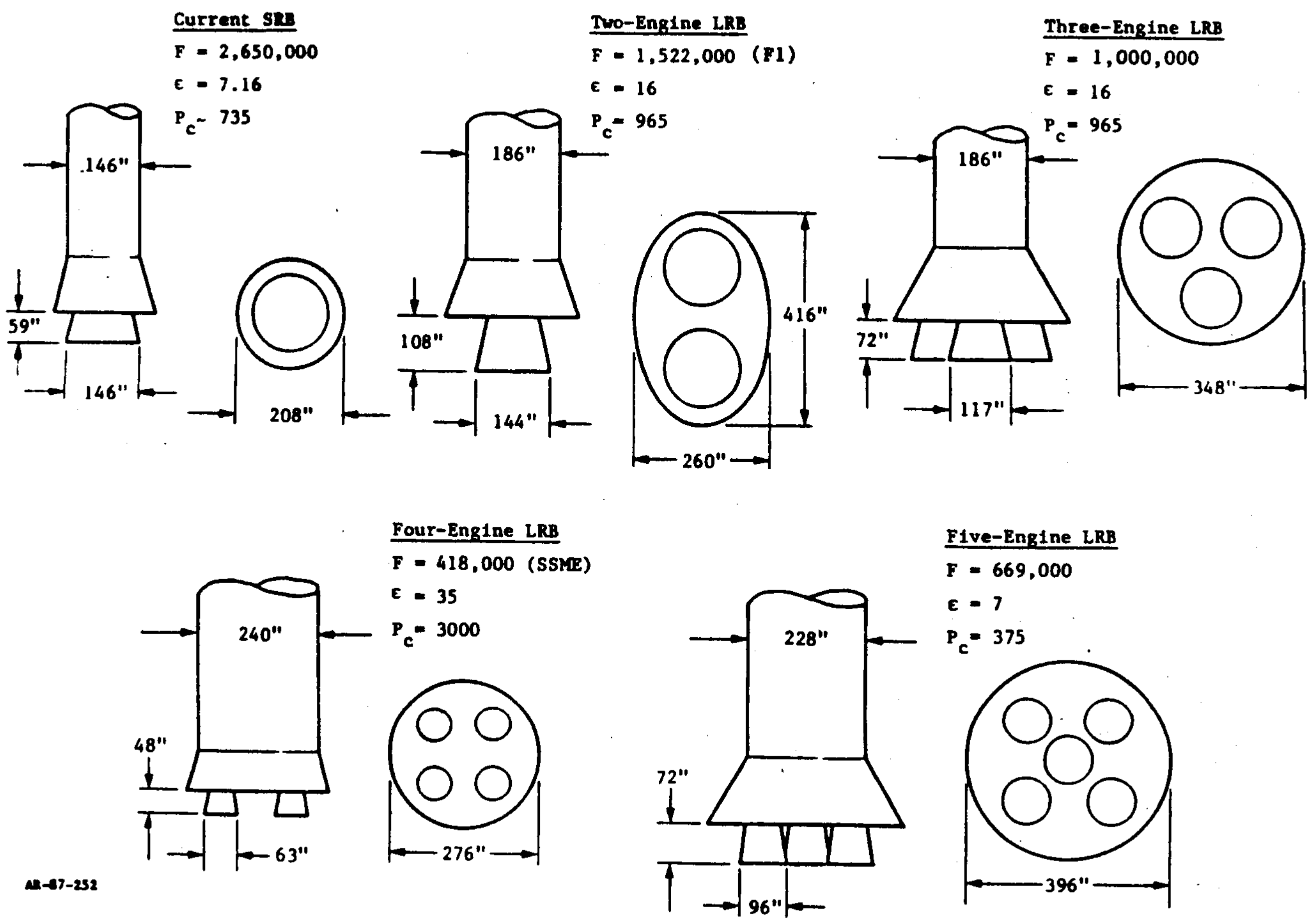

Fig. 2-19 Shuttle LRB Configurations Used In Study

Table 2-4 ANALYTICAL UNCERTAINTIES

PARAMETER	CONFIGURATION 2 LRB	3 LRB	4 LRB	5 LRB
SKIRT DIMENSION	E	E	E	E
NOZZLE AXIAL POSITION	E	E	E	E
SKIRT FLARE EFFECTS	EX	EX		EX
ENGINE THRUST		E		
ENGINE CHAMBER PRESSURE		E		
NOZZLE AREA RATIO		E		E
PLUME ANGLE VS ALTITUDE		E		E
MULTIPLE ENGINE PLUME EFFECTS			EX	
BASE PRESSURE ABOVE M = 2.0			EX	
ENGINE SPACING	E	E	E	E
ALTITUDE AND DYN PRESSURE VS MACH NO.	(1)	(1)	(1)	(1)
THRUST VS MACH NO.	(2)	(2)	(2)	(2)

E = ESTIMATED VALUE BASED ON MEASUREMENTS/CALCULATIONS
Ex = EXTRAPOLATION BEYOND EXISTING DATA BASE WAS PERFORMED.
(1) = ASSUMED SAME AS CURRENT SHUTTLE PROFILE
(2) = ASSUMED CONSTANT THRUST

The base pressure prediction technique was used to determine the base pressure coefficient for each booster configuration. Figures 2-20 and 2-21 present the Booster base pressure coefficients and external tank base pressure coefficients for each configuration at the Mach numbers used in the analysis. The base drag increment for the mated vehicle was determined and compared to current Shuttle data. Figure 2-22 presents the base drag increments for the booster configurations in comparison to the current STS. It was determined that the drag for the LRB is greater than that of the current shuttle because of the larger base area and the base pressure.

The normal force and pitching moment effects were calculated and compared to the current STS. Figs. 2-23 and 2-24 graphically present the comparison. Results showed that, for the LRB's, at $M > 1$, the pitching moment was significantly increased while normal force was significantly decreased. This was attributed to the decrease in ET base pressure due to a larger base area in the recirculation base from environment. Furthermore, the greater nozzle area ratios of the LRB configurations resulted in lower plume expansion angles and decreased base pressure.

The study recommended that delta base values <u>not</u> be incremented to account for plume effects for the following reasons:

1. Configuration uncertainties and assumptions are a significant factor
2. Drag increment is not large compared to total vehicle drag and thrust
3. Normal force increment is not larger compared to total vehicle values
4. Pitching moment has the most significant impact and could be an important factor.

It is recommended that an update to the plume analysis be conducted when more definition becomes available on LRB designs. This updated analysis was conducted and is discussed in section 7.

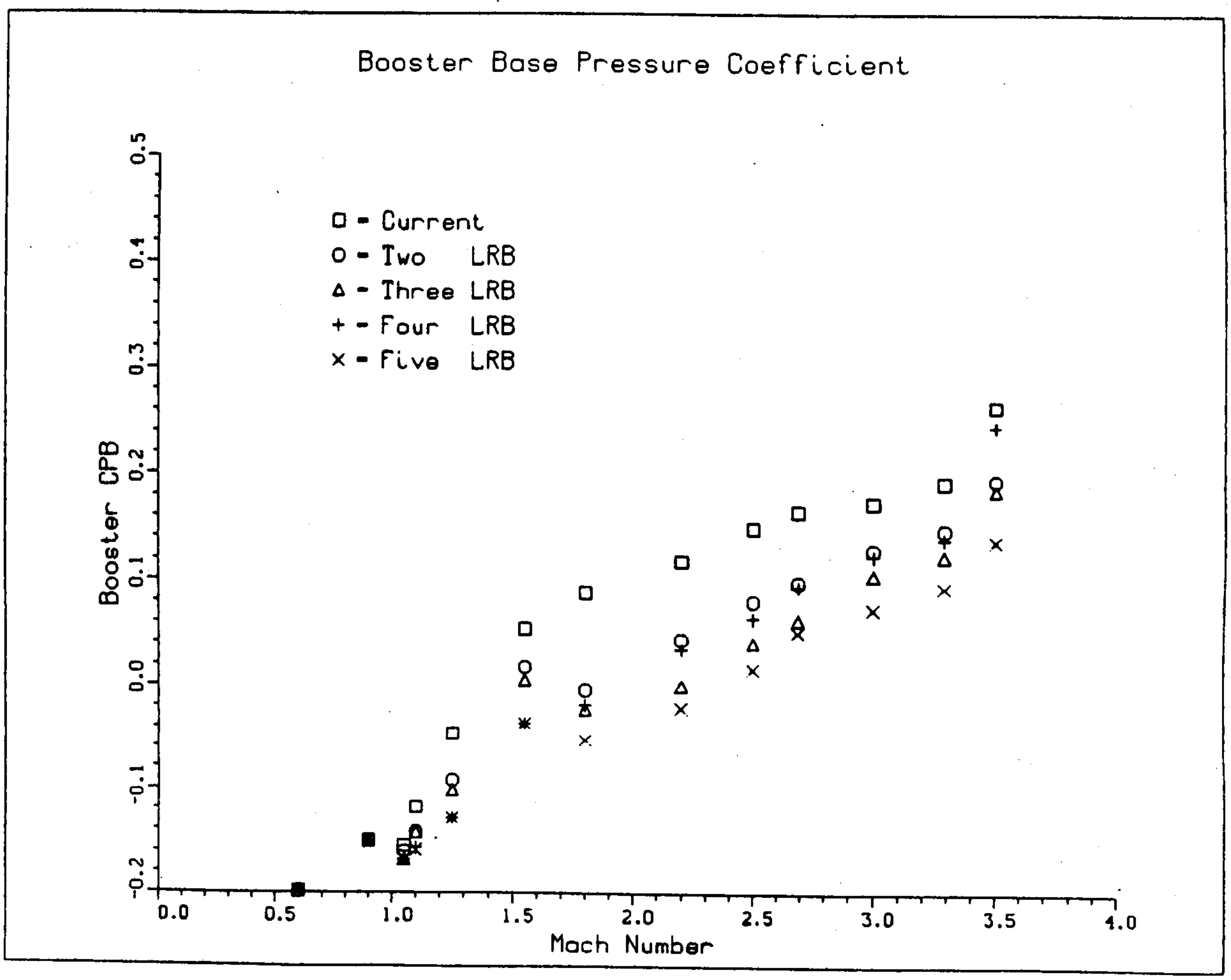

Fig. 2-20 Booster CPB vs Mach

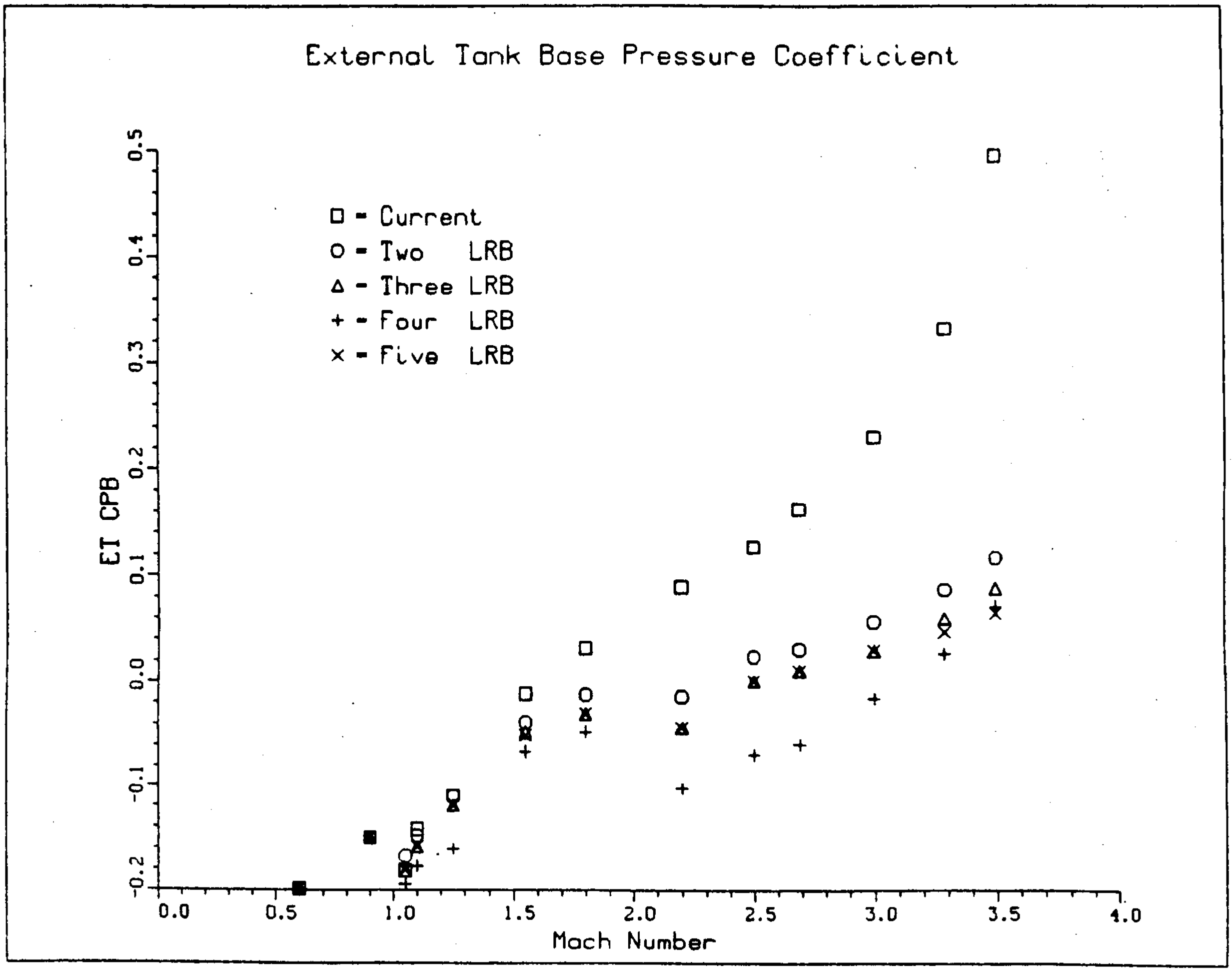

Fig. 2-21 ET CPB vs Mach

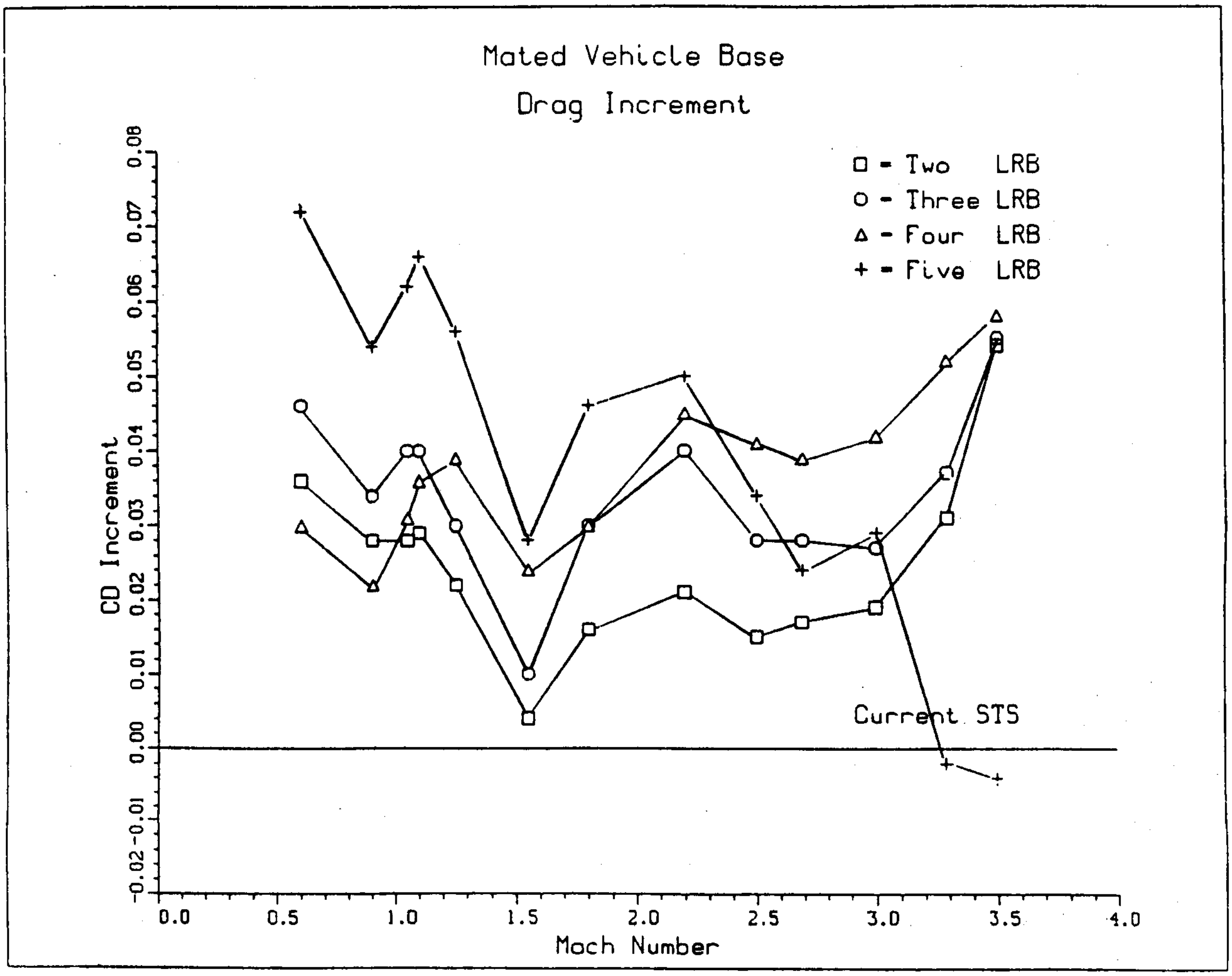

Fig. 2-22 CD Increment vs Mach

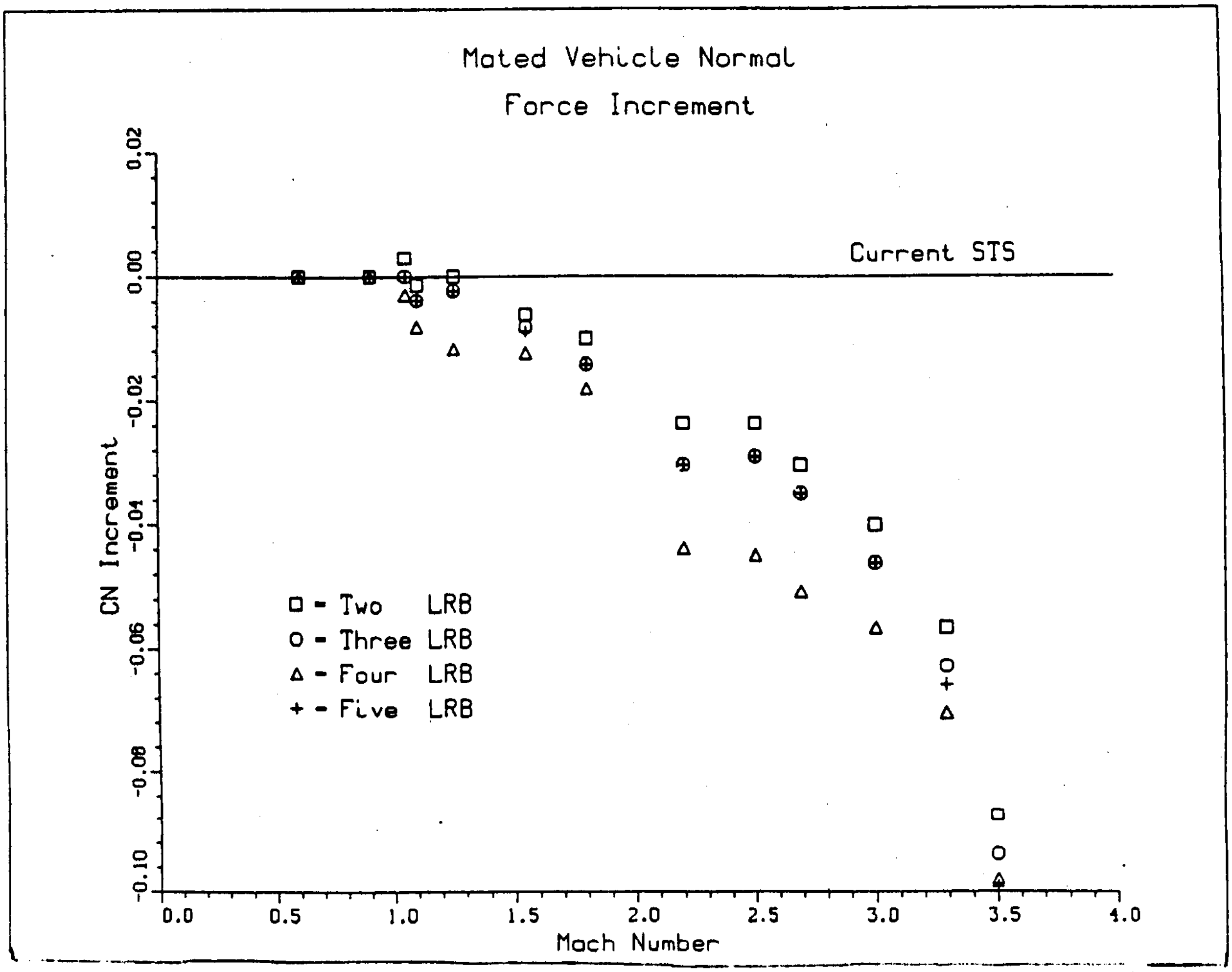

Fig. 2-23 CN Increment vs Mach

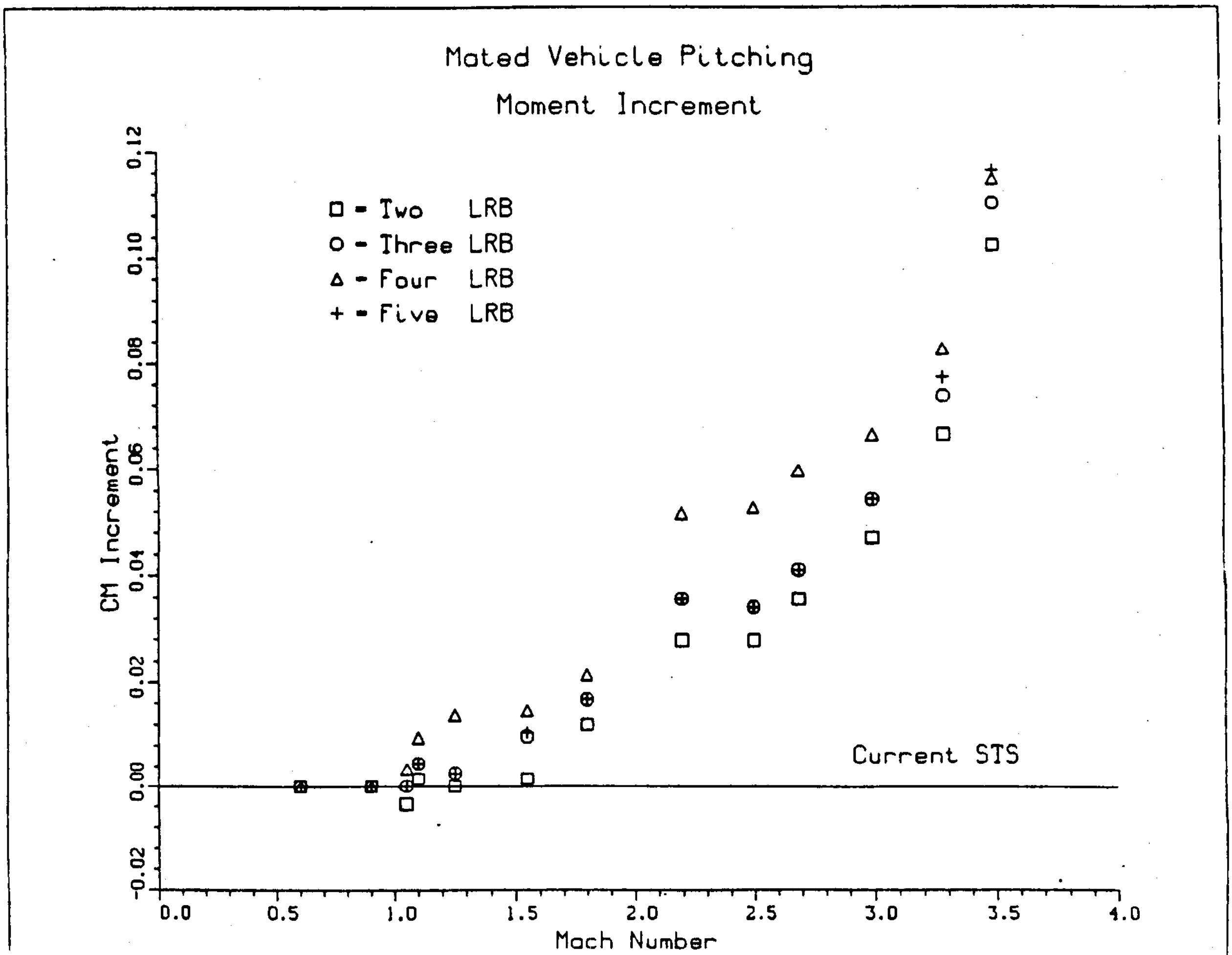

Fig. 2-24 CM Increment vs Mach

2.5 DATA ANALYSIS REVIEW

2.5.1 Data Analysis Review of Longitudinal Effects

Test data were analyzed to determine longitudinal effect at negative angles of attack. From the test data, it was concluded that the axial force coefficient (C_{AF}) increases with the diameter and length. The maximum C_{AF} occurs between 170 and 180 ft. See Fig. 2-25 for a plot of C_{AF} vs booster length and diameter.

The normal force coefficient (C_N) is relatively unaffected by changes in length. However, increases in diameter do produce a decrease or more negative C_N. This decrease is partially due to the larger nose of the vehicle. Since the nose of the LRB generated the majority of the normal force, increasing the nose area will increase the normal force produced, whereas increasing the length will have very minimal effect on C_N. The increased plan form area is also a contributing factor. See Fig. 2-26 for a plot of C_{NF} vs booster length and diameter.

The pitching moment coefficient decreases with an increase in length due to the forward movement of the LRB nose. An increase in diameter has minimal effects on C_M. The LRB length also changes the moment arm. See Fig. 2-27 for a plot of CMF vs booster length and diameter.

The aerodynamic center location moves forward with increases in length and diameter due to the increased loading and forward movement of the LRB nose. See Fig. 2-28 for a plot of X_{AC} vs booster length and diameter. A summary of vehicle longitudinal effects can be found in Table 2-4.

2.5.2 Data Analysis Review on Wing Loads

Analysis of the data with regard to wing loads indicated the wing root coefficients and elevon hinge moments are relatively unchanged by increase in length. However, an increase in diameter increases all wing loads including wing shear, root bending, root torsion, and inboard/outboard elevon hinge moments.

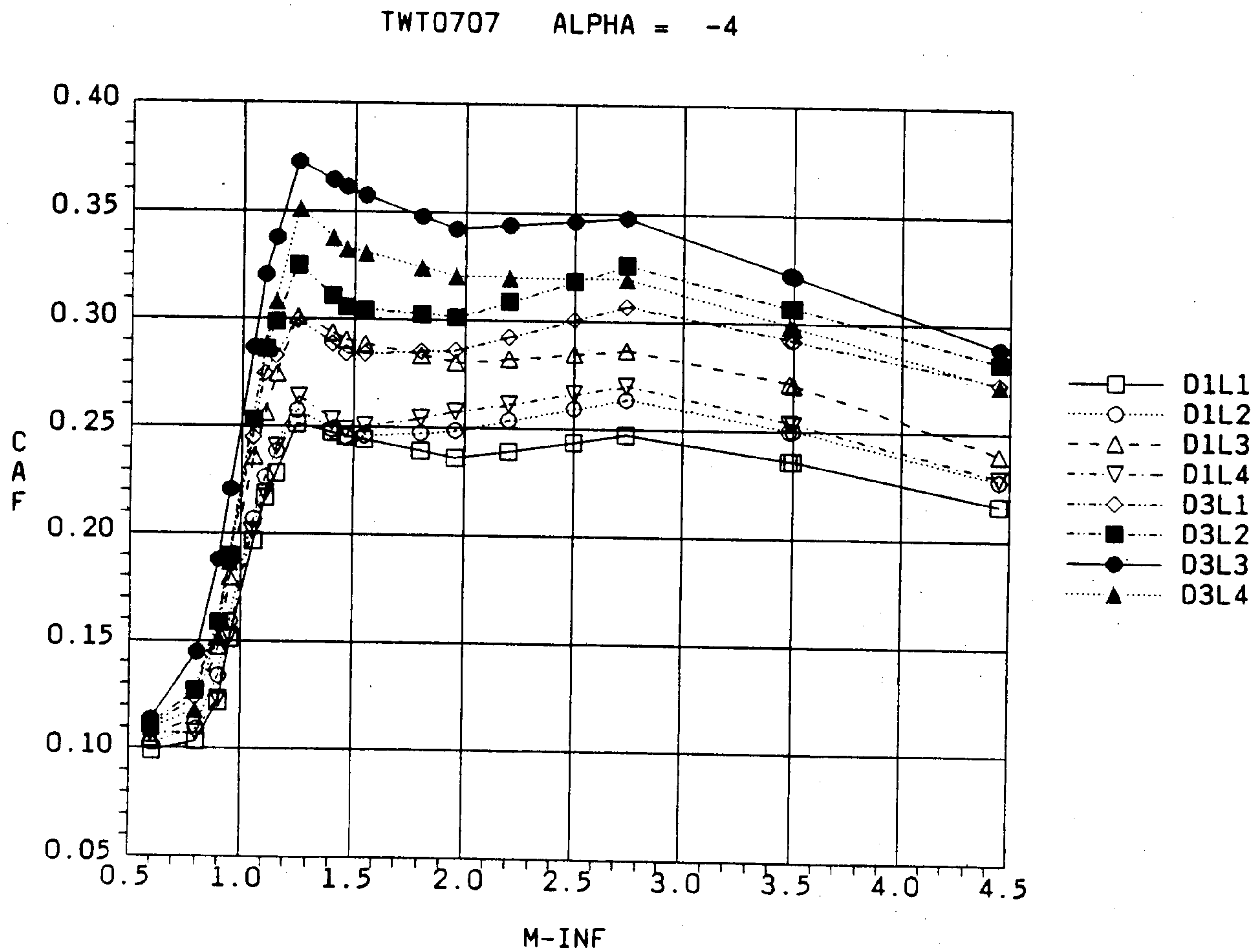

Fig. 2-25 CAF vs Mach (Length and Diameter Effects)

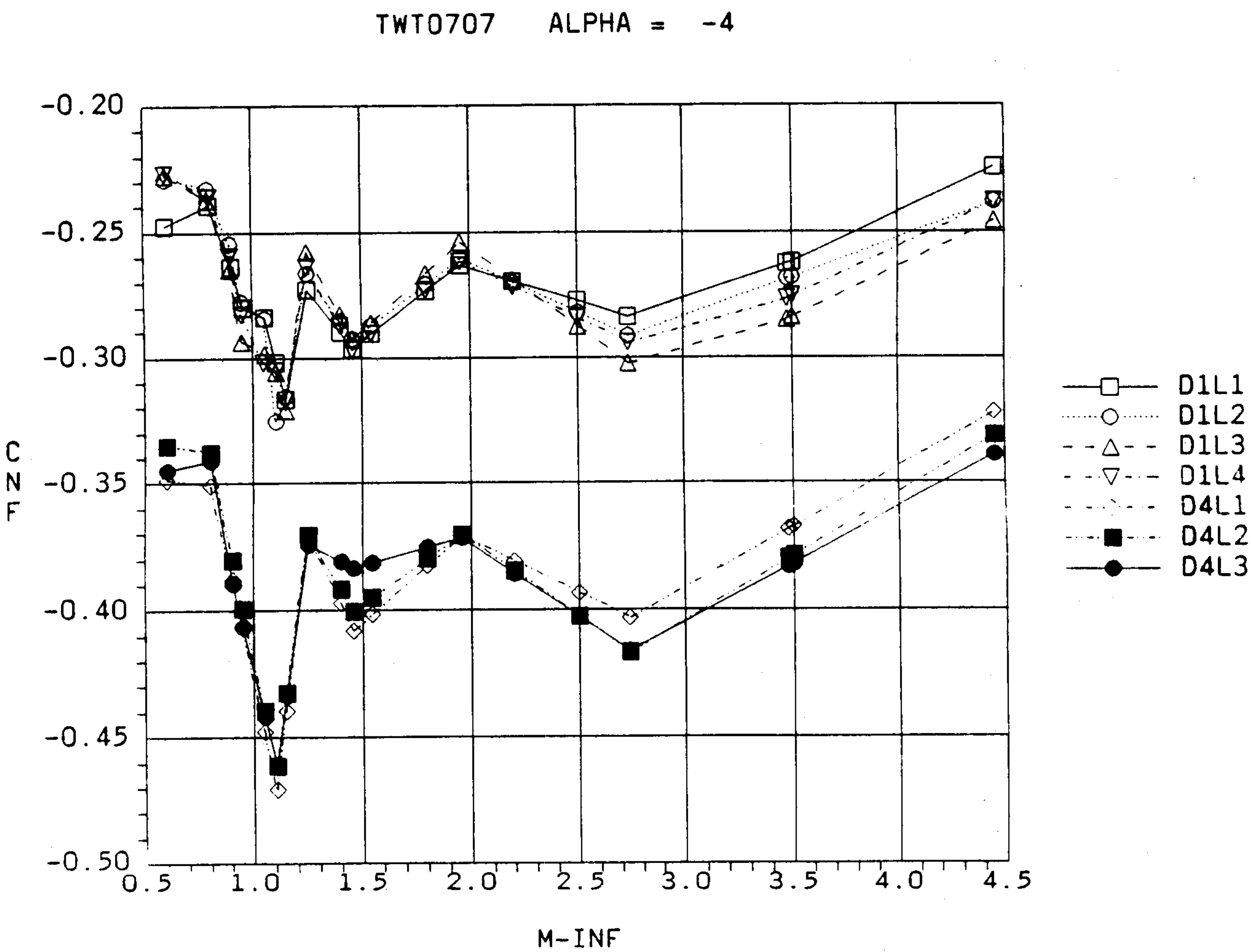

Fig. 2-26 CNF vs Mach (Length and Diameter Effects)

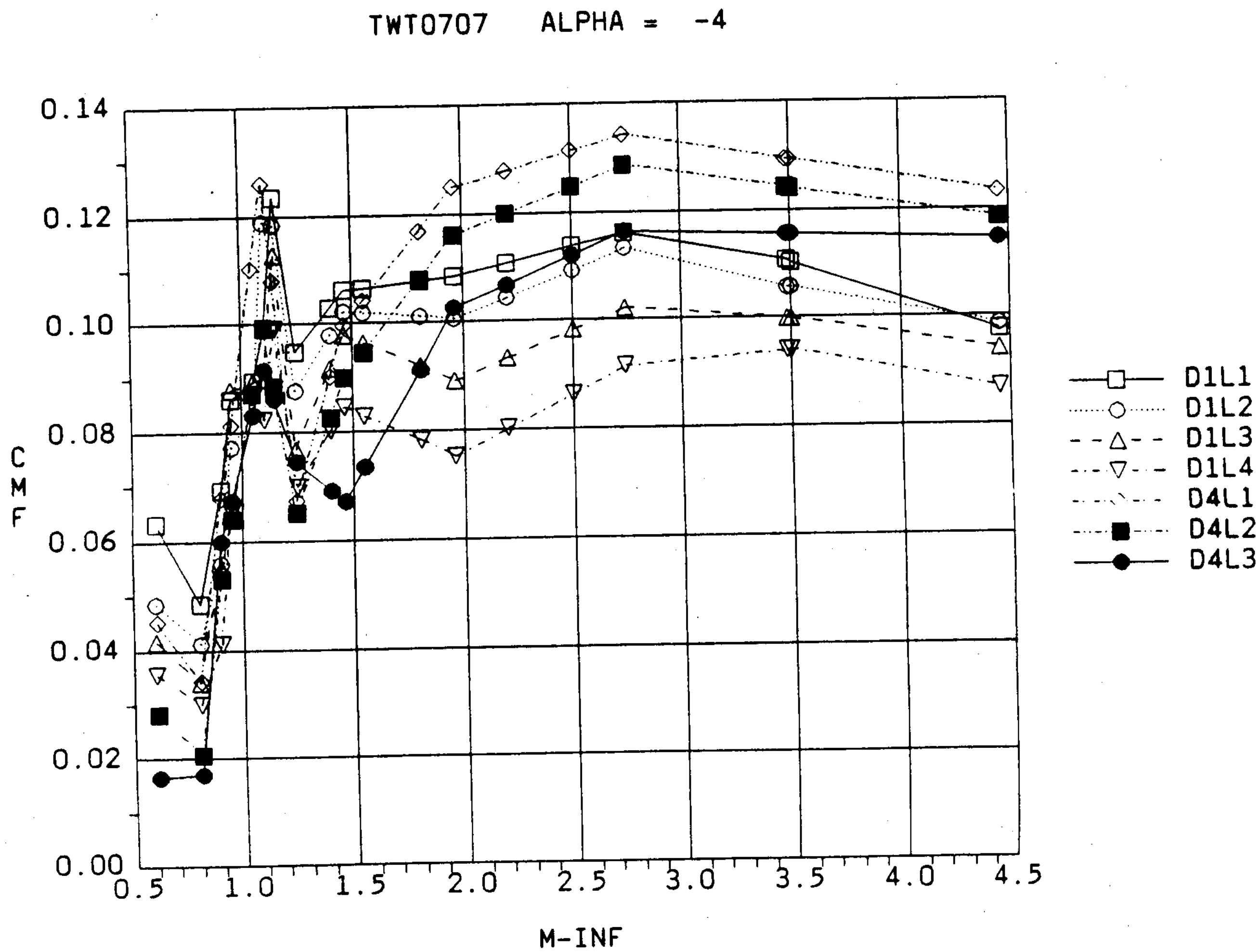

Fig. 2-27 CMF vs Mach (Length and Diameter Effects)

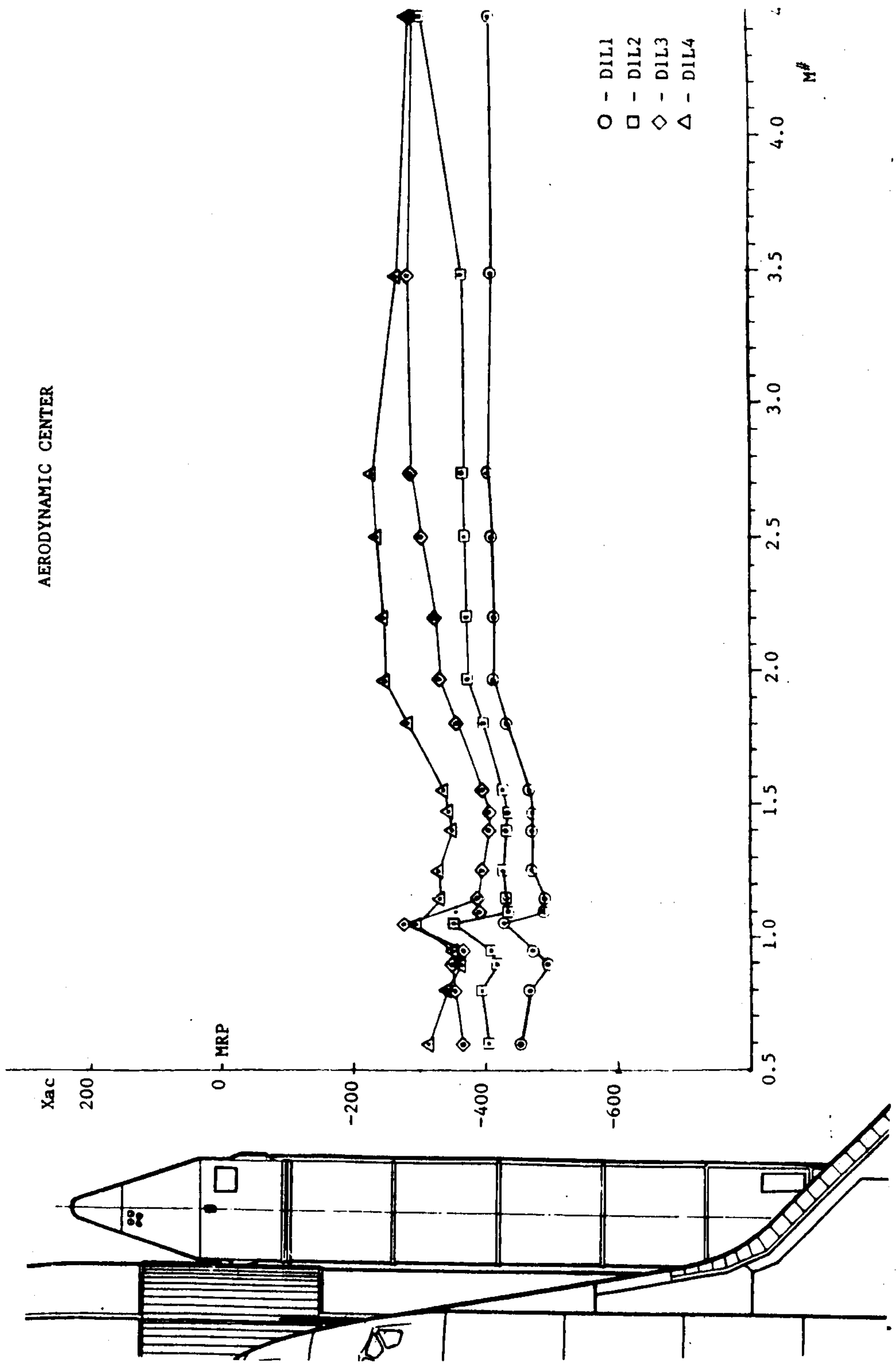

Fig. 2-28a X_{AC} vs Mach

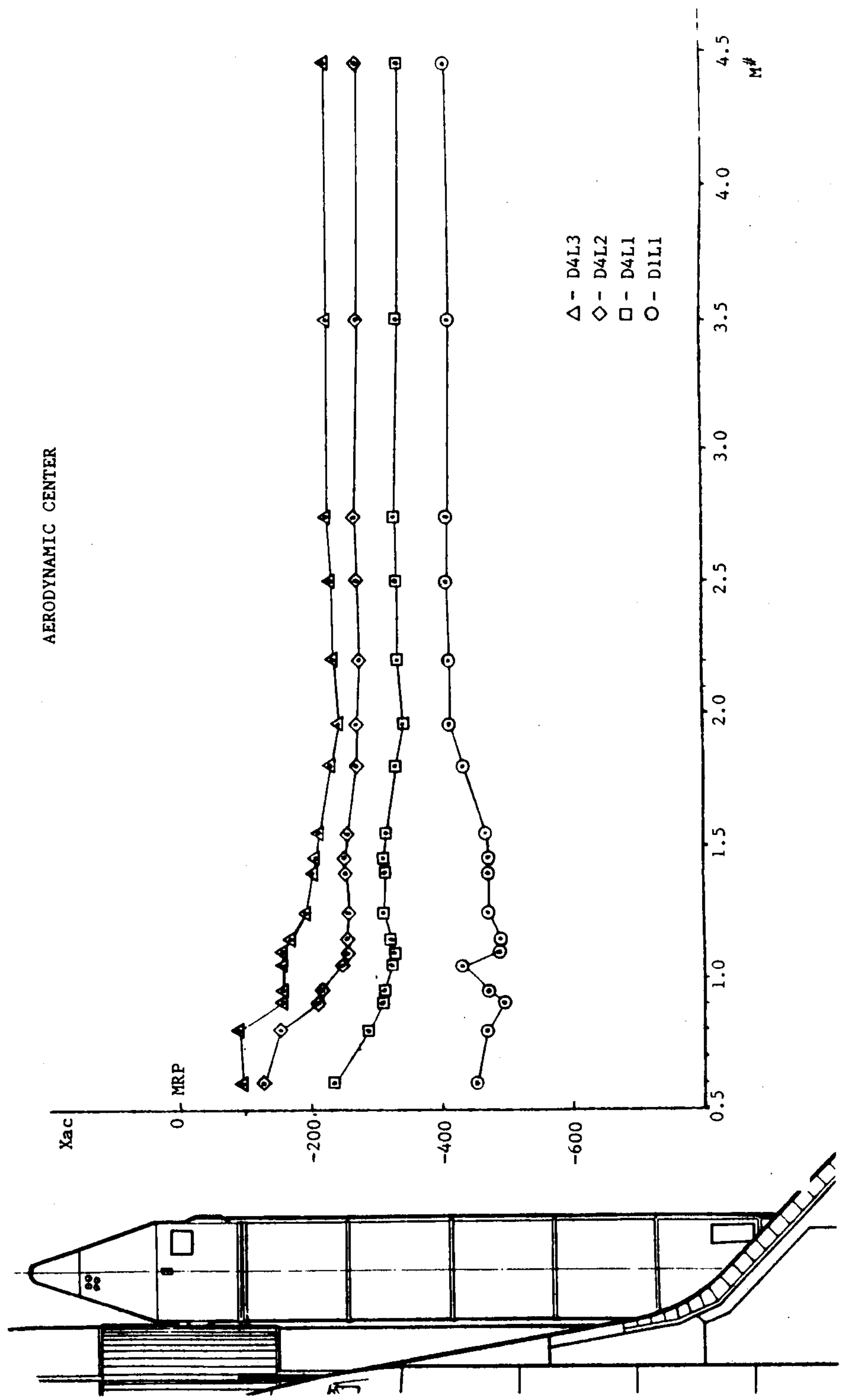

Fig. 2-28b X_{AC} vs Mach

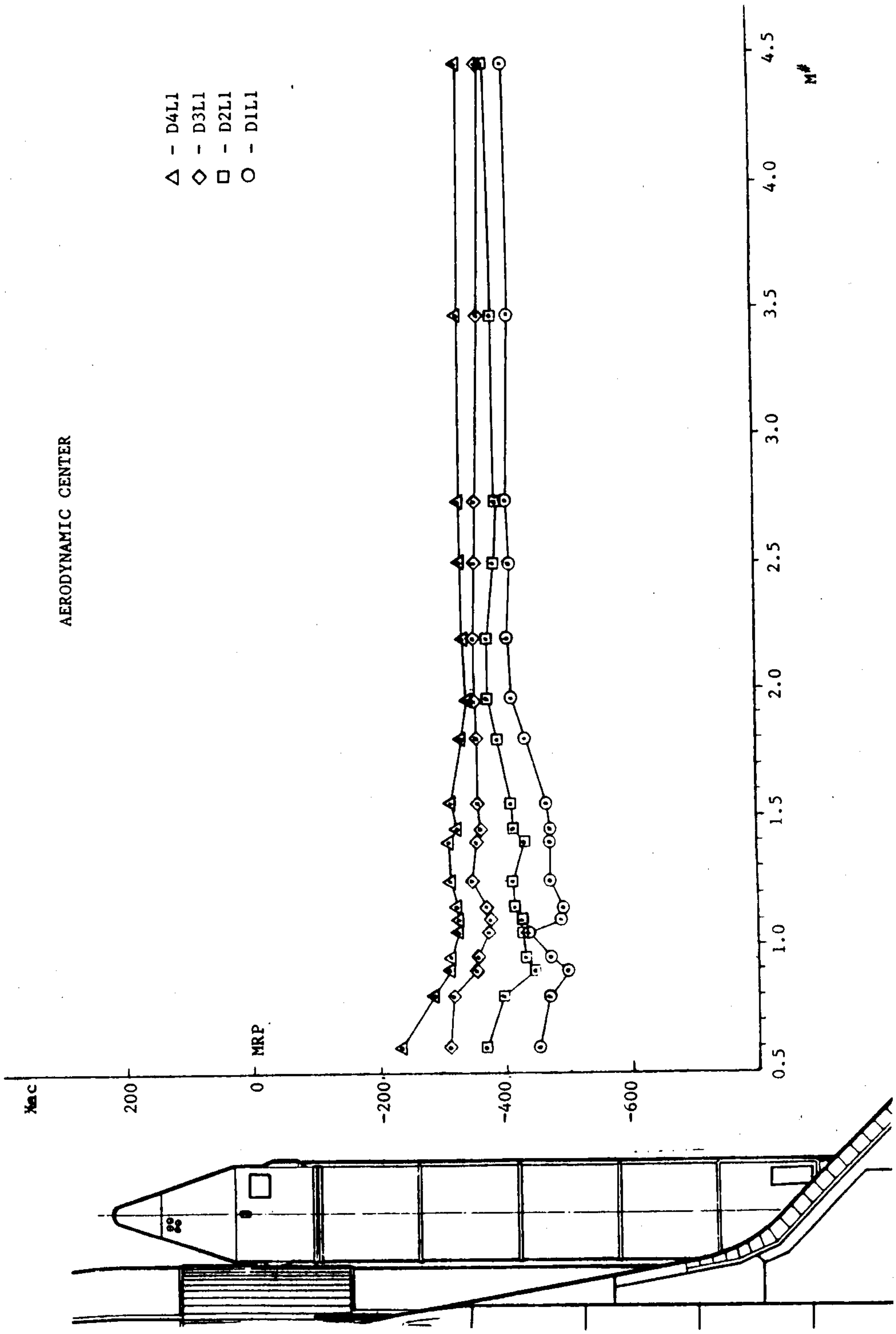

Fig. 2-28c X_{AC} vs Mach

Table 2-5 SUMMARY OF VEHICLE LONGITUDINAL EFFECTS

- AXIAL FORCE
  - C_{AF} Increases with Diameter (increased frontal area) and Length
  - Maximum C_{AF} Occurs at LRB Lengths between 170 and 180 ft.

- NORMAL FORCE
  - C_N Relatively Unaffected by Changes in Length
  - C_N Decreases (becomes more negative) with Increases in Diameter
    - Larger Nose is Partially Responsible
    - Increased Plan Form Area a Possible Contributor
  - $C_{N\alpha}$ Increases with Increase in Diameter
  - $C_{N\alpha}$ Relatively unaffected by Change in Length

- PITCHING MOMENT
  - C_M Decreases with Increase in Length
    - Caused by Forward Movement of LRB Nose
  - Increased Diameter Affects C_M as a Function of LRB Length
    - LRB Length changes Moment Arm
  - $C_{M\alpha}$ Decrease (slope becomes less negative) with Increases in Length and Diameter

- AERODYNAMIC CENTER LOCATION
  - X_{AC} moves Forward with Increases in Diameter
    - Increased loading on LRB Nose
  - X_{AC} moves Forward with Increases in Length
    - Forward movement of LRB Nose

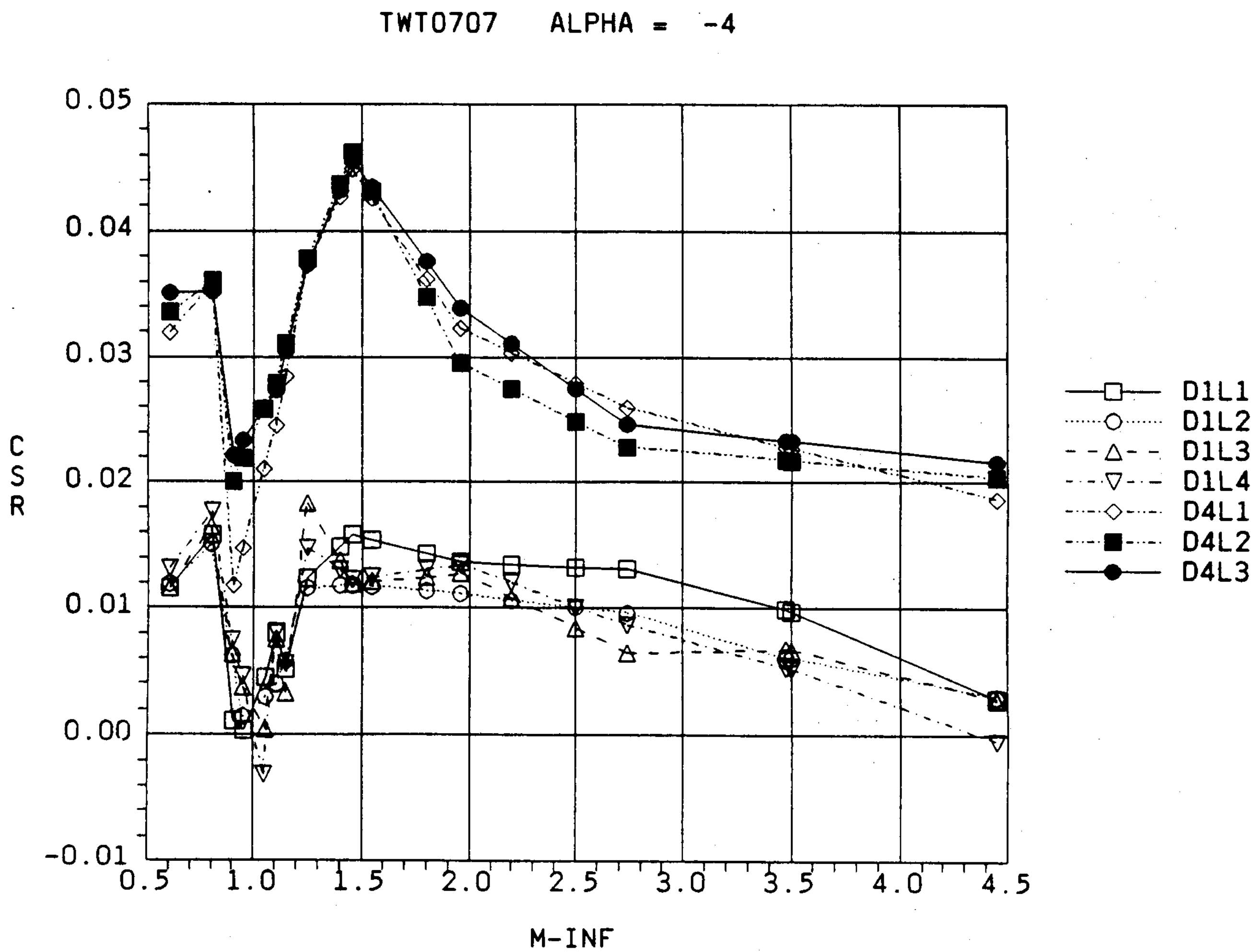

Fig. 2-29 C_{SR} vs Mach (Length and Diameter Effects)

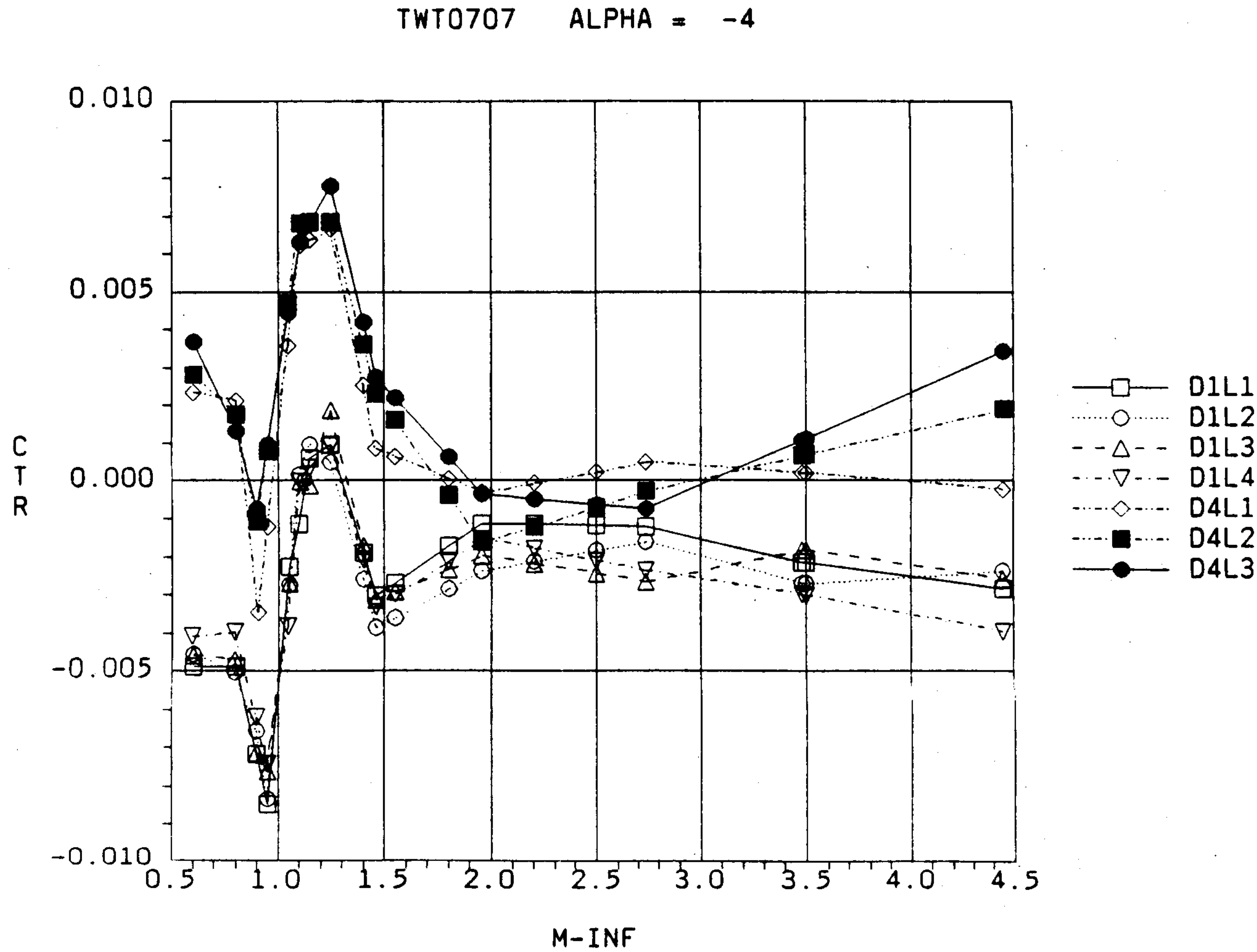

Fig. 2-30 C_{TR} vs Mach (Length and Diameter Effects)

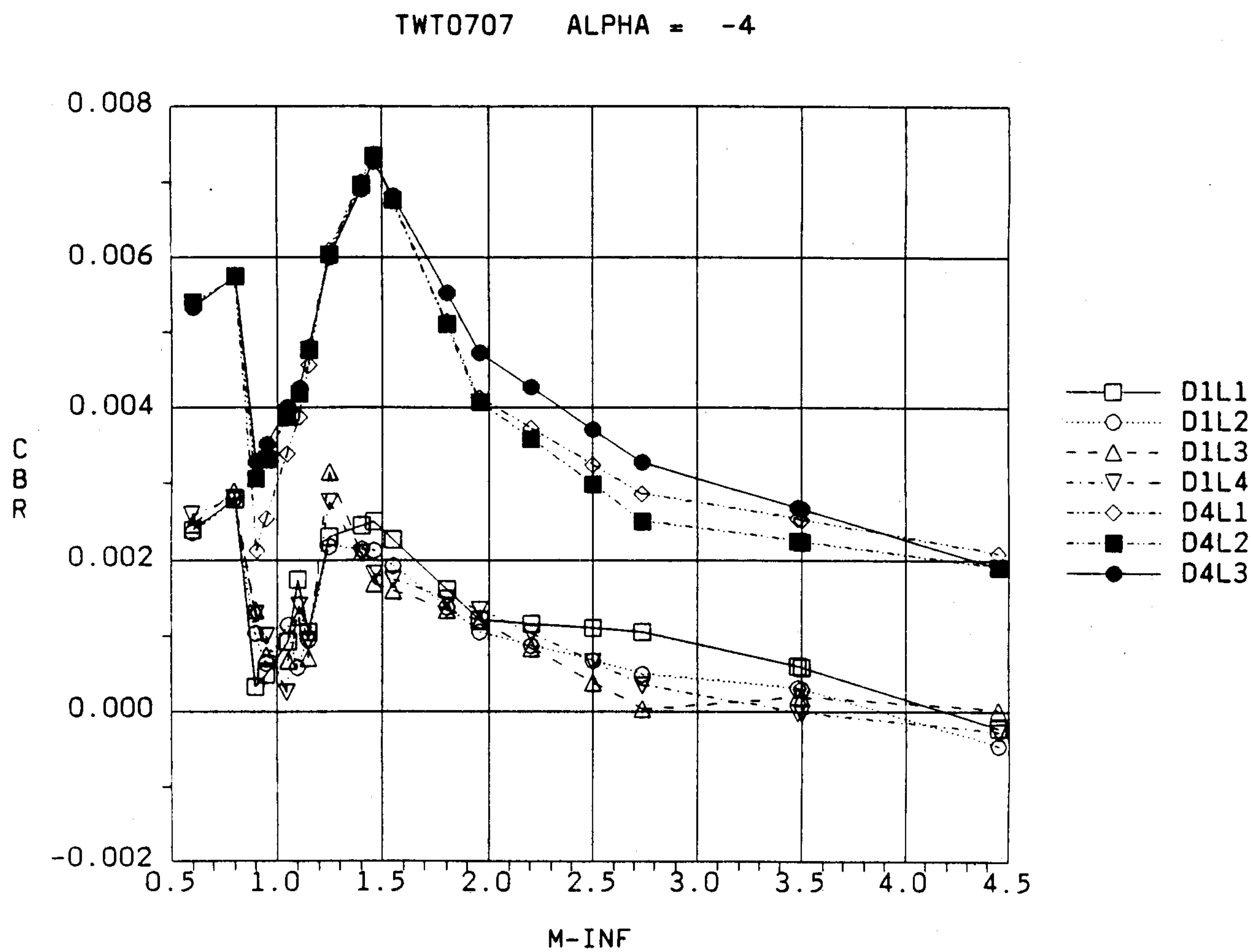

Fig. 2-31 C_{BR} vs Mach (Length and Diameter Effects)

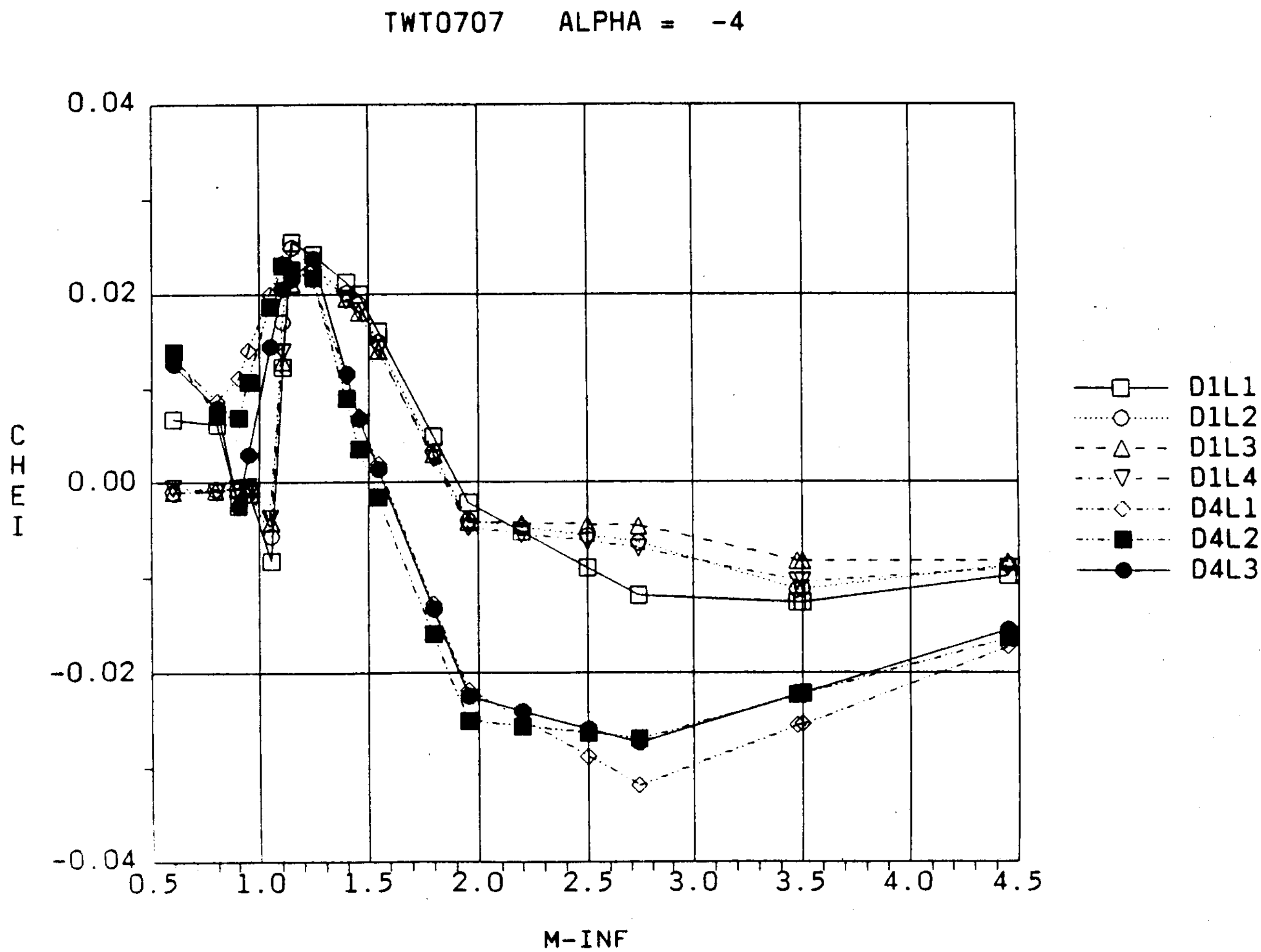

Fig. 2-32 CHEI vs Mach (Length and Diameter Effects)

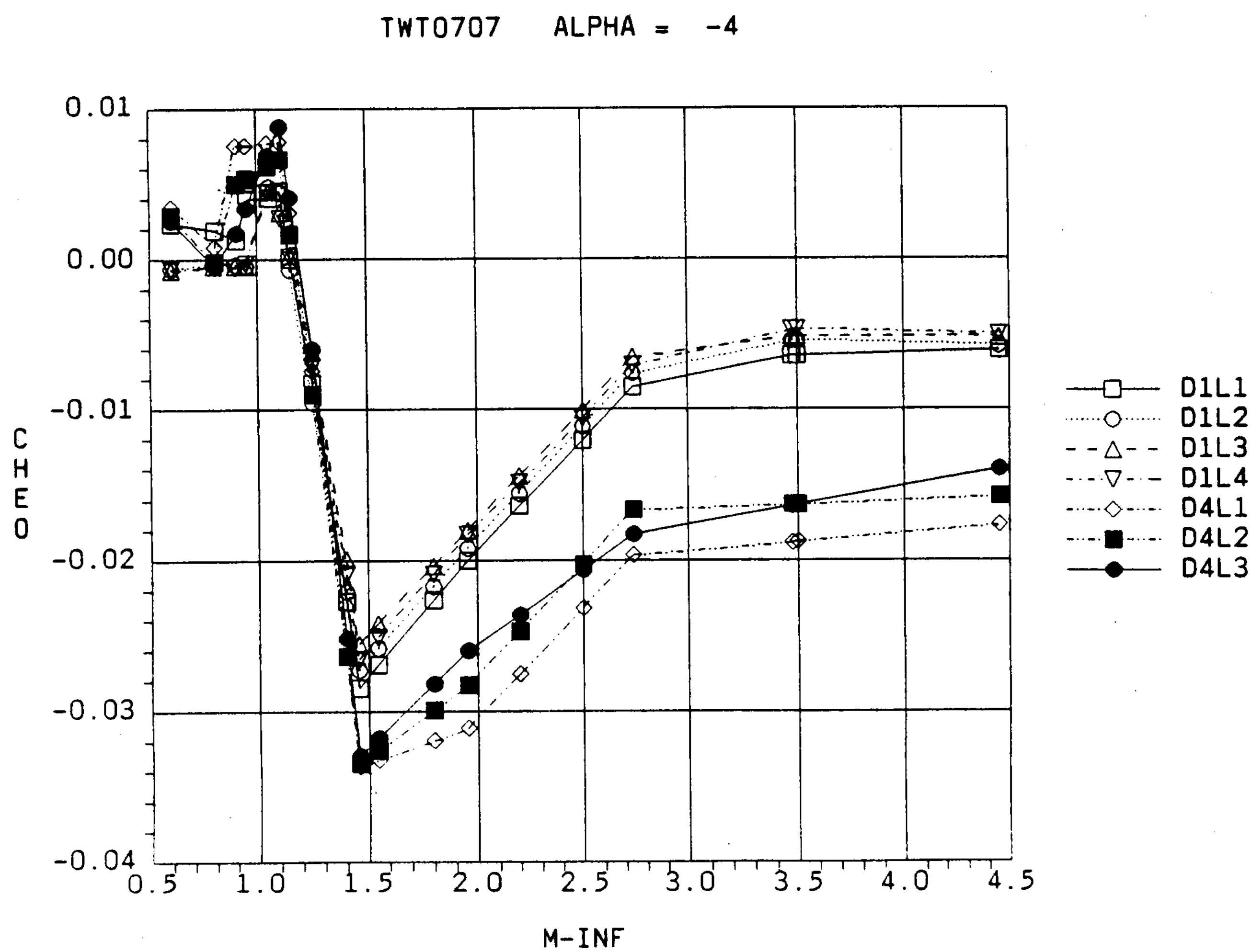

Fig. 2-33 CHEO vs Mach (Length and Diameter Effects)

3. PHASE II LIQUID ROCKET BOOSTER TESTING

The analysis of Phase I data indicated that increasing the diameter over 15 ft produced wing load levels that were unacceptable. In order to reduce the level of wing loads, various innovative configurations were designed and tested. Phase II data were the result of the wind tunnel testing for the new configurations. This section delineates the results of the Phase II configurations and a comparison between Phase I and II data.

3.1 TEST CONDITIONS AND CONFIGURATIONS

During Phase II a number of configurations were tested which included comparable Phase I designs (Fig. 3-1a), Hammerhead designs (Fig. 3-1b), a stacked booster design (Fig. 3-1c) and a rotated stack design Fig. 3-1d). Test conditions for these configurations can be found in Table 3-1.

3.2 TEST RESULTS

The majority of this section presents a comparison of Phase I and Phase II results. Therefore, most of the discussion will pertain to configurations SD12L1 and SD15. For a look at the results dealing with other configurations tested see Figs. 3-8a to 3-8i for increments vs Mach number and Figs. 3-9a to 3-9e for increments vs LRB diameter. Table 3-3 summarizes the effects of LRB diameter on increments for the hammerhead, stacked, and rotated stack configurations.

3.3 PHASE I AND II COMPARISONS

Comparison between Phase I and Phase II LRB wind tunnel test data revealed discrepancies in the incremental data of identical configurations at transonic Mach numbers. Through analysis it was determined that the cause of the differences was bad baseline data obtained during Phase I testing.

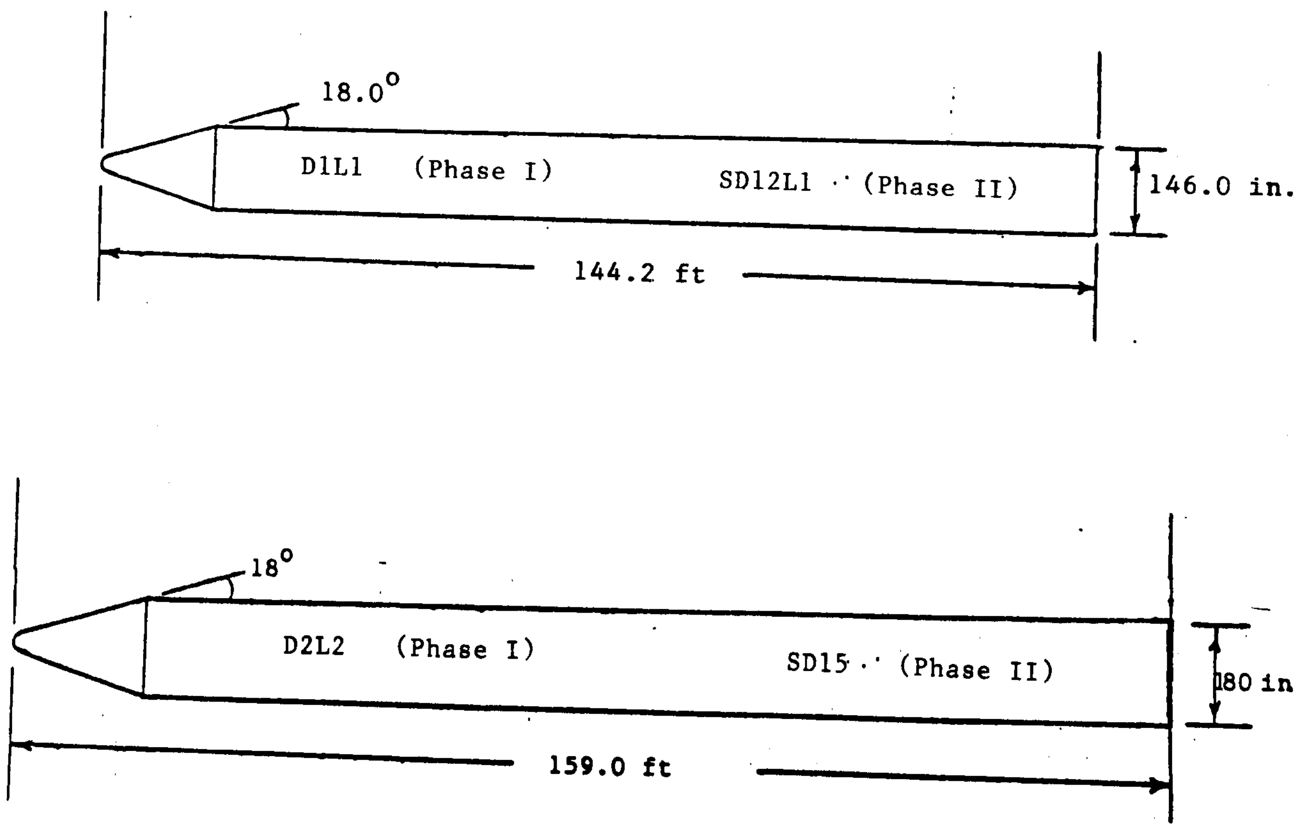

Fig. 3-1a Phase II Configurations (Phase I Comparison)

ORIGINAL PAGE IS
OF POOR QUALITY

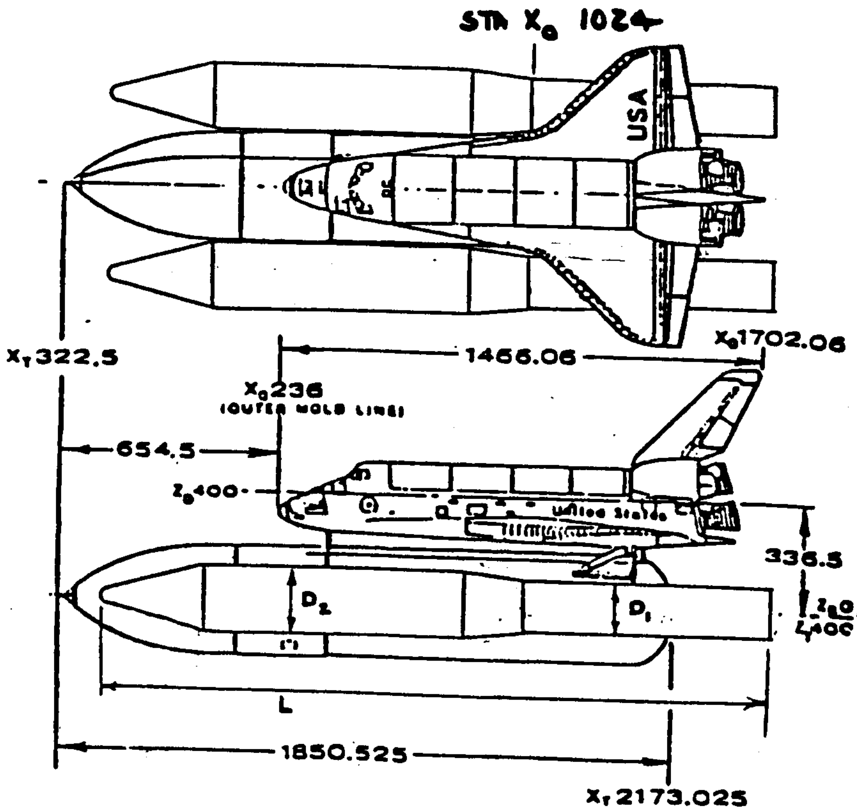

D_1 = 12.2 ft

D_2 = 15.0, 18.0 ft

L = 159 ft

Fig. 3-1b Phase II Configuration (MDXXXX Runs)

ORIGINAL PAGE IS
OF POOR QUALITY

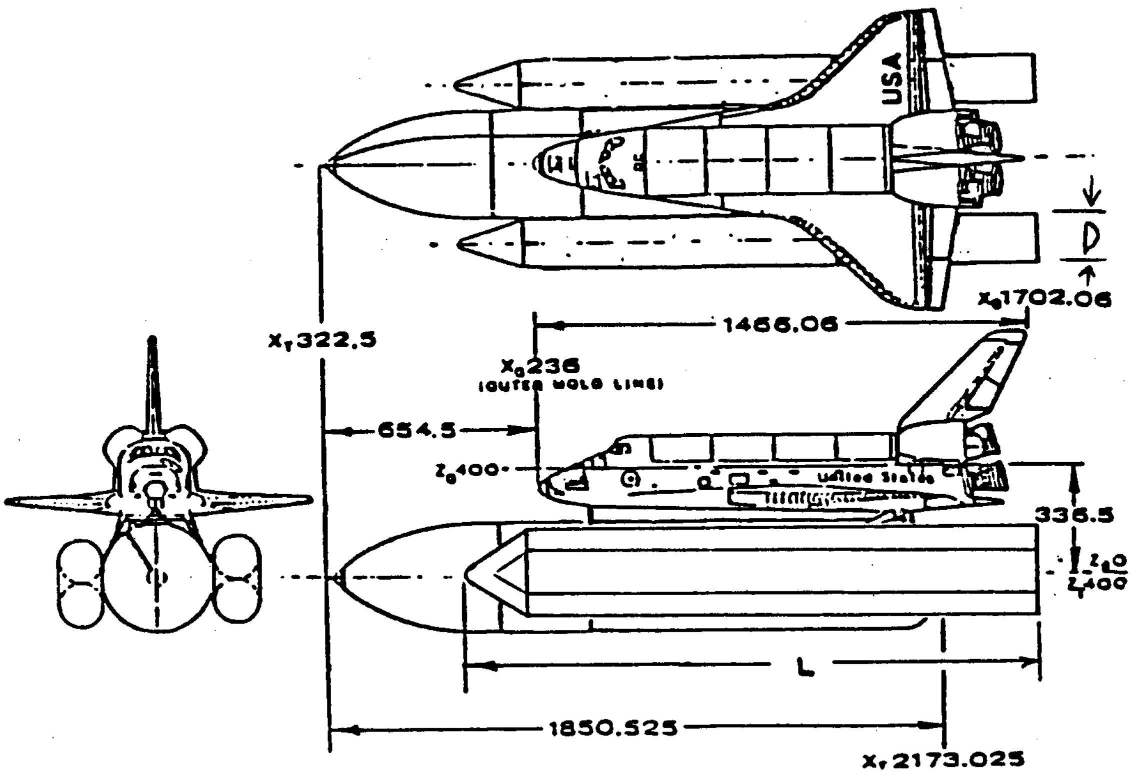

D = 12.2 ft

L = 159 ft

Fig. 3-1c Phase II Configuration (STXXXX Runs)

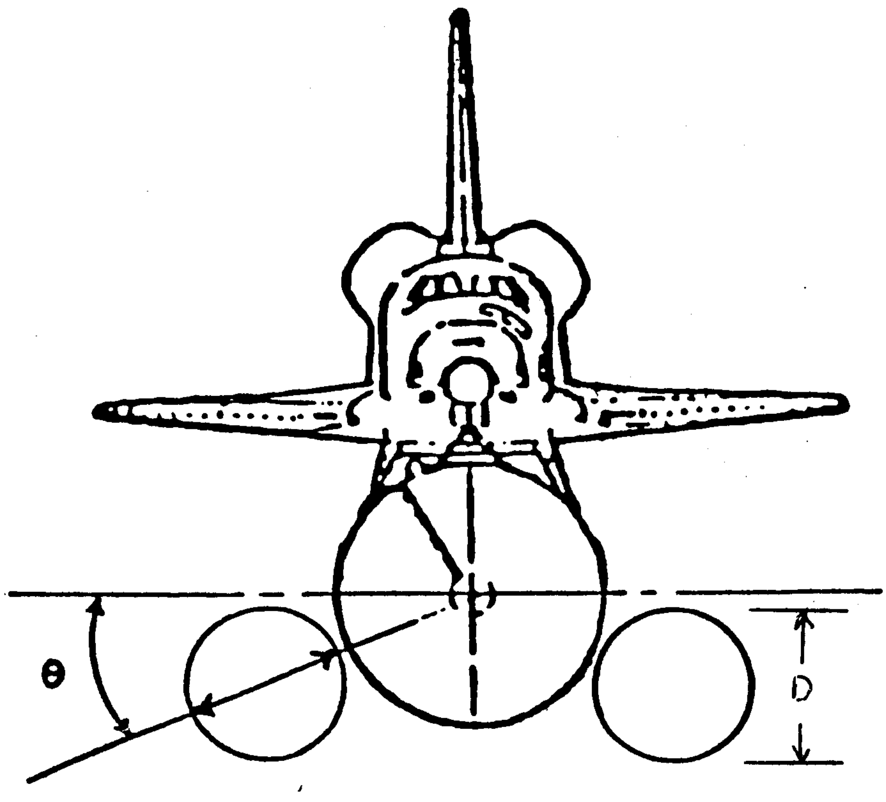

D = 15 ft

Θ = 3.6, 7.0, 10.0 deg.

Fig. 3-1d Phase II Configuration (OSXX Runs)

ORIGINAL PAGE IS
OF POOR QUALITY

Table 3-1 MATRIX OF DATA FILES USED TO GENERATE PHASE II DATA

TWT0711 LRB WIND TUNNEL DATA FILES

MACH/ CONFIG	0.60	0.80	0.90	0.95	1.05	1.10	1.15	1.25	1.46	1.96	2.74	3.48	4.45
SSLV-SD15	TWT001	TWT002	TWT003	TWT004	TWT005	TWT006	TWT007	TWT008	TWT009	TWT010	TWT011	TWT012	TWT013
SSLV-MD15	TWT014	TWT015	TWT016	TWT017	TWT018	TWT019	TWT020	TWT021	TWT022	TWT023	TWT024	TWT025	TWT026
SSLV-MD18	TWT027	TWT028	TWT029	TWT030	TWT031	TWT032	TWT033	TWT034	TWT035	TWT036	TWT037	TWT038	TWT039
SSLV-OS3	TWT053	TWT054	TWT055	TWT056	TWT057	TWT058	TWT059	TWT060	TWT061	TWT062	TWT063	TWT064	TWT065
SSLV-OS7	TWT066	TWT067	TWT068	TWT069	TWT070	TWT071	TWT072	TWT073	TWT074	TWT075	TWT076	TWT077	TWT078
SSLV-OS10	TWT079	TWT080	TWT081	TWT082	TWT083	TWT084	TWT085	TWT086	TWT087	TWT088	TWT089	TWT090	TWT091
SSLV-ST10	TWT092	TWT093	TWT094	TWT095	TWT096	TWT097	TWT098	TWT099	TWT100	TWT101	TWT102	TWT103	TWT104
SSLV-ST120S	TWT105	TWT106	TWT107	TWT108	TWT109	TWT110	TWT111	TWT112	TWT113	TWT114	TWT115	TWT116	TWT117
SSLV-SD12L1	TWT118	TWT119	TWT120	TWT121	TWT122	TWT123	TWT124	TWT125	TWT126	TWT127	TWT128	TWT129	TWT130

This section discusses the analysis performed to determine the validity of both sets of data. The conclusions and recommendations resulting from this analysis are presented at the end of the section.

3.3.1 Data Analysis

Figure 3-2 represents a sketch of the configurations for which data were obtained during Phase I tests. Table 3-2 provides the Phase I test matrix for wind tunnel tests. In order to distinguish between the Phase I and Phase II test data of identical configurations different nomenclatures were used. Similarly, SD12L1 represents the D1L1 (baseline) configuration. It is important to note that all coefficient data have been interpolated to even angles of attack. No data were generated by interpolating between test Mach numbers.

Comparisons between Phase I and Phase II incremental data are presented in Figs. 3.3a through 3.4f for the D2L2/SD15 configuration. The agreement between CNF, CMF, CSR, and CBR data is reasonably good except at the transonic Mach numbers of 1.10 and 1.25. The CAF and CTR data are in good agreement over the entire Mach number range.

Shown in Figs. 3.4a through 3.4f are comparisons between Phase I and Phase II total data obtained for the D2L2/SD15 configuration for Mach numbers ranging from 0.6 to 1.46. The agreement between the two sets of data is quite good for all coefficients. Figures 3.5a through 3.5f compare Phase I and Phase II total data obtained for the D1L1/ SD12L1 configuration. All of the data at Mach numbers less than 1.10 agree reasonably well. Additionally, CAF and CTR data continue to agree well throughout the entire transonic Mach number range. At Mach numbers ranging between 1.10 and 1.25, there is considerable difference between Phase I and Phase II results for CNF, CMF, CSR, and CBR.

From the data comparisons made thus far, it is clear that the cause of differences seen between the Phase I and Phase II incremental data is invalid baseline (D1L1/SD12L1) data. The problem now is to determine which set of data is incorrect.

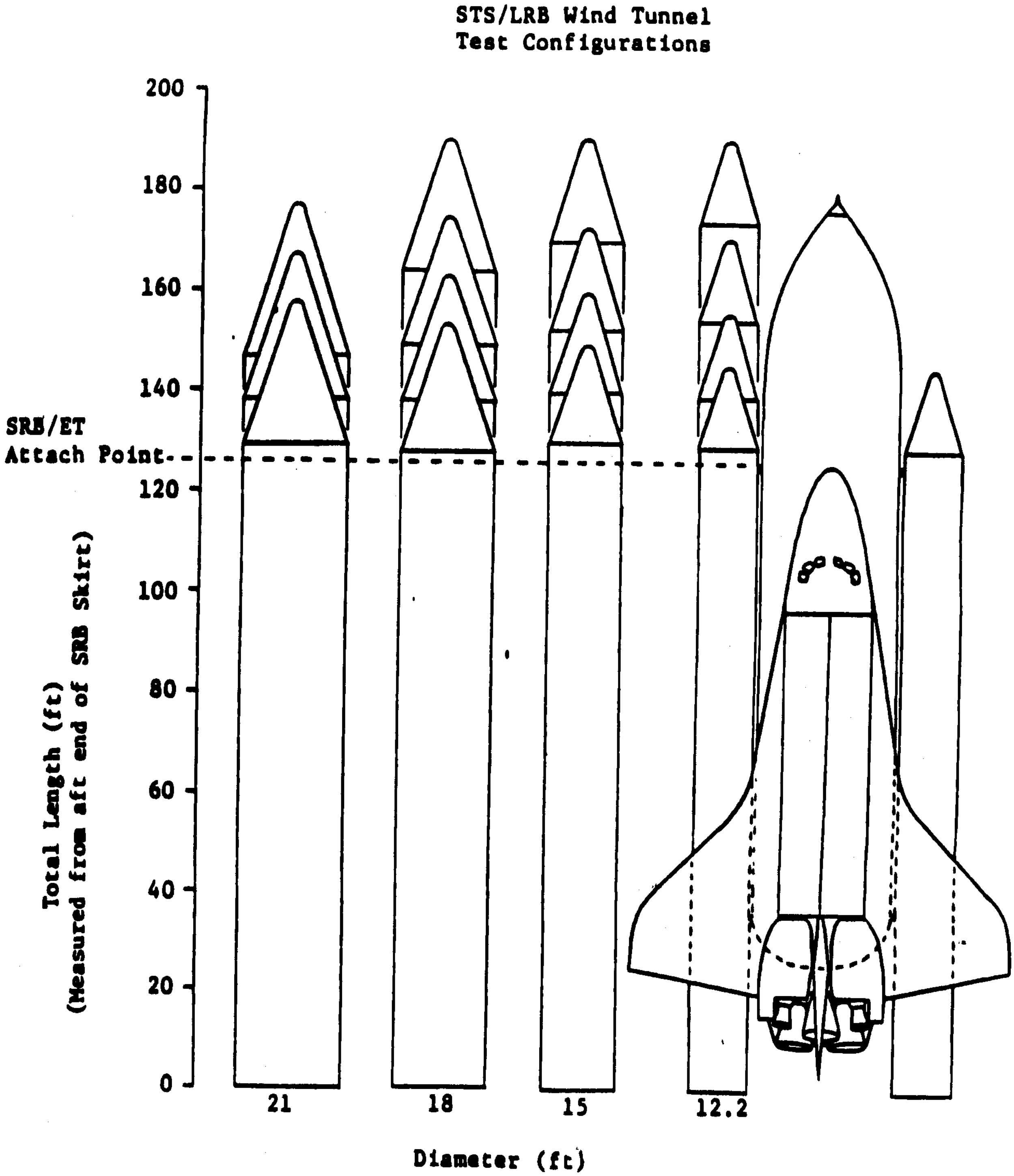

Fig. 3-2 Phase I LRB Wind Tunnel Test Configurations

Table 3-2 **MATRIX OF DATA FILES USED TO GENERATE THE PHASE I LRB INCREMENTAL DATA**

TWT0707 LRB WIND TUNNEL DATA FILES

MACH # CONFIG.	0.60	0.80	0.90	0.95	1.05	1.10	1.15	1.25	1.40	1.46	1.55	1.80	1.96	2.20	2.50	2.74	3.48	3.50	4.45
D1L1	TWT013	TWT017	TWT021	TWT025	TWT029	TWT033	TWT037	TWT041	*TWT197	TWT045	*TWT212	*TWT227	TWT049	*TWT242	*TWT257	TWT053	TWT057	*TWT283	TWT061
L2	TWT014	TWT018	TWT022	TWT026	TWT030	TWT034	TWT038	TWT042	*TWT198	TWT046	*TWT213	*TWT228	TWT050	*TWT243	*TWT258	TWT054	TWT058	*TWT284	TWT062
L3	TWT015	TWT019	TWT023	TWT027	TWT031	TWT035	TWT039	TWT043	*TWT199	TWT047	*TWT214	*TWT229	TWT051	*TWT244	*TWT259	TWT055	TWT059	*TWT285	TWT063
L4	TWT016	TWT020	TWT024	TWT028	TWT032	TWT036	TWT040	TWT044	*TWT200	TWT048	*TWT215	*TWT230	TWT052	*TWT245	*TWT260	TWT056	TWT060	*TWT286	TWT064
D2L1	TWT097	TWT093	TWT089	*TWT164	*TWT175	TWT085	*TWT186	TWT081	*TWT201	TWT077	*TWT216	*TWT231	TWT073	*TWT246	*TWT261	TWT069	*TWT272	*TWT287	TWT065
L2	TWT098	TWT094	TWT090	*TWT165	*TWT176	TWT086	*TWT187	TWT082	*TWT202	TWT078	*TWT217	*TWT232	TWT074	*TWT247	*TWT262	TWT070	*TWT273	*TWT288	TWT066
L3	TWT099	TWT095	TWT091	*TWT166	*TWT177	TWT087	*TWT188	TWT083	*TWT203	TWT079	*TWT218	*TWT233	TWT075	*TWT248	*TWT263	TWT071	*TWT274	*TWT289	TWT067
L4	TWT100	TWT096	TWT092	*TWT167	*TWT178	TWT088	*TWT189	TWT084	*TWT204	TWT080	*TWT219	*TWT234	TWT076	*TWT249	*TWT264	TWT072	*TWT275	*TWT290	TWT068
D3L1	TWT101	TWT105	TWT109	*TWT168	*TWT179	TWT113	*TWT190	TWT117	*TWT205	TWT121	*TWT220	*TWT235	TWT125	*TWT250	*TWT265	TWT129	*TWT276	*TWT291	TWT133
L2	TWT102	TWT106	TWT110	*TWT169	*TWT180	TWT114	*TWT191	TWT118	*TWT206	TWT122	*TWT221	*TWT236	TWT126	*TWT251	*TWT266	TWT130	*TWT277	*TWT292	TWT134
L3	TWT103	TWT107	TWT111	*TWT170	*TWT181	TWT115	*TWT192	TWT119	*TWT207	TWT123	*TWT222	*TWT237	TWT127	*TWT252	*TWT267	TWT131	*TWT278	*TWT293	TWT135
L4	TWT104	TWT108	TWT112	*TWT171	*TWT182	TWT116	*TWT193	TWT120	*TWT208	TWT124	*TWT223	*TWT238	TWT128	*TWT253	*TWT268	TWT132	*TWT279	*TWT294	TWT136
D4L1	TWT161	TWT158	TWT155	*TWT172	*TWT183	TWT152	*TWT194	TWT149	*TWT209	TWT146	*TWT224	*TWT239	TWT143	*TWT254	*TWT269	TWT140	*TWT280	*TWT295	TWT137
L2	TWT162	TWT159	TWT156	*TWT173	*TWT184	TWT153	*TWT195	TWT150	*TWT210	TWT147	*TWT225	*TWT240	TWT144	*TWT255	*TWT270	TWT141	*TWT281	*TWT296	TWT138
L3	TWT163	TWT160	TWT157	*TWT174	*TWT185	TWT154	*TWT196	TWT151	*TWT211	TWT148	*TWT226	*TWT241	TWT145	*TWT256	*TWT271	TWT142	*TWT282	*TWT297	TWT139

* - INTERPOLATED

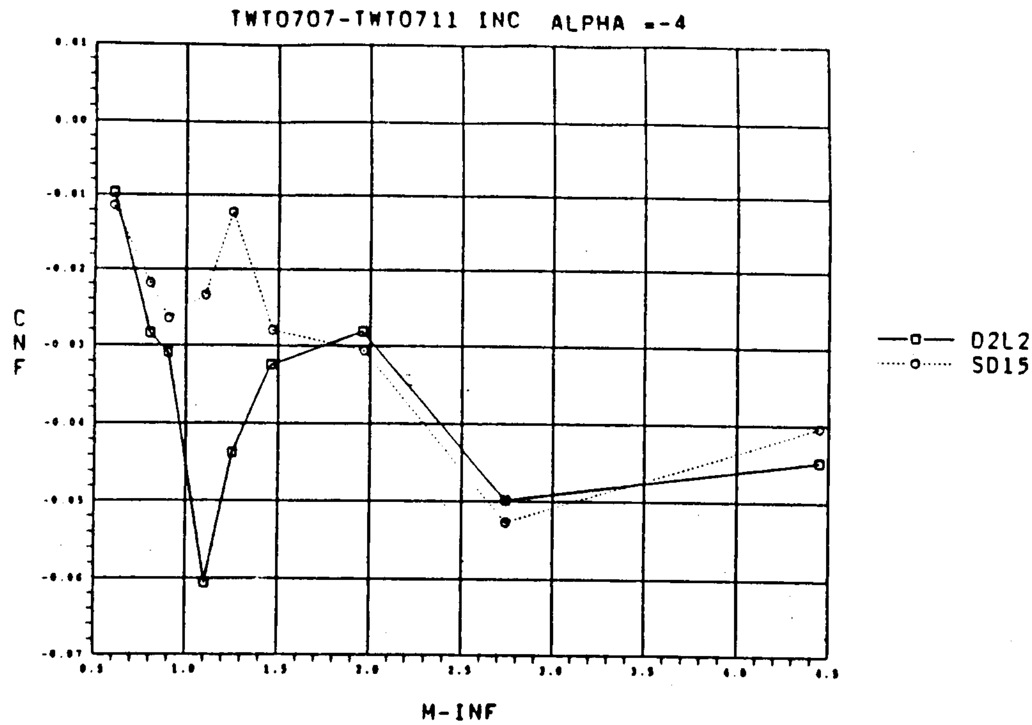

a. CNF; α = -4

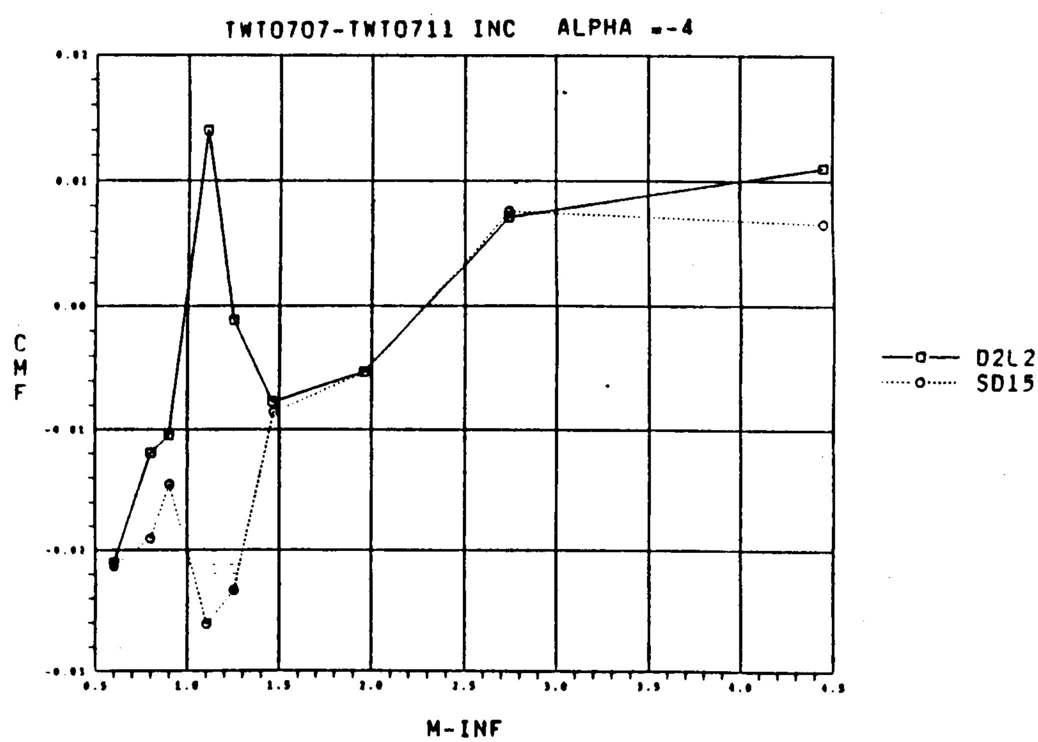

b. CMF; α = -4

Fig. 3-3 Phase I/Phase II Incremental Data, D2L2/SD15 Configuration

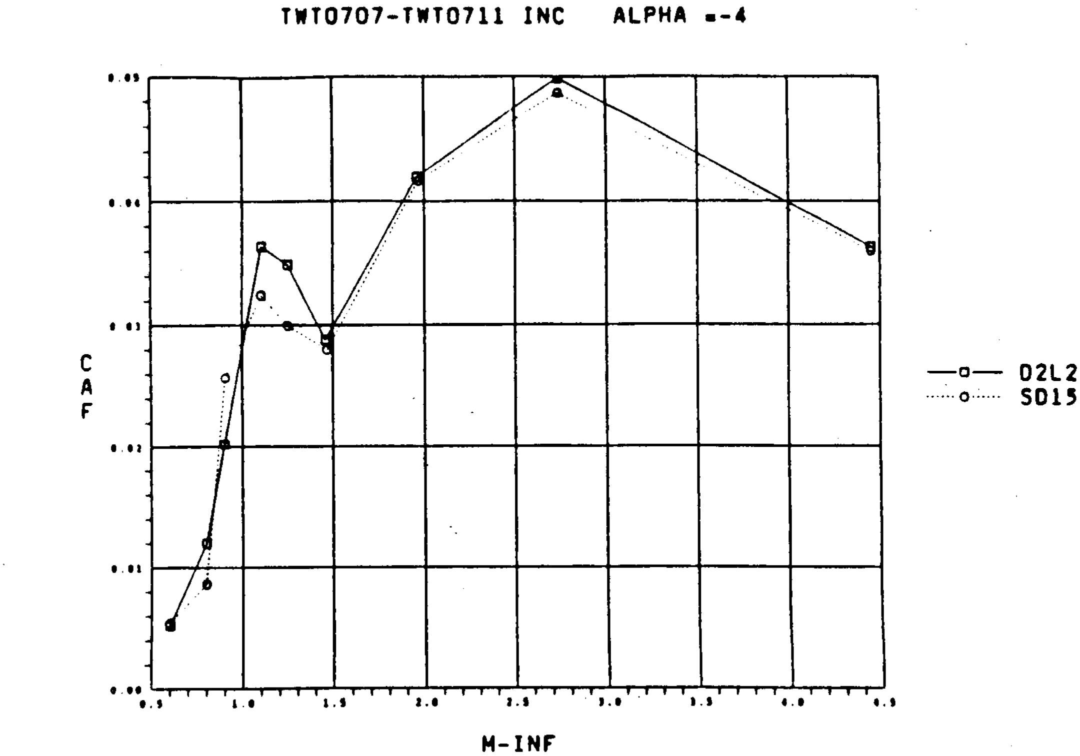

c. CAF; α = -4

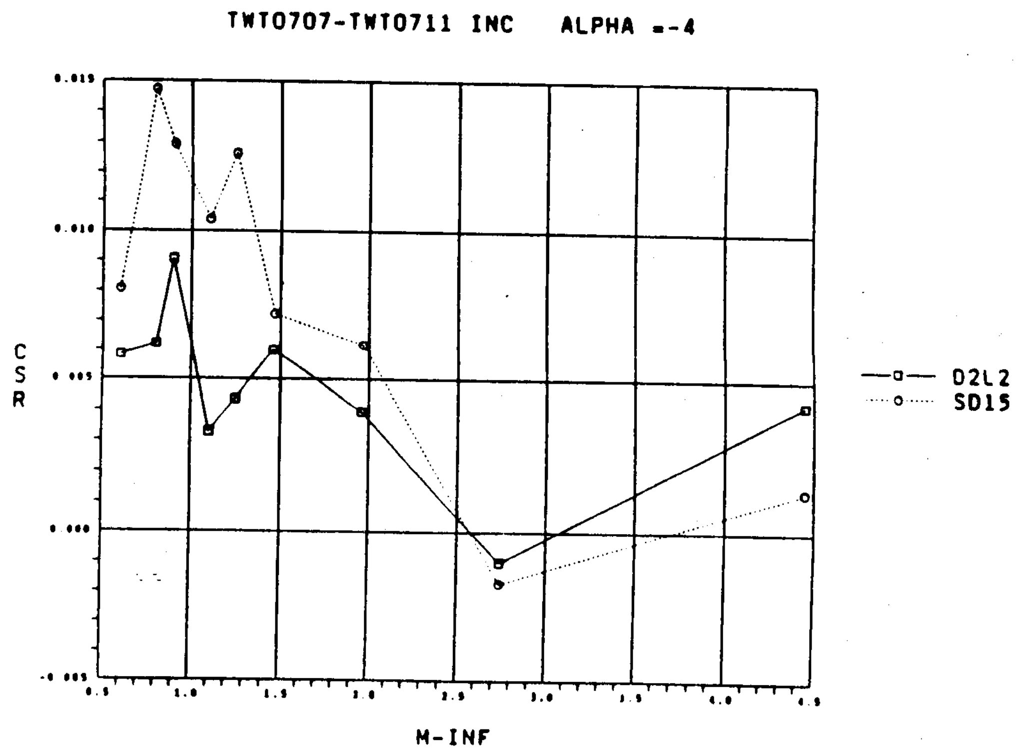

d. CSR; α = -4

Fig. 3-3 Phase I/Phase II Incremental Data, D2L2/SD15 Configuration (Continued)

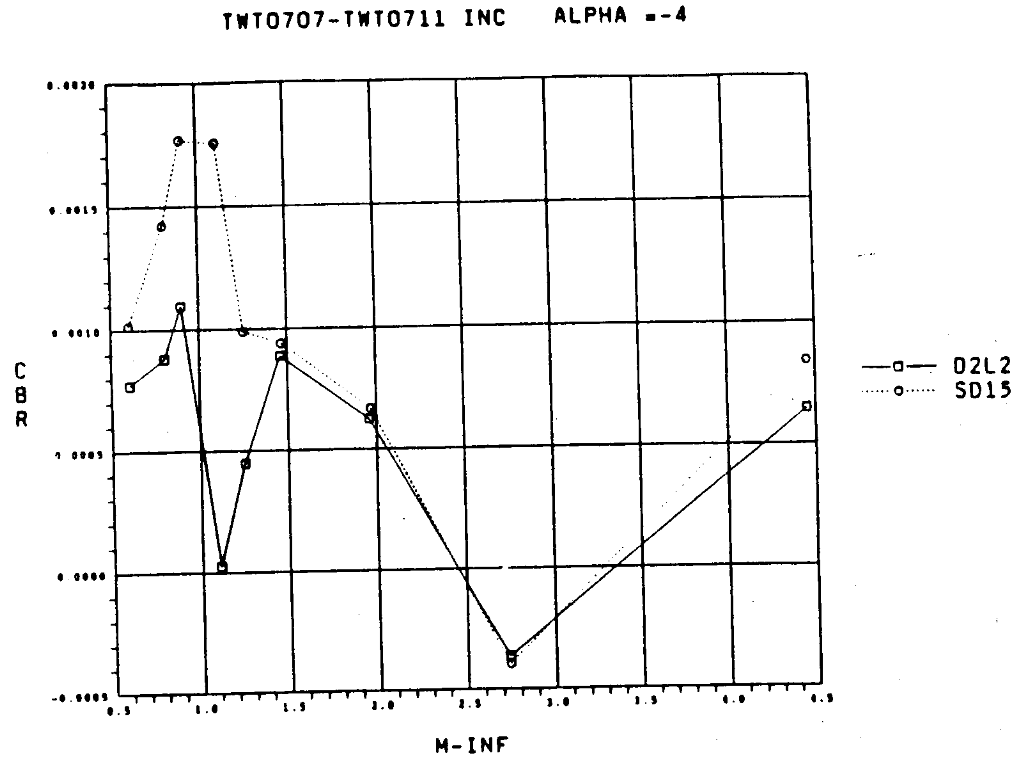

e. CBR; α = -4

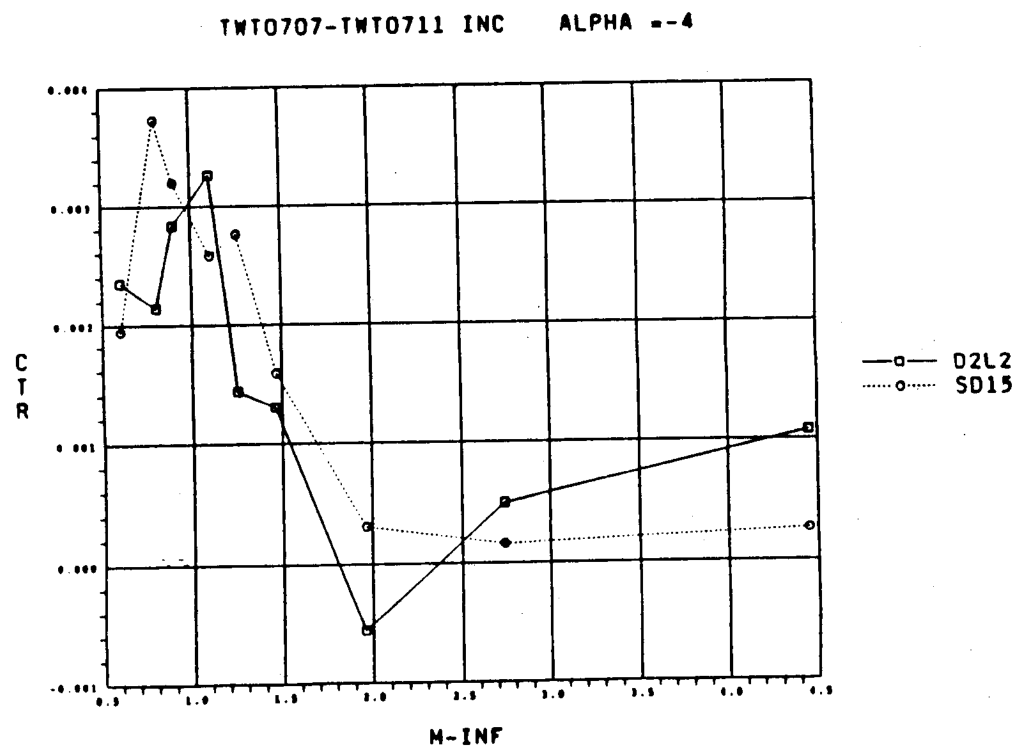

f. CTR; α = -4

Fig. 3-3 Phase I/Phase II Incremental Data, D2L2/SD15 Configuration (Concluded)

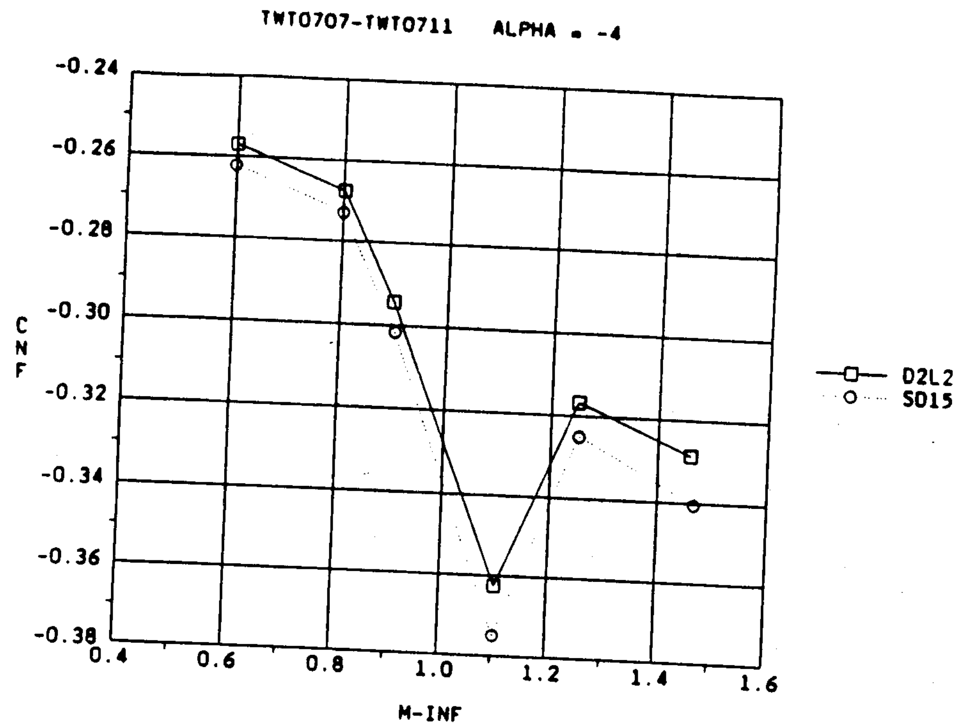

a. CNF; α = -4

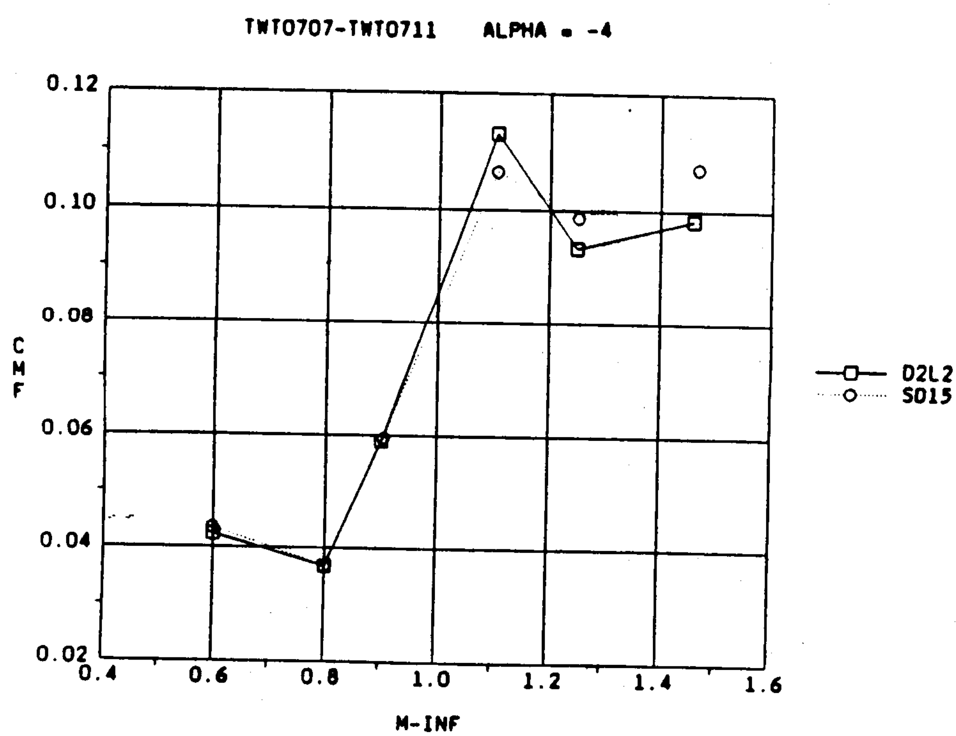

b. CMF; α = -4

Fig. 3-4 Phase I/Phase II Total Data Comparison, D2L2/SD15 Configuration

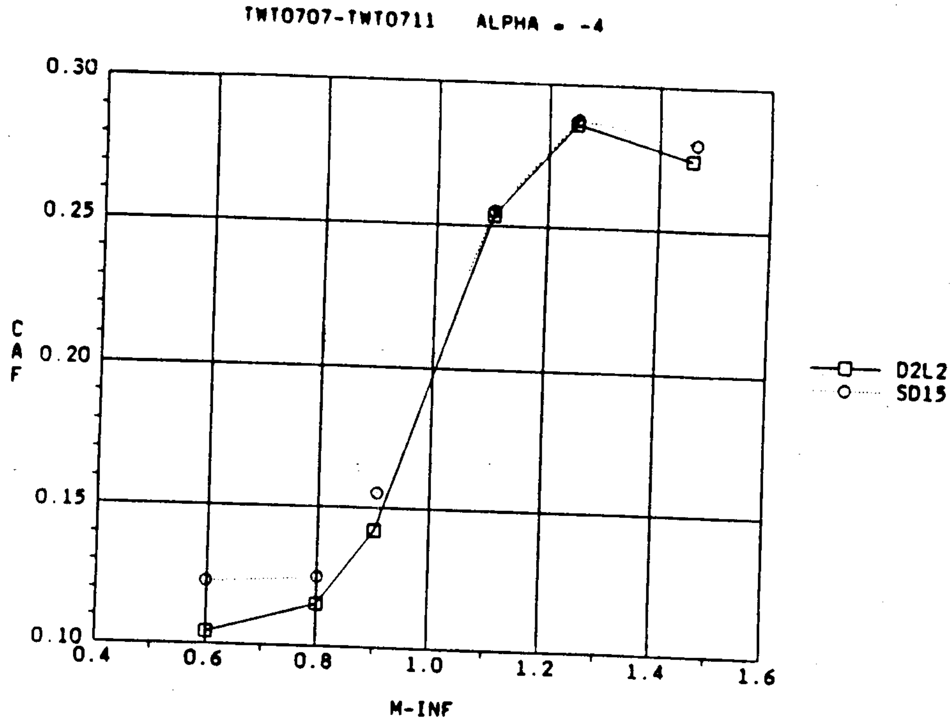

c. CAF; α = -4

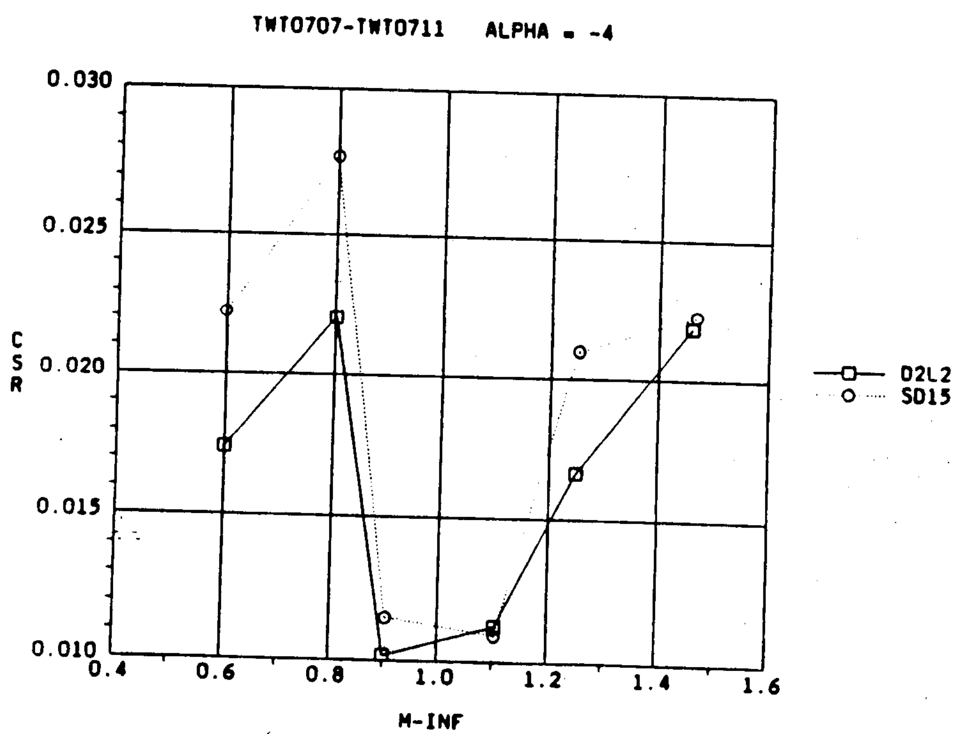

d. CSR; α = -4

Fig. 3-4 Phase I/Phase II Total Data Comparison, D2L2/SD15 Configuration (Continued)

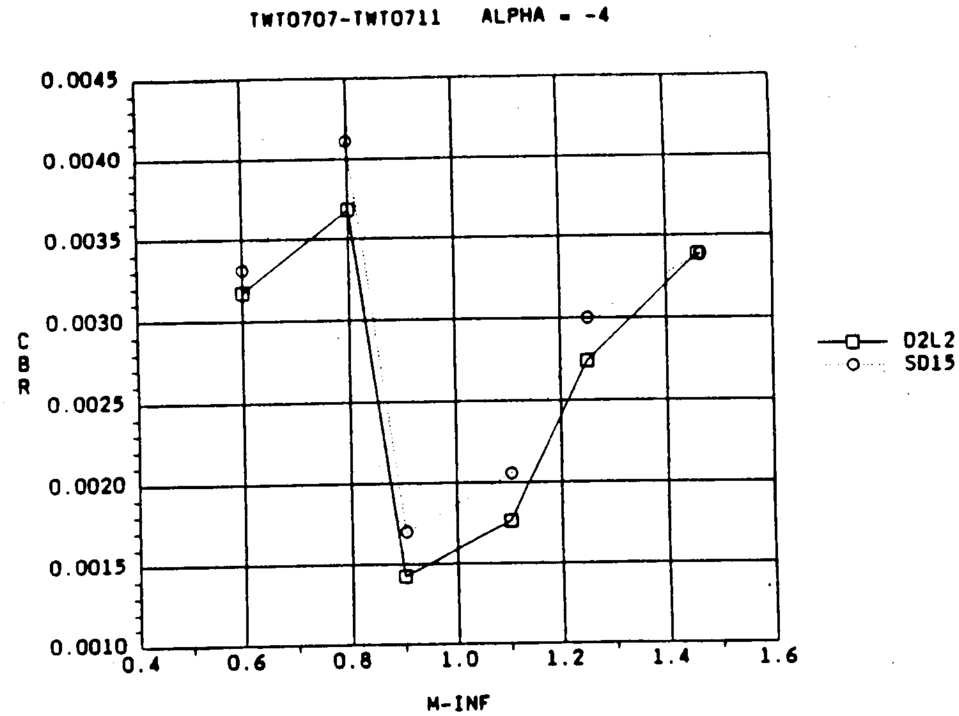

e. CBR; α = -4

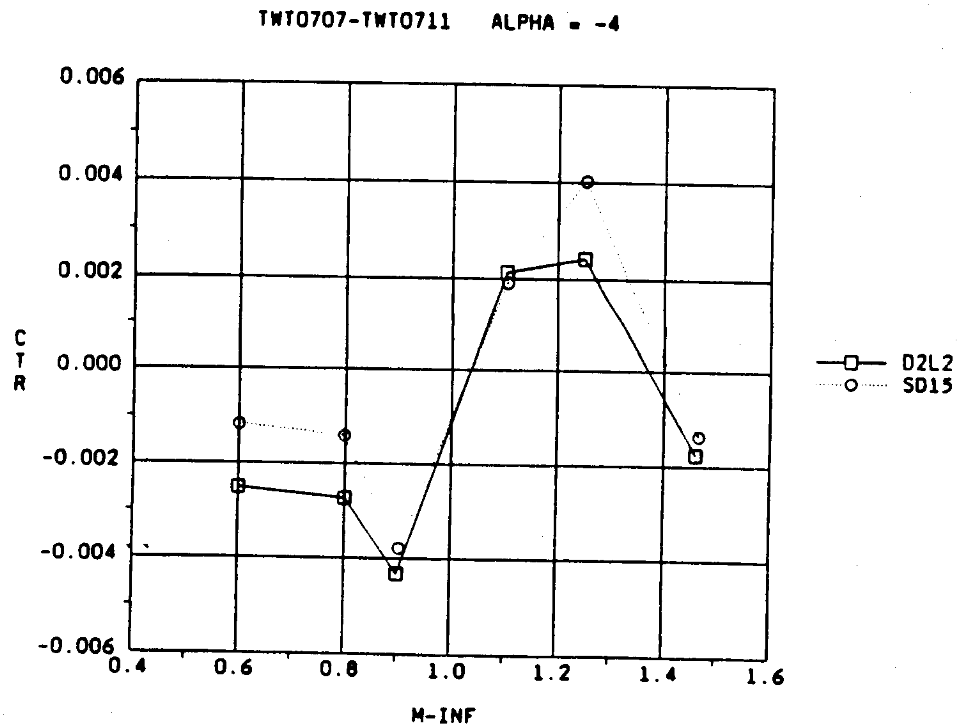

f. CTR; α = -4

Fig. 3-4 Phase I/Phase II Total Data Comparison, D2L2/SD15 Configuration (Concluded)

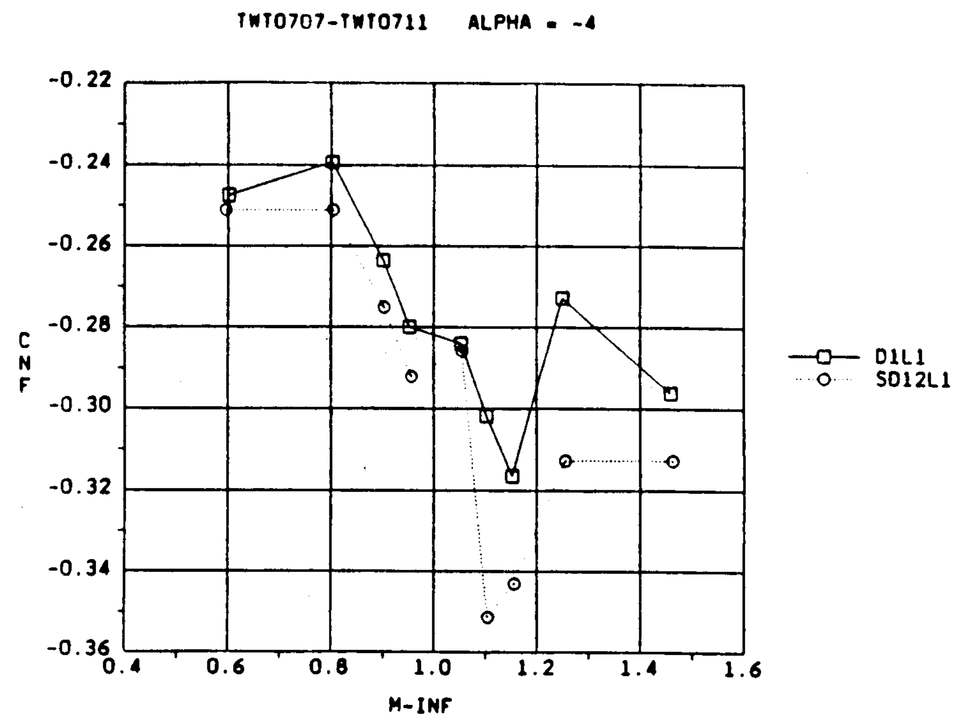

a. CNF; α = -4

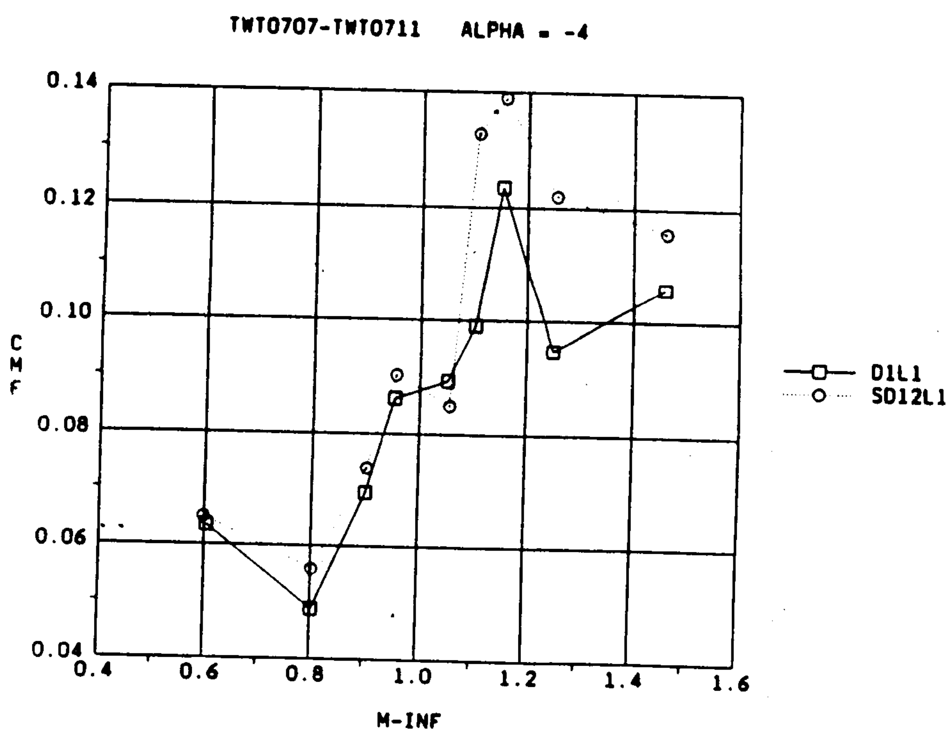

b. CMF; α = -4

Fig. 3-5 Phase I/Phase II Total Data Comparison, D1L1/SD12L1 Configuration

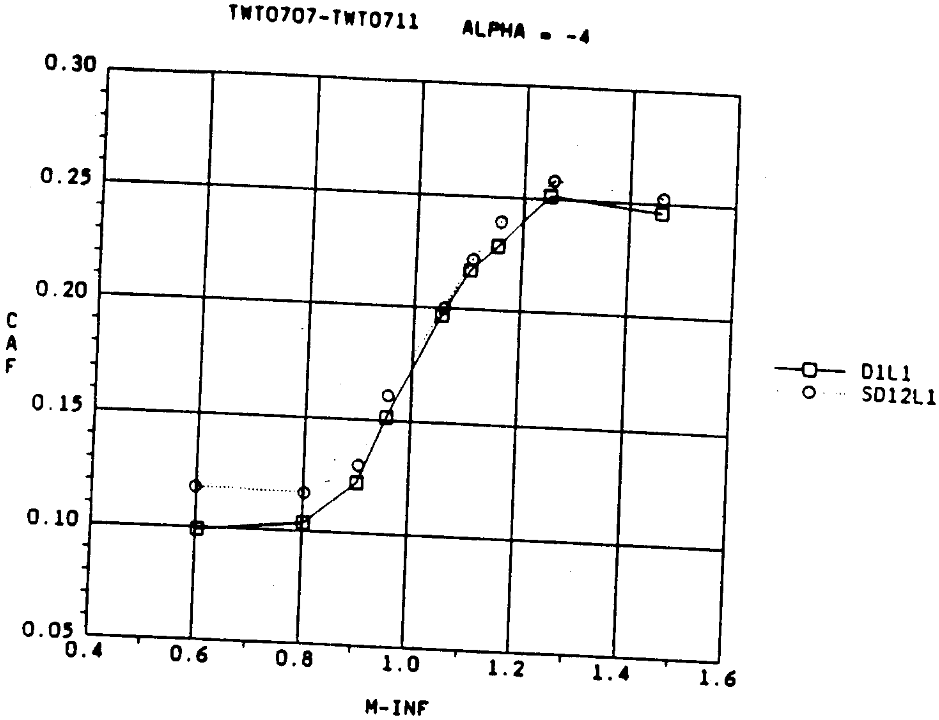

c. CAF; α = −4

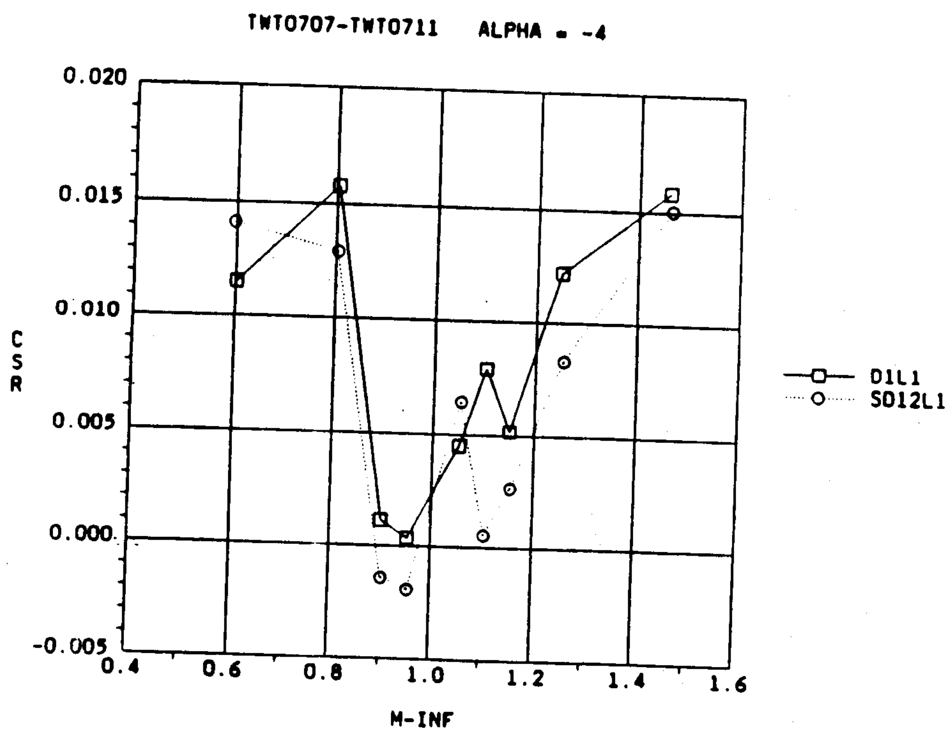

d. CSR; α = −4

Fig. 3-5 Phase I/Phase II Total Data Comparison, D1L1/SD12L1 Configuration (Continued)

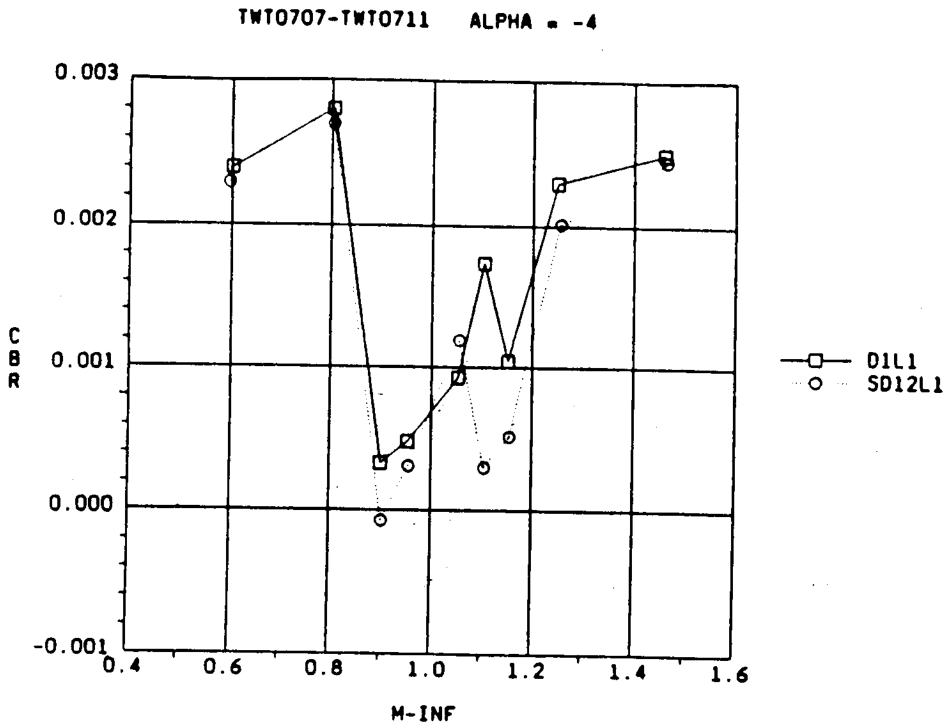

e. CBR; α = -4

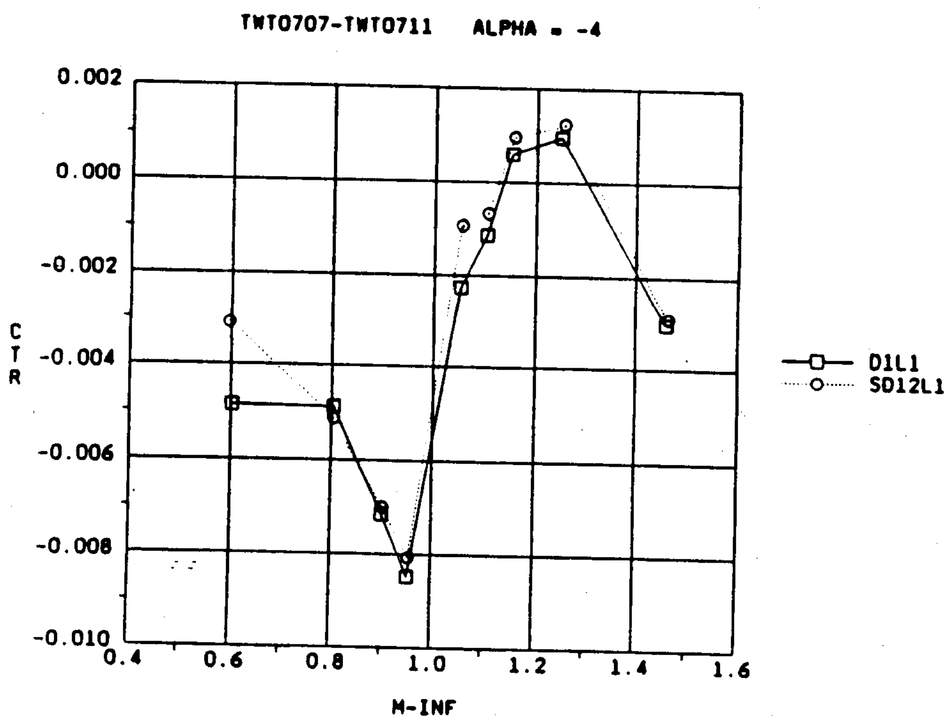

f. CTR; α = -4

Fig. 3-5 Phase I/Phase II Total Data Comparison, D1L1/SD12L1 Configuration (Concluded)

3.3.2 Angle of Attack Trends.

From the analyses conducted thus far, it is obvious that the Phase I D1L1/SD12L1 CNF, CMF, CSR, and CBR data are incorrect at Mach numbers between 1.10 and 1.25 at an angle of an attack of -4 deg. Presented in Figs. 3-6a through 3-6h are plots of total coefficient data which show both angle of attack trends and diameter trends for different LRB configurations. From Figs. 3-6a through 3-6h, it is quite clear that there are significant differences between Phase I and Phase II results for the D1L1/SD12L1 configuration at angles of attack ranging from -4 deg to 0 deg. Although positive angle of attack data are not presented in Figs. 3-6a through 3-6h, previous analyses have shown that significant differences between Phase I and Phase II D1L1/SD12L1 data do exist throughout the entire angle-of-attack range.

Figures 3-6a through 3-6h also show that the Phase I and Phase II D2L2/SD15 data are in good agreement at angles of attack between -4 deg and 0 deg. Once again, previous analyses have shown that this agreement continues at positive angles of attack.

3.3.3 Results of Data Comparison

It has been determined that the Phase I D1L1/SD12L1 total CNF, CMF, CSR, and CBR data are invalid at Mach numbers between 1.10 and 1.25. Thus, all of the Phase I incremental data that were generated at these Mach numbers are also invalid.

Most likely, the cause of the bad Phase I data is potential tunnel operating errors. Table 3-2 is a matrix of the Phase I test runs. It has been shown that runs TWT033, TWT0037, and TWT041 contain bad data. If indeed the potential tunnel errors resulted in the bad data, then it is quite likely that all of the "D1" data at Mach numbers between 1.10 and 1.25 (runs TWT033 through TWT044) are also bad due to the consecutive order in which the runs were conducted.

Figures 3-7a through 3-7f contain comparisons of Phase I "D1" data and Phase II D1L1/SD12L1 data. Figures 3-7a through 3-7f show that some of the inconsistencies seen in the Phase I D1L1/SD12L1 data at Mach numbers between 1.10 and 1.25 are also present in the D1L2, D1L3, and D1L4 data. Thus, the validity of the Phase I D1L2, D1L3, and D1L4 total data at Mach numbers between 1.10 and 1.25 cannot be confirmed.

It appears that the extent of the bad Phase I data is limited to runs TWT033 through TWT044 (i.e., only the "D1" configurations). Referring back to Figs. 3-6a through 3-6h, the trends produced by the larger diameter configurations appear to follow the initial trends of the valid (Phase II) D1L1/SD12L1 data and the D2L2/SD15 data. Unfortunately, there are no Phase II data available to confirm the validity of the Phase I "D3" and "D4" data.

It is recommended that a modified Phase I data base be developed. This would be a relatively simple task requiring an additional six test runs. The additional runs that would be needed are given in Table 3-3. It is further recommended that the increment development method documented in Lockheed-Huntsville IDC 88FT44 be used in creating the new Phase I LRB incremental data base.

Table 3-3 ADDITIONAL TEST RUNS SUGGESTED TO REDEVELOP PHASE I DATA BASE

Configuration	M = 1.10	M = 1.25
D1L2	X	X
D1L3	X	X
D1L4	X	X

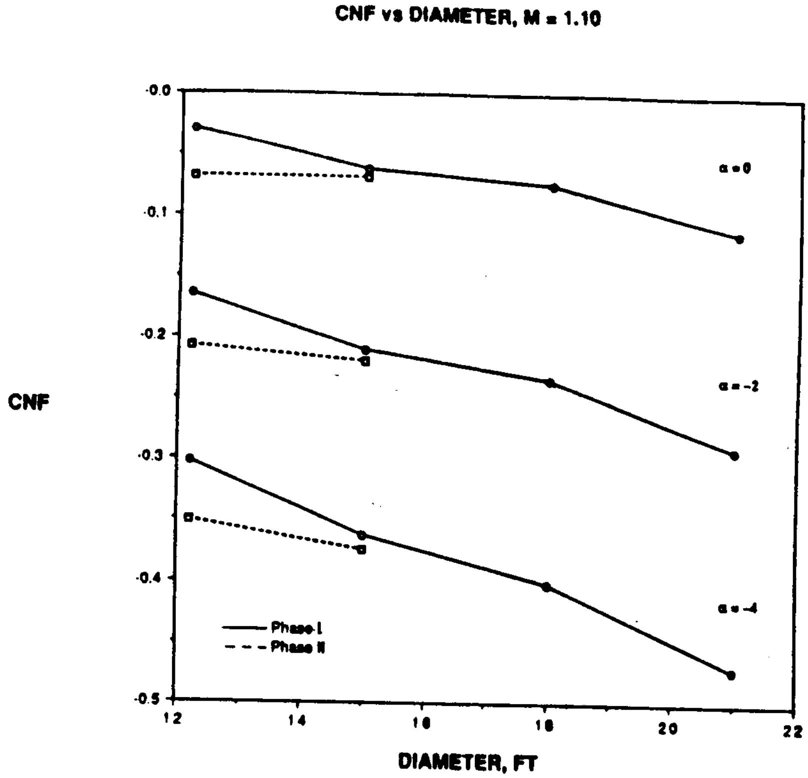

a. CNF; M = 1.10

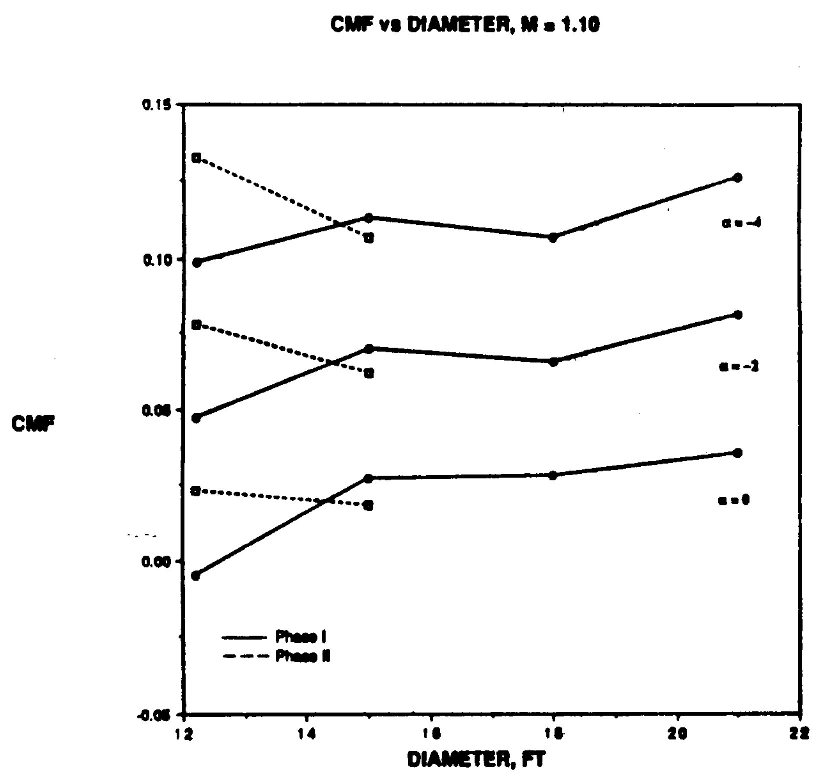

b. CMF; M = 1.10

Fig. 3-6 Angle of Attack and Diameter Effects on Phase I/Phase II Data

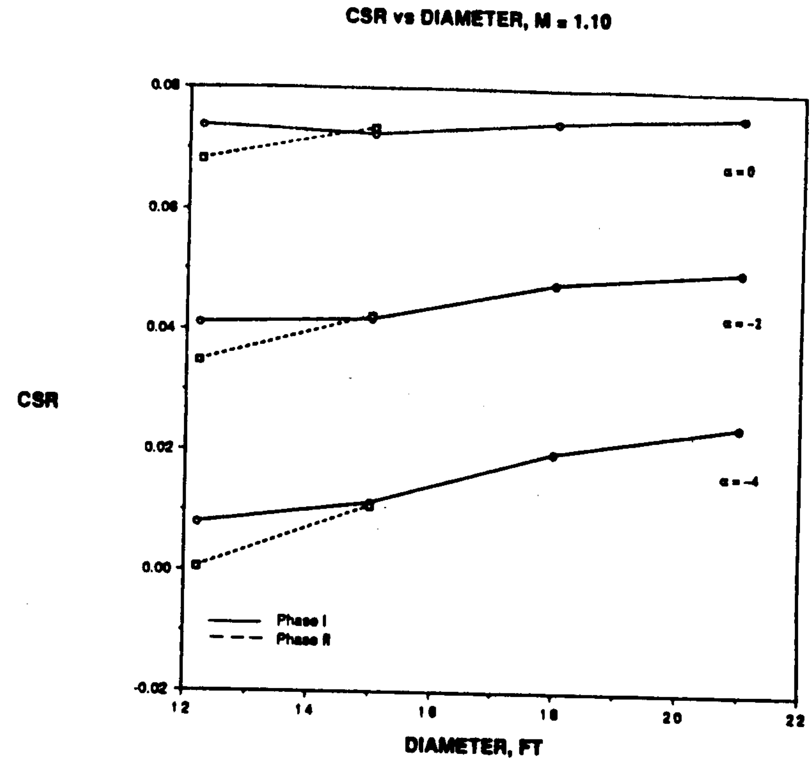

c. CSR; M = 1.10

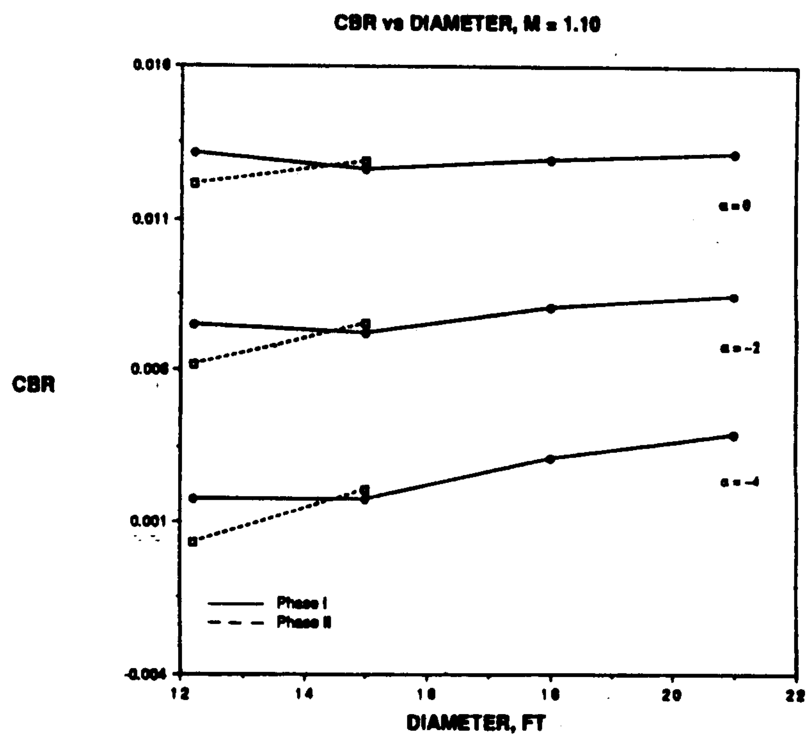

d. CBR; M = 1.10

Fig. 3-6 Angle of Attack and Diameter Effects on Phase I/Phase II Data (Continued)

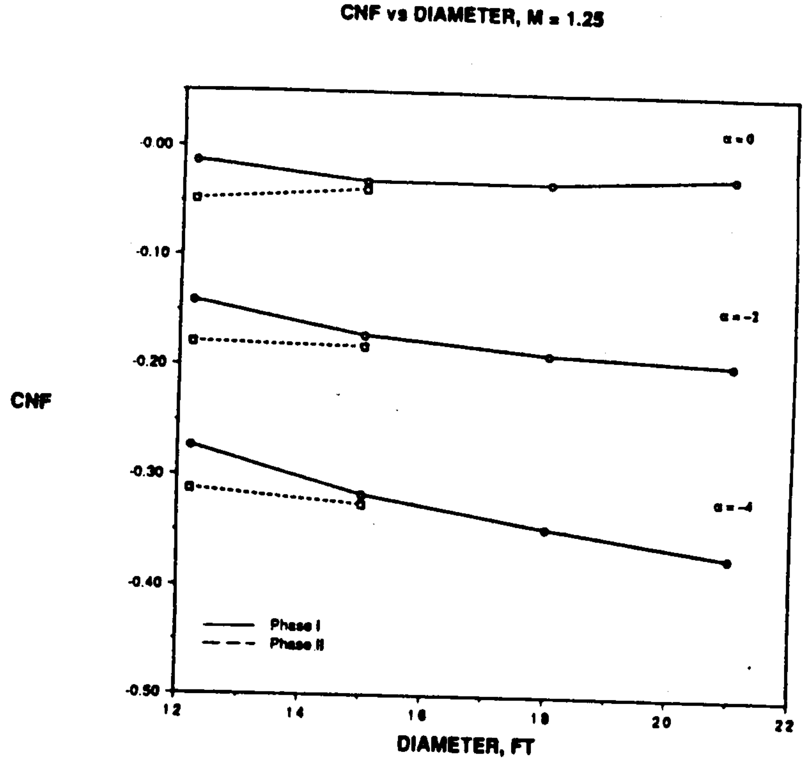

e. CNF; M = 1.25

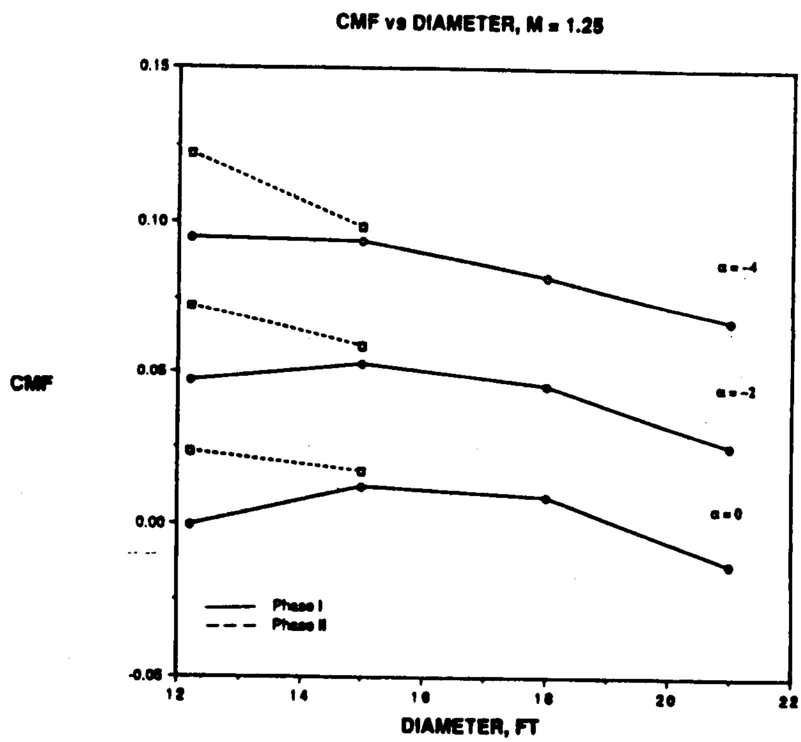

f. CMF; M = 1.25

Fig. 3-6 Angle of Attack and Diameter Effects on Phase I/Phase II Data (Continued)

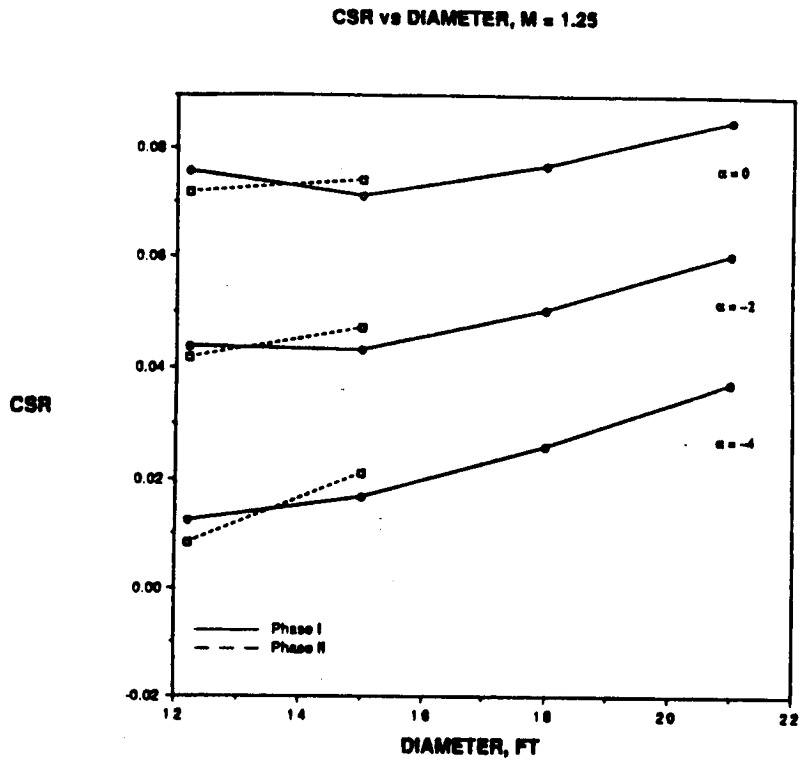

g. CSR; M = 1.25

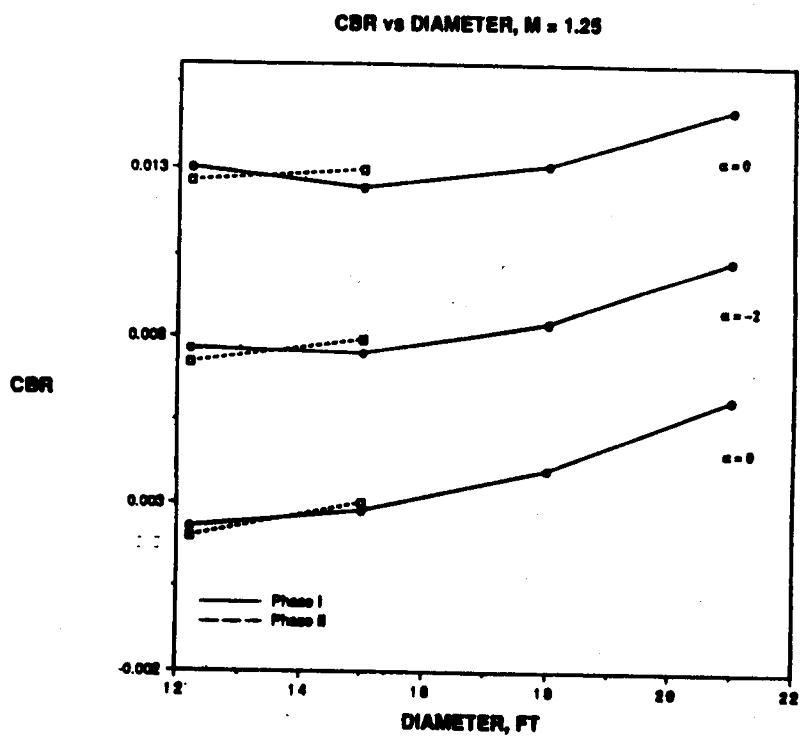

h. CBR; M = 1.25

Fig. 3-6 Angle of Attack and Diameter Effects on Phase I/Phase II Data (Concluded)

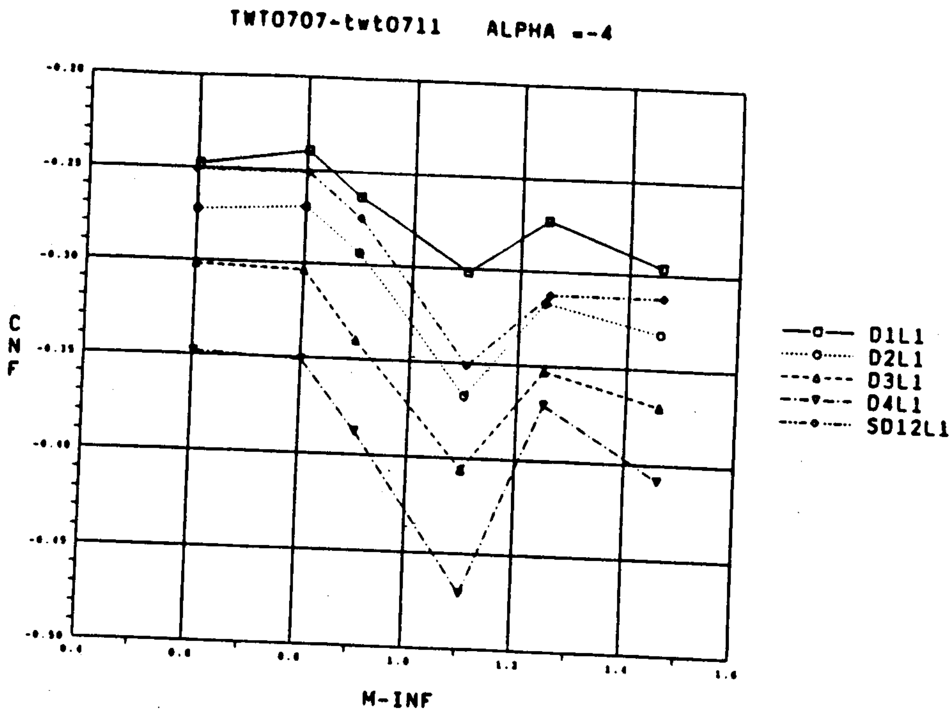

a. CNF; α = -4

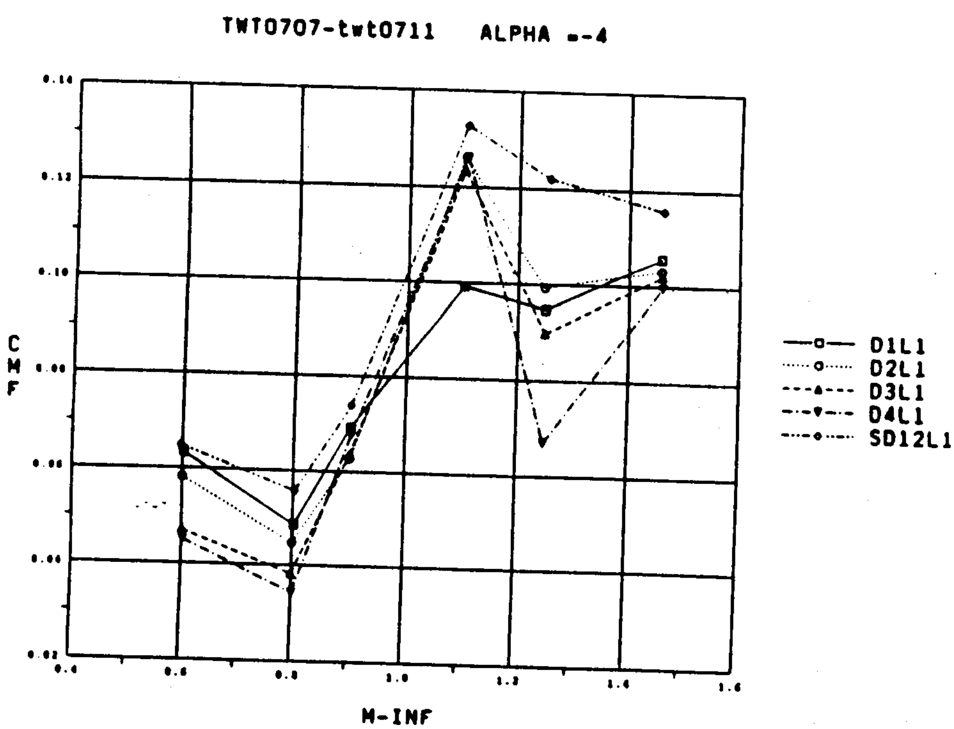

b. CMF; α = -4

Fig. 3-7 LRB Diameter Effects

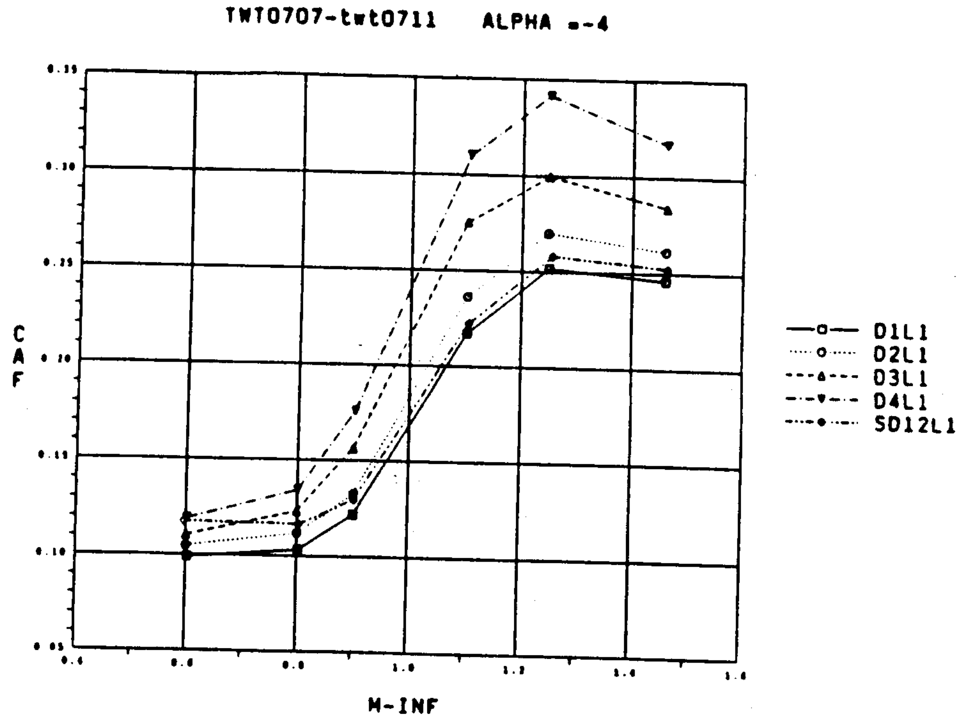

c. CAF; α = -4

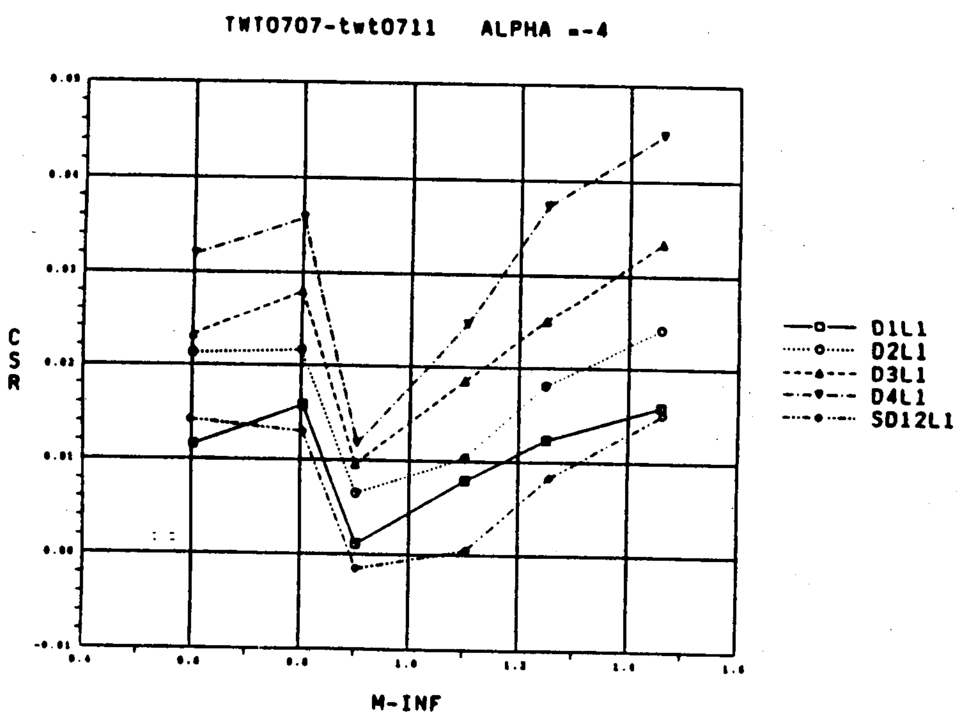

d. CSR; α = -4

Fig. 3-7 LRB Diameter Effects (Continued)

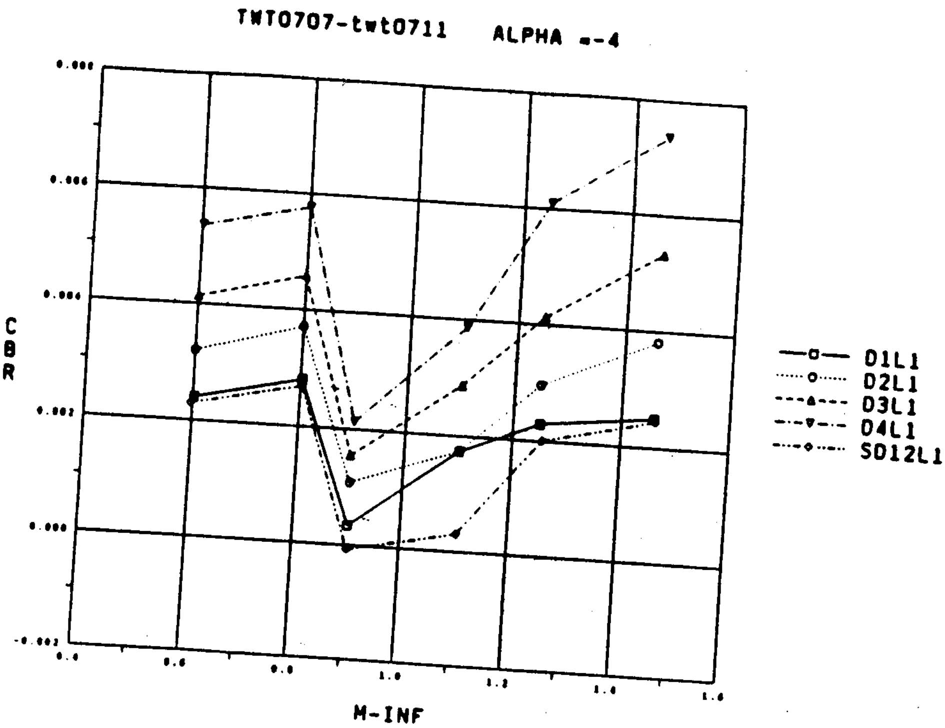

e. CBR; α = −4

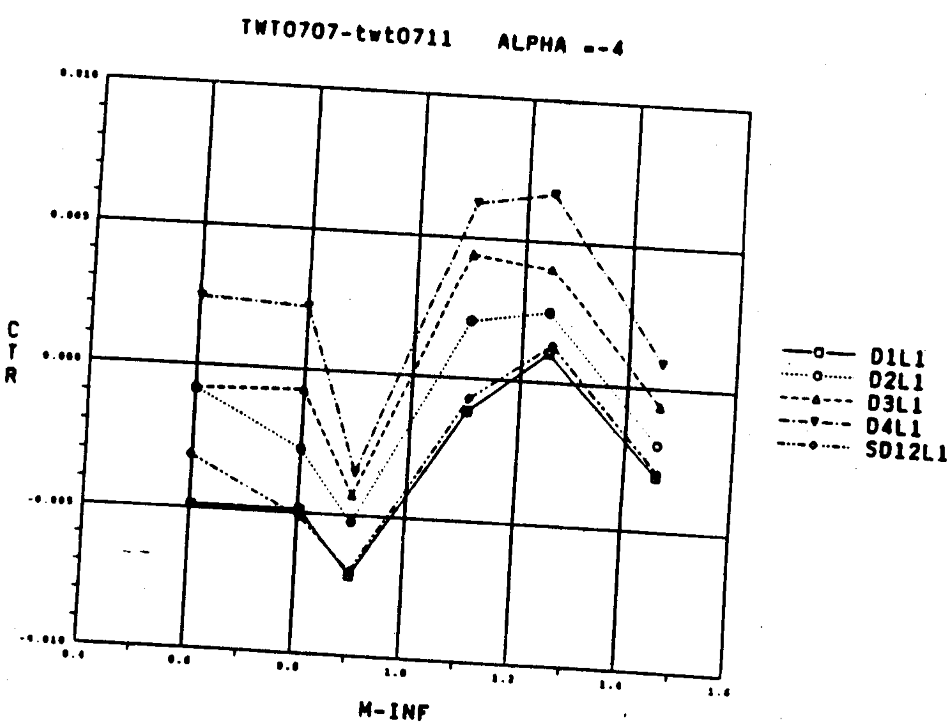

f. CTR; α = −4

Fig. 3-7 LRB Diameter Effects (Concluded)

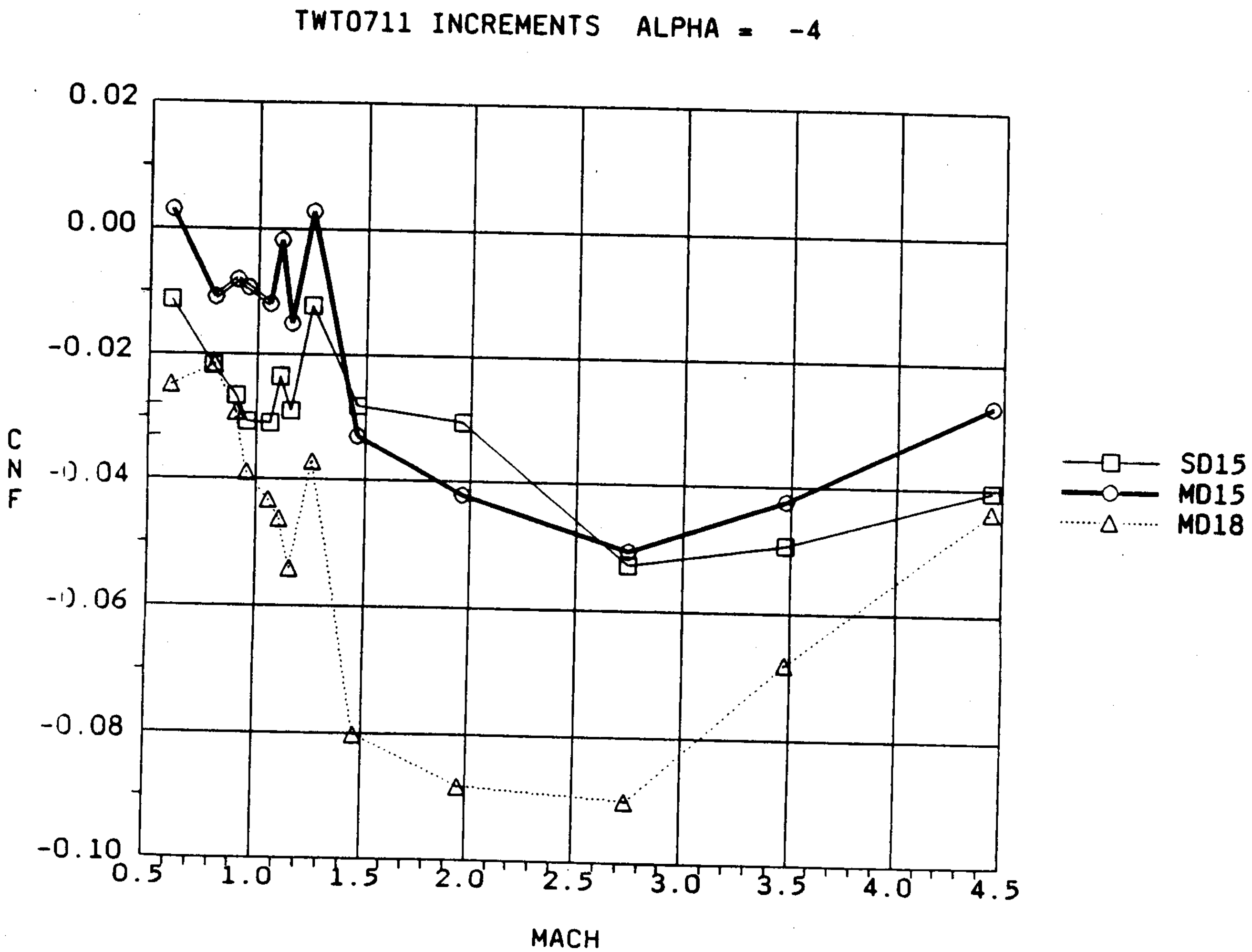

Fig. 3-8a Normal Force Increments

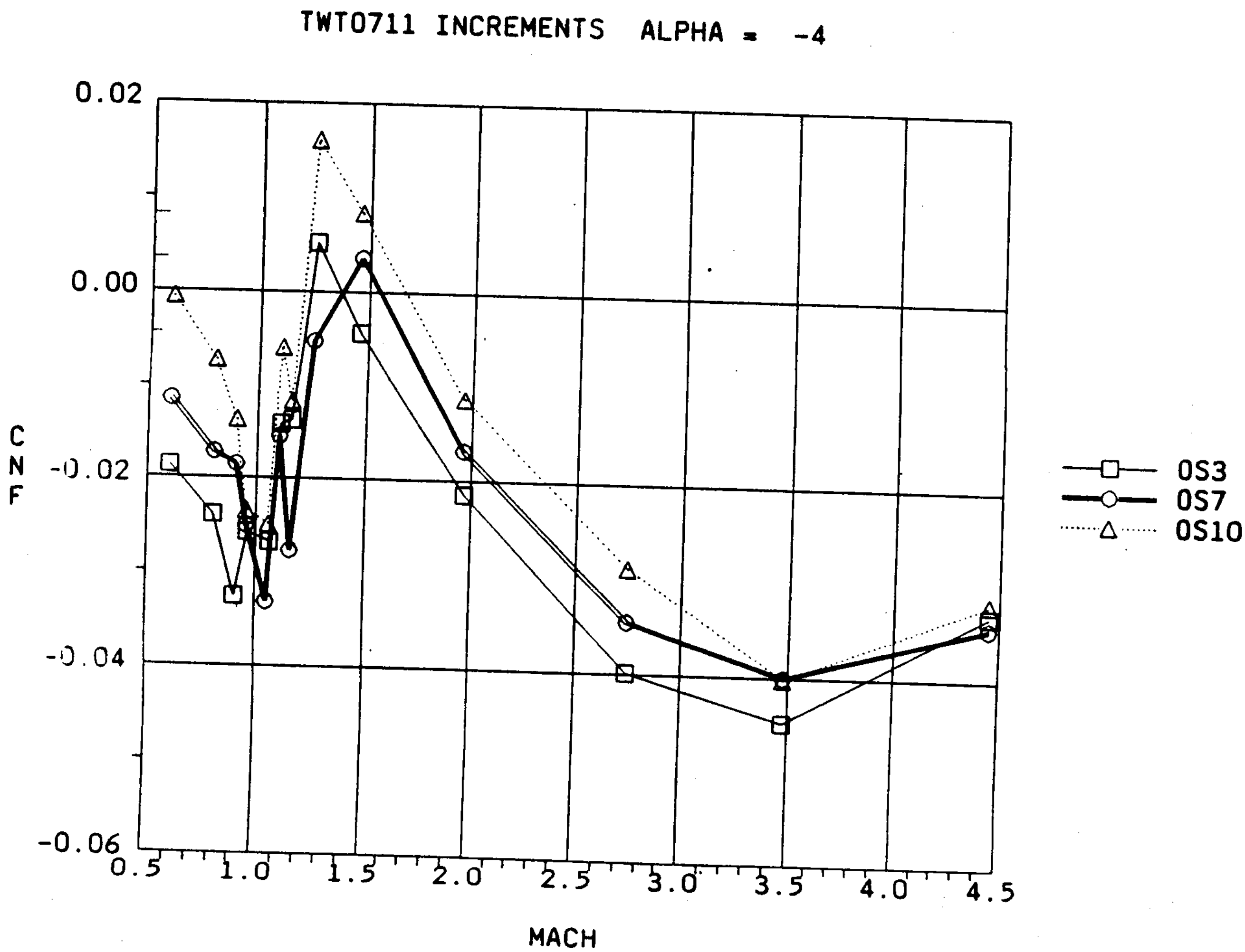

Fig. 3-8b Normal Force Increments

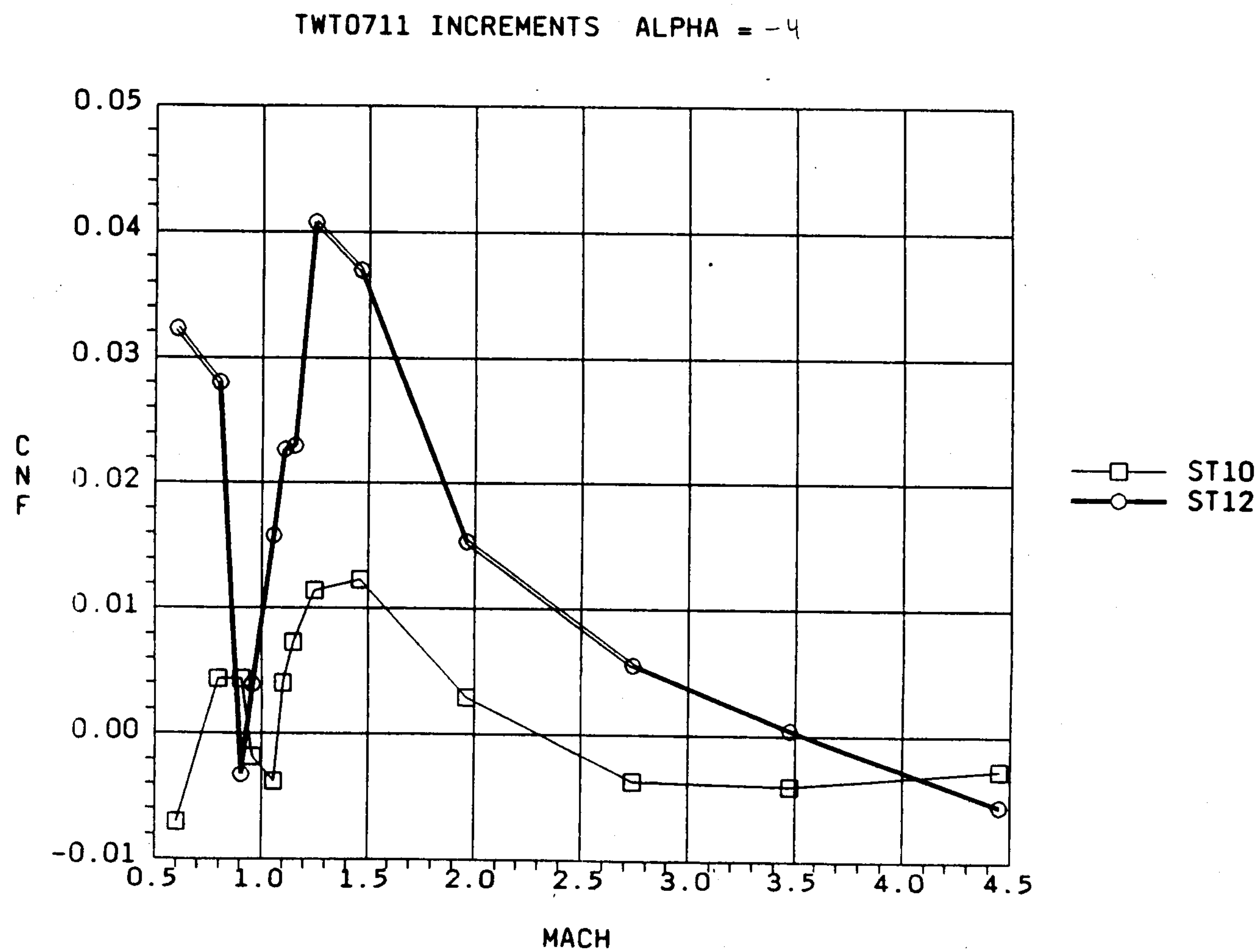

Fig. 3-8c Normal Force Increments

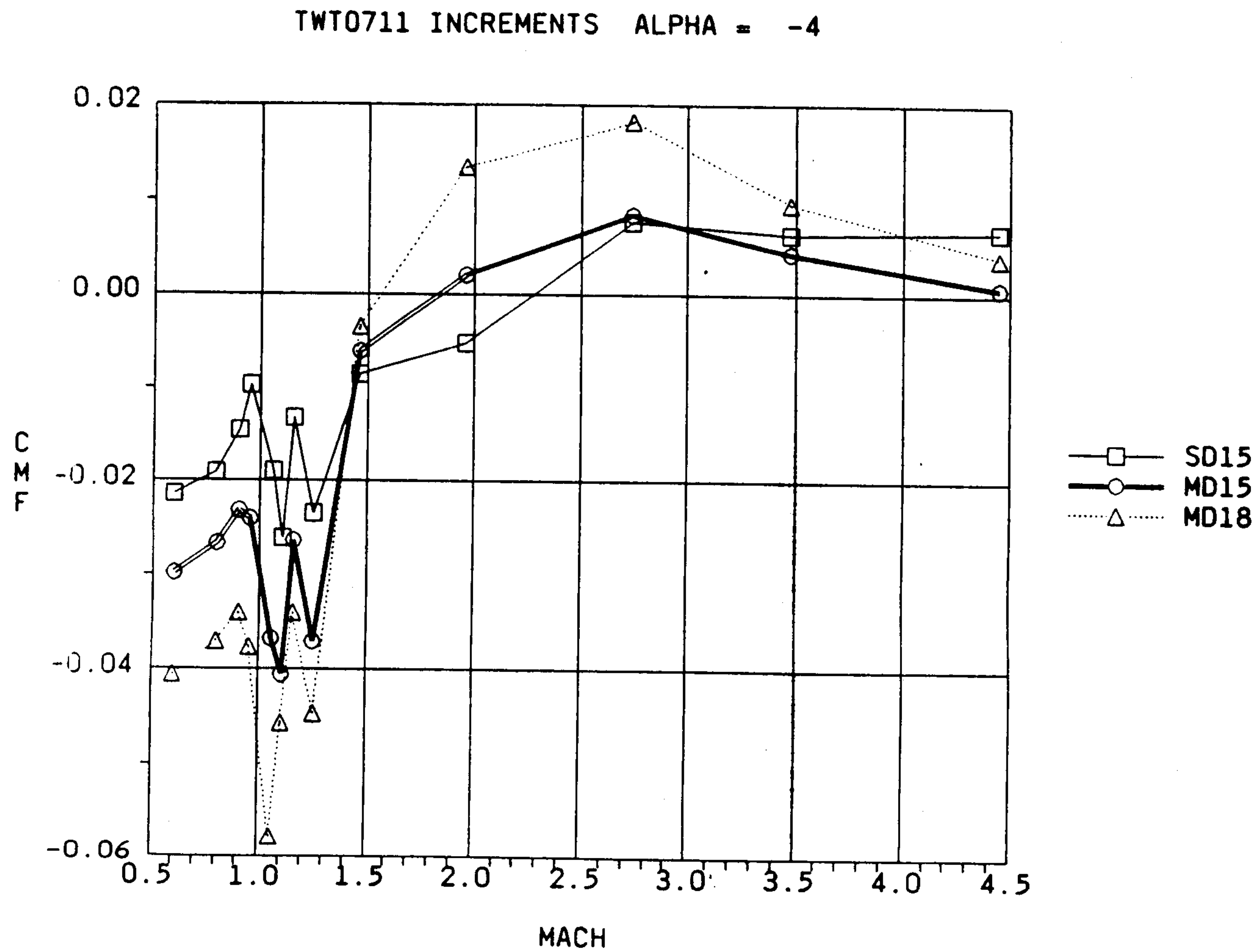

Fig. 3-8d Pitching Moment Increments

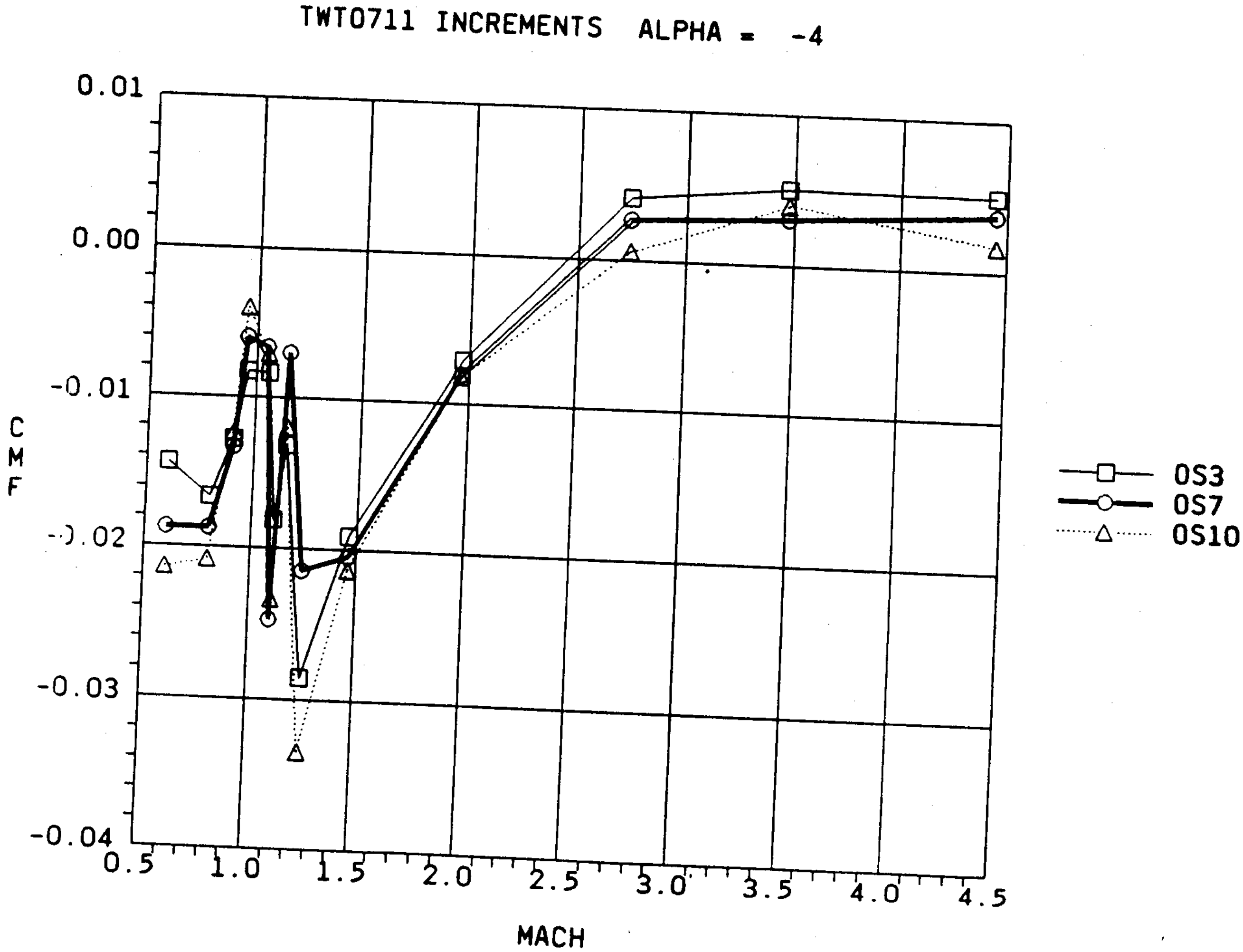

Fig. 3-8e Pitching Moment Increments

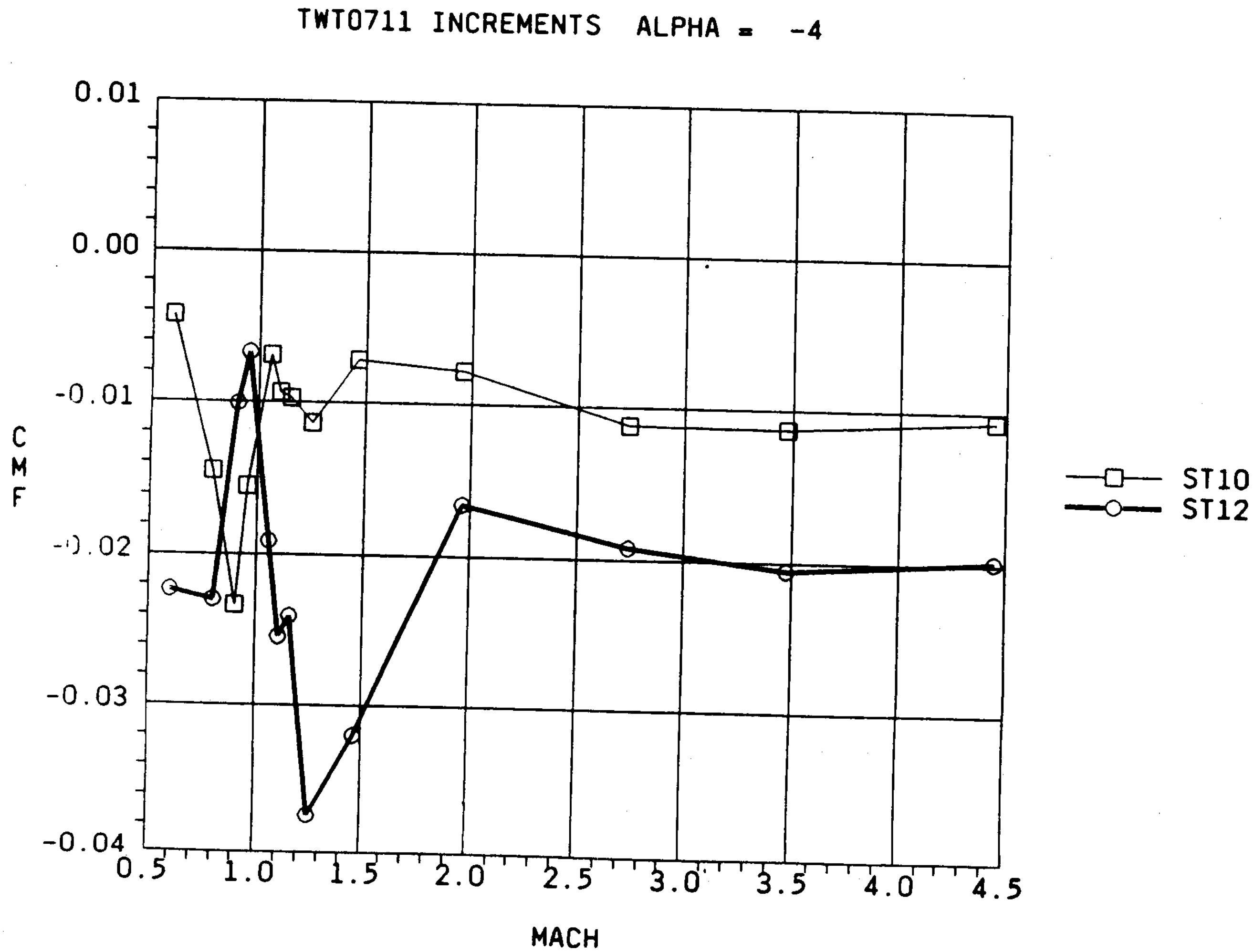

Fig. 3-8f Pitching Moment Increments

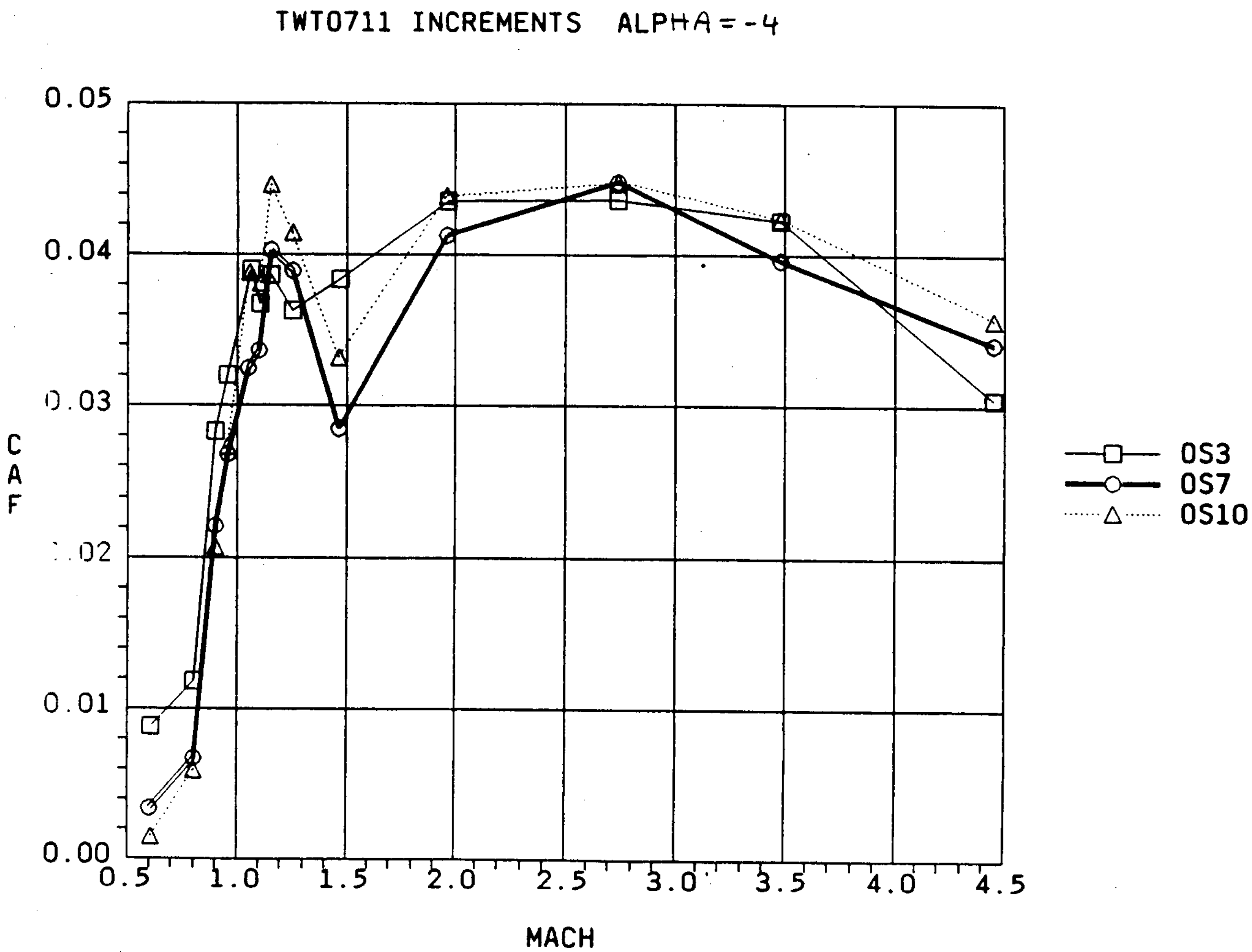

Fig. 3-8g Axial Force Increments

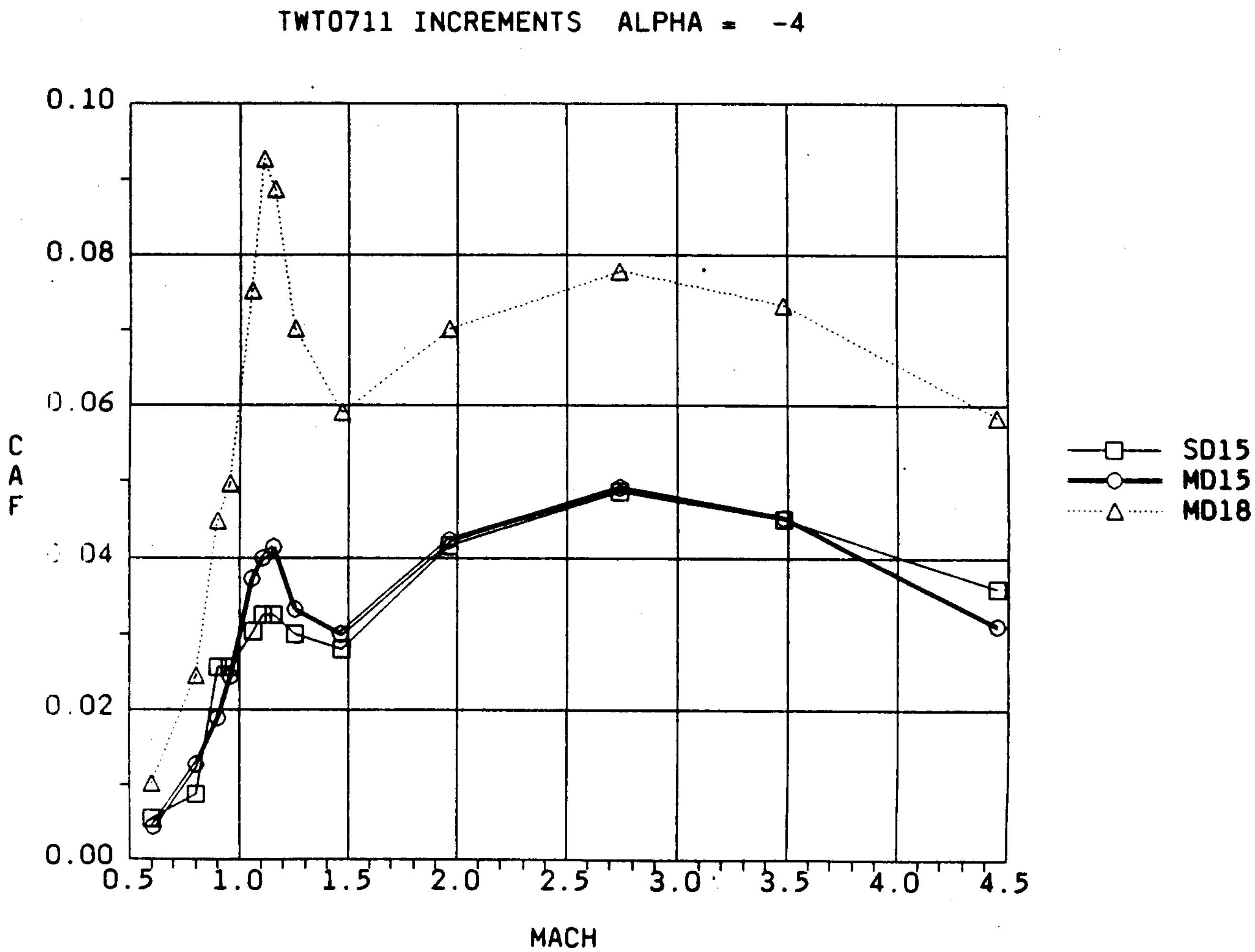

Fig. 3-8h Axial Force Increments

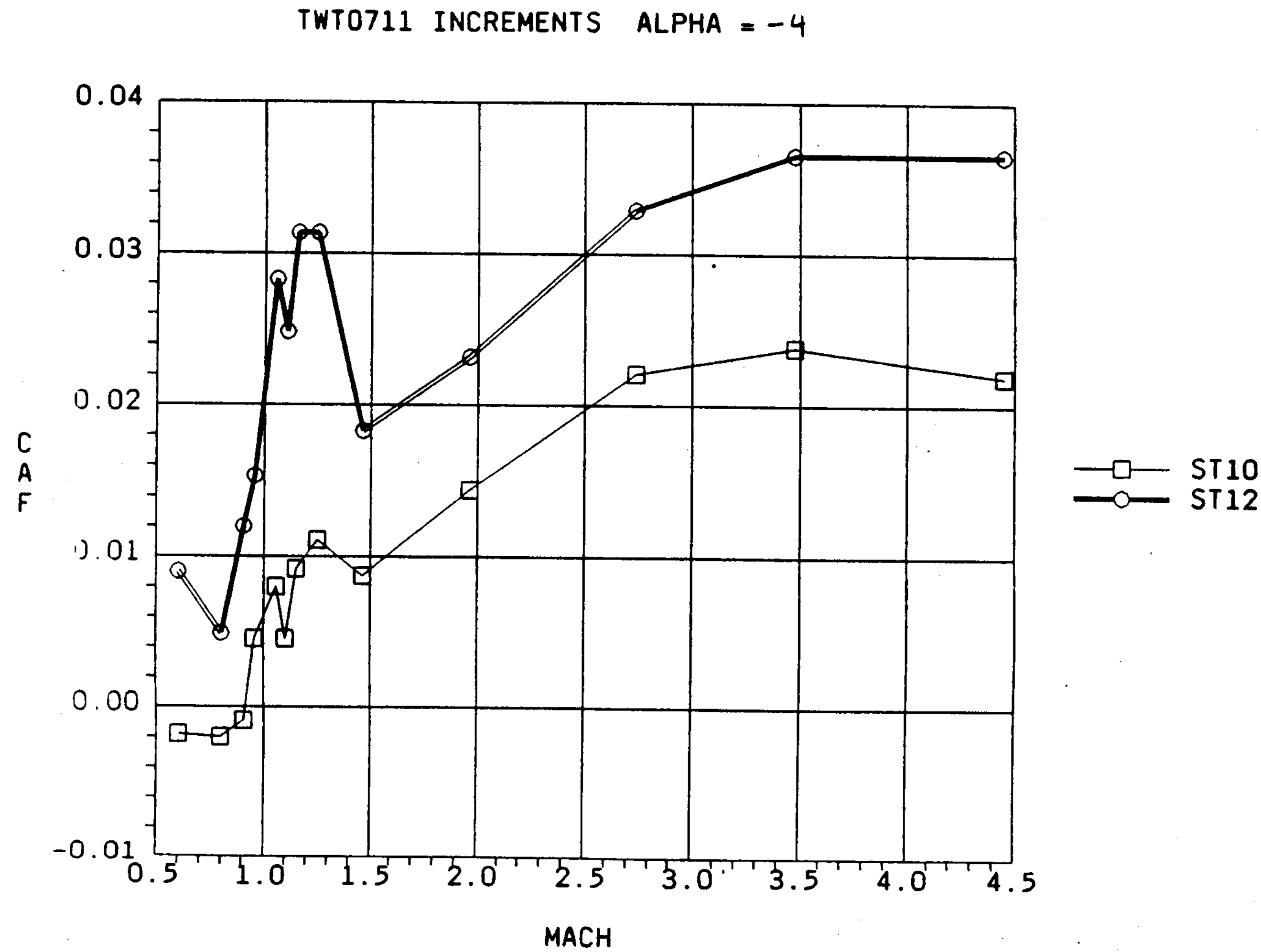

Fig. 3-8i Axial Force Increments

C-2

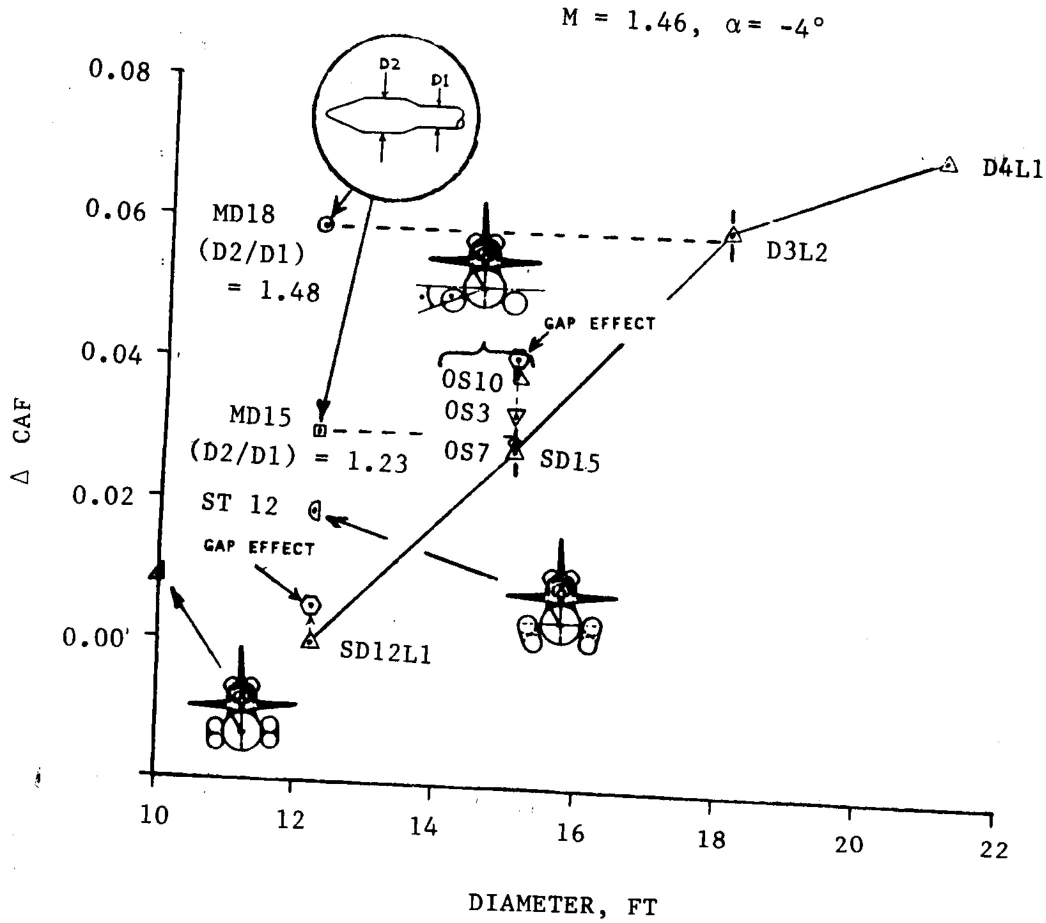

Fig. 3-9a Δ CAF vs Diameter

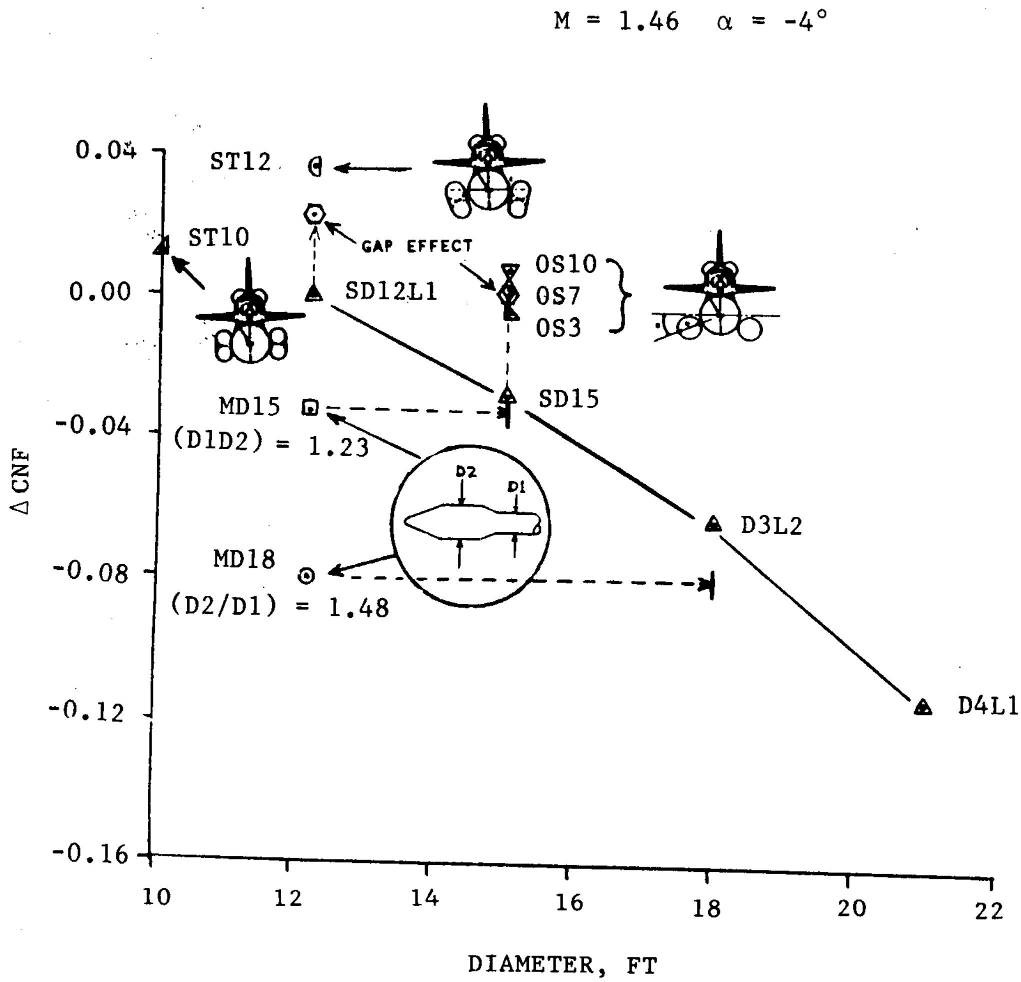

Fig. 3-9b Δ CNF vs Diameter

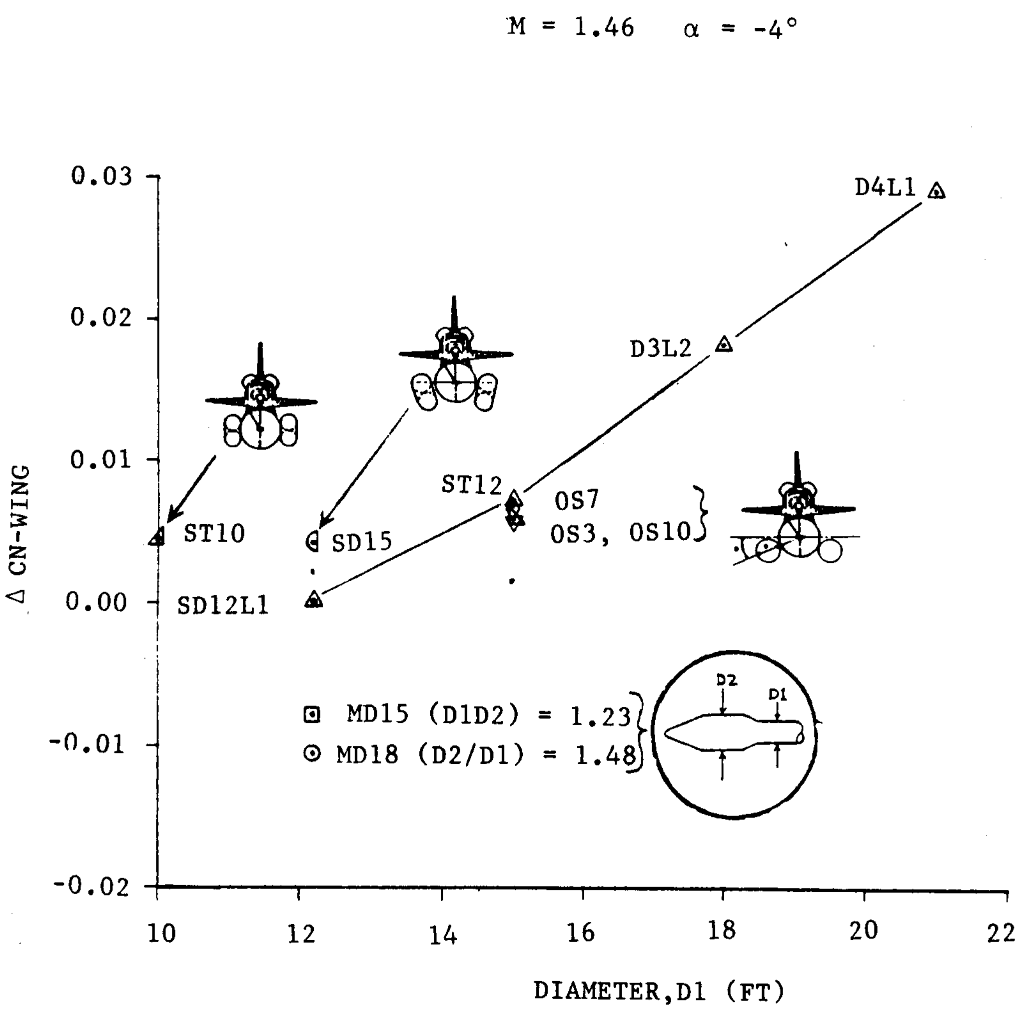

Fig. 3-9c Δ CN-Wing vs Diameter

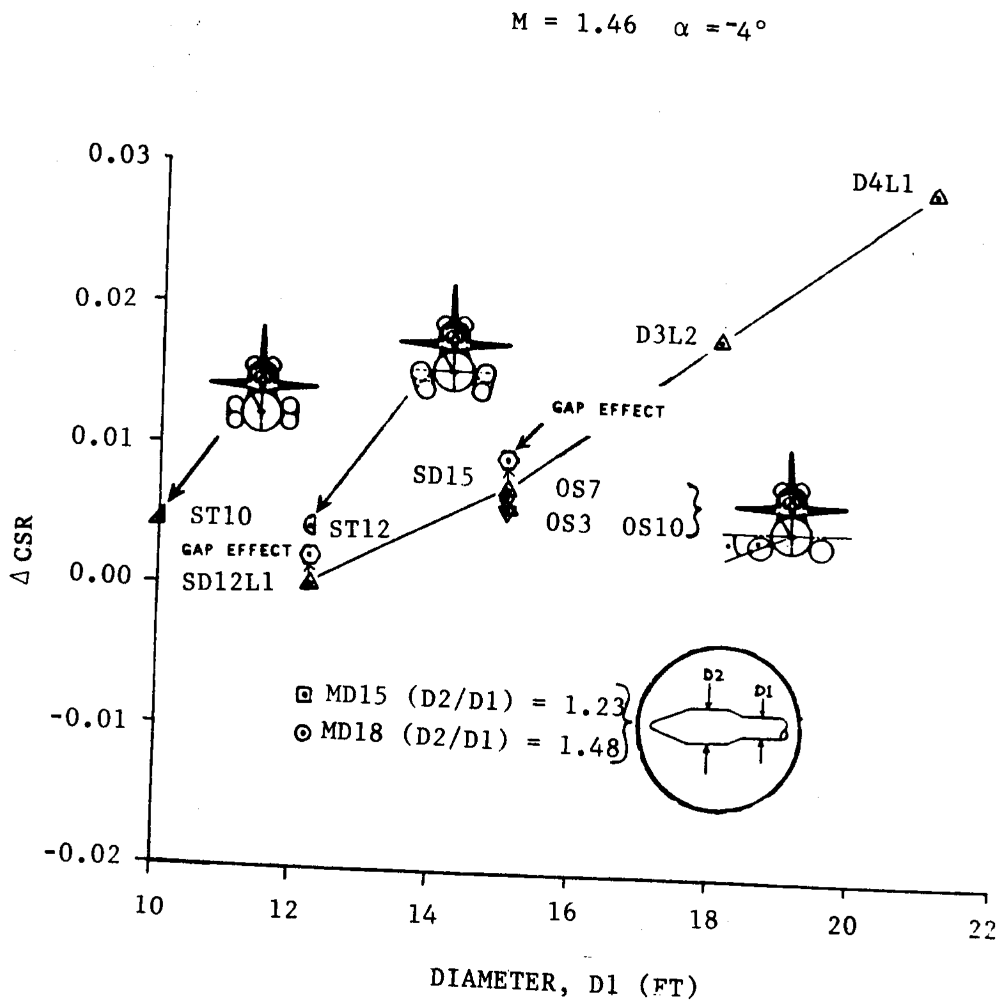

Fig. 3-9d Δ CSR vs Diameter

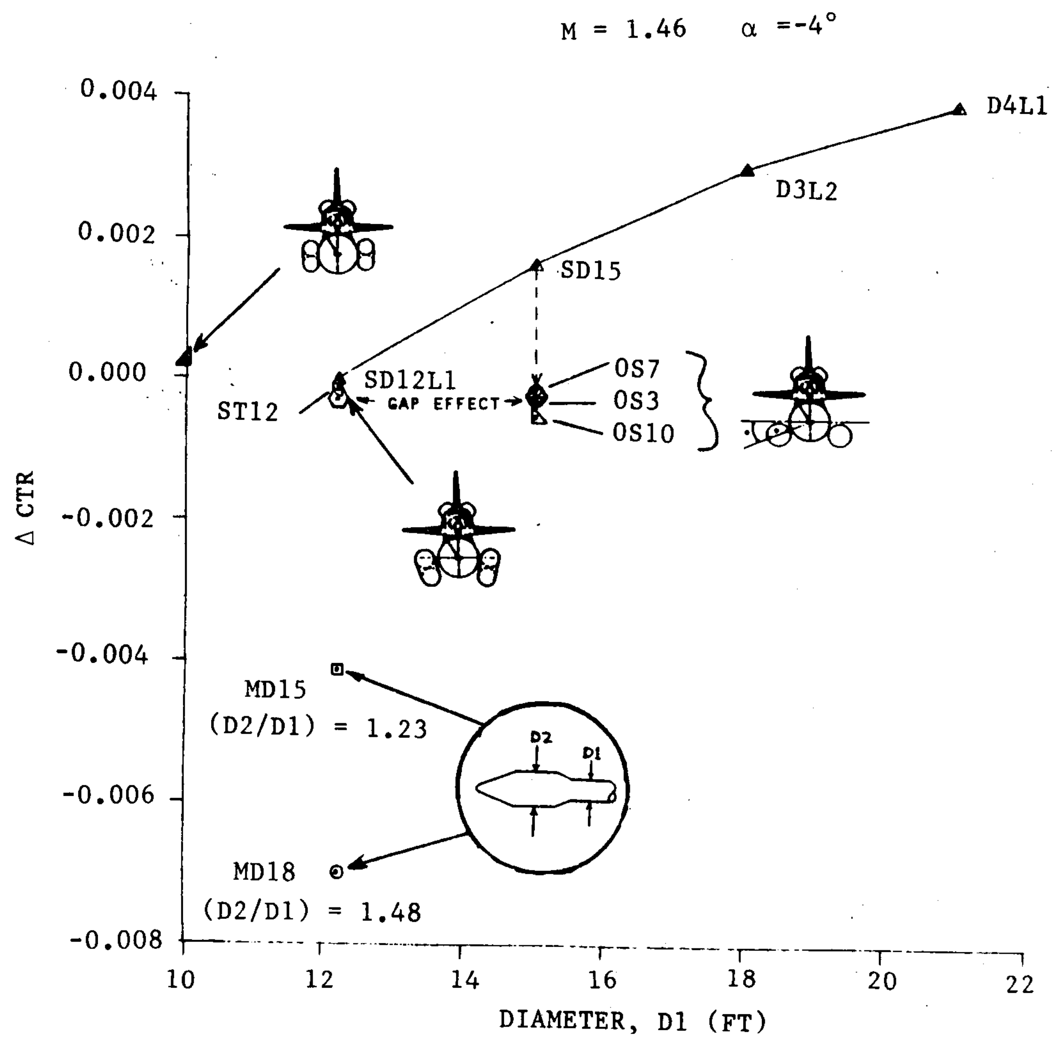

Fig. 3-9e Δ CTR vs Diameter

4. LRB LATERAL/DIRECTIONAL WIND TUNNEL DATA

The LRB Lateral/Directional incremental data were taken from Wind Tunnel Test TWT0716. The test was conducted from April 1988 to June 1988 to investigate length and diameter effects on the lateral/directional aerodynamic characteristics of the SSLV. Figure 4-1 presents the scope of the test. The configurations used in the test are presented in Figure 4-2.

The aerodynamic increment coefficients were for the total vehicle and were generated using the following equation:

Δ DXLY = DXLY - D1L1

where: X = either 2 or 3 (15' or 18' diameter)
Y = either 1,2,3, or 4 (length variations ranging from 149' to 190').

The increments can be used to determine the coefficient increment for any LRB configuration. New LRB coefficients equal the current SSLV values plus the increments.

The wing data (bending, shear, torsion) increments are for the right wing. The elevon data (inboard and outboard) increments are for the left wing. All data are for alpha - 0 and have been uniformly shifted by an incremental value so that beta = 0. Sign conventions for the launch vehicle, wing, and elevon data are shown in Figure 4-3.

Diameter (ft) / Length (ft)	D1	D2	D3	D4
	12.2*	15	18	21
L1	144*	149	154	
L2		159	163	
L3		172	175	
L4		190	190	-

M = 0.6, 0.8, 0.9, 0.95, 1.05, 1.10, 1.15, 1.25,

1.46, 1.96, 2.75, 3.48, 4.45

$\alpha = 0°$, $\beta = -6.0$ to 6.0

Fig. 4-1 Scope of Test (TWT 016)

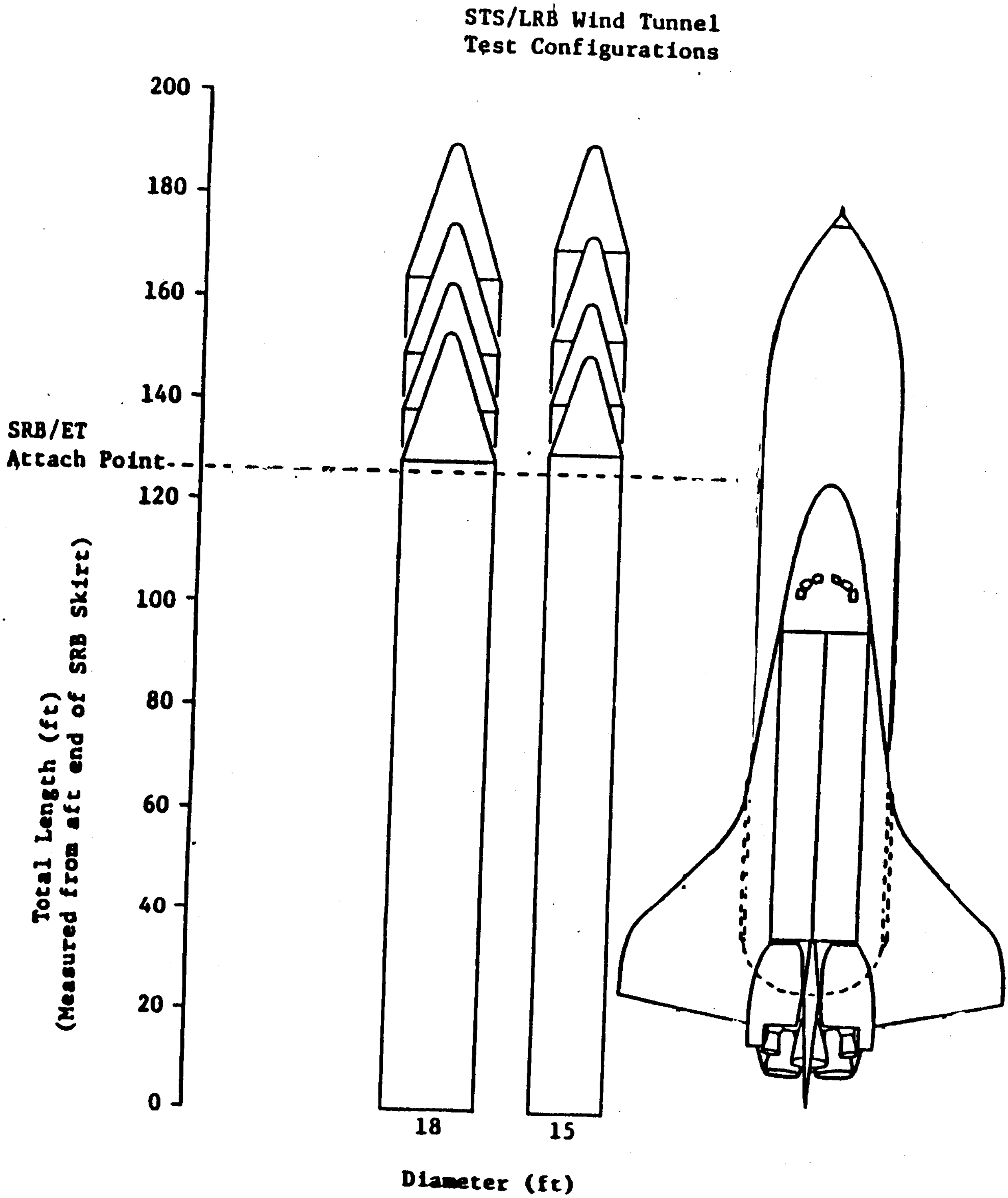

Fig. 4-2 Test Configurations (TWT 716)

ORIGINAL PAGE IS
OF POOR QUALITY

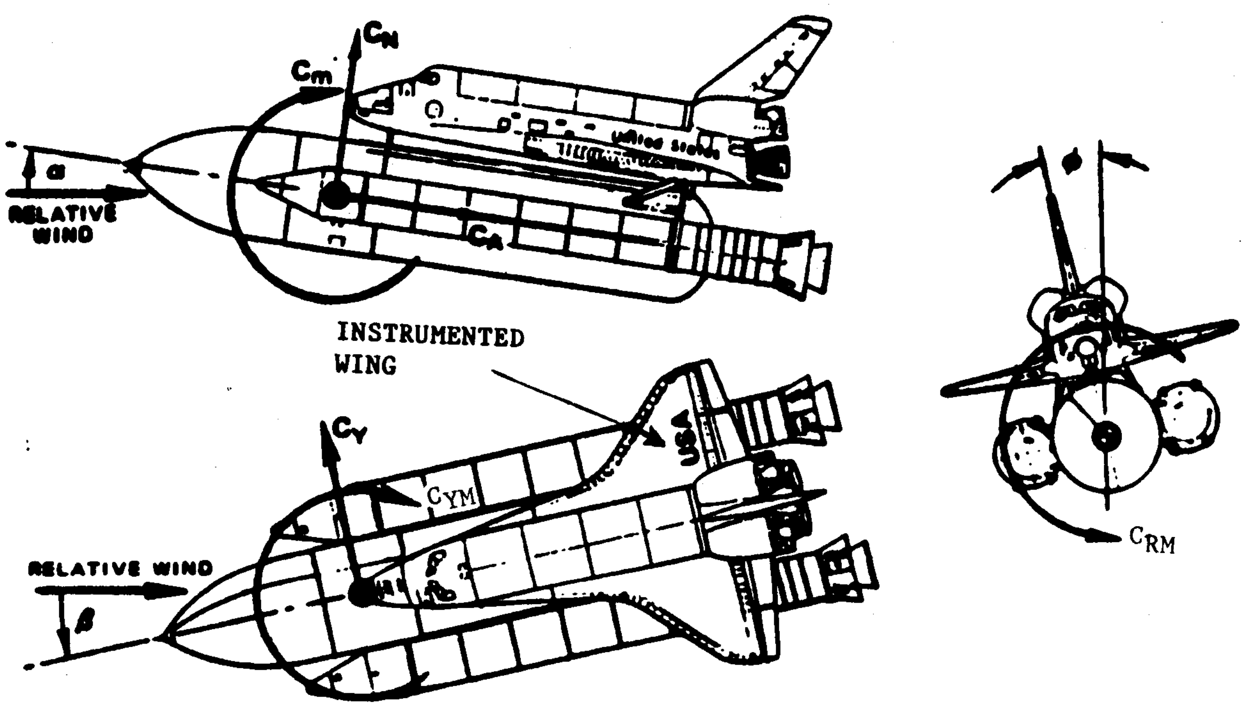

Fig. 4-3a Launch Vehicle Sign Convention

ORIGINAL PAGE IS
OF POOR QUALITY

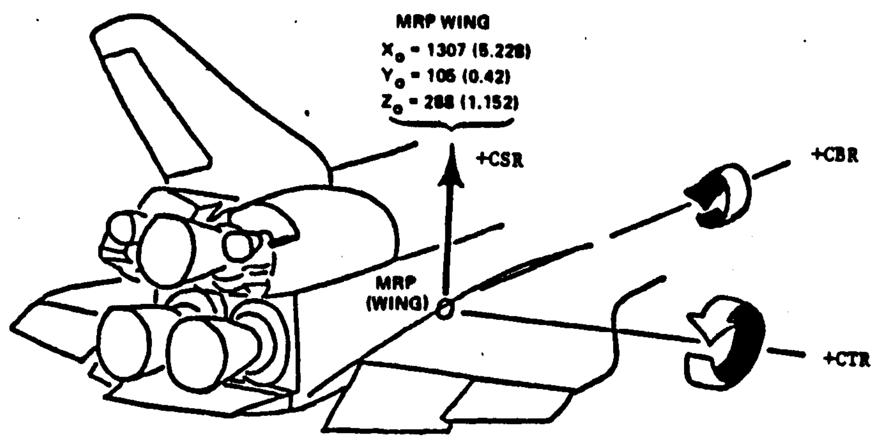

ALL DIMENSIONS IN INCHES
MODEL SCALE IN PARENTHESES

Wing Coordinate Axes
(Ref. Dimensions and Axes are
the same for all Databases)

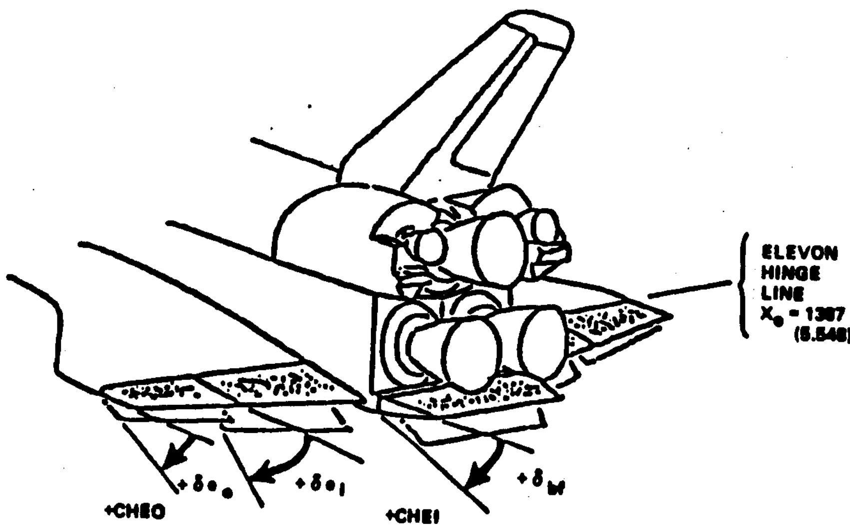

ALL DIMENSIONS IN INCHES
MODEL SCALE IN PARENTHESES

Elevon Coordinate Axes
(Ref. Dimensions and Axes are
the same for all Databases)

Fig. 4-3b Launch Vehicle Sign Convention

During analysis of the LRB lateral/directional data, some basic trends were observed. The trends are for unshifted increments and are given below.

1. CY Trends

- Generally $|CY_\beta|$ increases in diameter. Thus, for a given β, $|\Delta CY|$ increases with increases in diameter.
- For $M \leq 1.05$, LRB length variation has no significant effect on CY_β.
- For $1.05 < M < 1.80$, $|CY_\beta|$ generally decreases with increases in LRB length.
- For $M \geq 1.80$, length trends switch so that $|CY_\beta|$ generally increases in LRB length.
- Typically, LRB length and diameter effects on SSLV CY_β values are less than 15%.

2. CYM Trends

- Generally, $|CYM_\beta|$ increases with increases in diameter. Thus, for a given β, $|\Delta CYM|$ increases with increases in diameter.
- Generally, $|CYM_\beta|$ decreases with increases in LRB length.
- Typically, length and diameter effects on SSLV CYM_β values are less than 20%.

3. CRM Trends

- Generally, $|CRM_\beta|$ decreases with increases in diameter. Thus, for a given β, $|\Delta CRM|$ increases with increase in diameter.
- LRB length generally has a small effect on ΔCRM and thus CRM_β.
- Typically, length and diameter effects on SSLV CRM_β values are less than 20%.

4. CSR Trends - Right Wing

- For all β values, ΔCSR generally increases as LRB diameter increases.

- For β > 0 and a given diameter, ΔCSR generally increases as β increases for all M.

- LRB length effects on ΔCSR are small.

5. CBR Trends - Right Wing

- For all β values, ΔCBR generally increases with increases in LRB diameter.

- For β > 0 and a given diameter, ΔCBR typically decreases as β becomes more negative.

- LRB length effects on ΔCBR typically decreases as β becomes more negative.

- LRB length effects on ΔCBR values are small.

6. CTR Trends - Right Wing

- For $1.80 \leq M < 3.48$, diameter increases typically cause ΔCTR to decrease for all β. For other Mach numbers, ΔCTR usually increase with increases in LRB diameter.

- No consistent β trends appear to exist for the Mach numbers tested.

- LRB length effects on ΔCTR values are small.

7. Hinge Moment Trends - Left Wing

- Inboard - ΔCHEI

• ΔCHEI generally increases with increases in diameter except for $1.8 \leq M \leq 2.5$, where it decreases as β increases.

• ΔCHEI typically decreases as β increases.

• LRB length effects on ΔCHEI are small.

- Outboard - ΔCHEO

- ΔCHEO generally increases with increases in diameter except for 1.8 ≤ M ≤ 2.5, where it increases in diameter.
- No consistent β trends are apparent.
- LRB length effects on ΔCHEO are small.

8. Additional Trends

- β effects on ΔCNF, ΔCMF, ΔCAF are small for all configurations.

The data from the wind tunnel test were analyzed with regard to yaw angle effects of shuttle wing loads. At Mach = 1.96 the incremental wing loads are a strong function of both LRB length and yaw angle. Unlike the longitudinal data, the LRB diameter was found to have a small effect on wing loads.

Analysis of the test data for the various configurations leads to the conclusion that the aft skirt on D1L1 configurations does not significantly affect wing loads. It was also determined that the MD15 (hammerhead) configuration greatly reduces the wing loads over the entire yaw angle range tested. The maximum incremental loading on a wing occurs when it is on the leeward side.

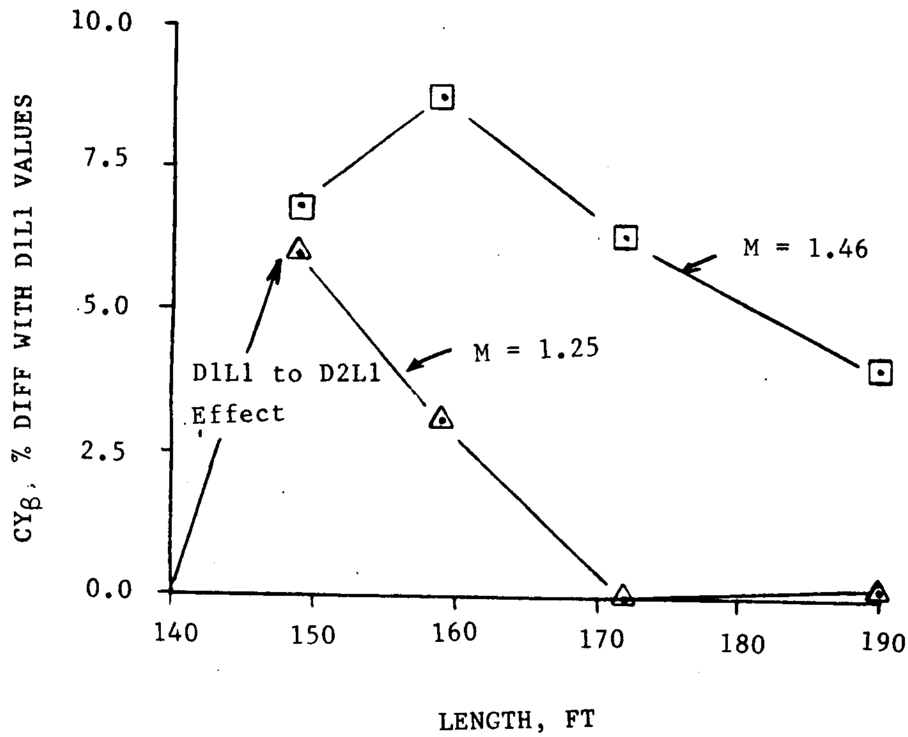

Fig. 4-4 CY_{β} vs Length

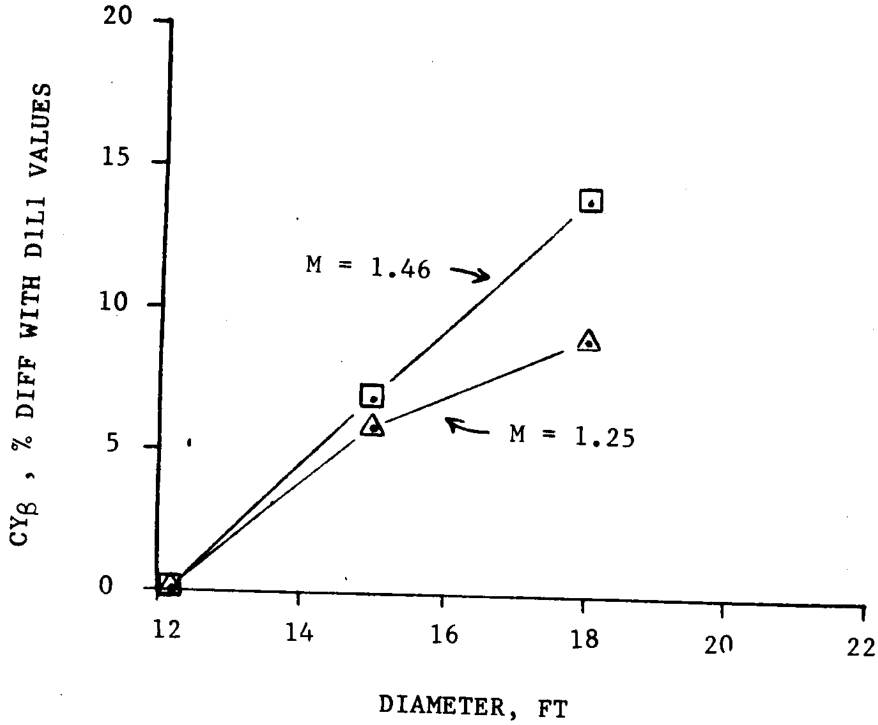

Fig. 4-5 CY_β VS DIAMETER

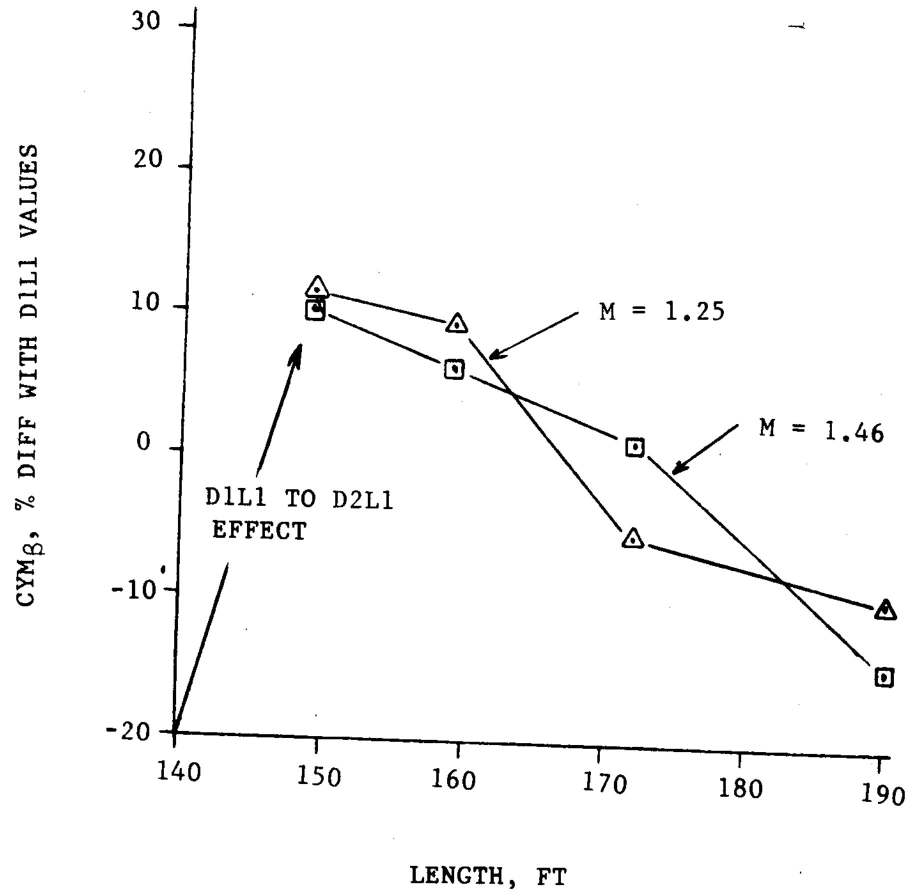

Fig. 4-6 CYM$_\beta$ VS LENGTH

ORIGINAL PAGE IS
OF POOR QUALITY

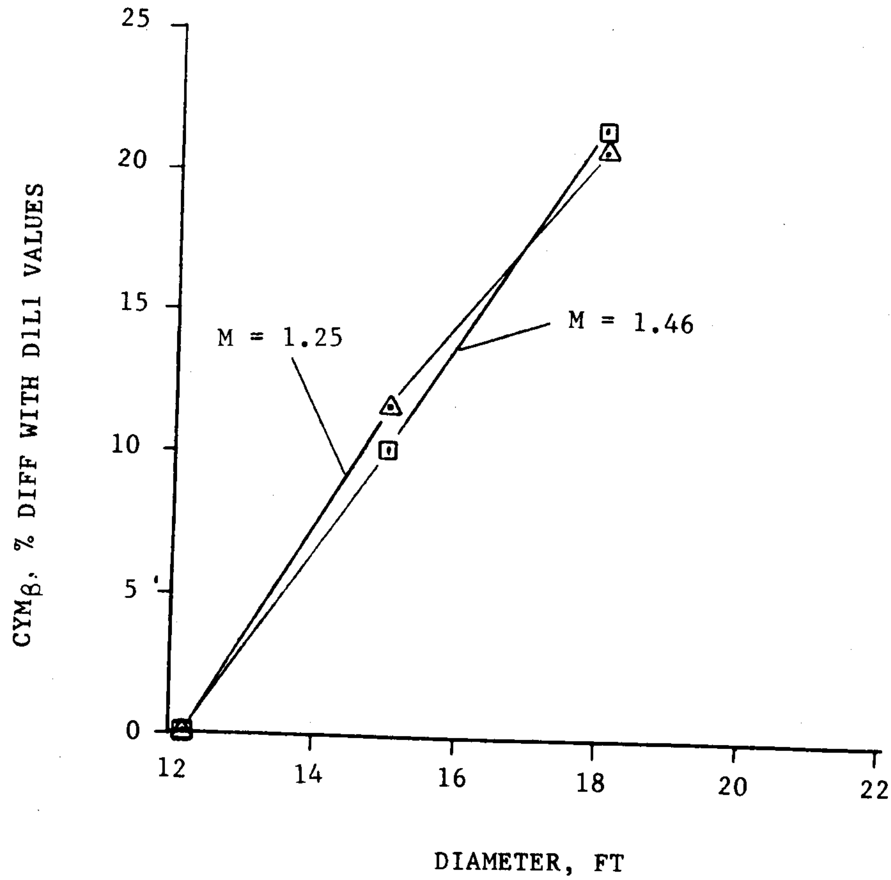

Fig. 4-7 CYM_{β} vs Diameter

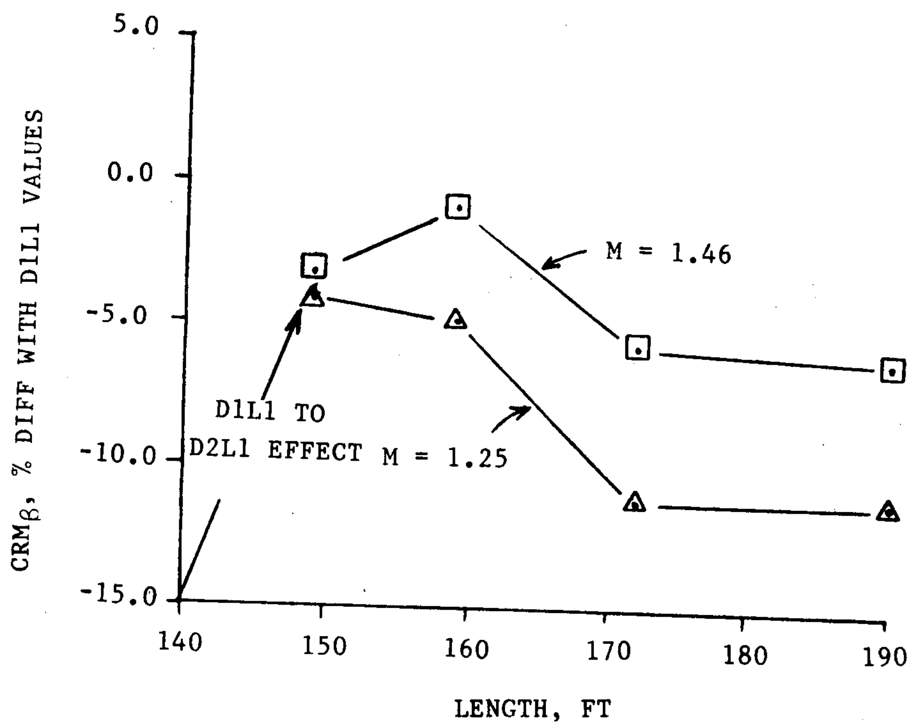

Fig. 4-8 CRM_β vs Length

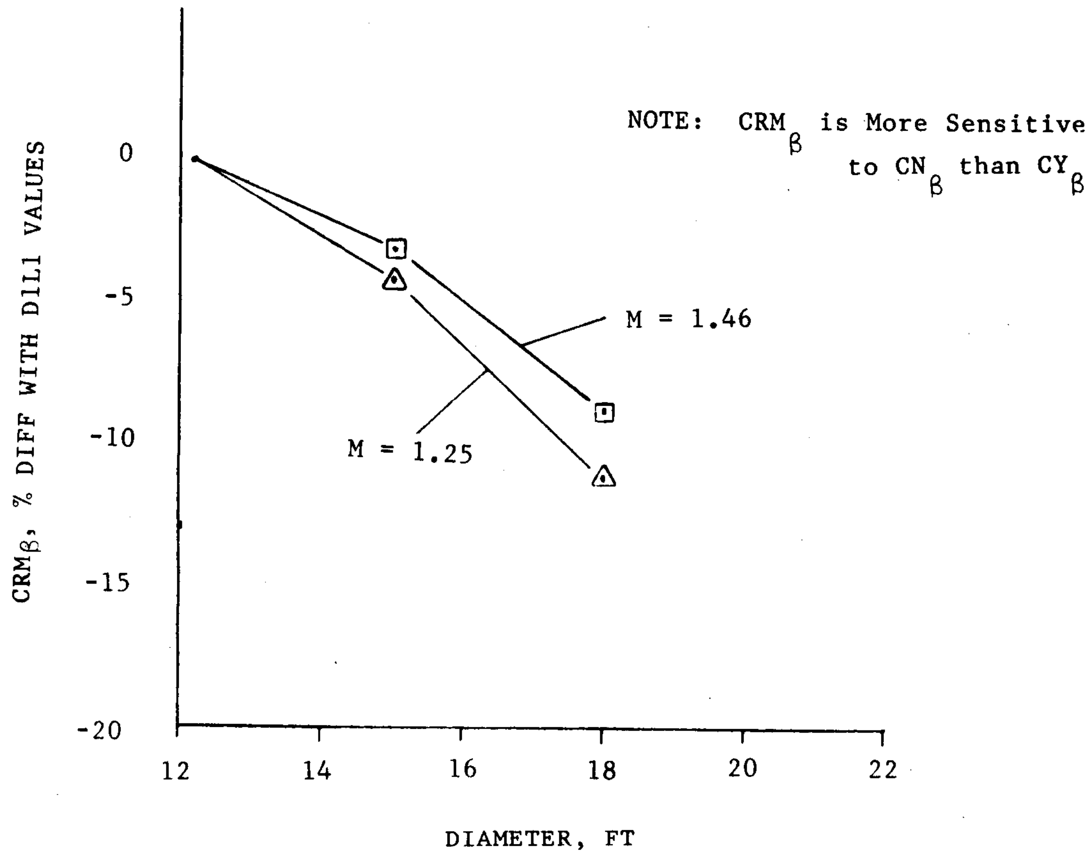

Fig. 4-9 CRM$_\beta$ vs Diameter

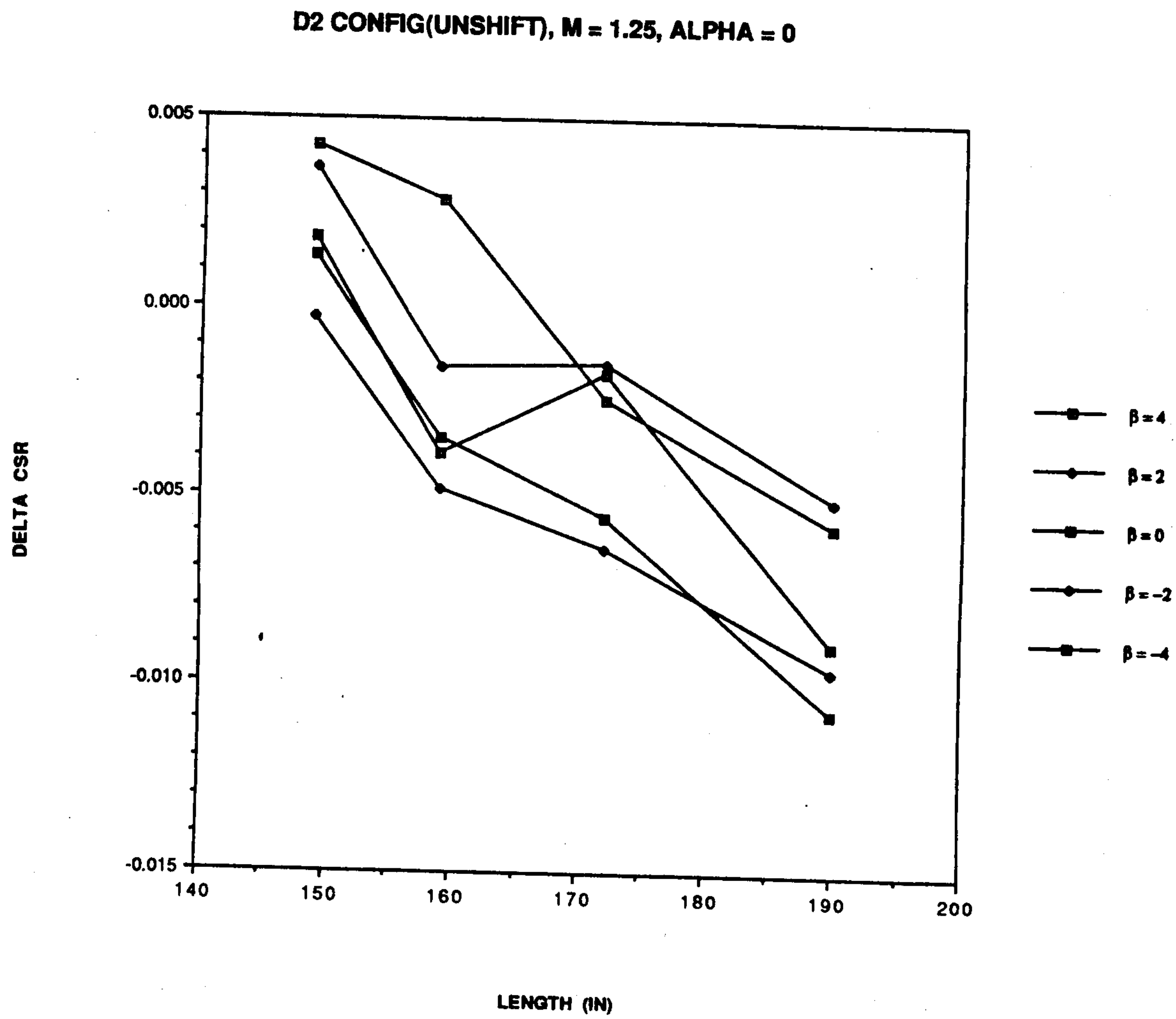

Fig. 4-10 $\Delta\ C_{SR}$ vs Length

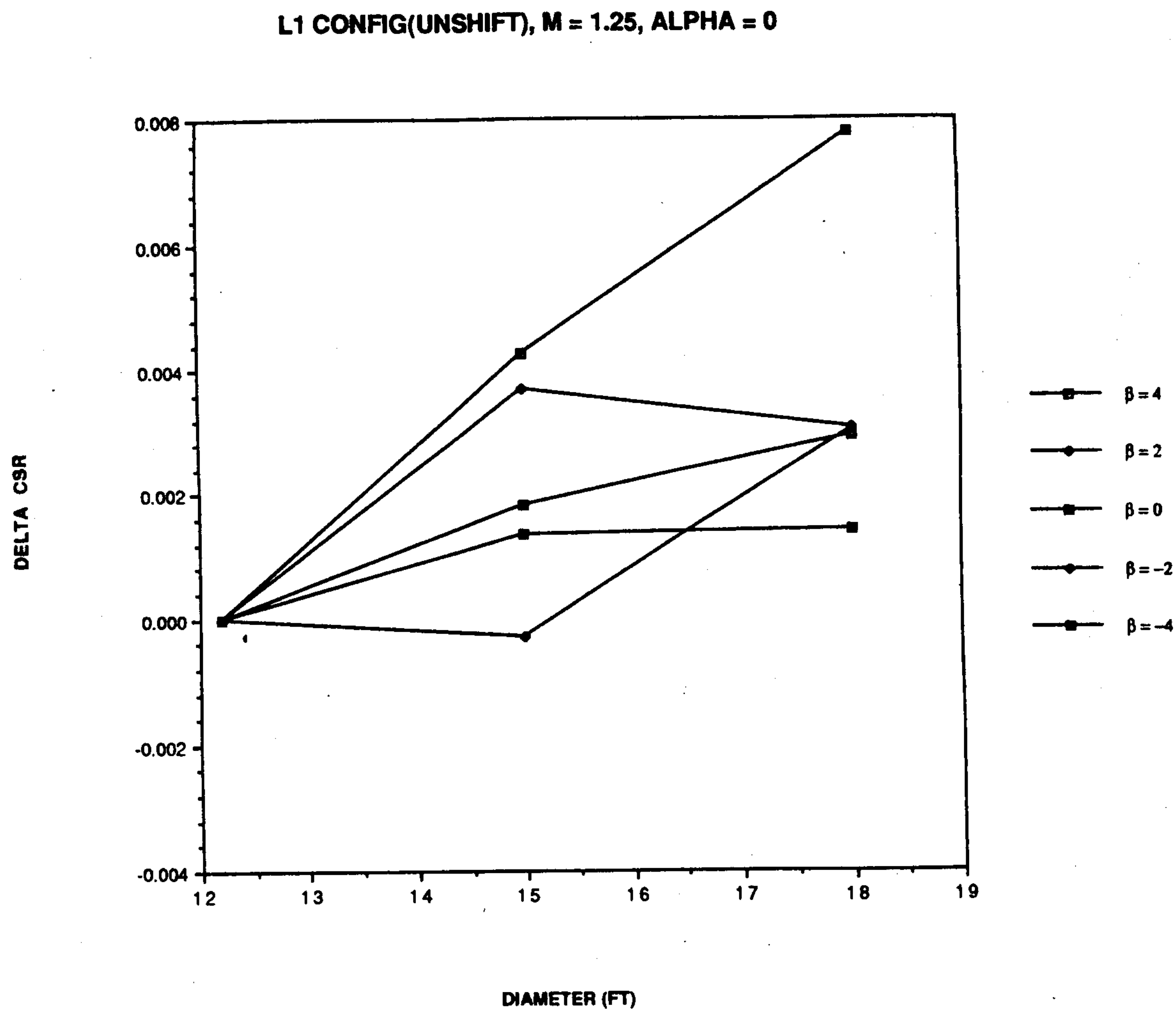

Fig. 4-11 ΔC_{SR} vs Diameter

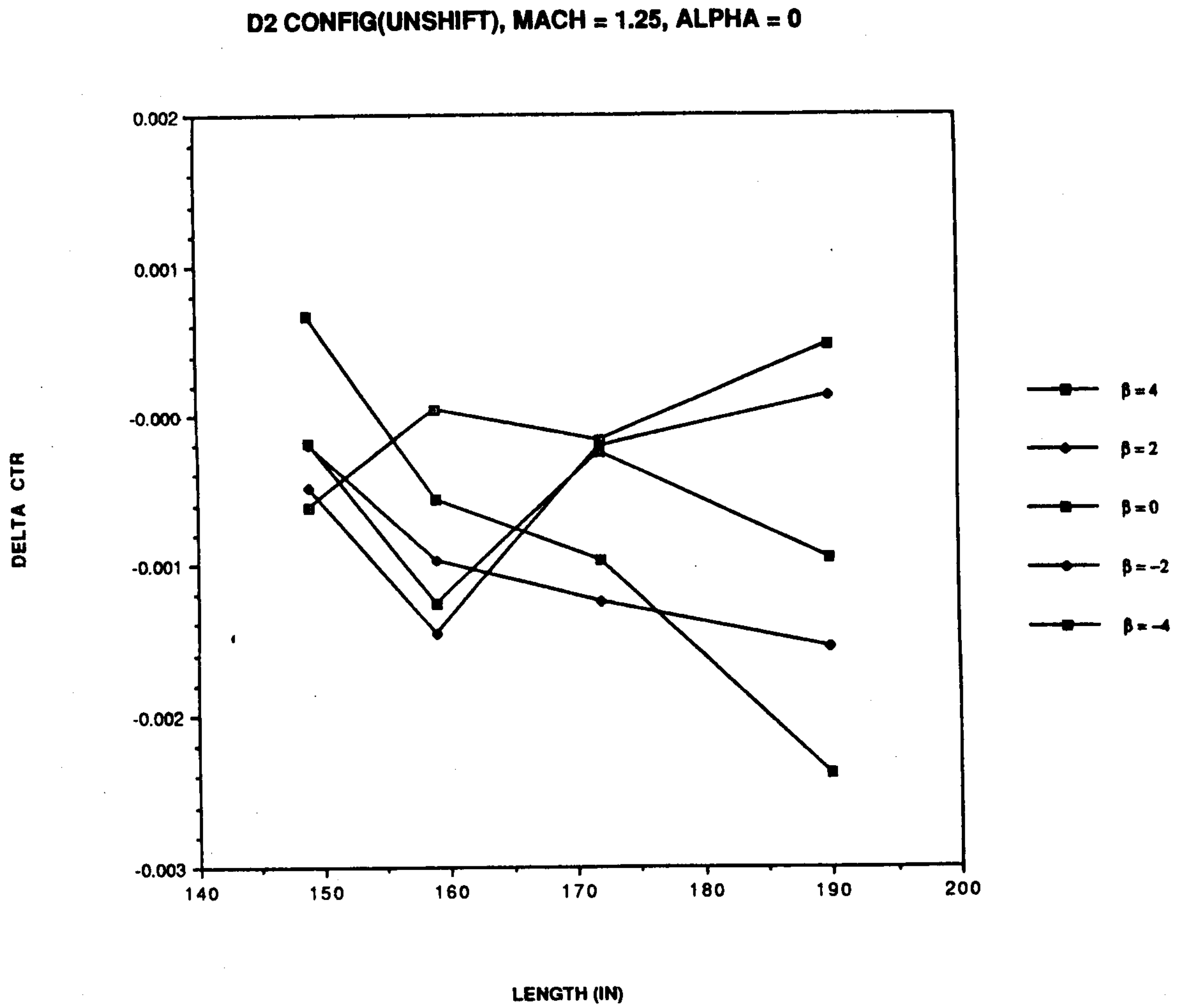

Fig. 4-12 ΔC_{TR} vs Length

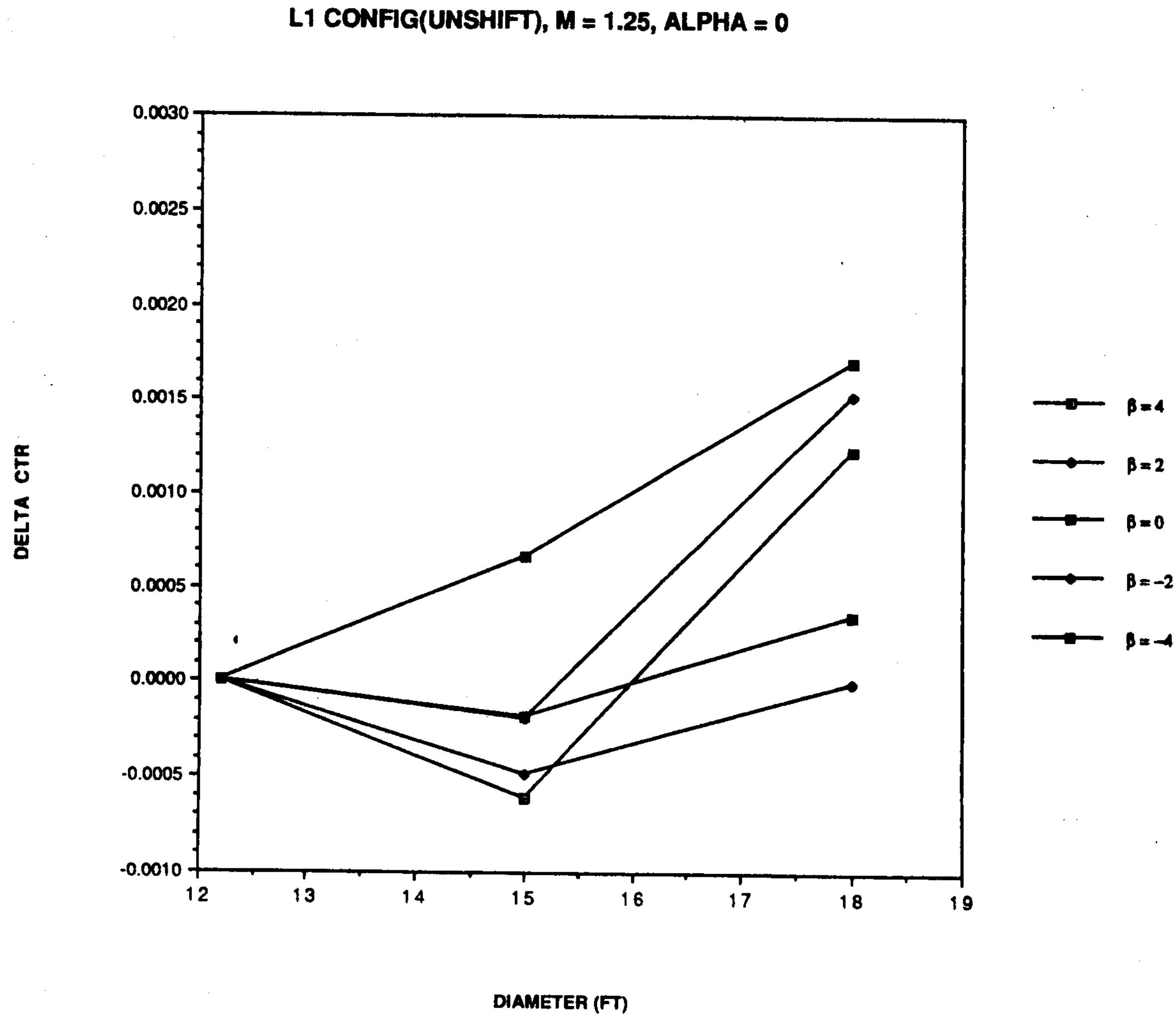

Fig. 4-13 $\Delta\ C_{TR}$ vs Diameter

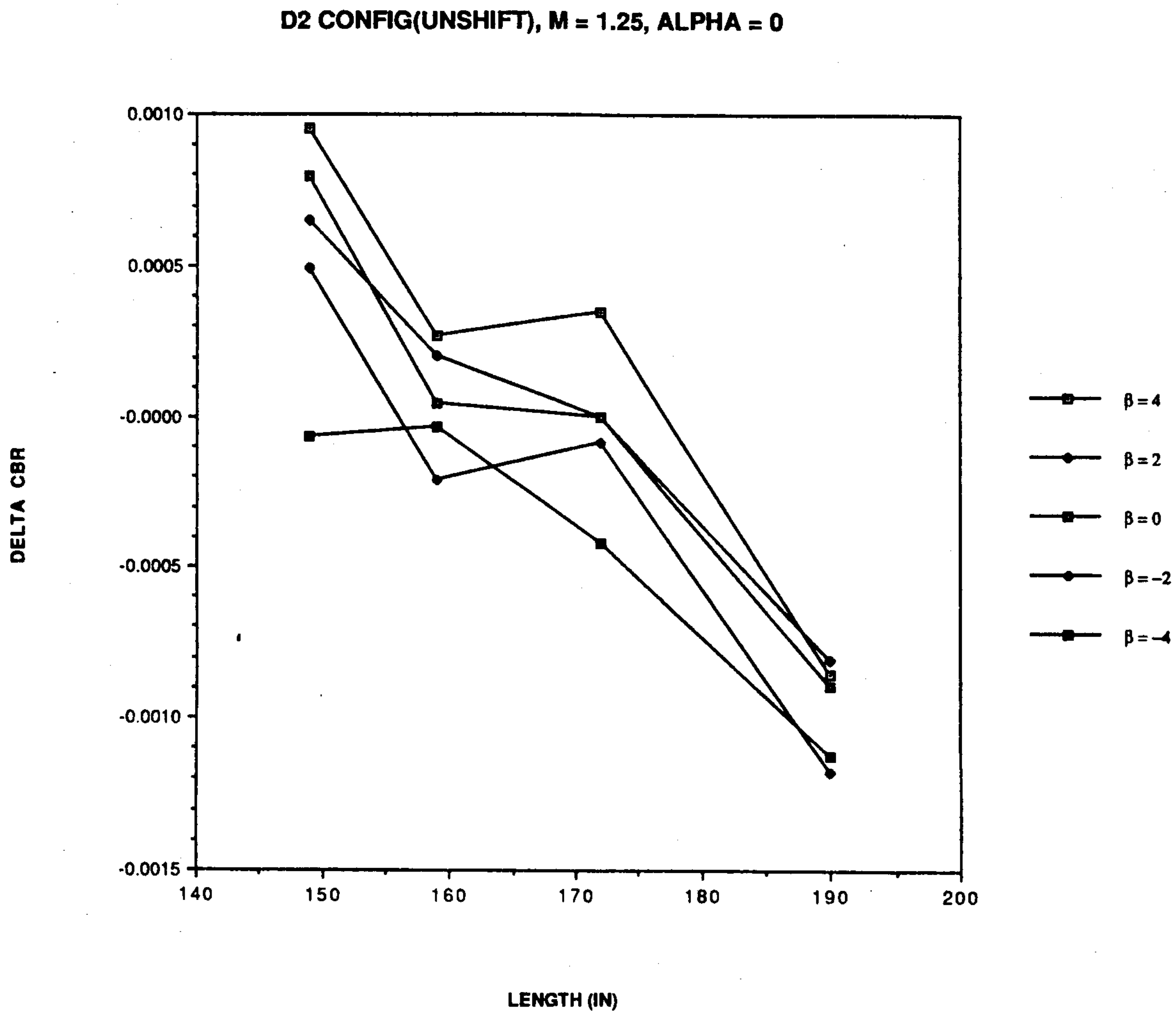

Fig. 4-14 $\Delta\ C_{BR}$ vs Length

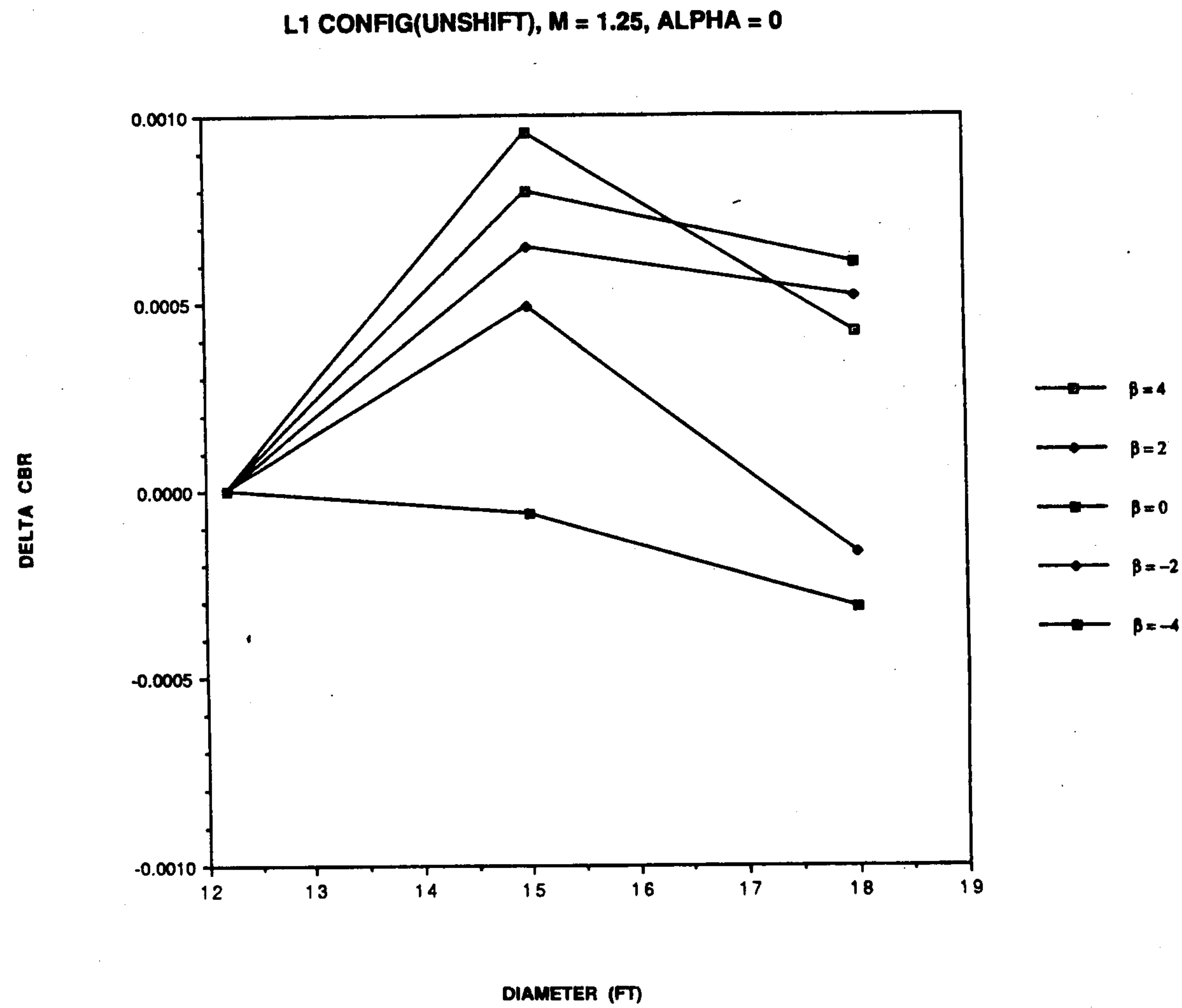

Fig. 4-15 $\Delta\ C_{BR}$ vs Diameter

Table 4-1 DIAMETER EFFECTS OF PHASE II CONFIGURATIONS

- DIAMETER EFFECTS - AN INCREASE IN DIAMETER INCREASES ΔCNF, MOVES X_{CP} FORWARD, INCREASES BOTH ΔC_N-WING AND ΔC_{TR}
- LRB ROTATION EFFECTS (OSXXXX RUNS) - ROTATING THE LRBs DOWNWARD HAS A SMALL EFFECT ON ΔC_{MF} VALUES, PLACE X_{CP} OF THE INCREMENTAL LOADING ON THE MOON, HAS A SMALL EFFECT ON BOTH ΔC_N-WING AND ΔC_{TR}
- HAMMERHEAD EFFECTS (MDXXXX RUNS) - MULTI-DIAMETER LRBs CREATE LARGE CHANGES IN ΔC_{NF} VALUES, HAVE A SMALL EFFECT ON ΔC_{MF} VALUES MOVE X_{CP} FORWARD, CAUSE A DECREASE IN $\Delta\ C_N$-WING AND ΔC_{TR}
- STACKED CONFIGURATION EFFECTS (STXXXX RUNS) - STACKING LRBs CREATE LARGE CHANGES IN ΔC_{NF} VALUES AND ΔC_{MF}, PLACES X_{CP} AT THE BASE OF THE ORBITER, CAUSES A SMALL INCREASE IN C_N-WING
- HAMMER GAP AND FLOW EXPANSION ARE EFFECTIVE IN REDUCING WING LOADS.

5. PROTUBERANCE EFFECTS

Wind tunnel testing was conducted to investigate the aerodynamic effects of protuberances on the SSLV. This section details the results of protuberance analysis from wind tunnel testing. Three configurations were tested: a baseline SRB, an SRB without protuberances, and an SRB with out the IEA Cover. The fairing configurations were also varied. Figures 5-1 and 5-2 present the four configurations analyzed. A Mach number range of 0.8 to 4.45 was used for testing. Results from the test can be found in Figs. 5-3 to 5-20 which depict protuberance and fairing efforts.

5.1 PROTUBERANCE EFFECTS

Analysis indicated that SRB protuberances have major effects on wing loads. A significant increase in the vehicle normal force increment is exhibited in the presence of SRB protuberances. The majority of the increase can be attributed to orbiter wing shear. Further, the SRB/ET aft attach ring/ IEA position and geometry have adverse effects on the orbiter ascent wing loads. Wind tunnel testing suggested that ascent wing load reduction can be accomplished by removal or modification of the IEA/attach ring. Additional efforts, however, would be required to study the impact of the IEA relocation. Also a trajectory analysis should be considered to determine performance or launch probability increase due to wing load reduction. Finally, a complete evaluation of the fairing configurations should be performed with regard to aerodynamic enhancement.

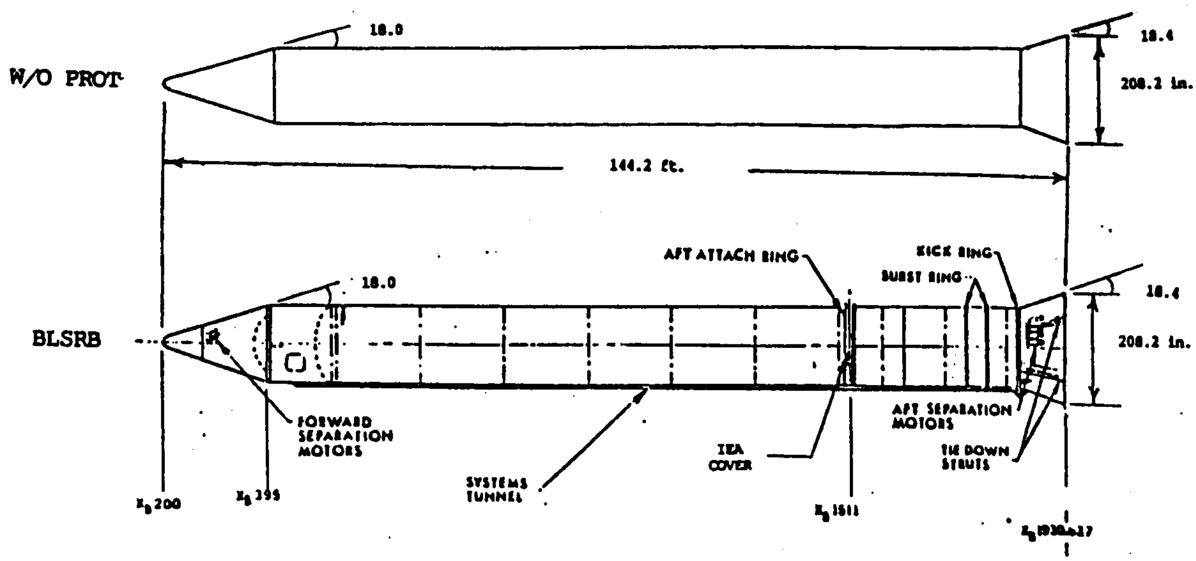

Fig. 5-1 SRB Protuberance Configurations

ORIGINAL PAGE IS
OF POOR QUALITY

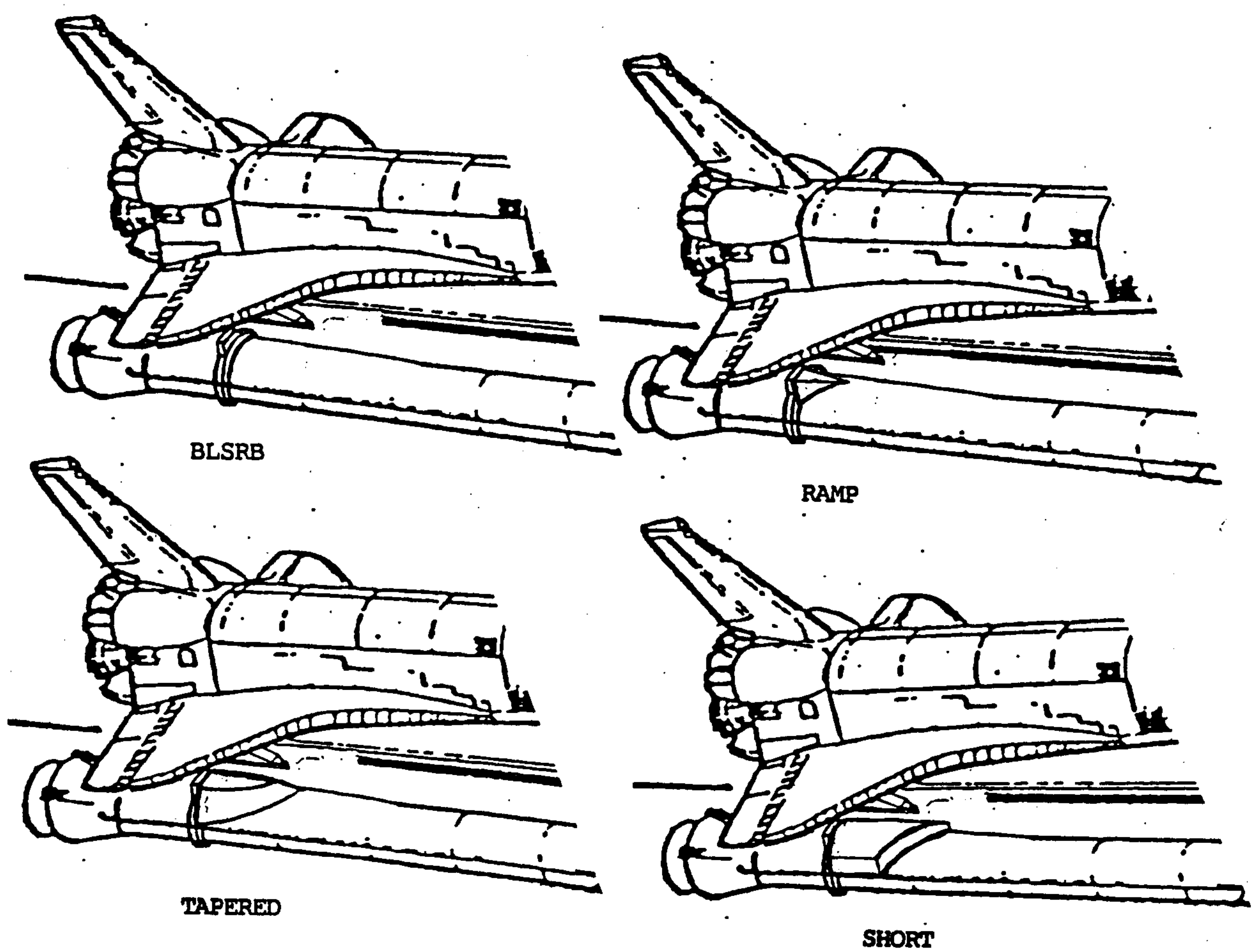

Fig. 5-2 SRB Fairing Configurations

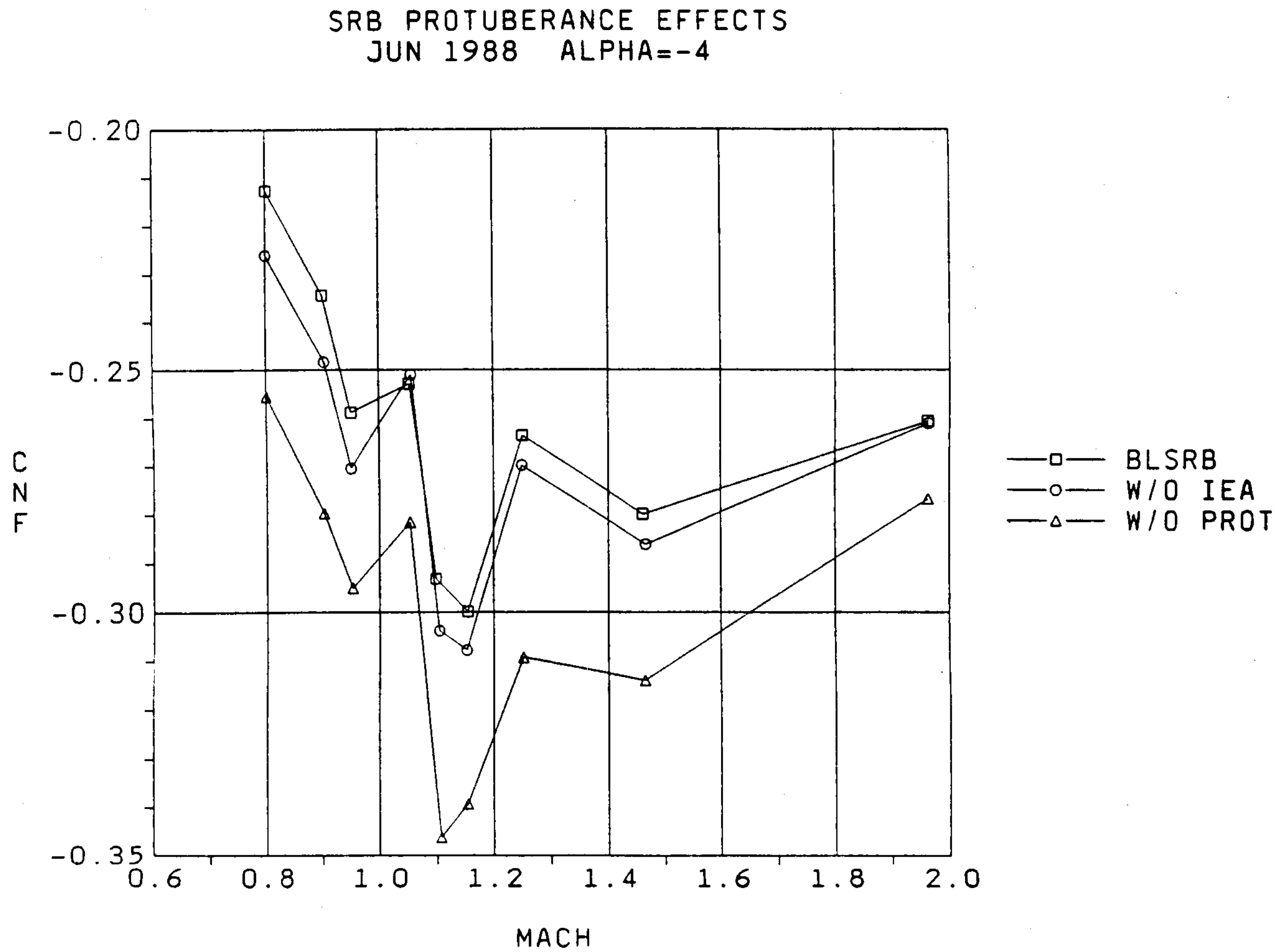

Fig. 5-3 CNF (Protuberance Effects)

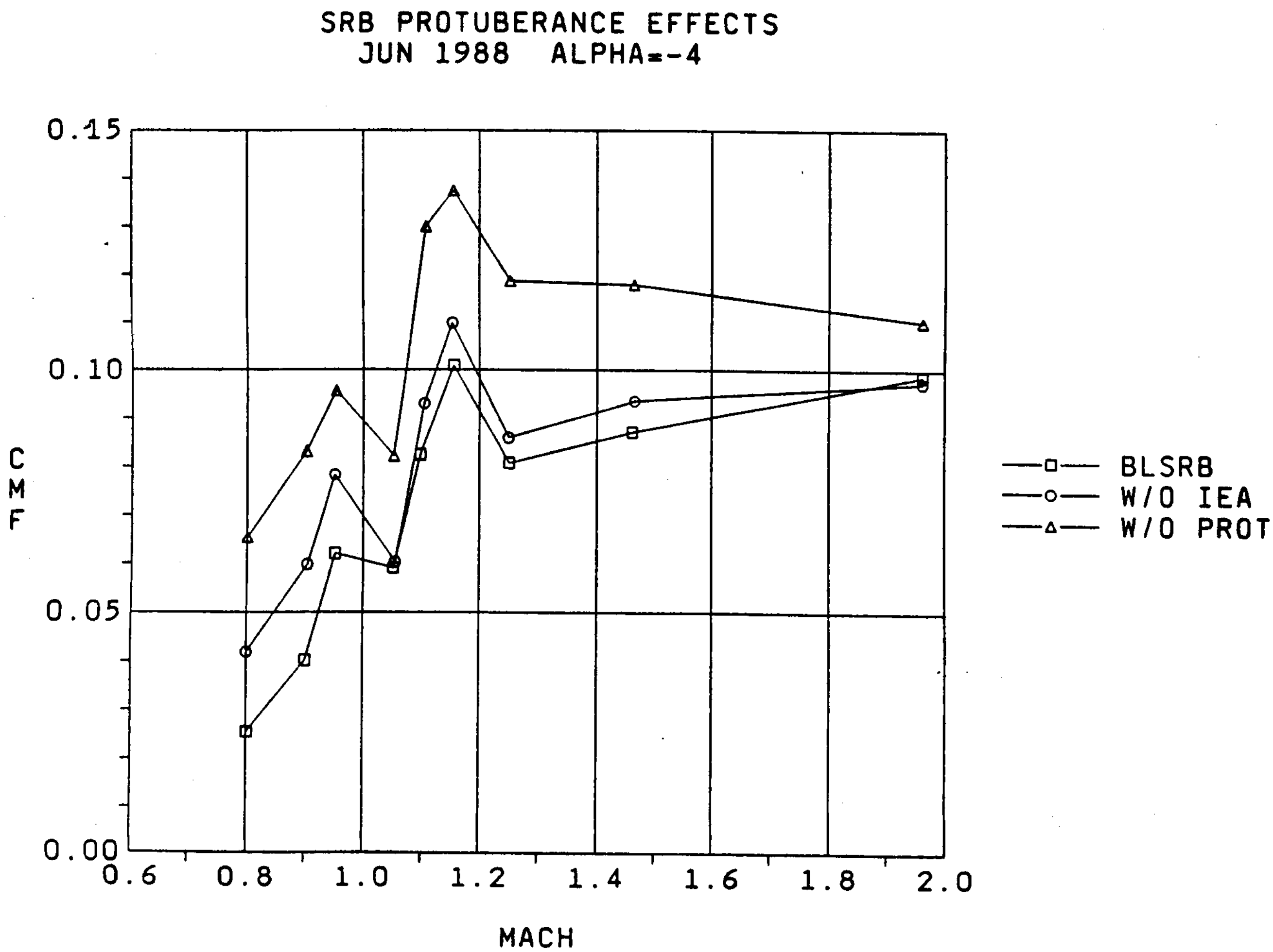

Fig. 5-4 CMF (Protuberance Effects)

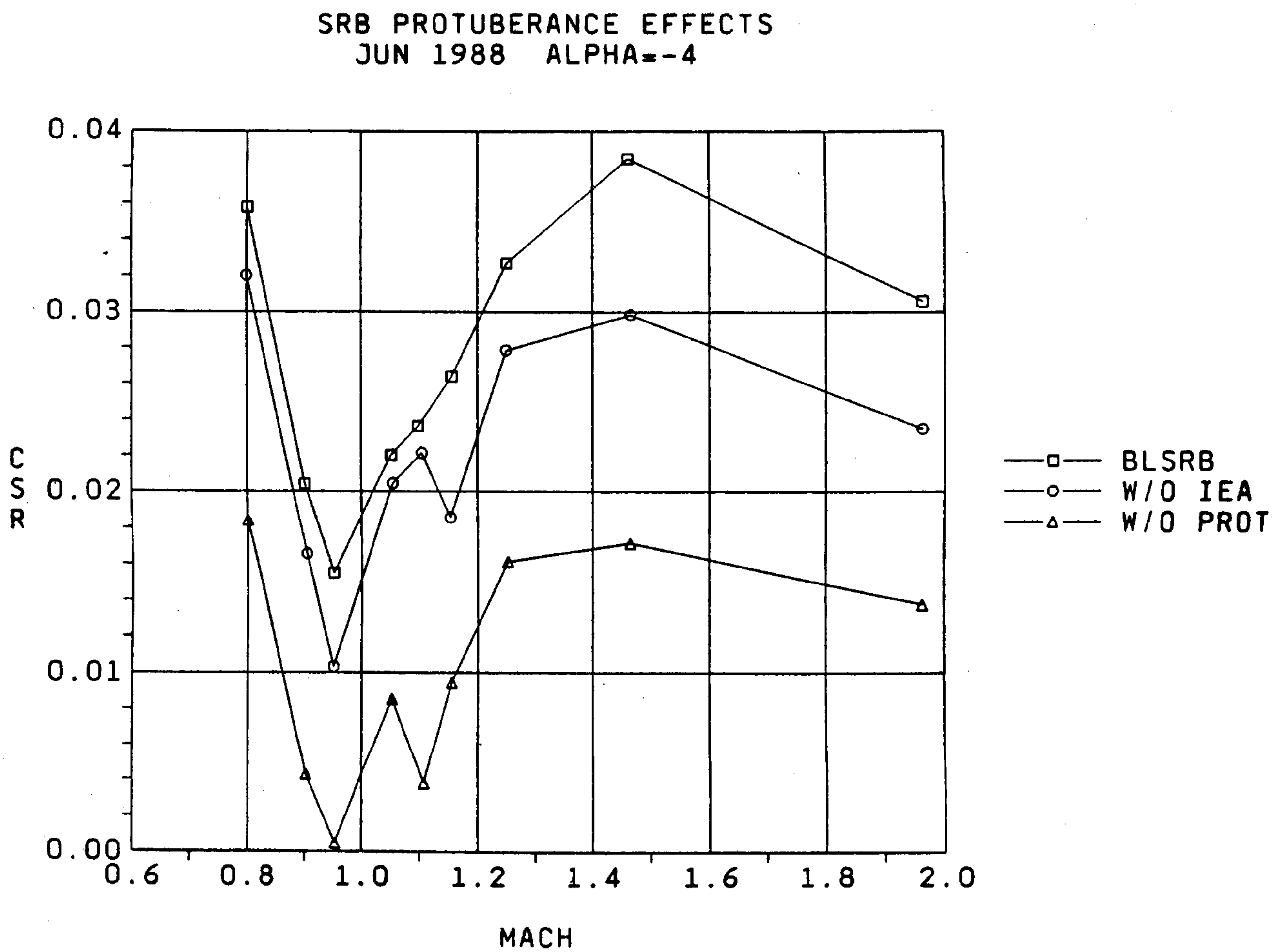

Fig. 5-5 CSR (Protuberance Effects)

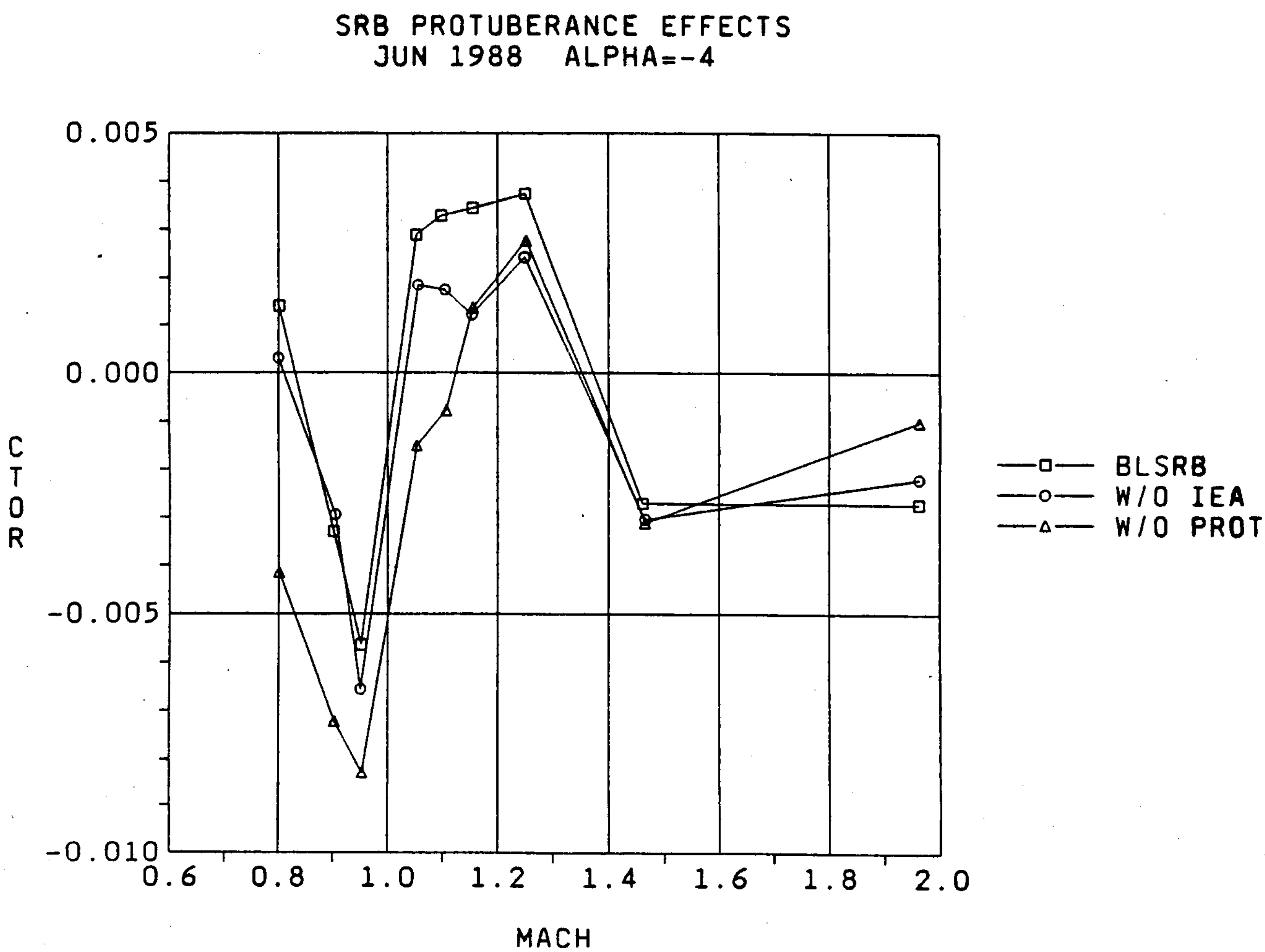

Fig. 5-6 CTOR (Protuberance Effects)

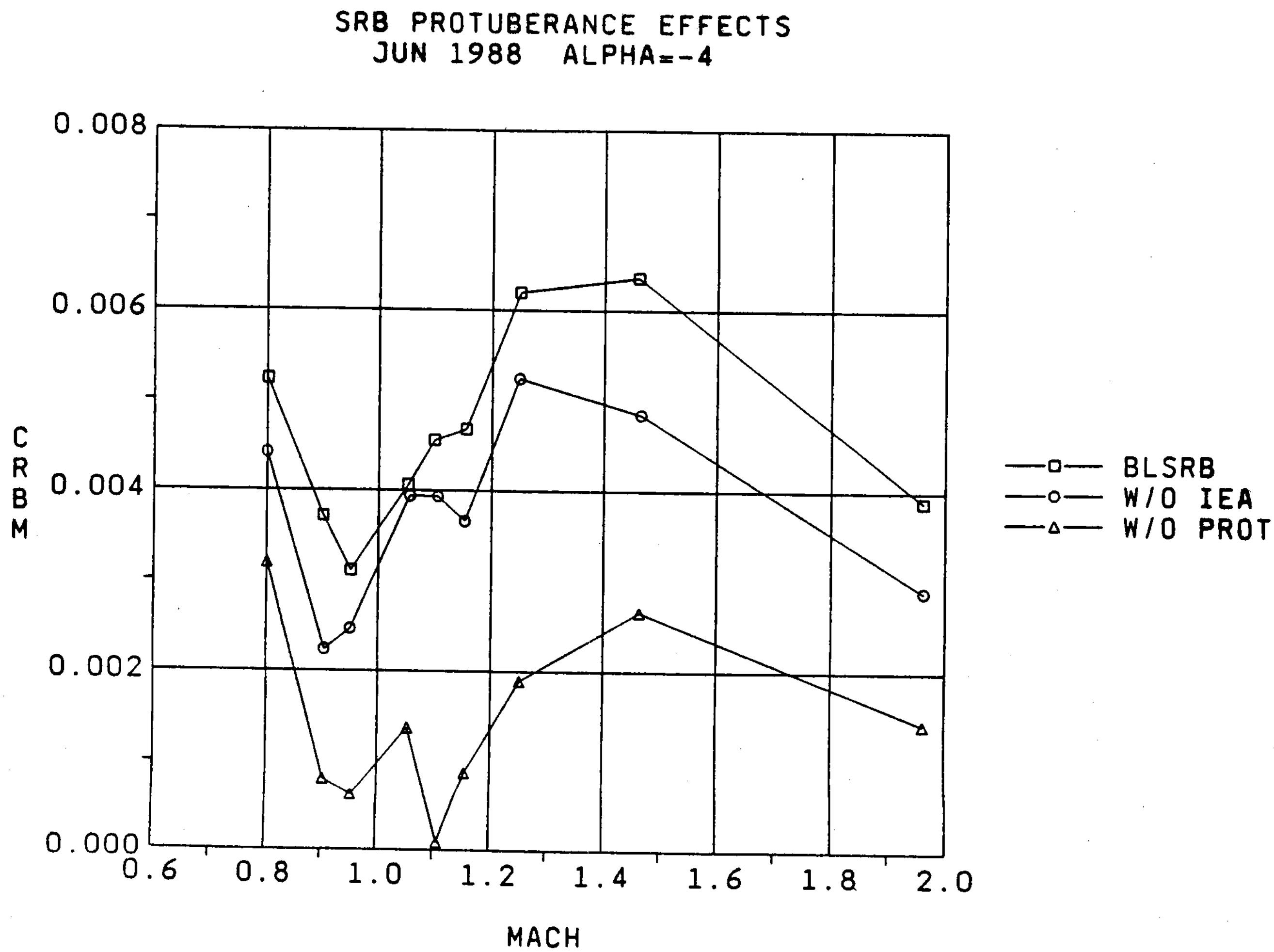

Fig. 5-7 CRBM (Protuberance Effects)

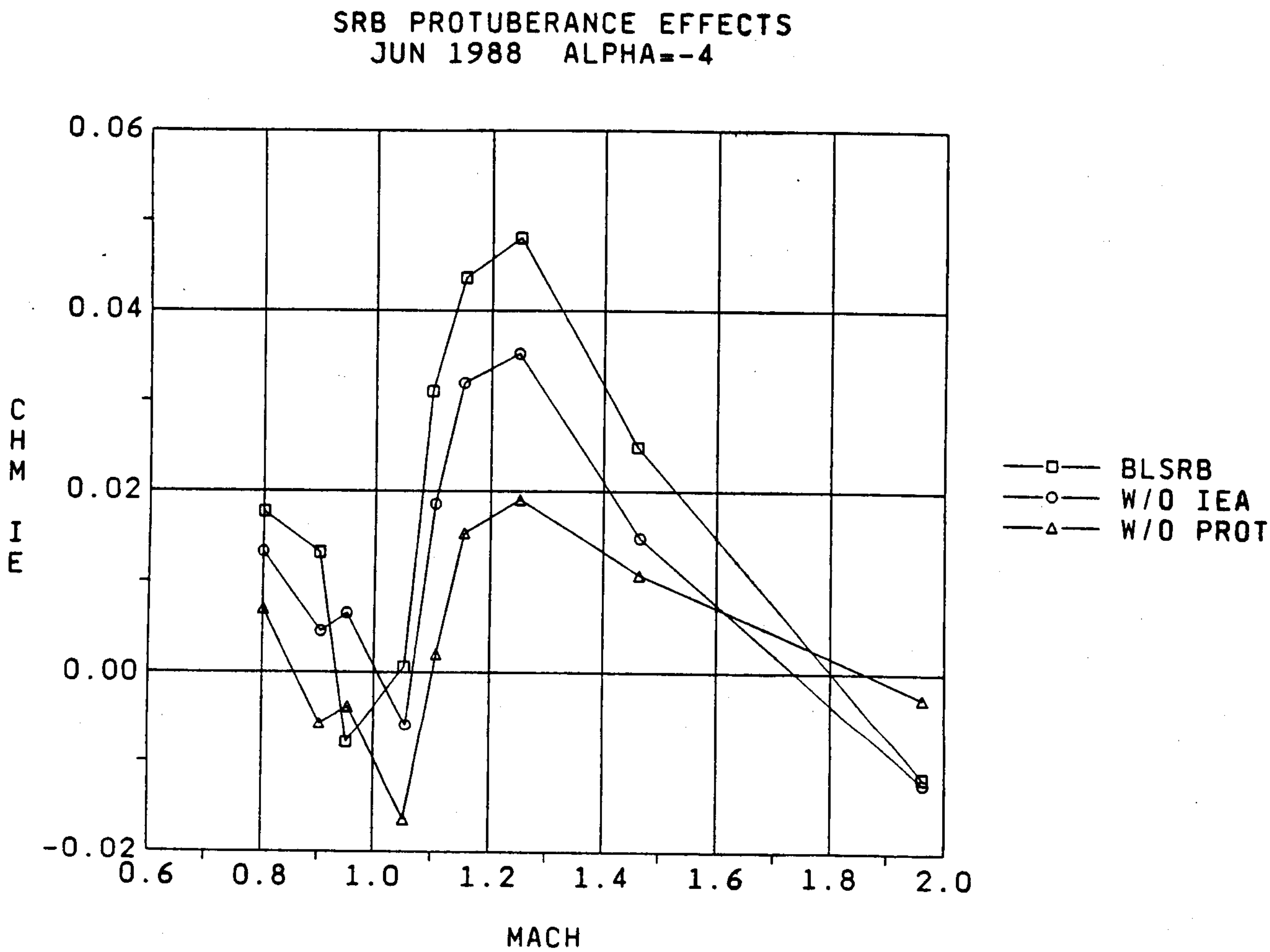

Fig. 5-8 CHMIE (Protuberance Effects)

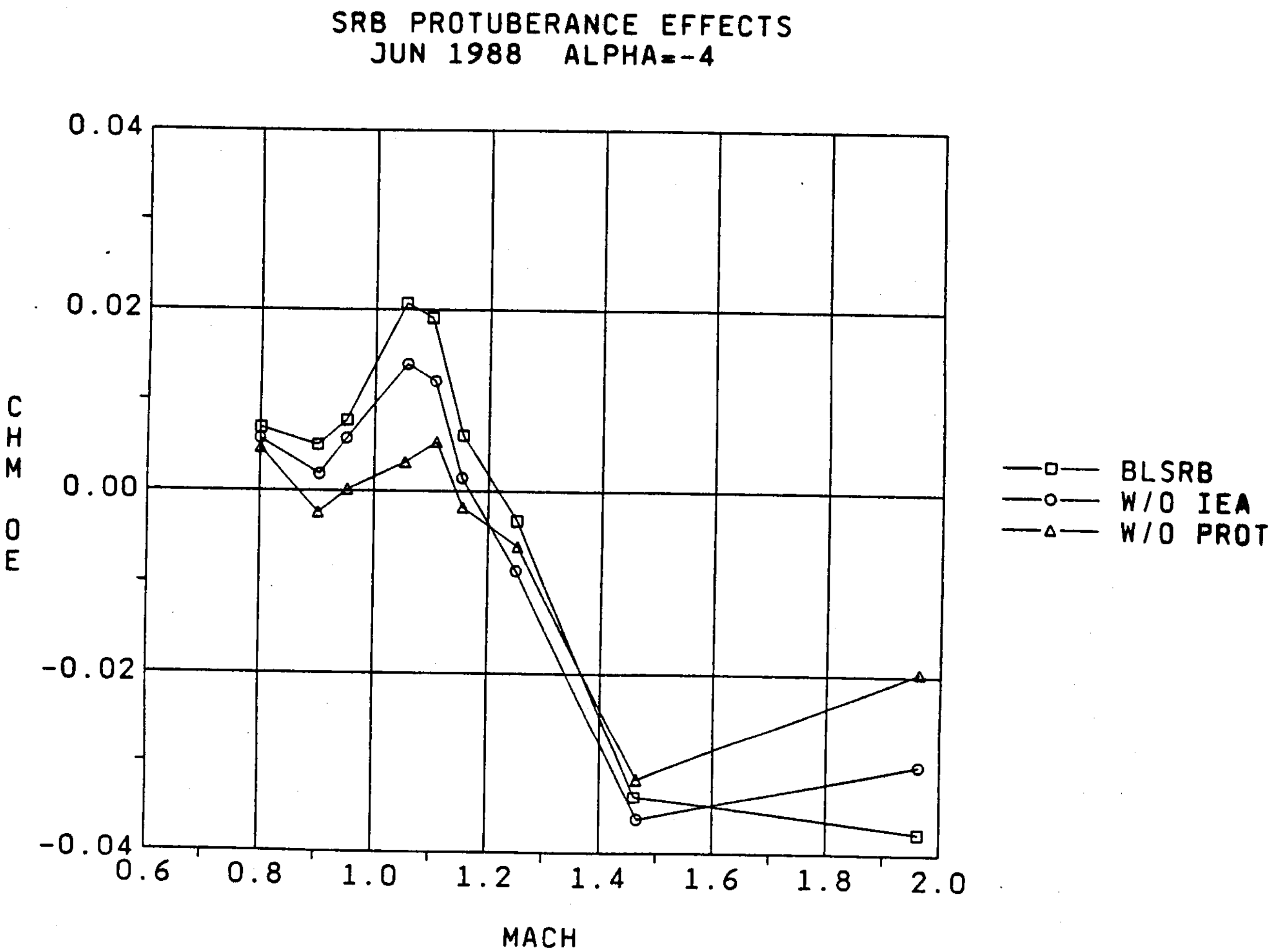

Fig. 5-9 CHMOE (Protuberance Effects)

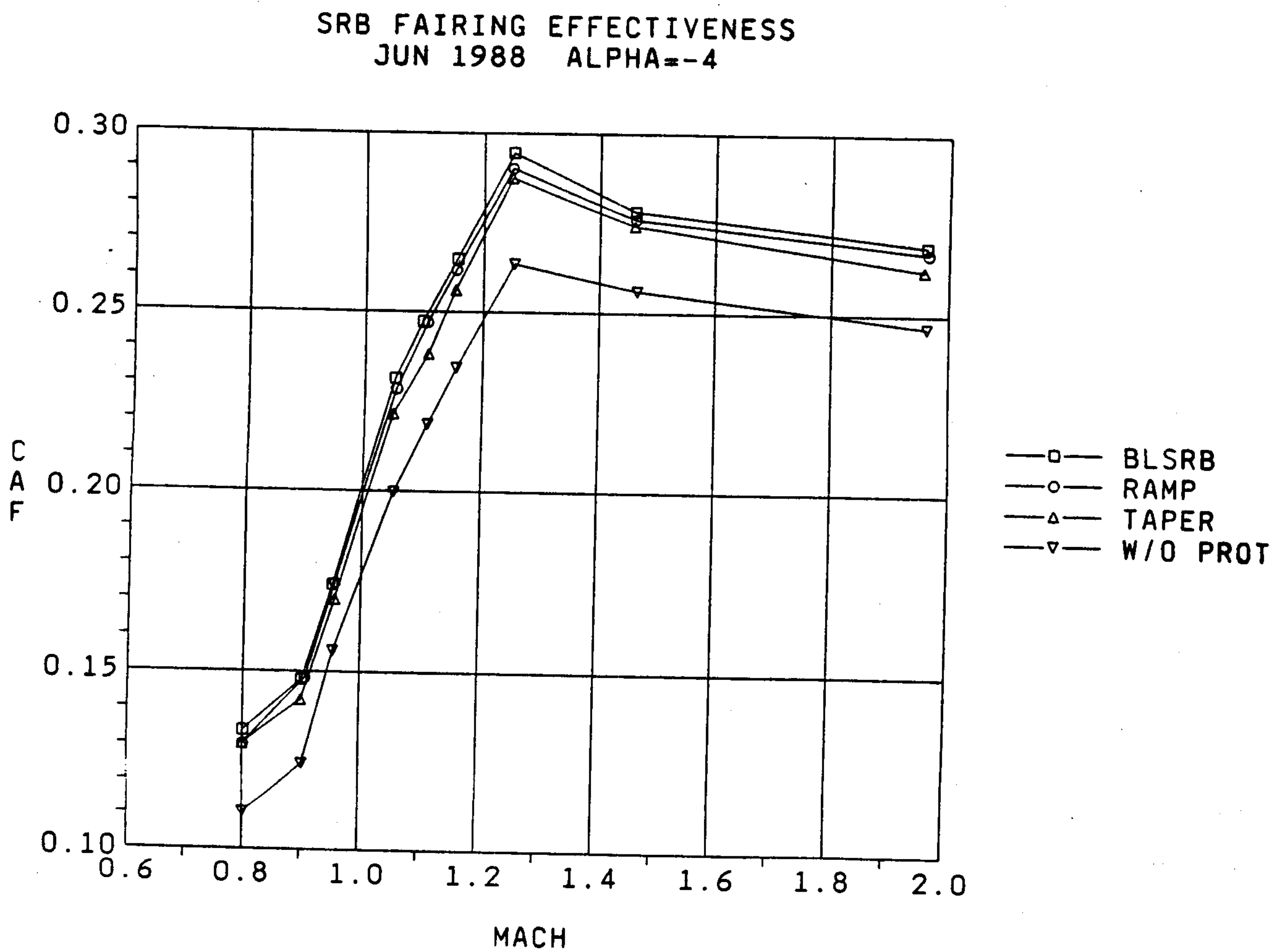

Fig. 5-10 CAF (Fairing/Protuberance Effects)

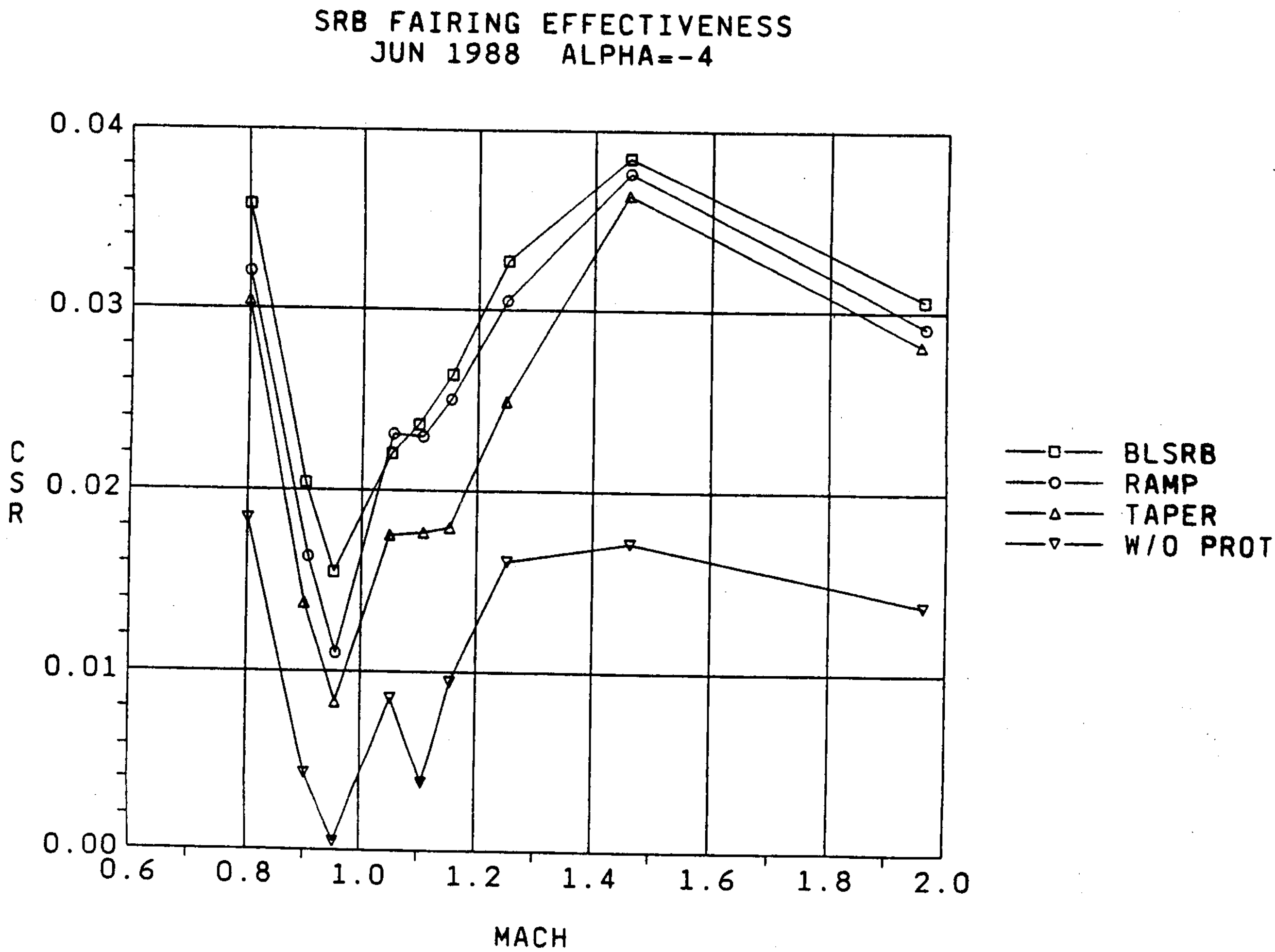

Fig. 5-11 CSR (Fairing/Protuberance Effects)

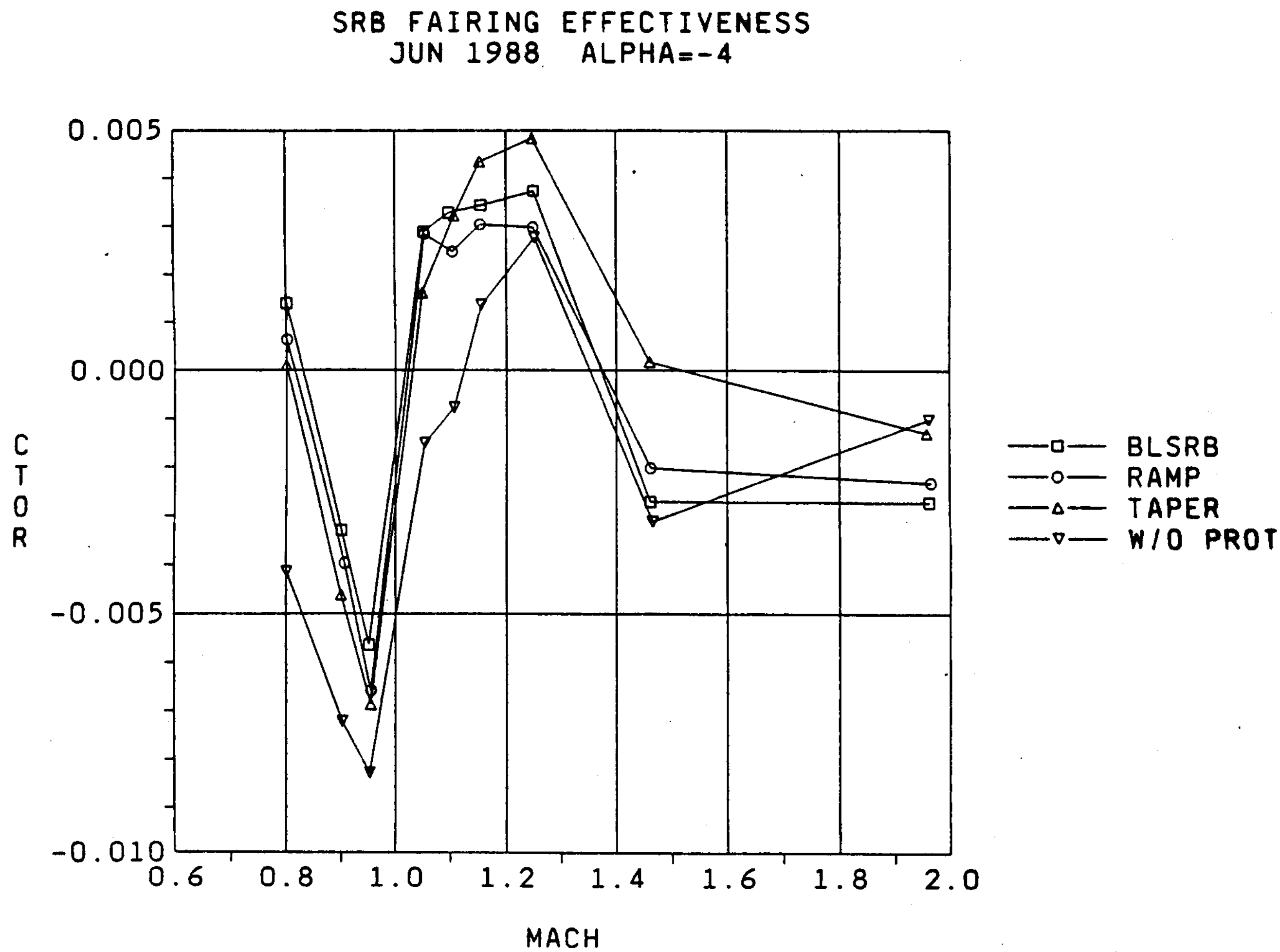

Fig. 5-12 CTOR (Fairing/Protuberance Effects)

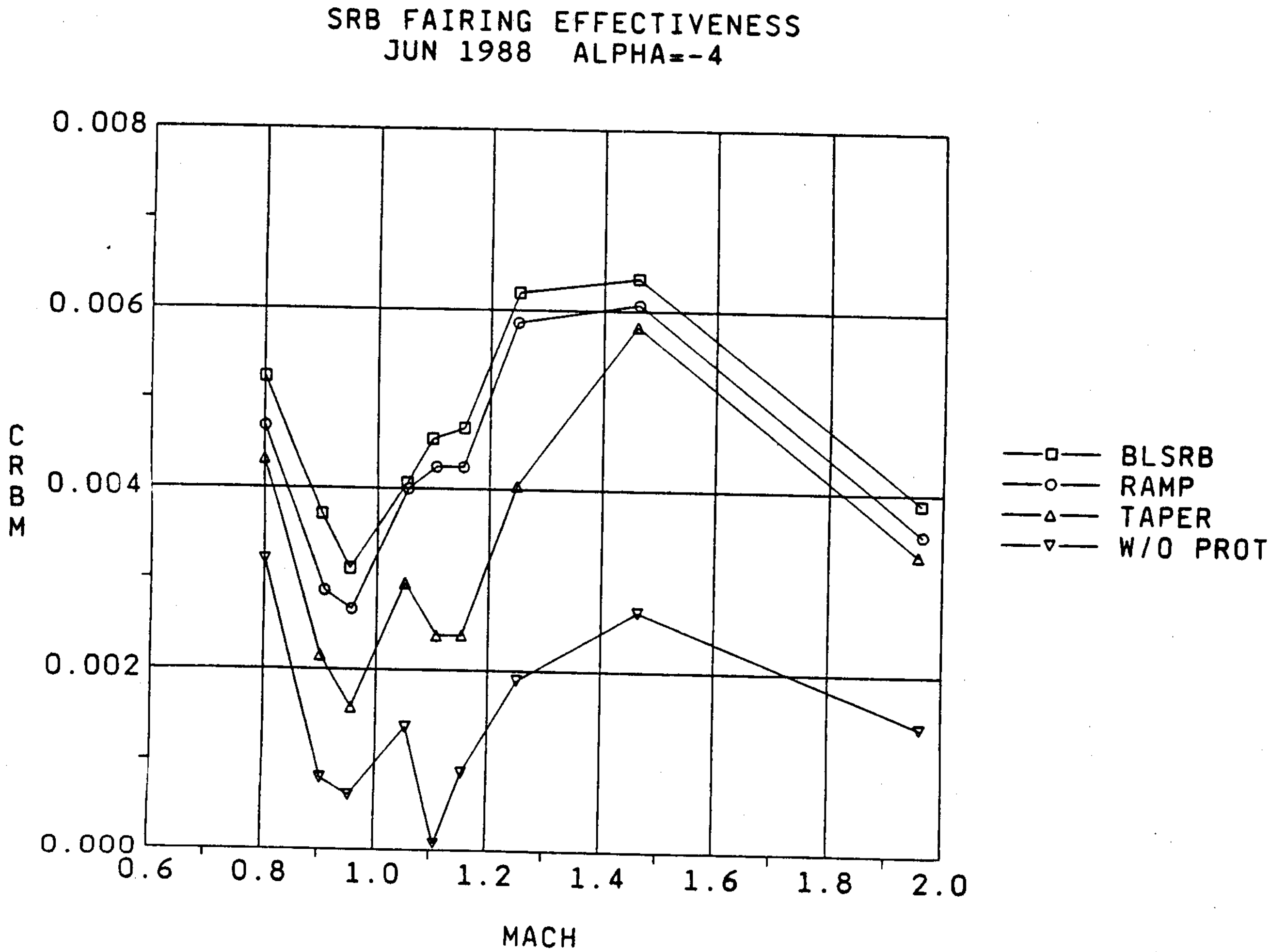

Fig. 5-13 CRBM (Fairing/Protuberance Effects)

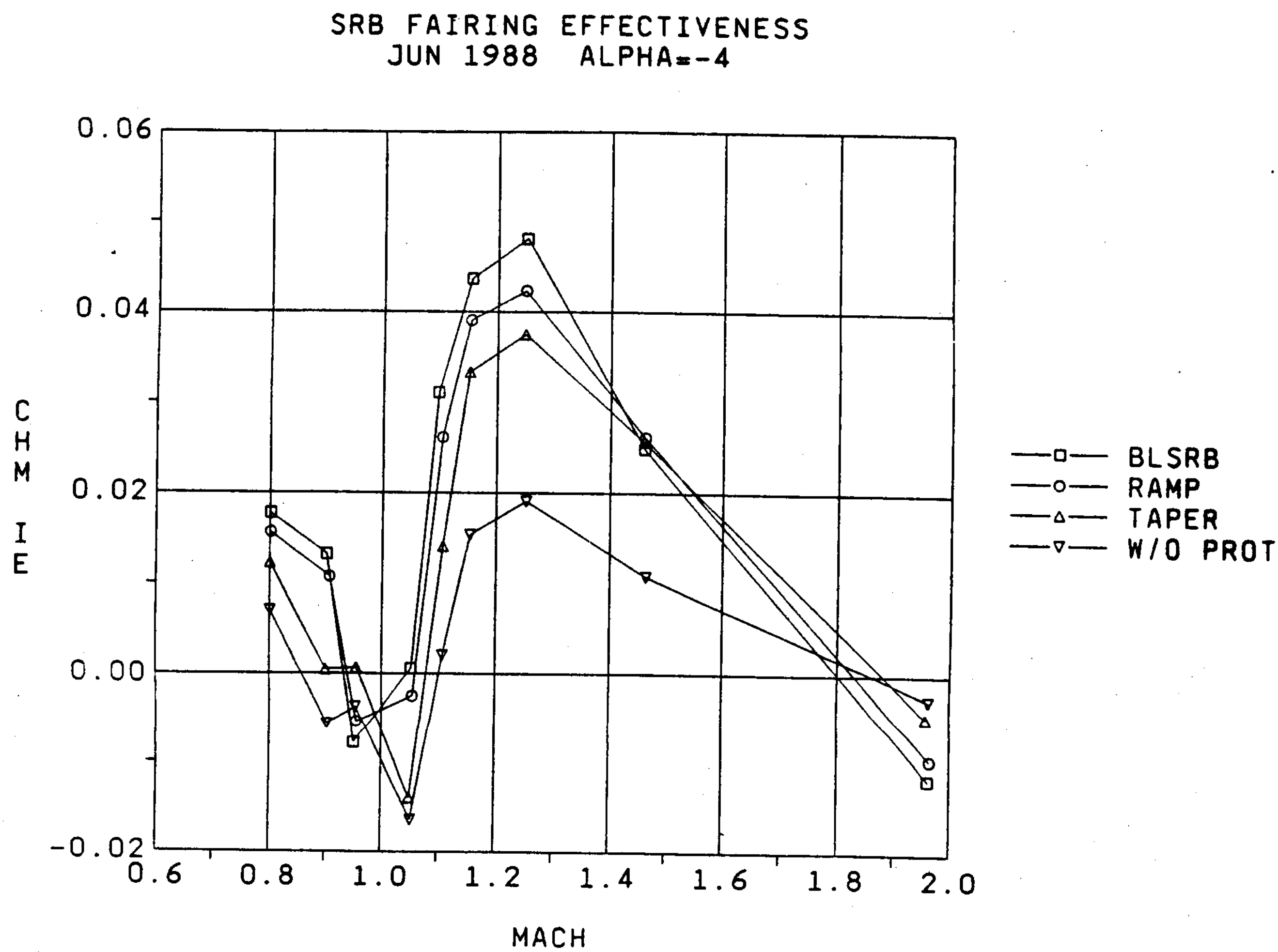

Fig. 5-14 CHMIE (Fairing/Protuberance Effects)

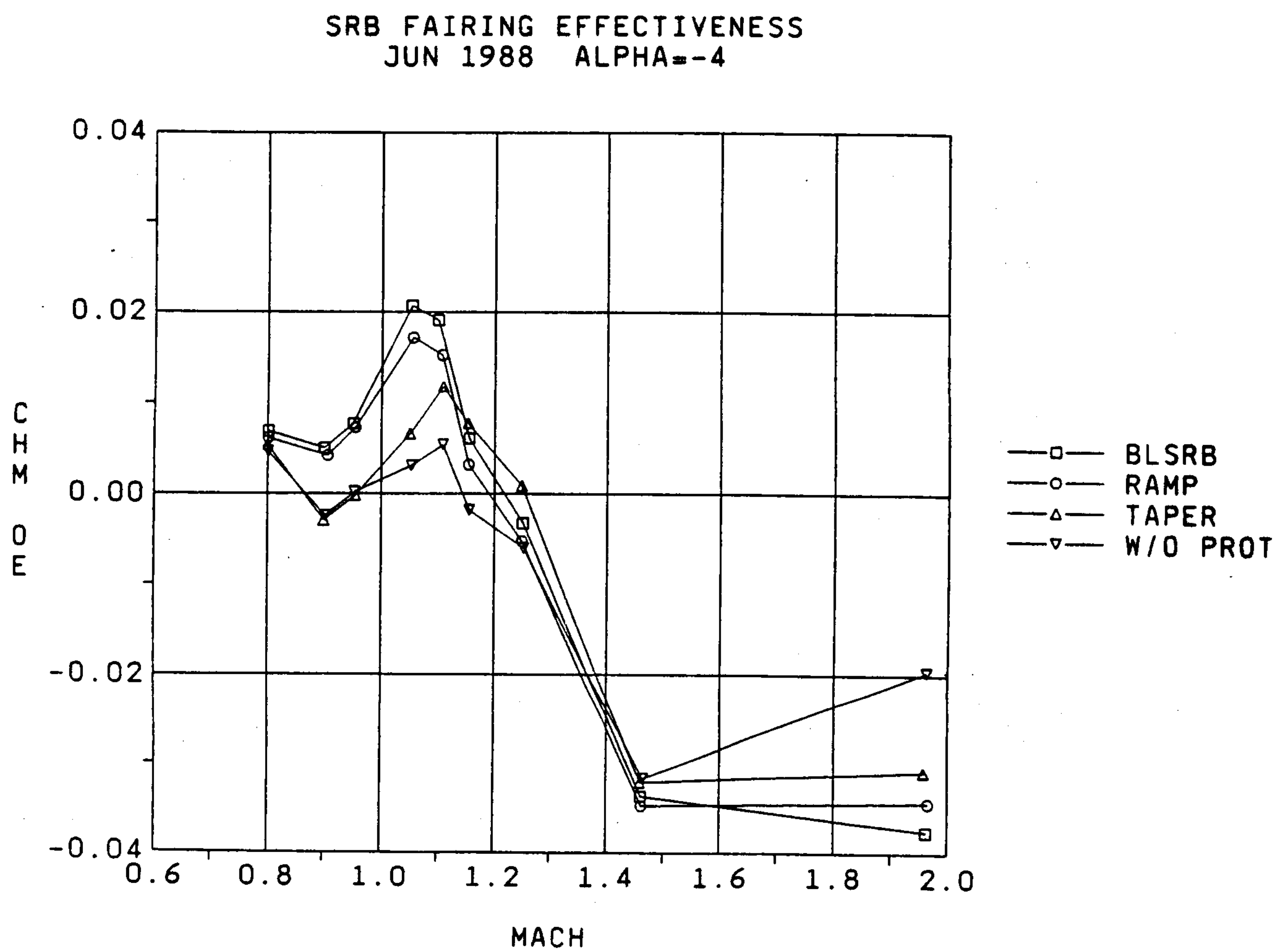

Fig. 5-15 CHMOE (Fairing/Protuberance Effects)

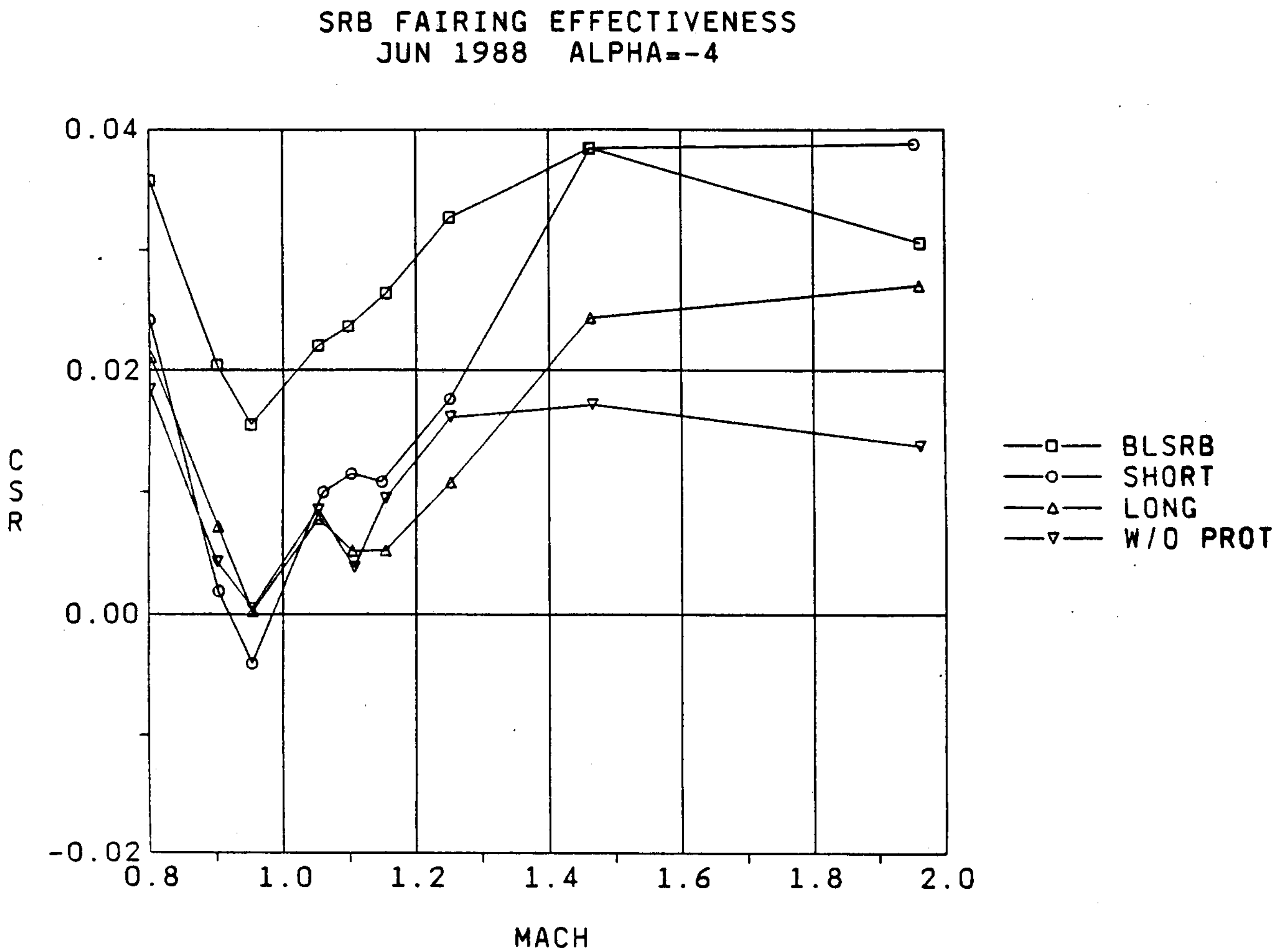

Fig. 5-16 CSR (Fairing/Protuberance Effects)

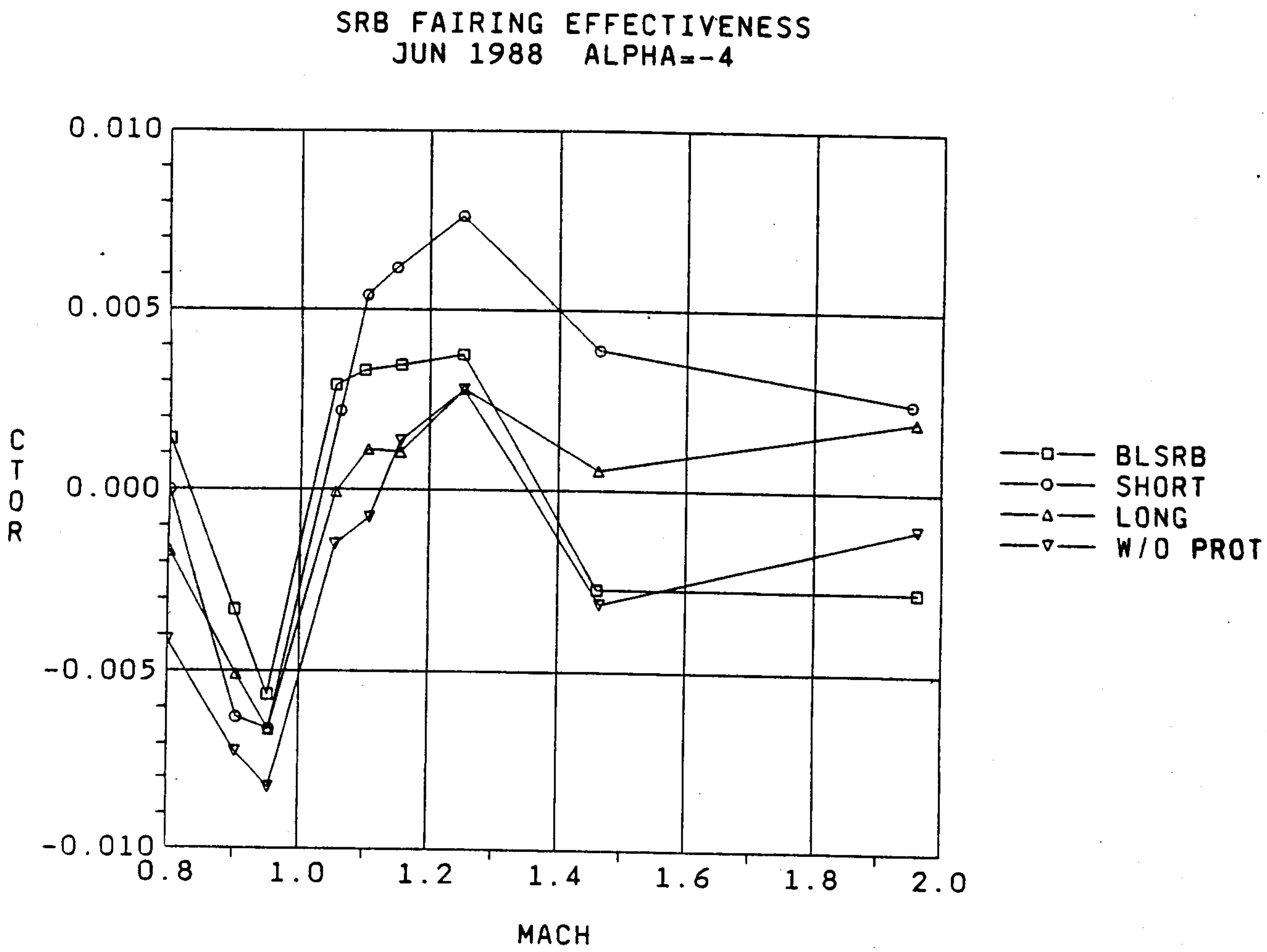

Fig. 5-17 CTOR (Fairing/Protuberance Effects)

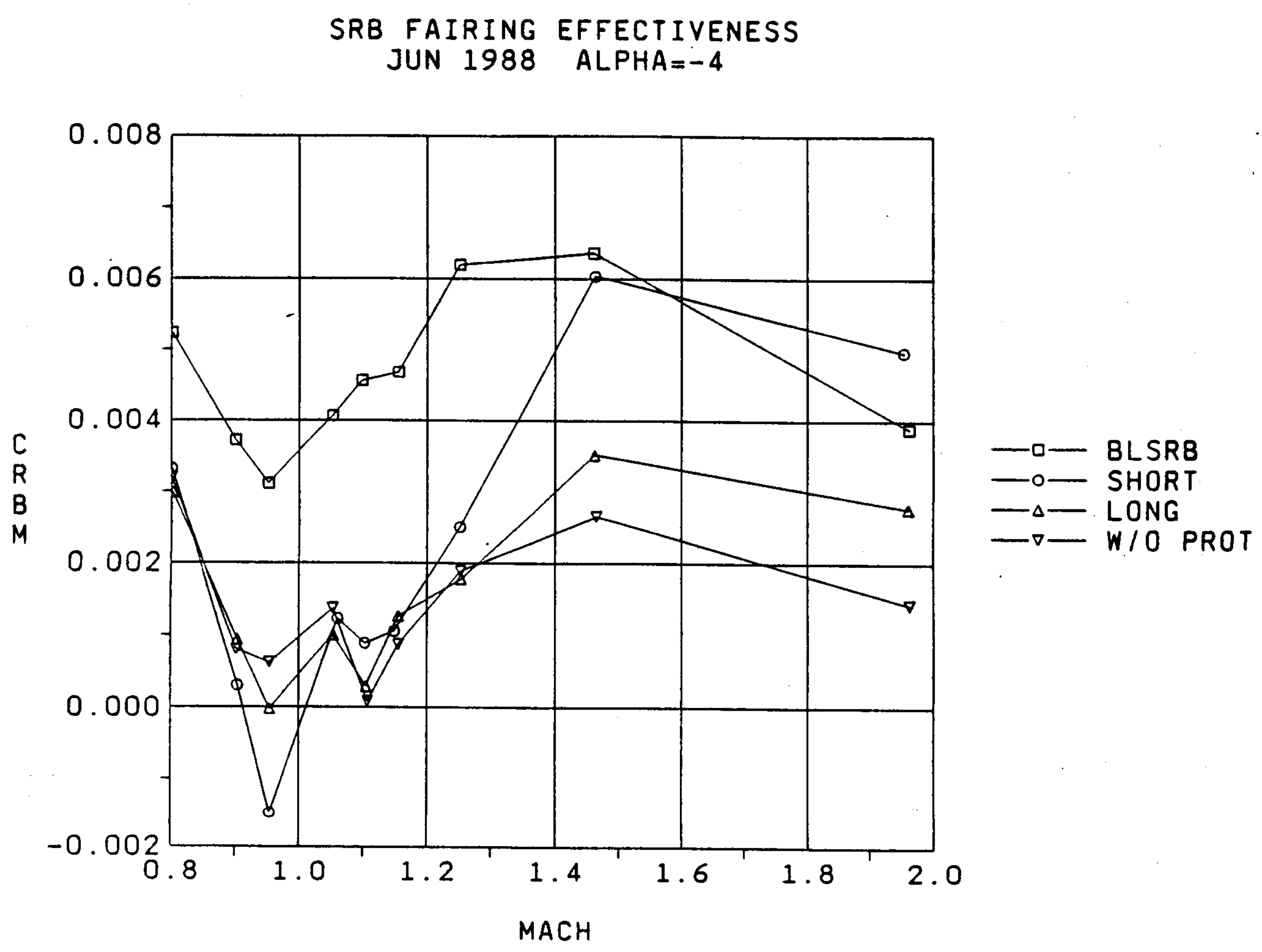

Fig. 5-18 CRBM (Fairing/Protuberance Effects)

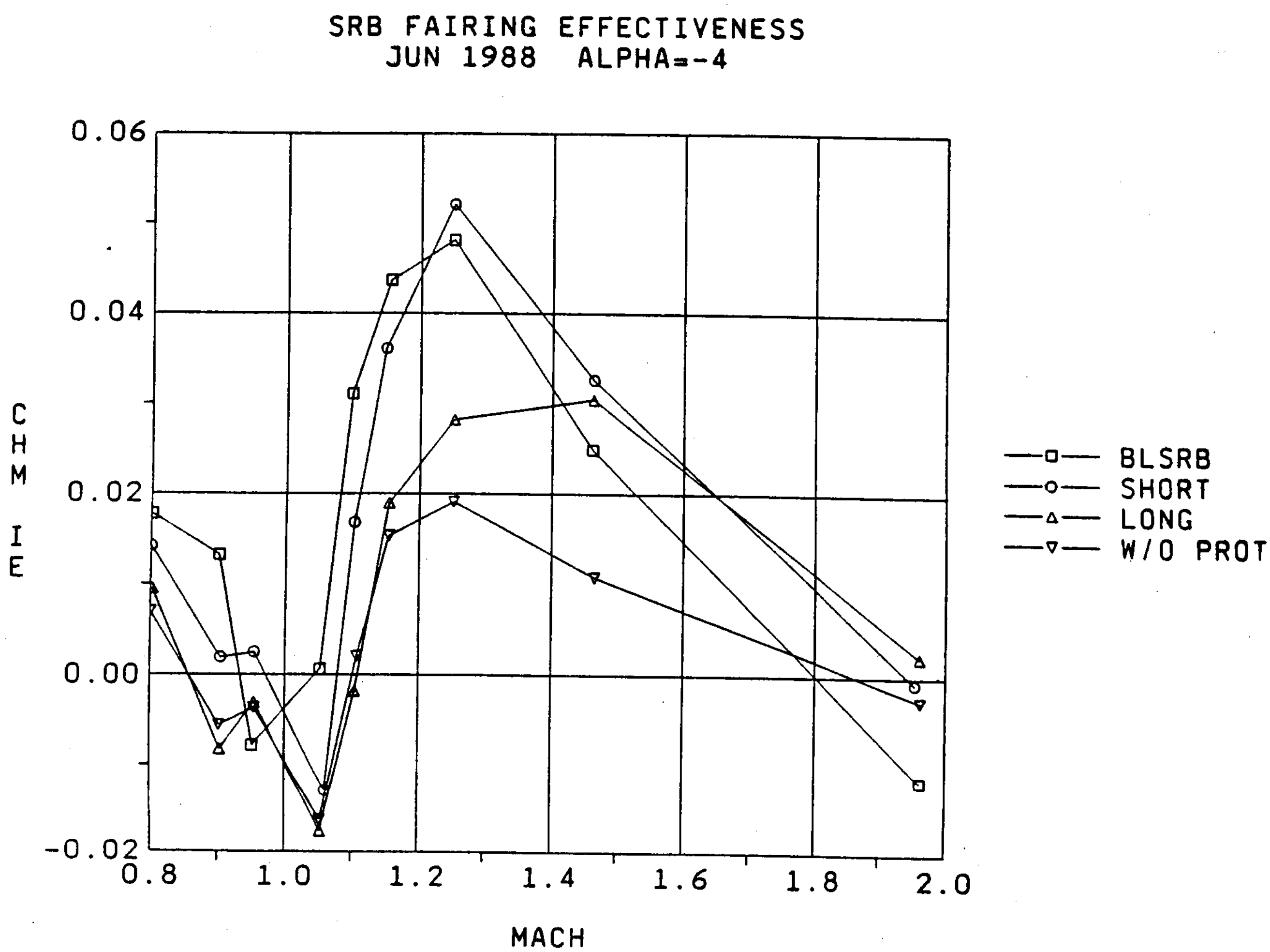

Fig. 5-19 CHMIE (Fairing/Protuberance Effects)

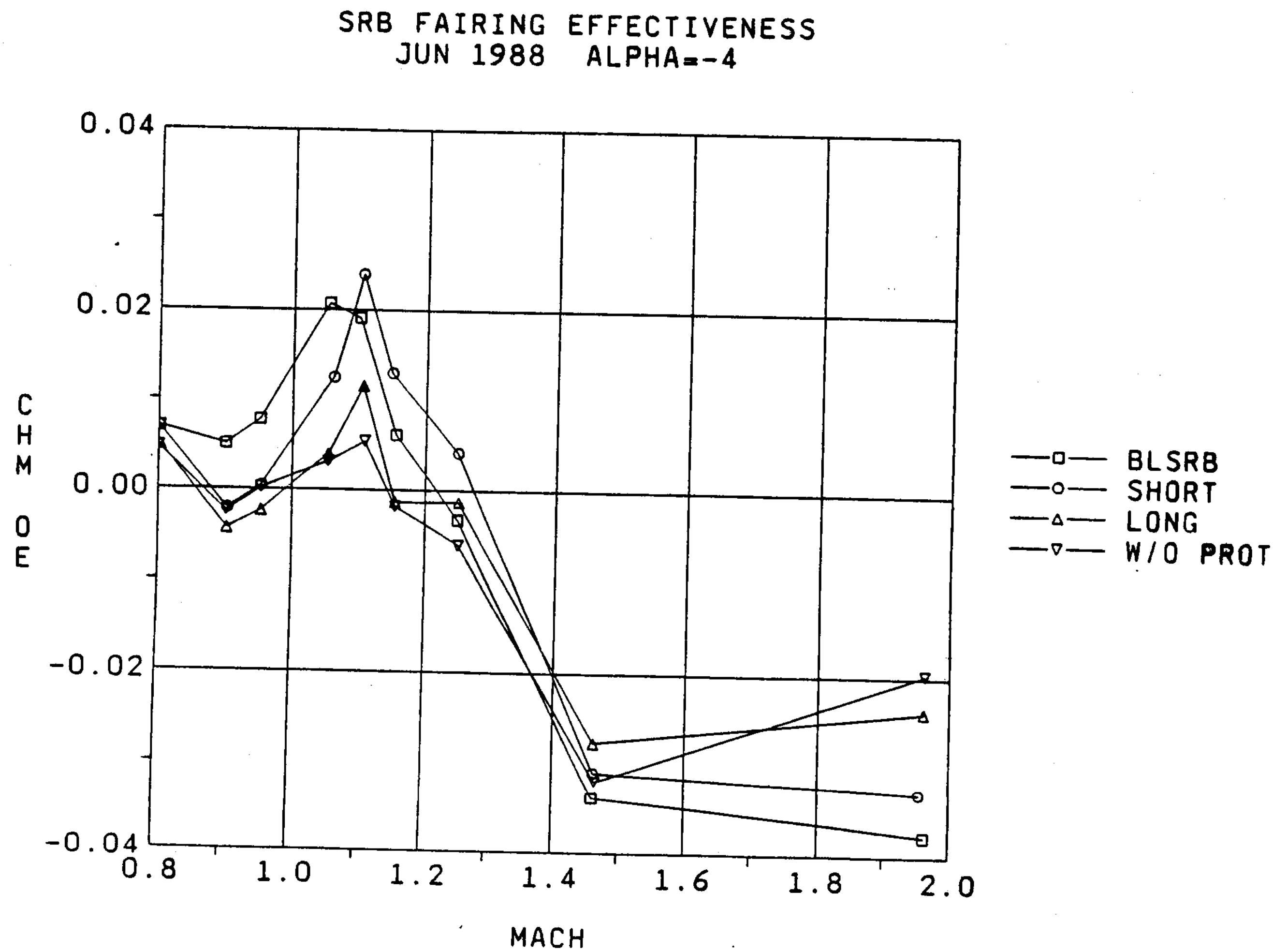

Fig. 5-20 CHMOE (Fairing/Protuberance Effects)

for an identical SSLV configuration less protuberances. Analysis of the SRB protuberance data increments can be summarized as follows:

- The longitudinal and wing total data show uniform shifts between BLSRB and SD12L1+AS. Corresponding increment plots show data scatter only.

- Hinge moment protuberance total data do not always give consistent changes for changes in alpha. A single number will not always give a good representation of the protuberance increment.

- For M = 1.46, the change in normal force at $\alpha = -2$ is 0.04. The corresponding change in shear is 0.0191 (2 x 0.0191 - 0.0382). Hence an increase in normal force is mostly due to an increase in wing shear. This shows that the data are consistent.

- All increment data fall within a reasonable band, as shown in the maximum and minimum coefficient table.

- Some Xcp values are questionable at higher Mach numbers ($\geq$ 2.74).

- Wing Xcp values are reasonable, moving aft and slightly inward with higher Mach numbers. The exception is M = 4.43, where the wing Scp values are located within the body.

It was then determined that LRB configurations that do not utilize the SRB type protuberances need to have the protuberance increments subtracted from the aerodynamic data base. To completely exclude the effects of SRB protuberances from a configuration using Phase I LRB data bases, the coefficients should be subtracted from the corresponding coefficients of that configuration.

5.2 SRB INCREMENT DATA BASE SUMMARY

Data analysis resulted in the generation of a protuberance incremental data base. The protuberance incremental data were generated by taking the difference between the baseline aerodynamic coefficient data of the SSLV with the baseline protuberances included and the aerodynamic coefficients obtained for an identical SSLV configuration less protuberances. Analysis of the SRB protuberance data increments can be summarized as follows:

- The longitudinal and wing total data show uniform shifts between BLSRB and SD12L1+AS. Corresponding increment plots show data scatter only.
- Hinge moment protuberance total data do not always give consistent changes for changes in alpha. A single number will not always give a good representation of the protuberance increment.
- For M = 1.46, the change in normal force at $\alpha = -2$ is 0.04. The corresponding change in shear is 0.0191 (2 x 0.0191 - 0.0382). Hence an increase in normal force is mostly due to an increase in wing shear. This shows that the data are consistent.
- All increment data fall within a reasonable band, as shown in the maximum and minimum coefficient table.
- Some Xcp values are questionable at higher Mach numbers ($\geq$ 2.74).
- Wing Xcp values are reasonable, moving aft and slightly inward with higher Mach numbers. The exception is M = 4.43, where the wing Scp values are located within the body.

It was then determined that LRB configurations that do not utilize the SRB type protuberances need to have the protuberance increments subtracted from the aerodynamic data base. To completely exclude the effects of SRB protuberances from a configuration using Phase I LRB data bases, the coefficients should be subtracted from the corresponding coefficients of that configuration.

6. GAP AND AFT SKIRT EFFECTS

The effects of the LRB/ET separation gap width and the aft skirt on the aerodynamics of the SSLV were analyzed. Data were obtained from wind tunnel testing on two configurations at Mach speeds from .9 to 1.5. Figures 6-1 and 6-2 present the configurations analyzed and the corresponding nomenclatures. The gap width was varied on both configurations from 12 in to 33 in. Angles of attack ranged from -4 to zero in increments of two. Analysis of the gap width was conducted with respect to changes in C_{NF}, C_{AF}, C_{SR}, C_{BR}, and C_{TR} values. The objectives of the aft skirt analysis were to determine the protuberances, diameter, and length effects on wing loading.

6.1 GAP EFFECTS SUMMARY

The data from the wind tunnel were analyzed to determine the effect of gap width on the aerodynamic coefficients. Figures 6-3 to 6-17 show results for D1L1 configurations, Figs. 6-18 to 6-32 for the D2L2 configurations. It was determined that increasing the gap width causes an increase in C_{NF} values and a decrease in C_{MF} values at negative angles of attack and transonic Mach numbers. C_{AF} values tend to increase with increasing gap size in the transonic and supersonic image.

At Mach 1.46, increases in the gap width cause a slight increase in C_{SR} values for both the D1L1 (baseline) and D2L2 configuration. However, at Mach 1.25 a slight increase occurs in the C_{SR} values for the D1L1 configuration where as a slight decreases occurs in the D2L2 values. At the same Mach numbers, it was observed that the C_{BR} values for both configurations increase as the gap width increases. The C_{TR} values and elevon hinge moments decrease slightly on both configurations as gap width increases.

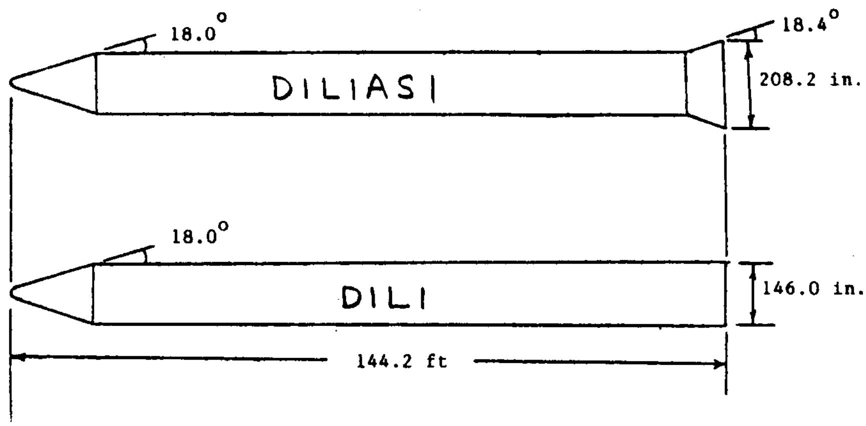

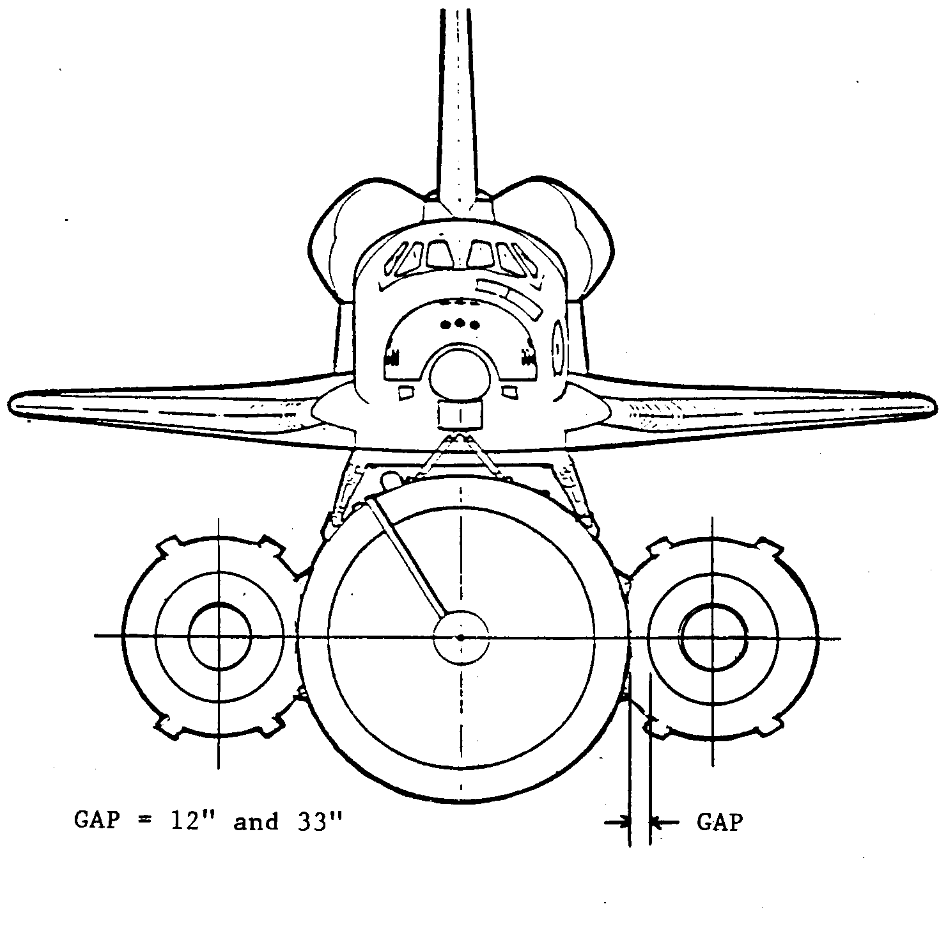

Fig. 6-1 Gap Effect Configurations (D1L1)

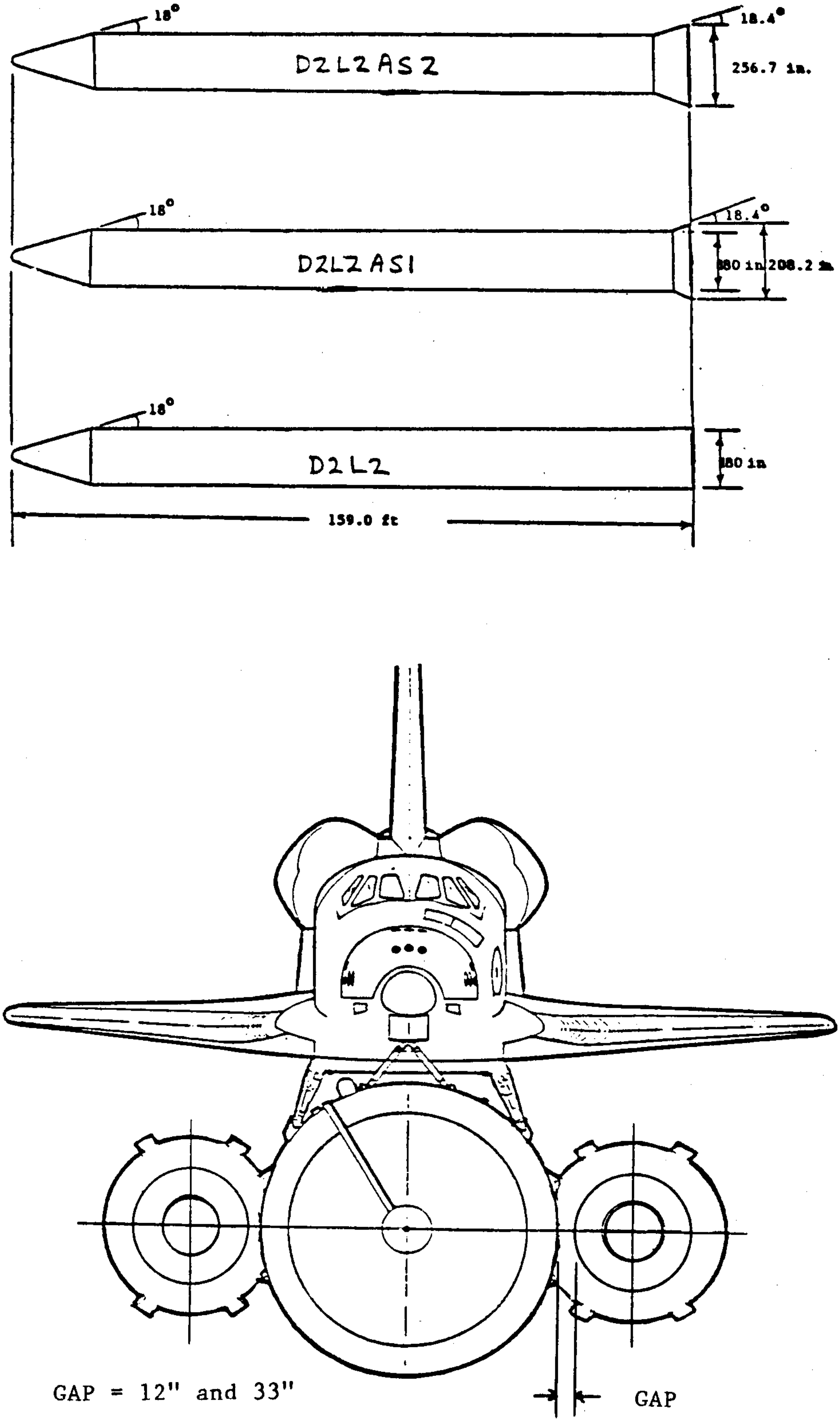

Fig. 6-2 Gap Effect Configurations (D2L2)

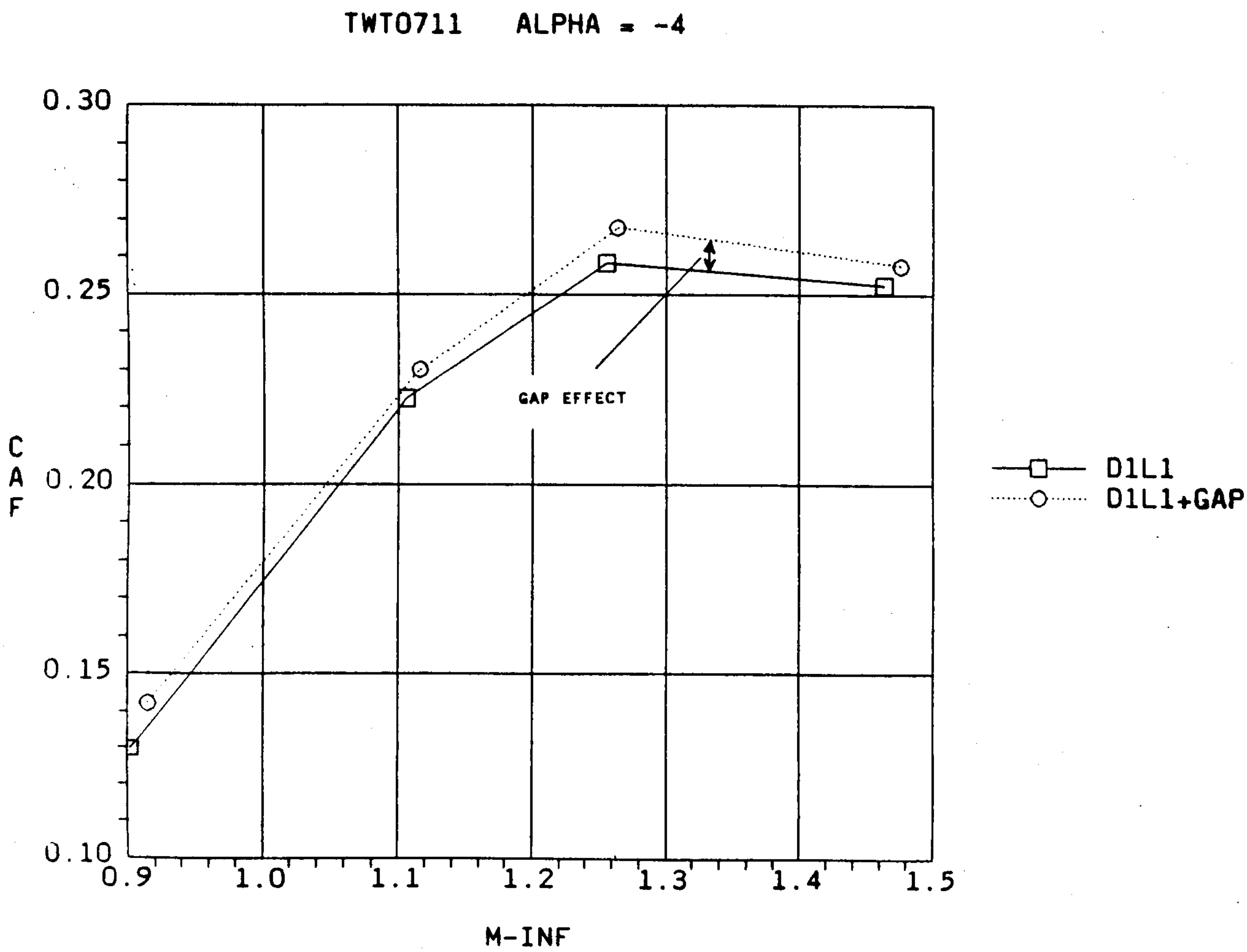

Fig. 6-3 C_{AF} vs Mach (D1L1)

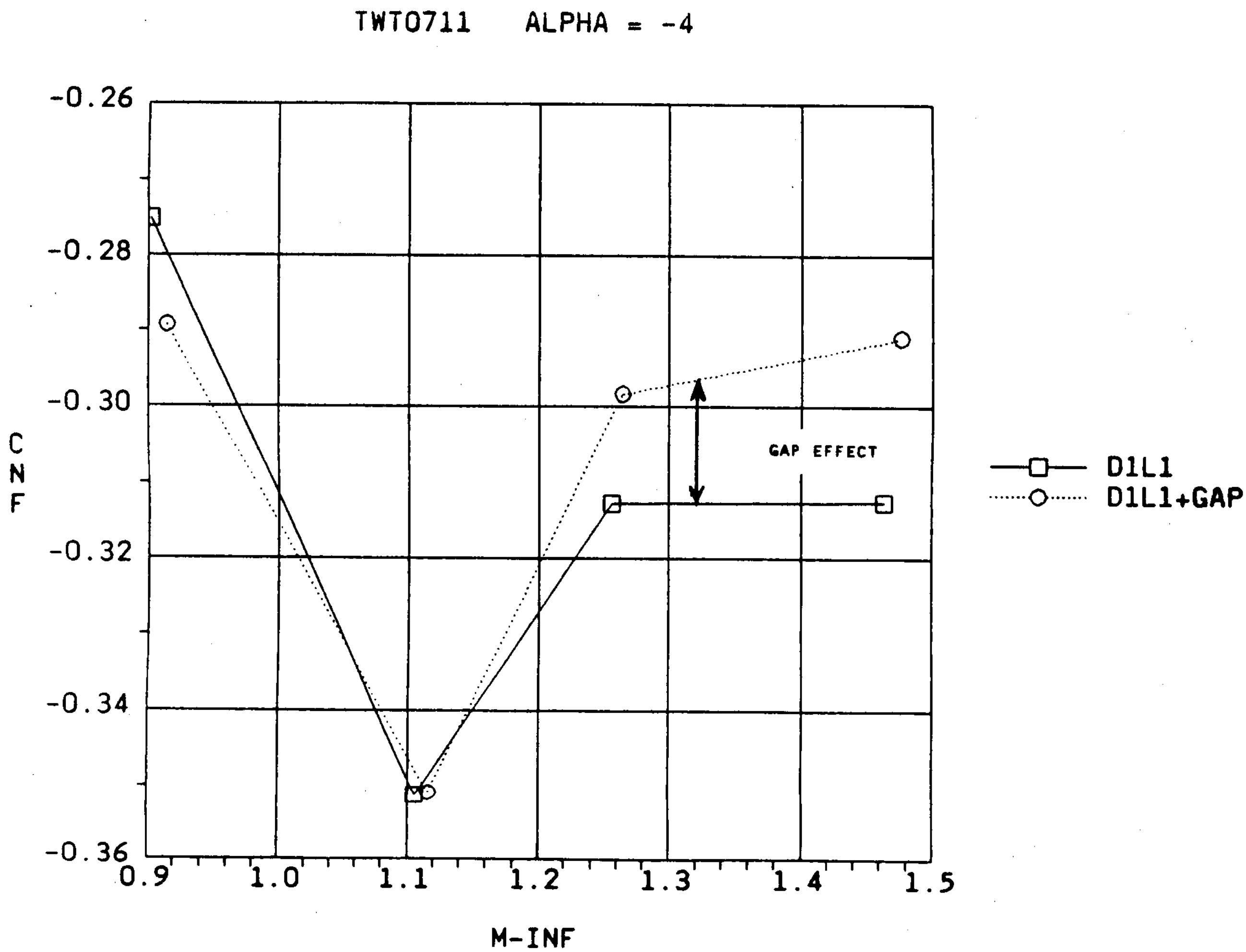

Fig. 6-4 C_{NF} vs Mach (D1L1)

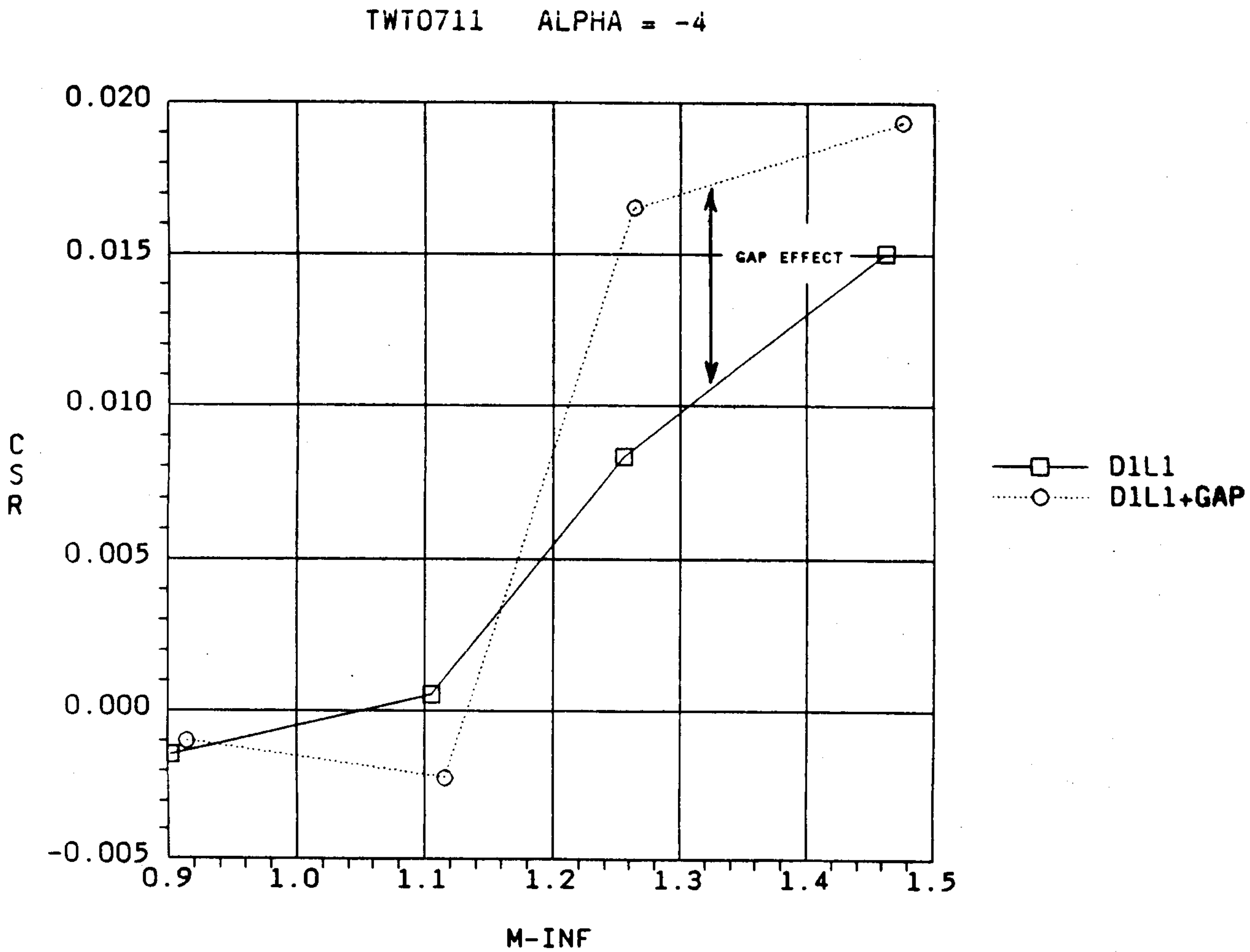

Fig. 6-5 C_{SR} vs Mach (D1L1)

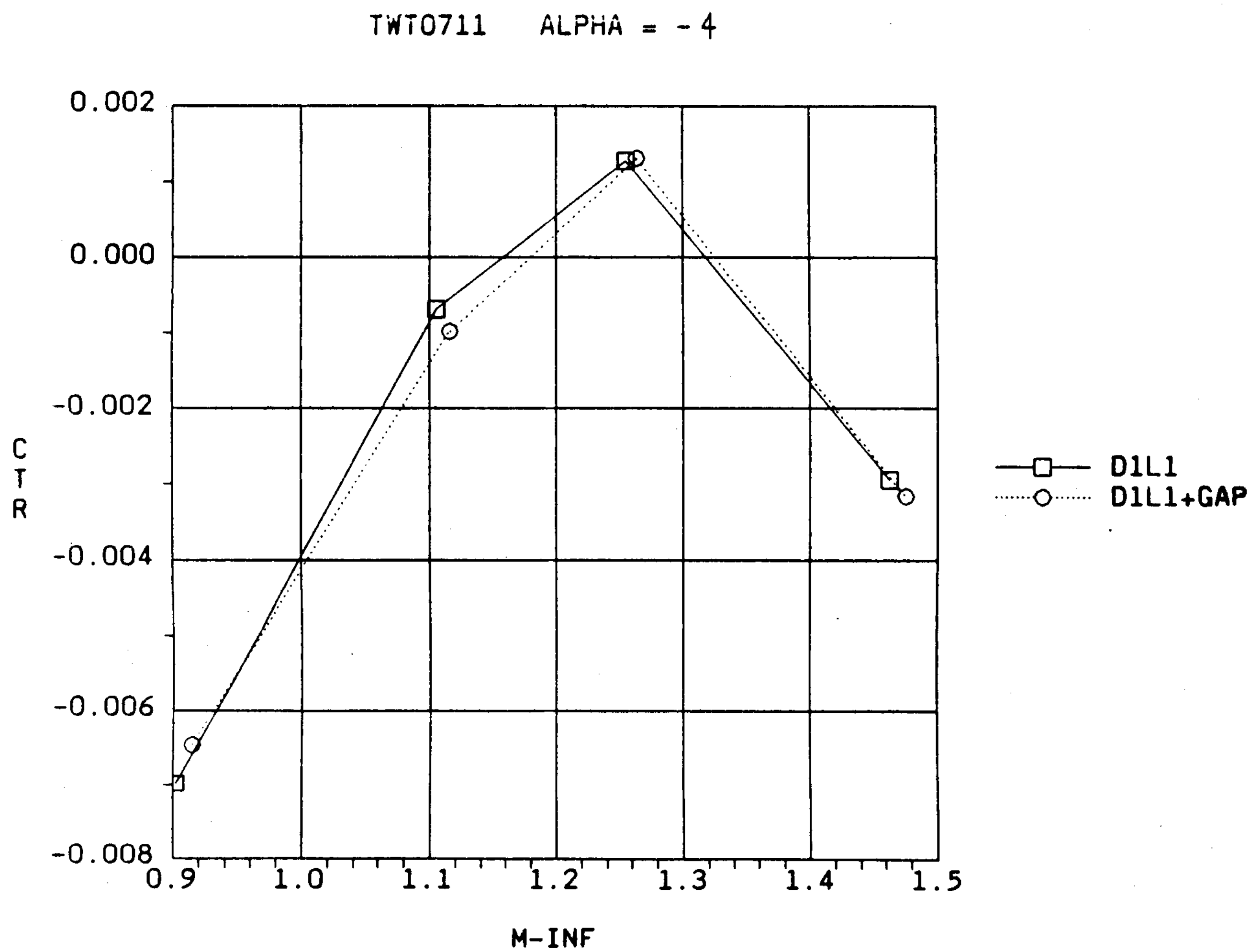

Fig. 6-6 C_{TR} vs Mach (D1L1)

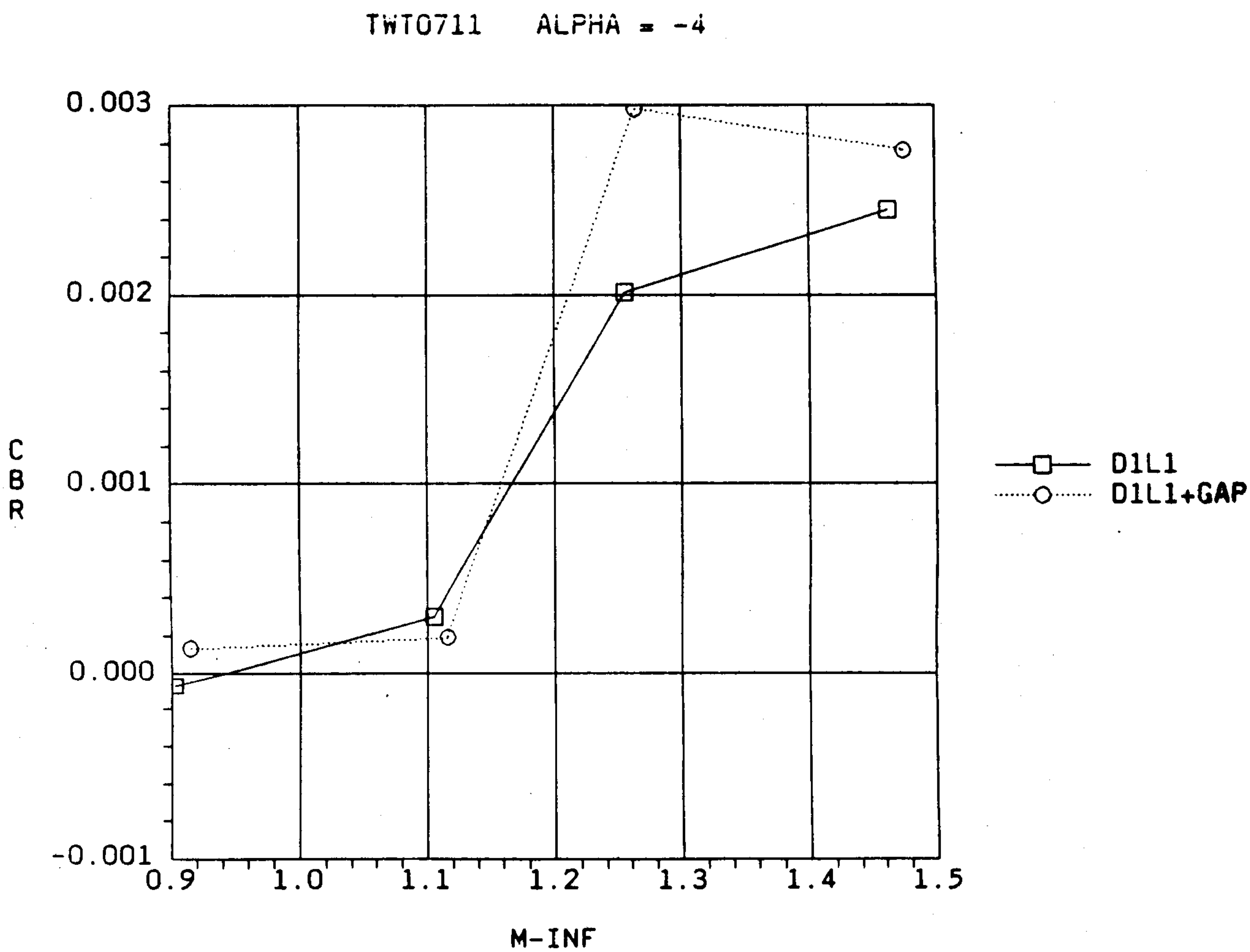

Fig. 6-7 C_{BR} vs Mach (D1L1)

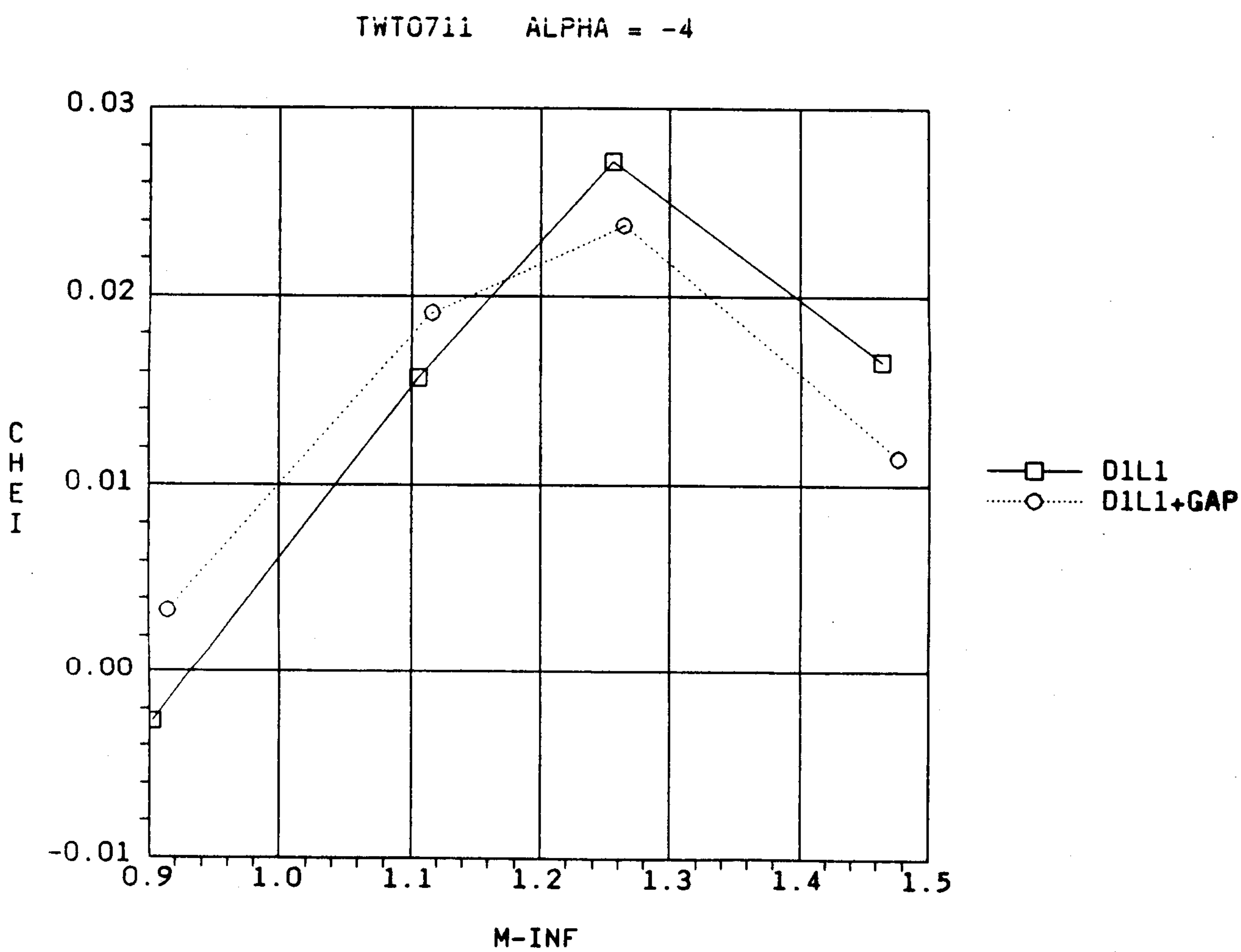

Fig. 6-8 CHEI vs Mach (D1L1)

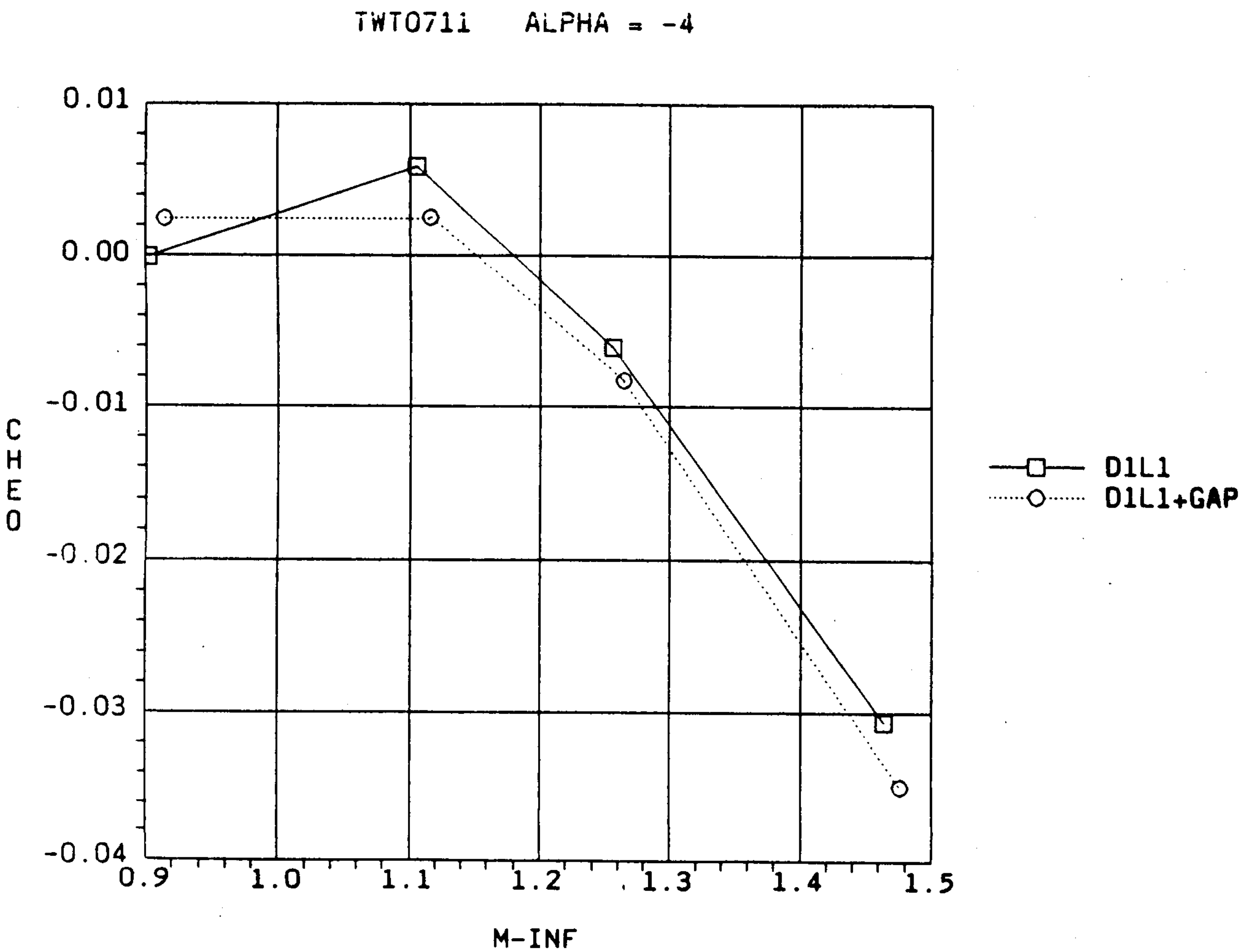

Fig. 6-9 CHEO vs Mach (D1L1)

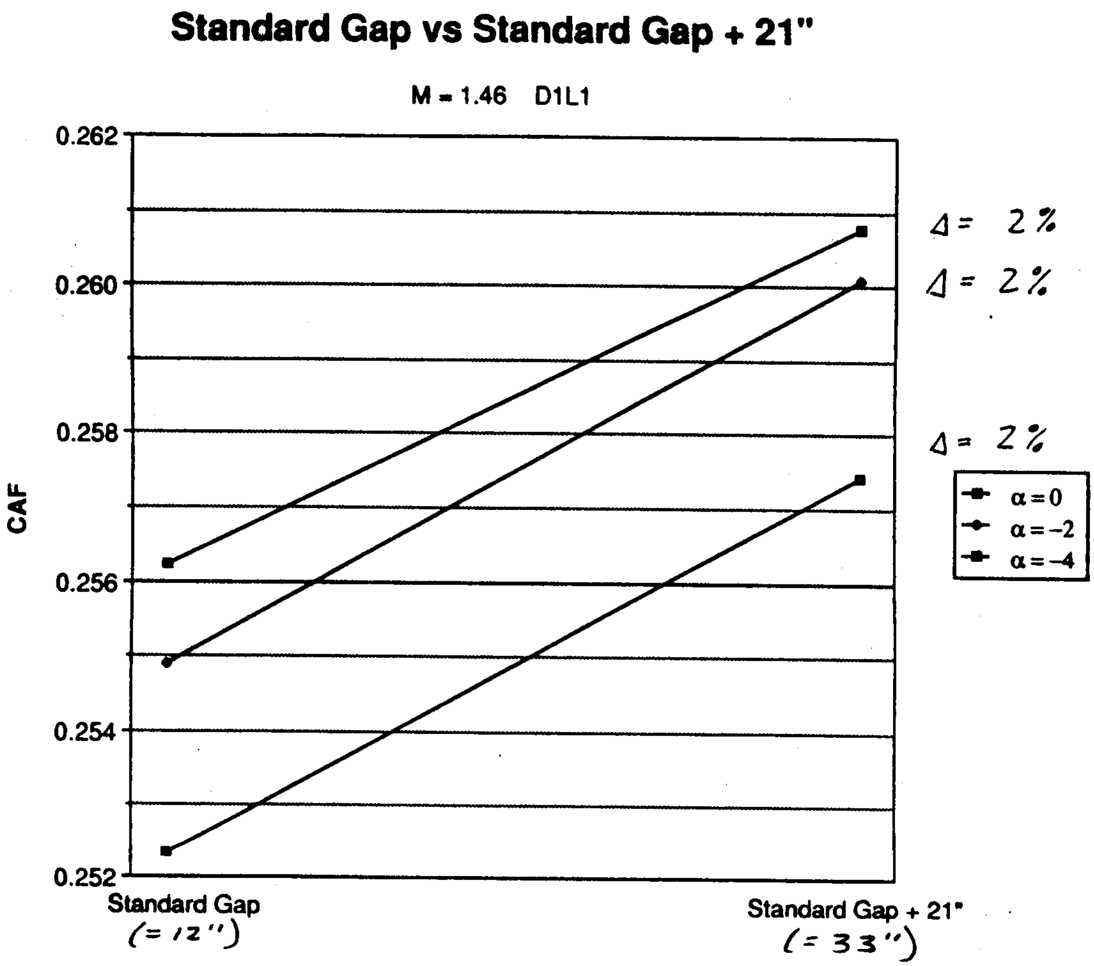

Fig. 6-10 C_{AF} vs Gap (D1L1)

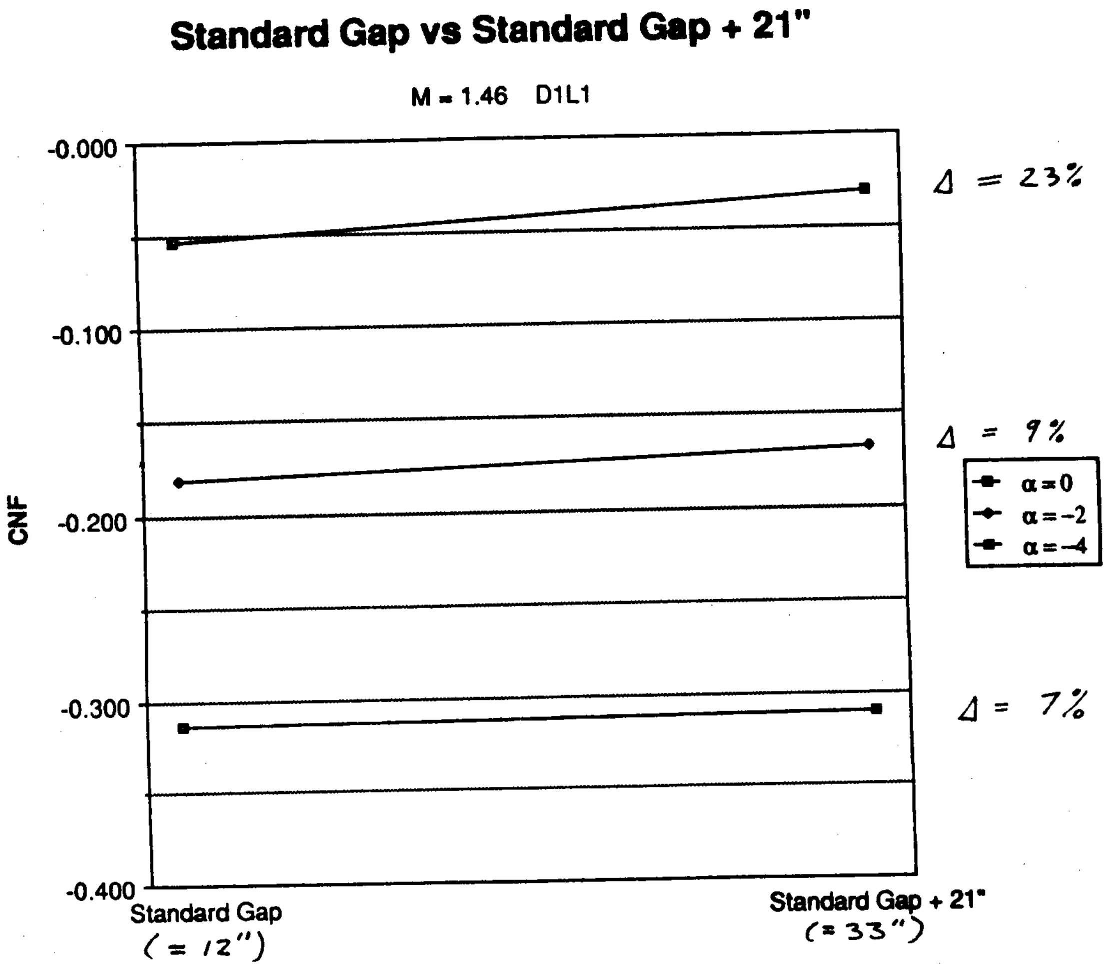

Fig. 6-11 C_{NF} vs Gap (D1L1)

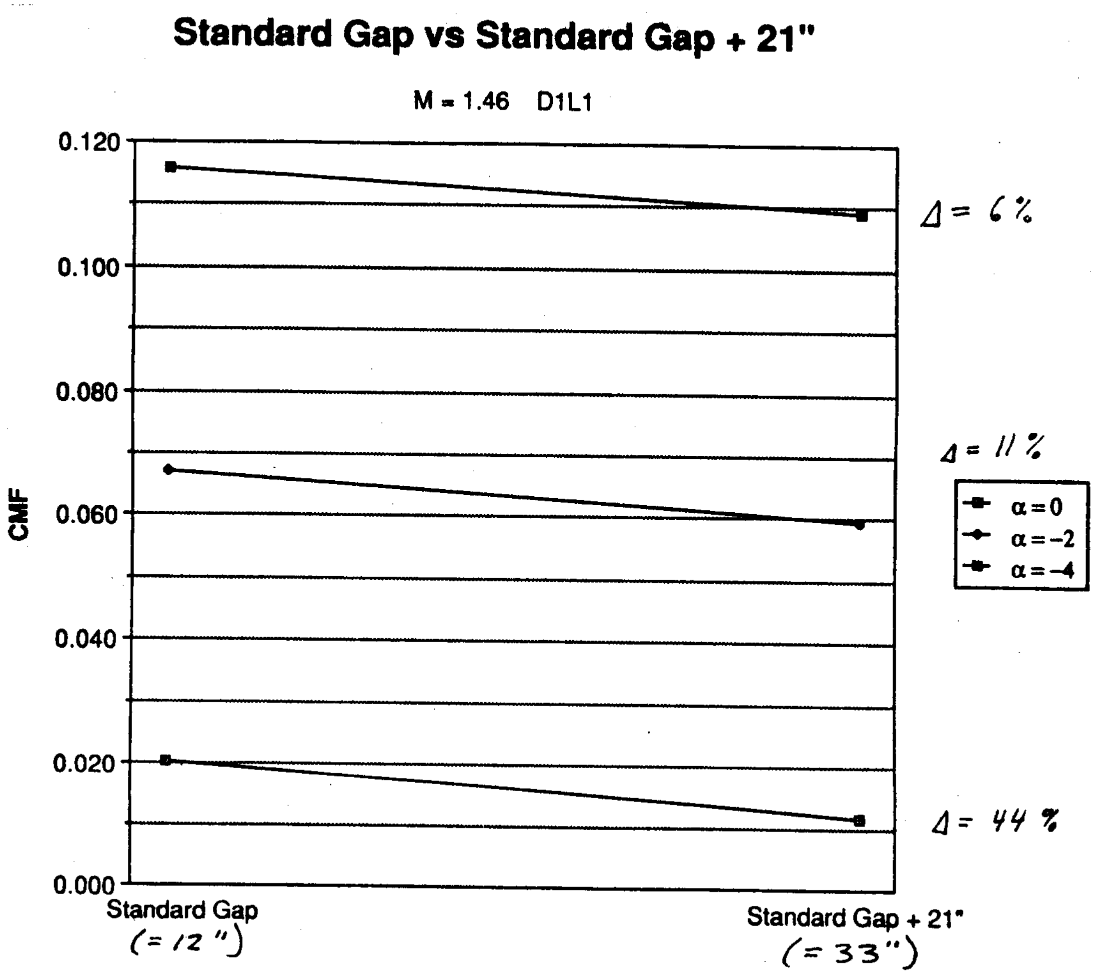

Fig. 6-12 C_{MF} vs Gap (D1L1)

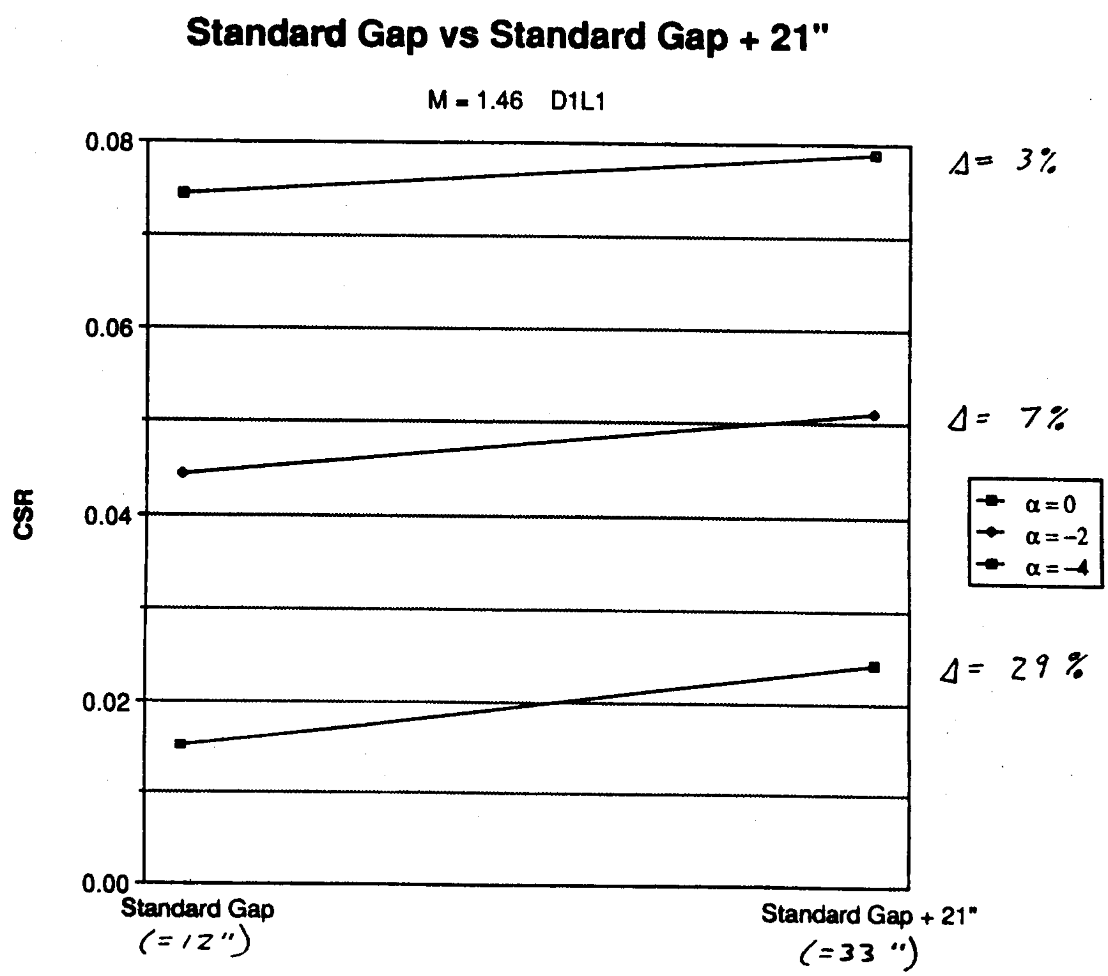

Fig. 6-13 C_{SR} vs Gap (D1L1)

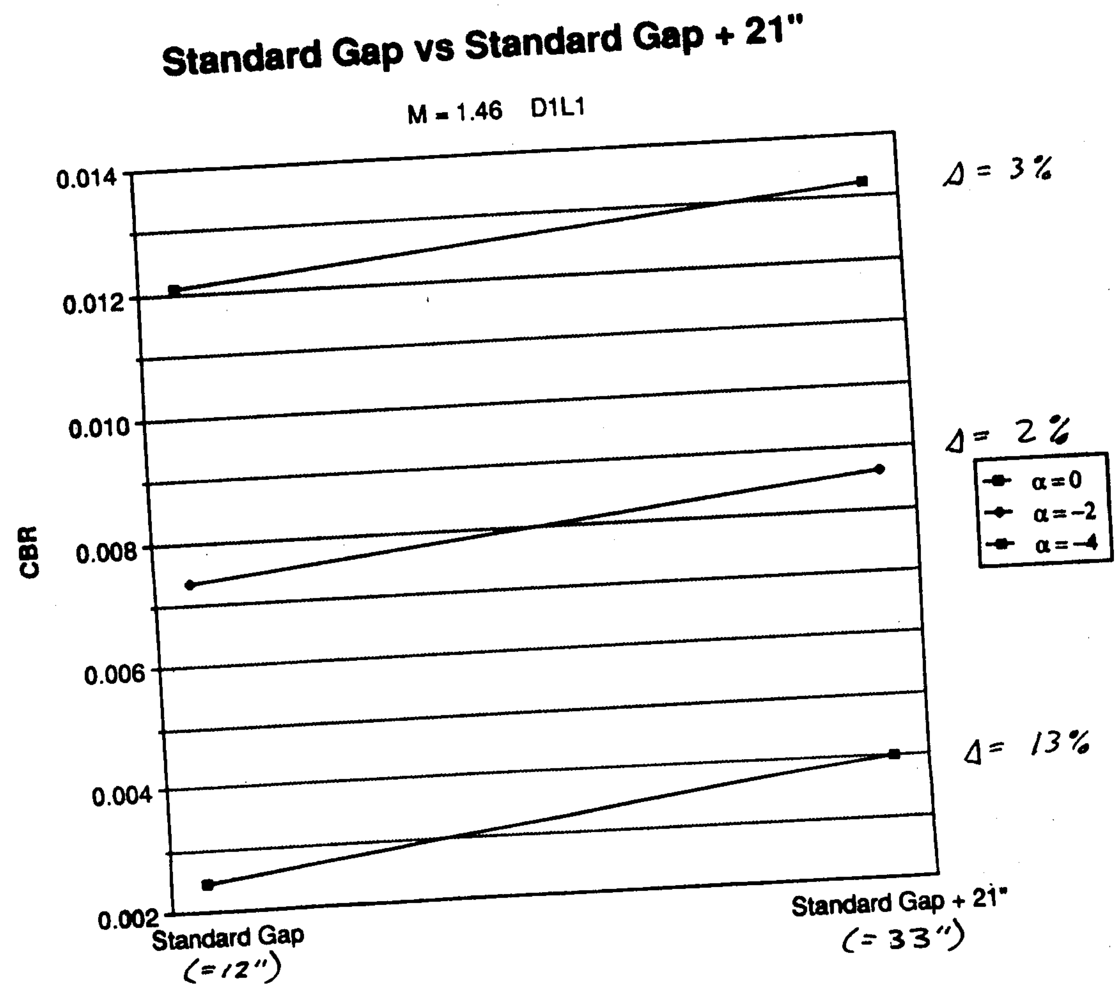

Fig. 6-14 C_{BR} vs Gap (D1L1)

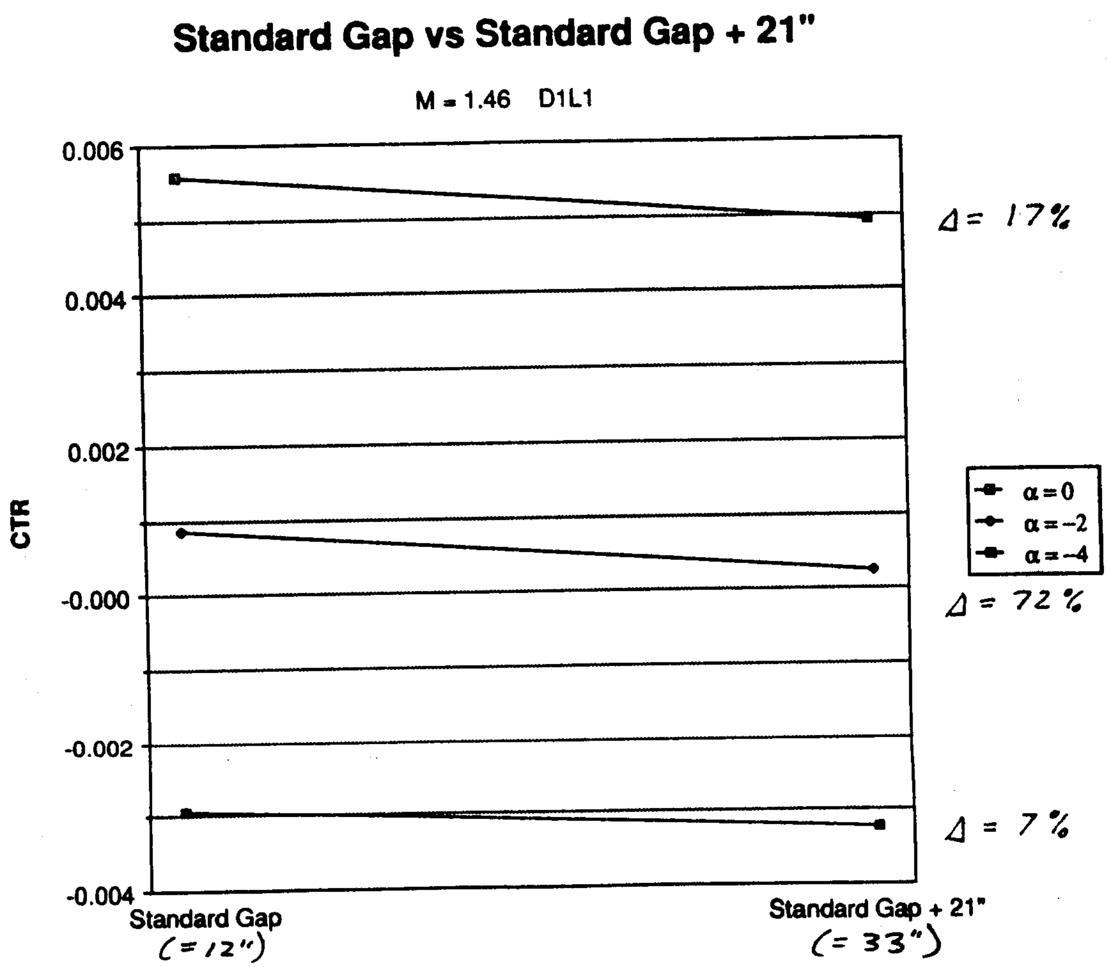

Fig. 6-15 C_{TR} vs Gap (D1L1)

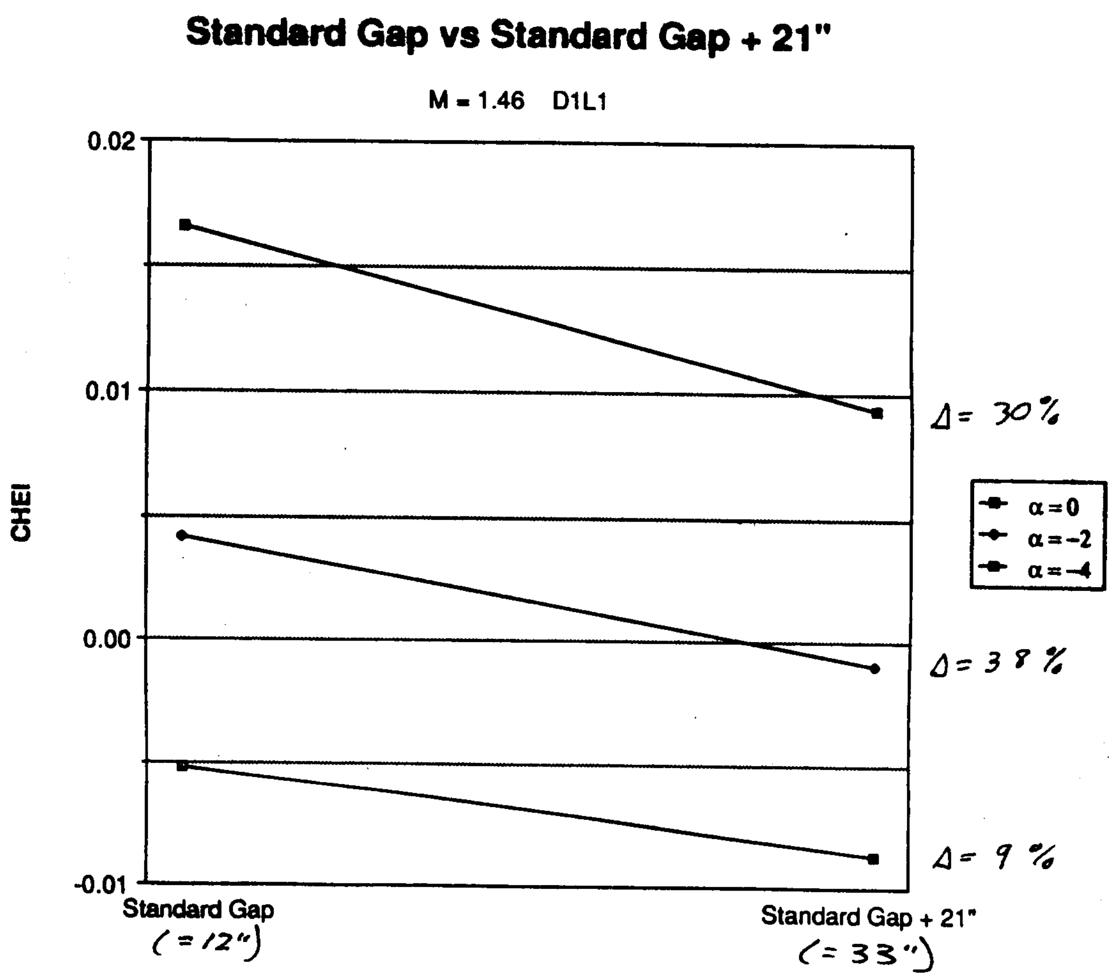

Fig. 6-16 CHEI vs Gap (D1L1)

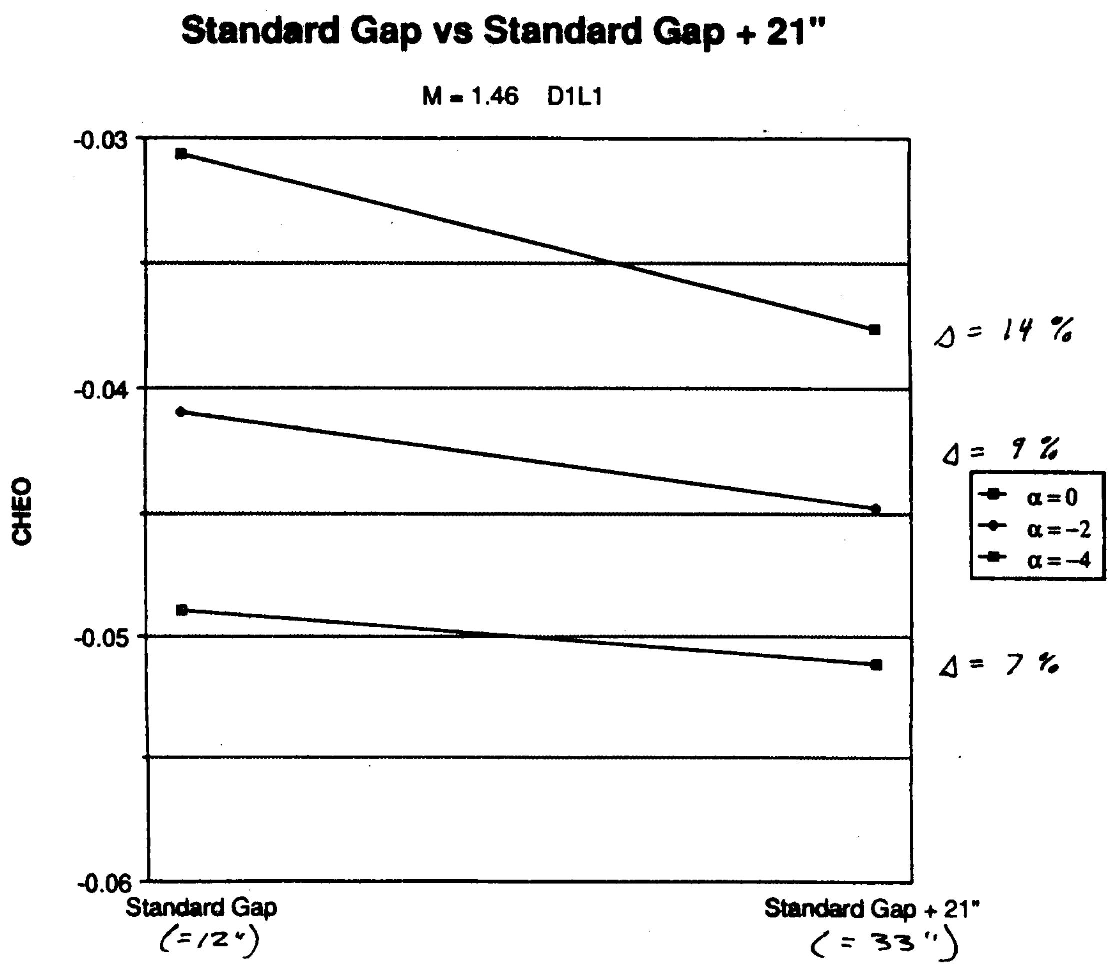

Fig. 6-17 CHEO vs Gap (D1L1)

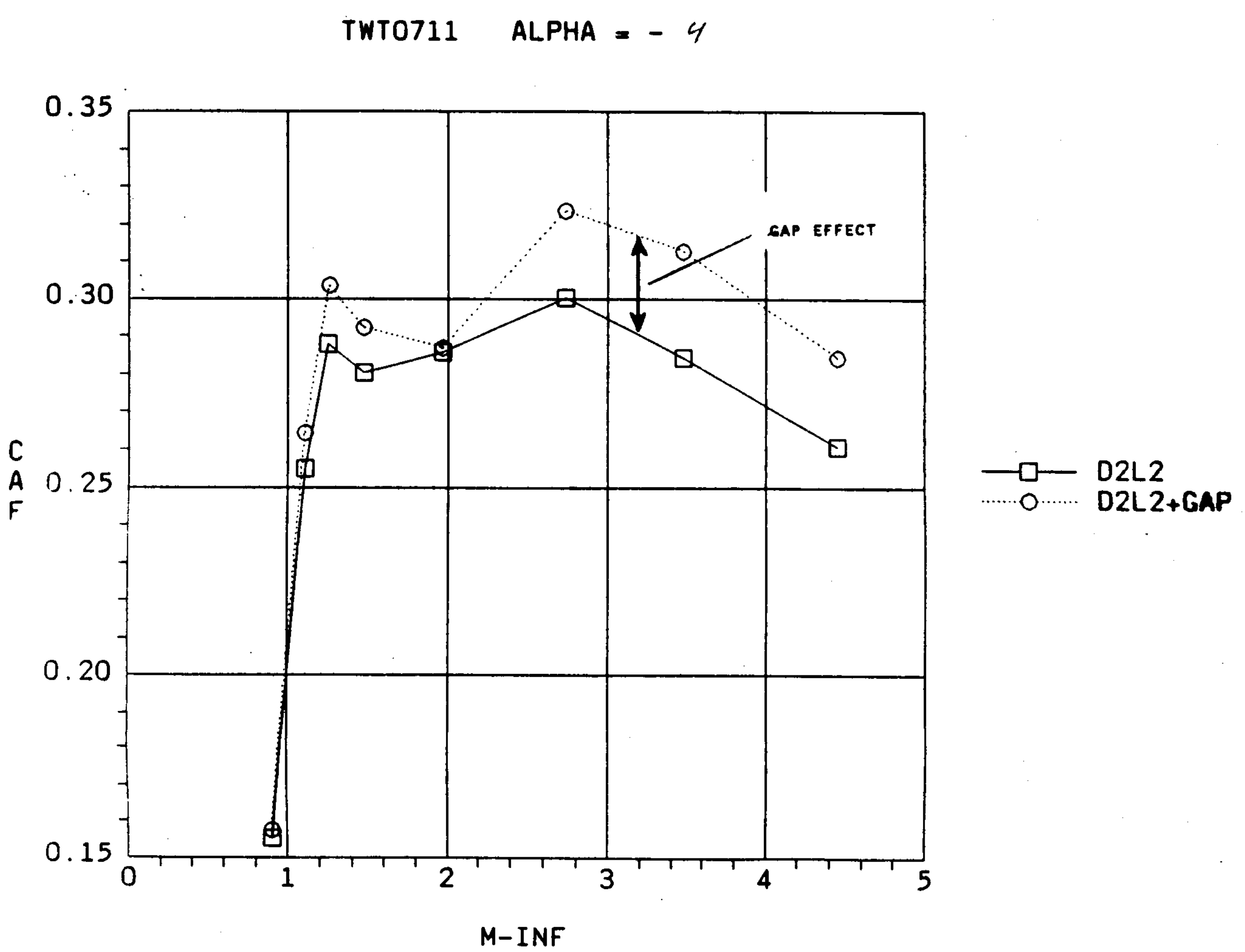

Fig. 6-18 C_{AF} vs Mach (D2L2)

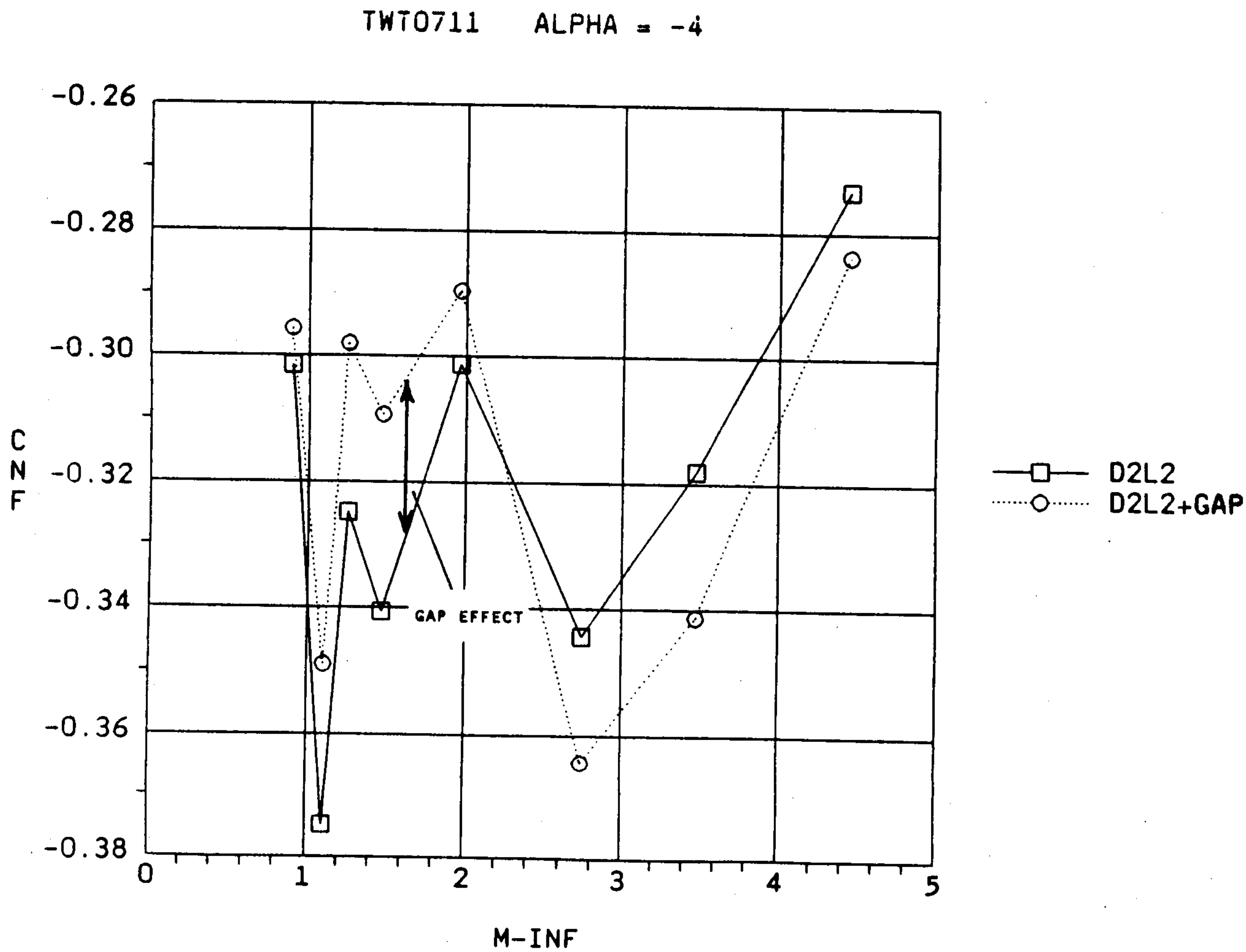

Fig. 6-19 C_{NF} vs Mach (D2L2)

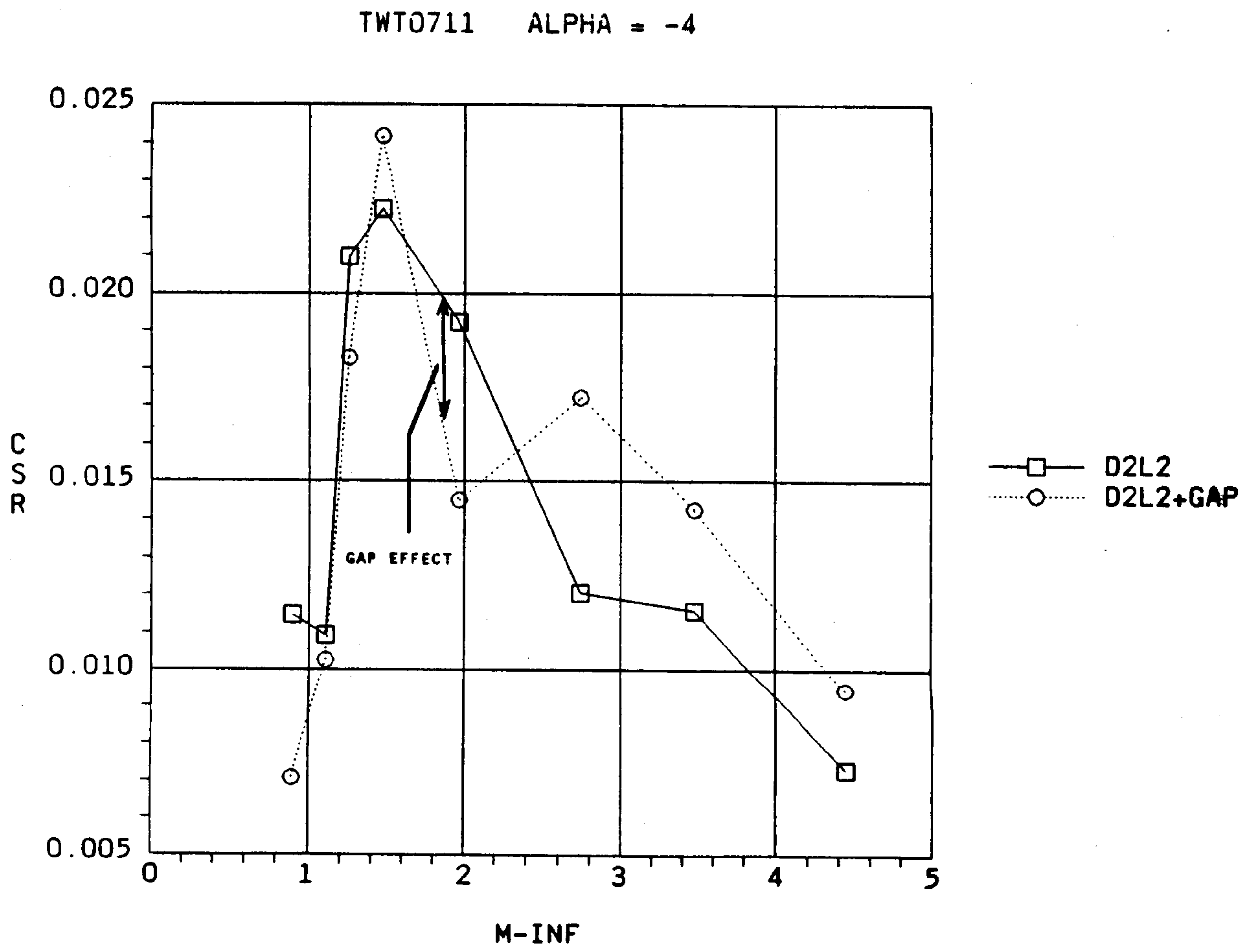

Fig. 6-20 C_{SR} vs Mach (D2L2)

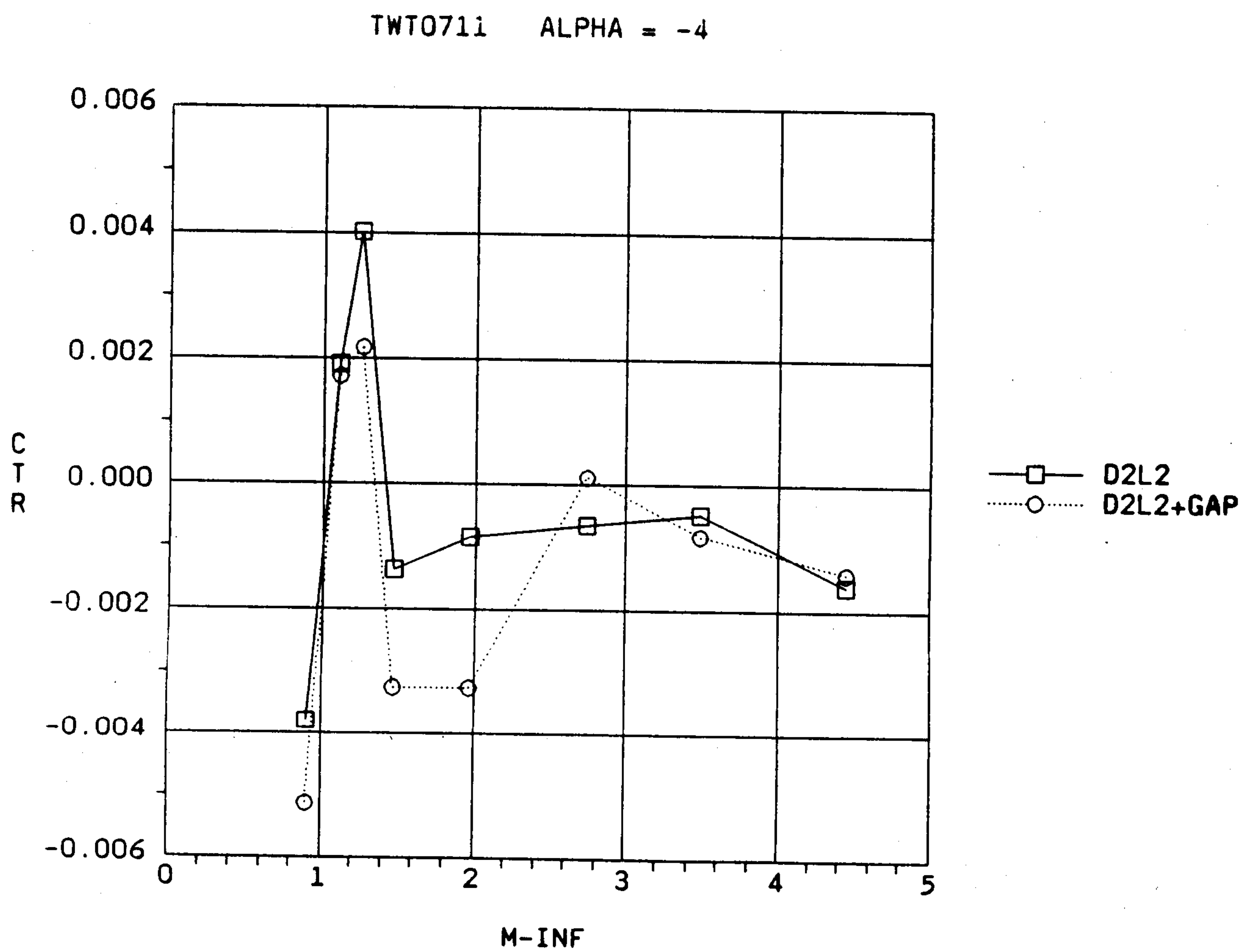

Fig. 6-21 C_{TR} vs Mach (D2L2)

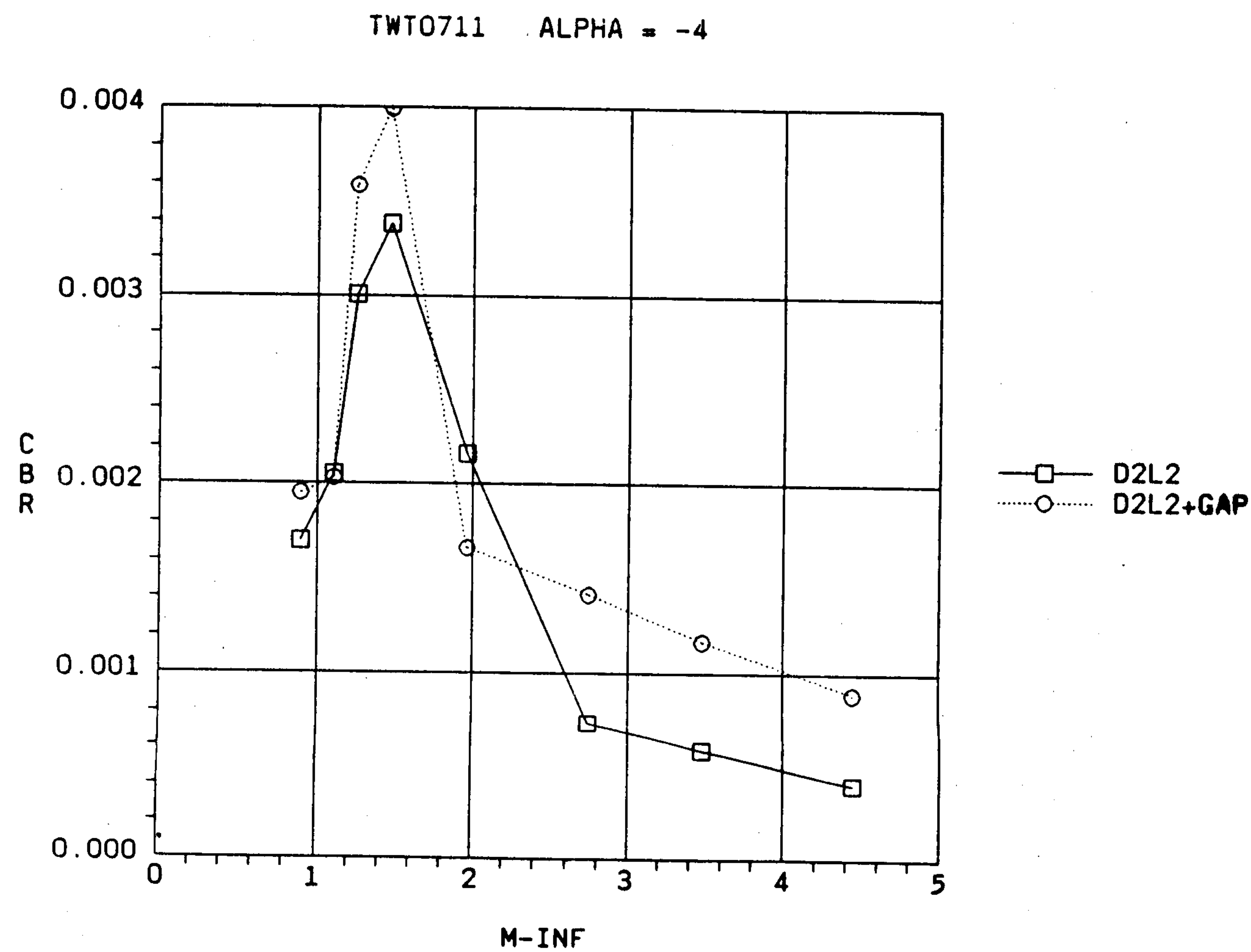

Fig. 6-22 C_{BR} vs Mach (D2L2)

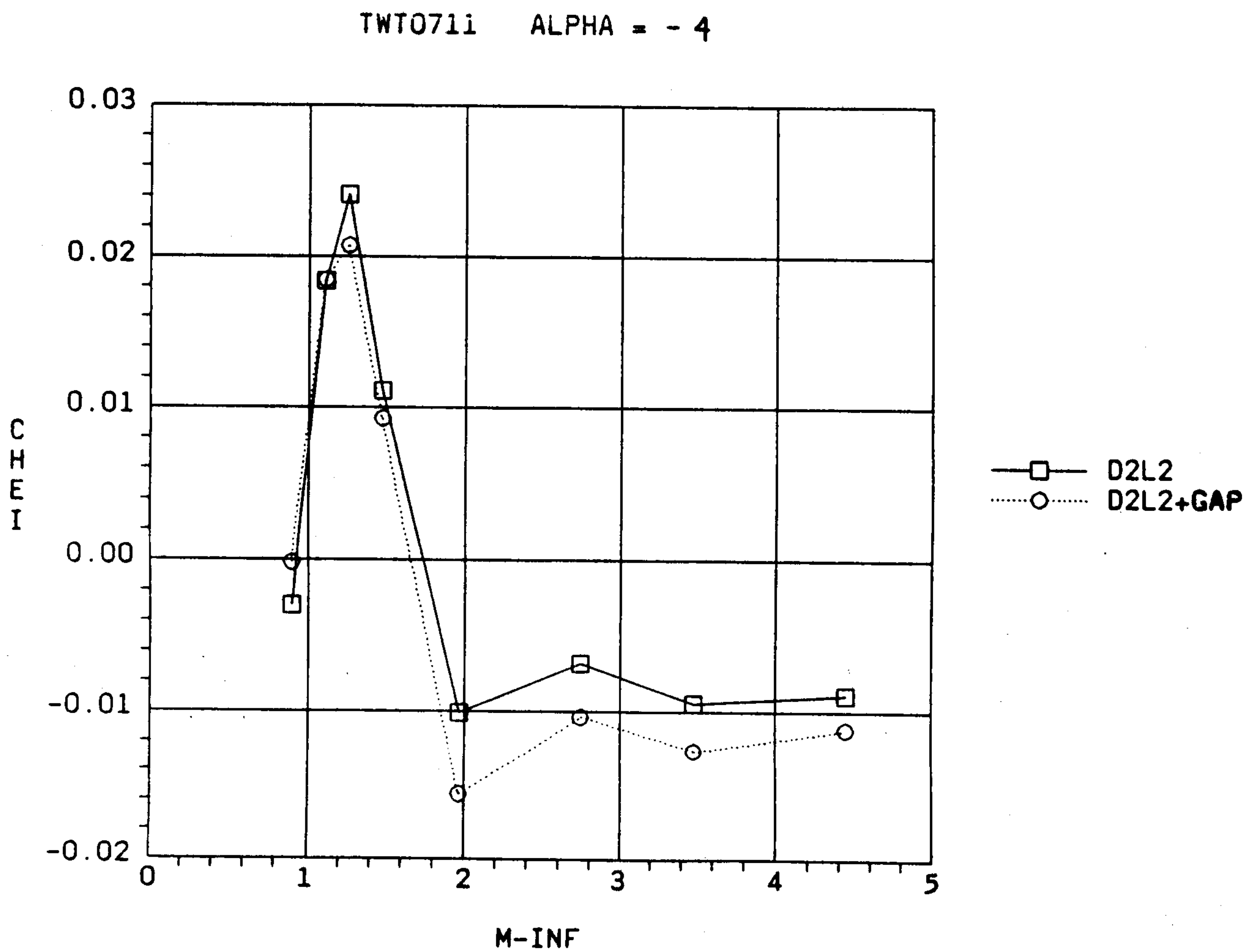

Fig. 6-23 CHEI vs Mach (D2L2)

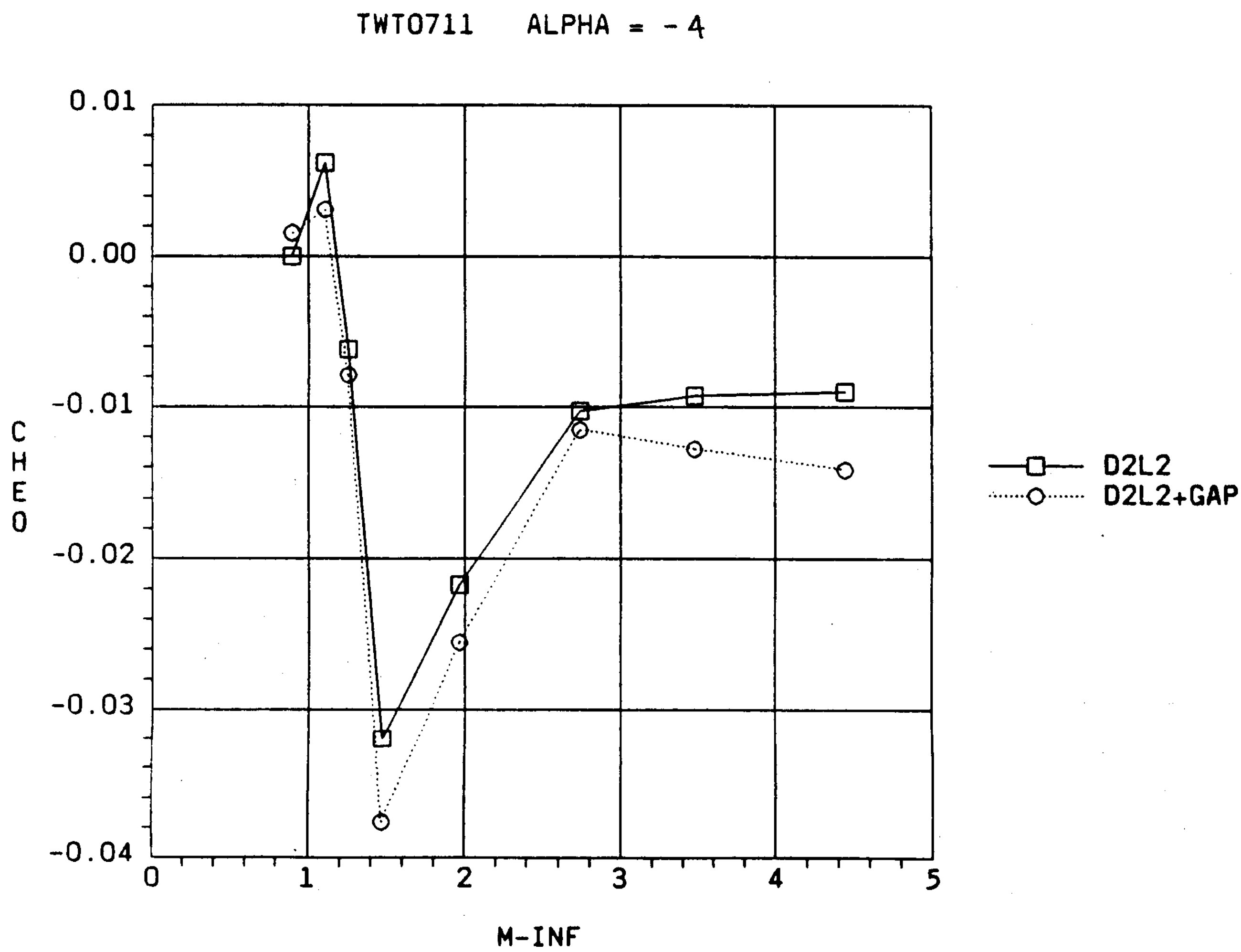

Fig. 6-24 CHEO vs Mach (D2L2)

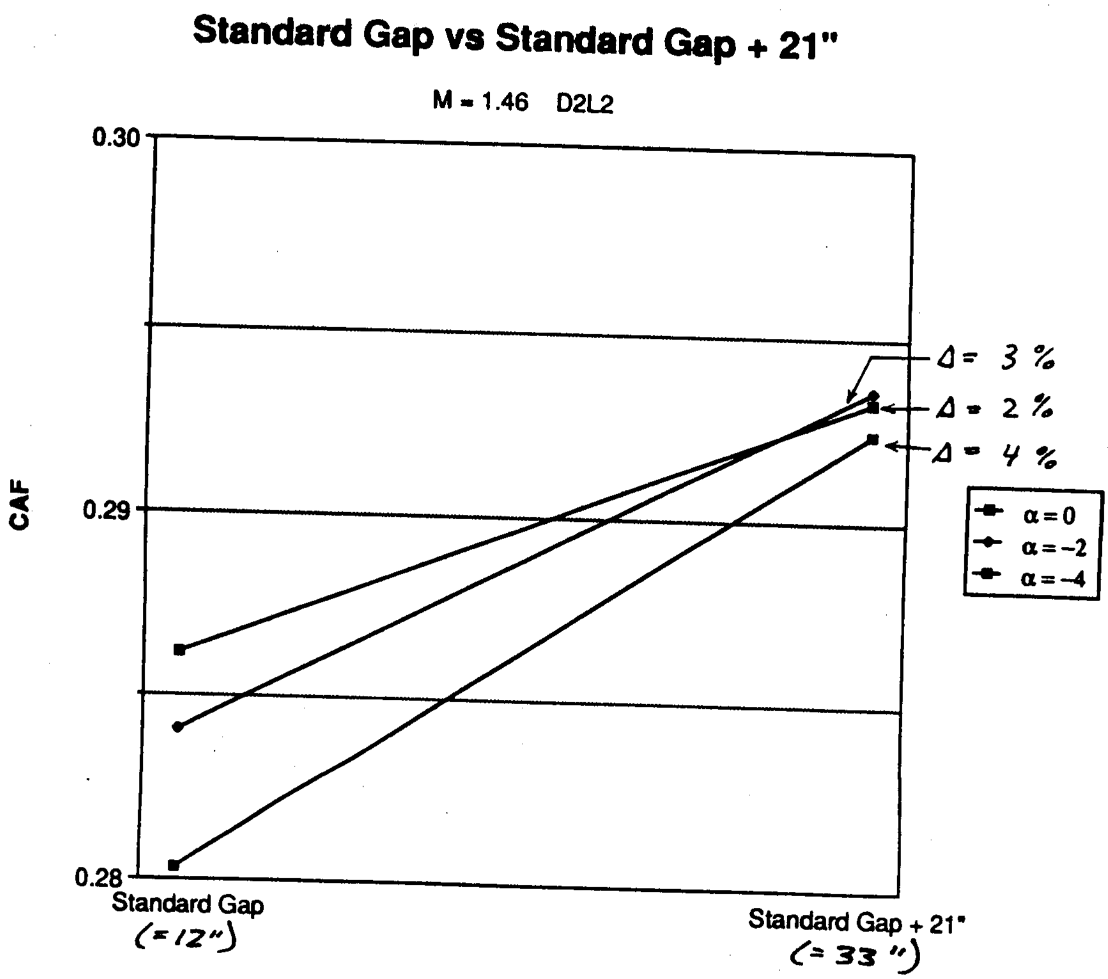

Fig. 6-25 C_{AF} vs Gap (D2L2)

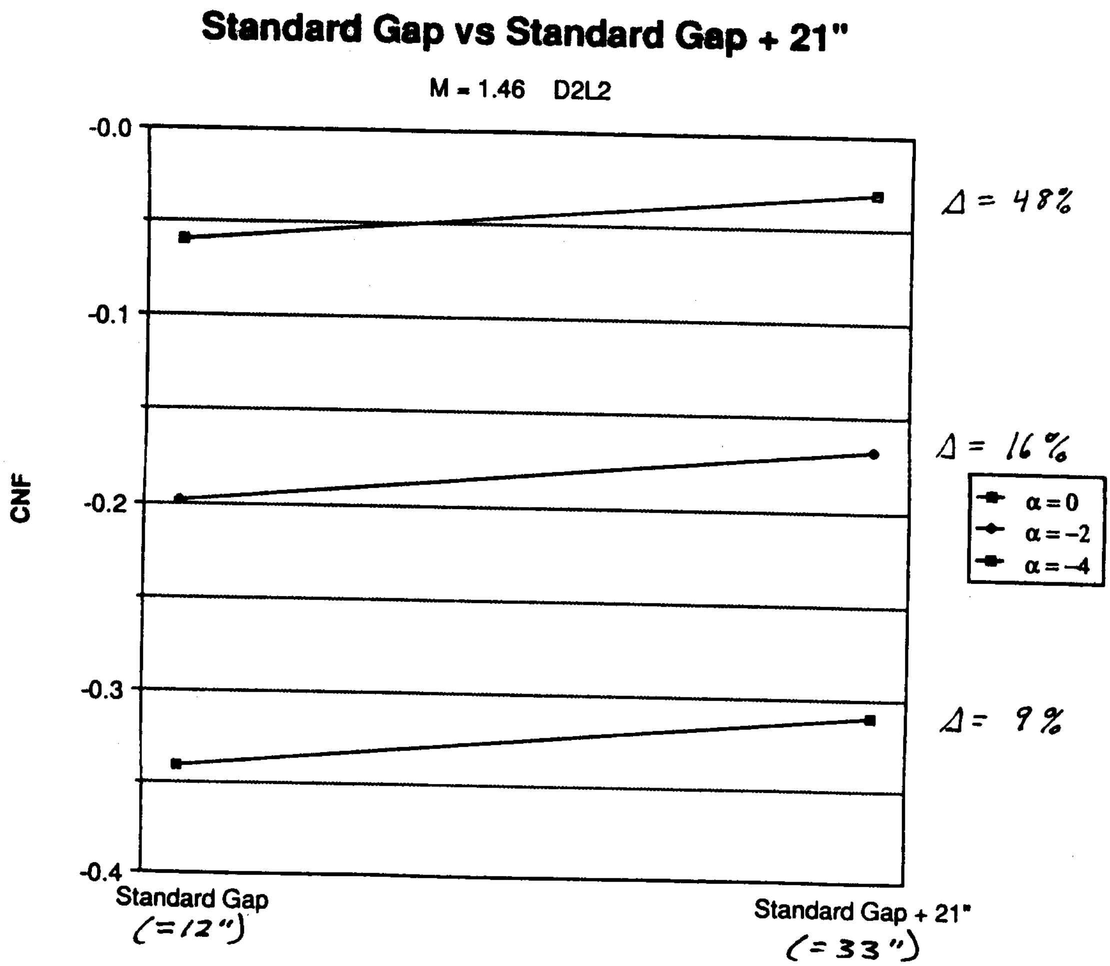

Fig. 6-26 C_{NF} vs Gap (D2L2)

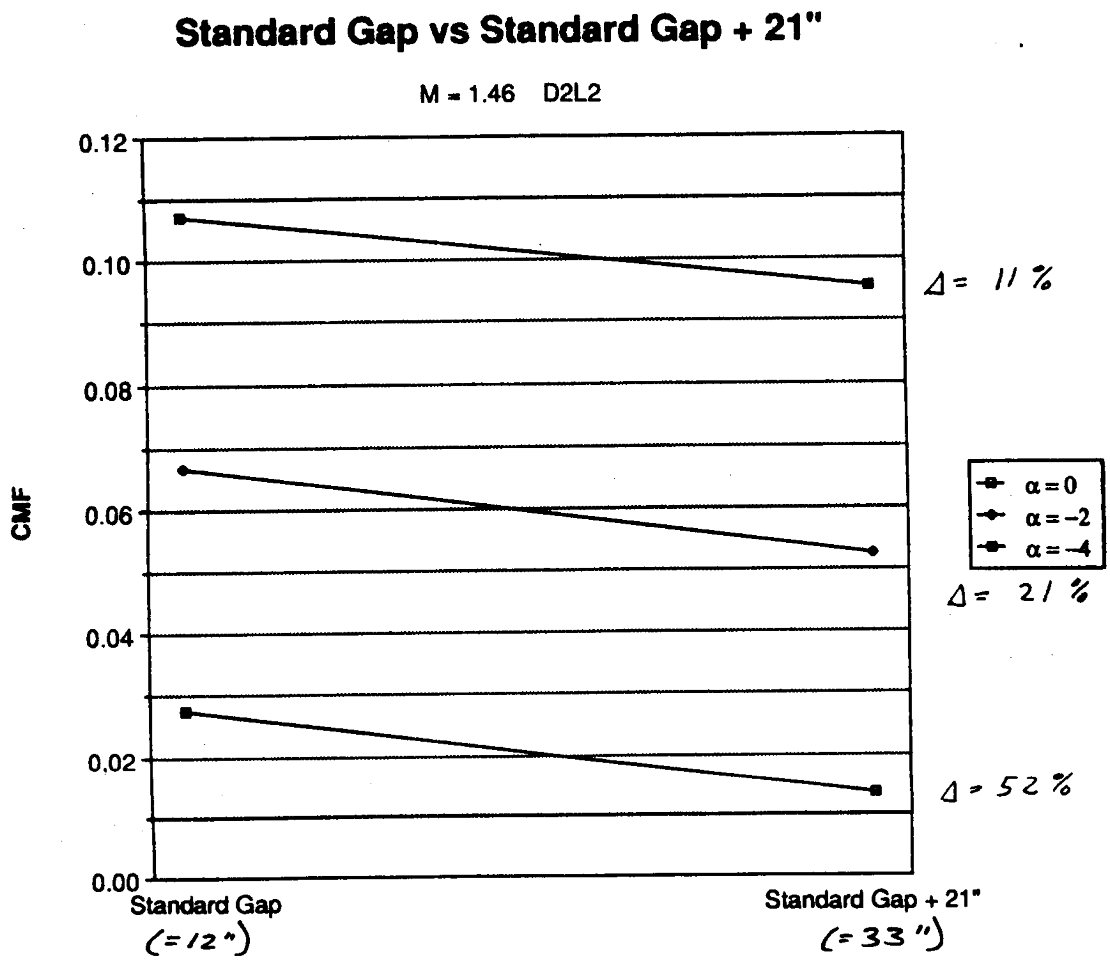

Fig. 6-27 C_{MF} vs Gap (D2L2)

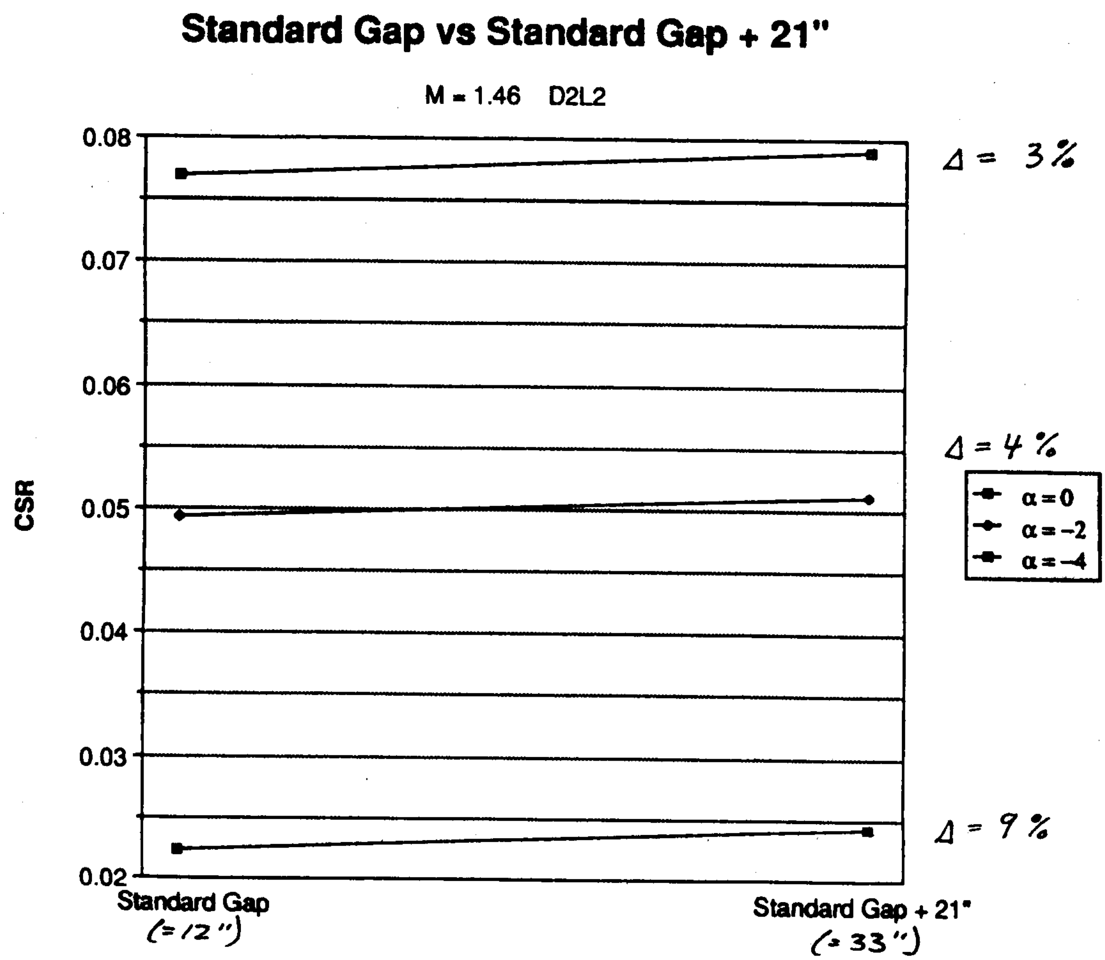

Fig. 6-28 C_{SR} vs Gap (D2L2)

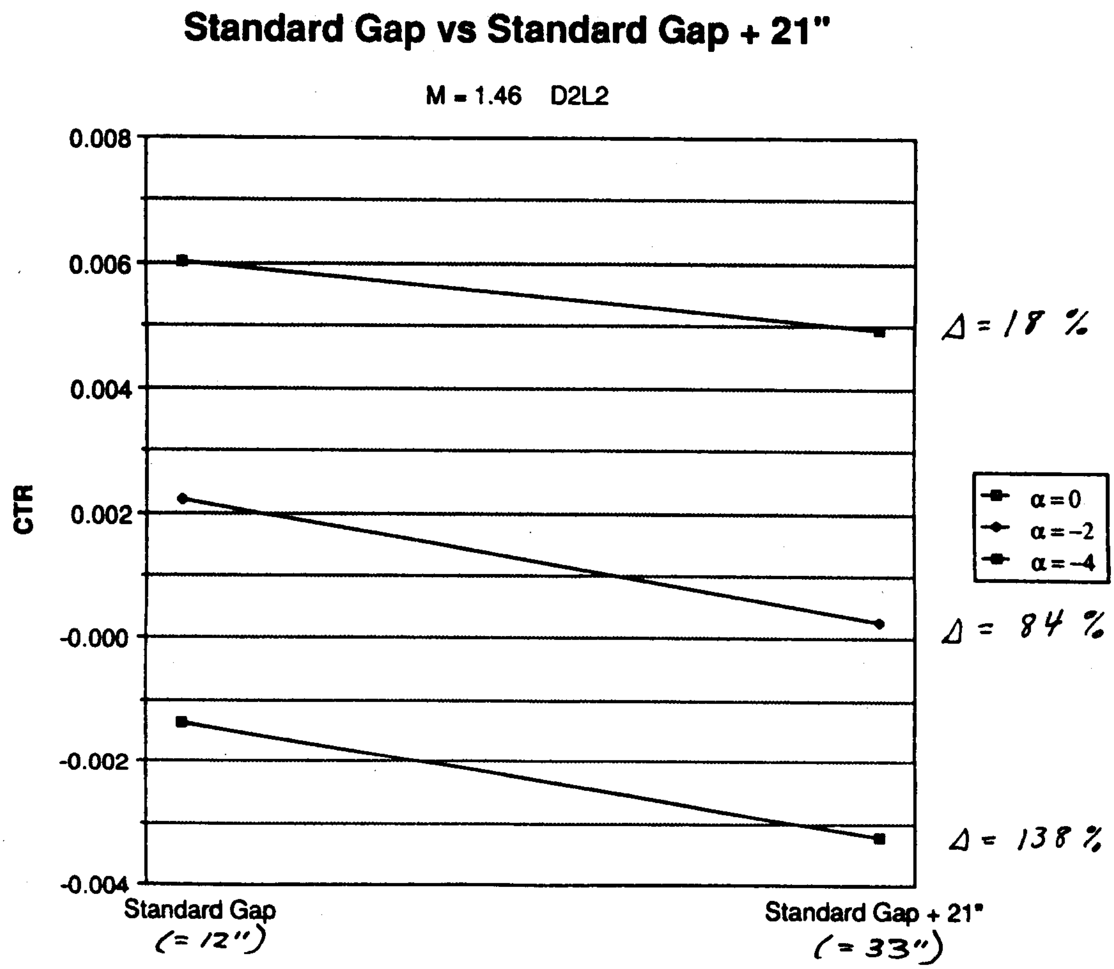

Fig. 6-29 C_{TR} vs GAP (D2L2)

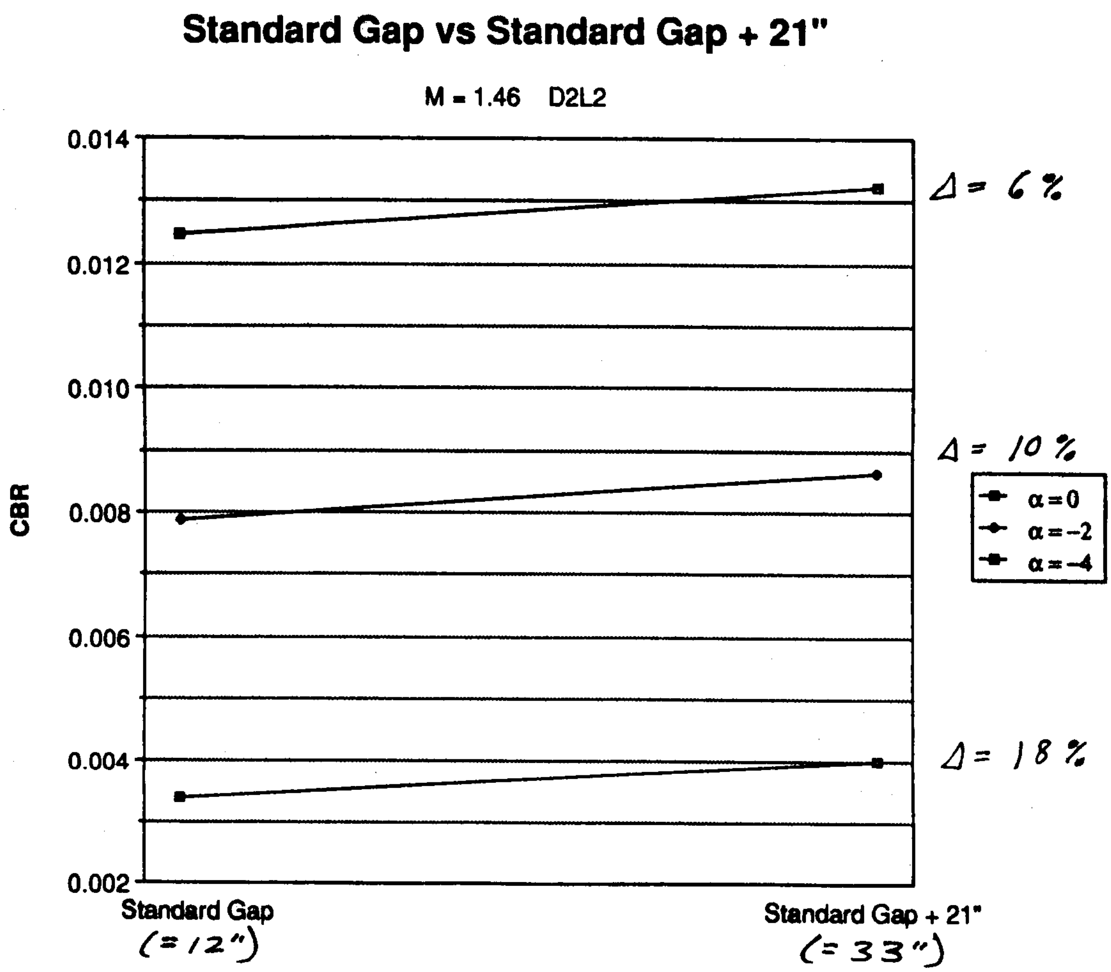

Fig. 6-30 C_{BR} vs GAP (D2L2)

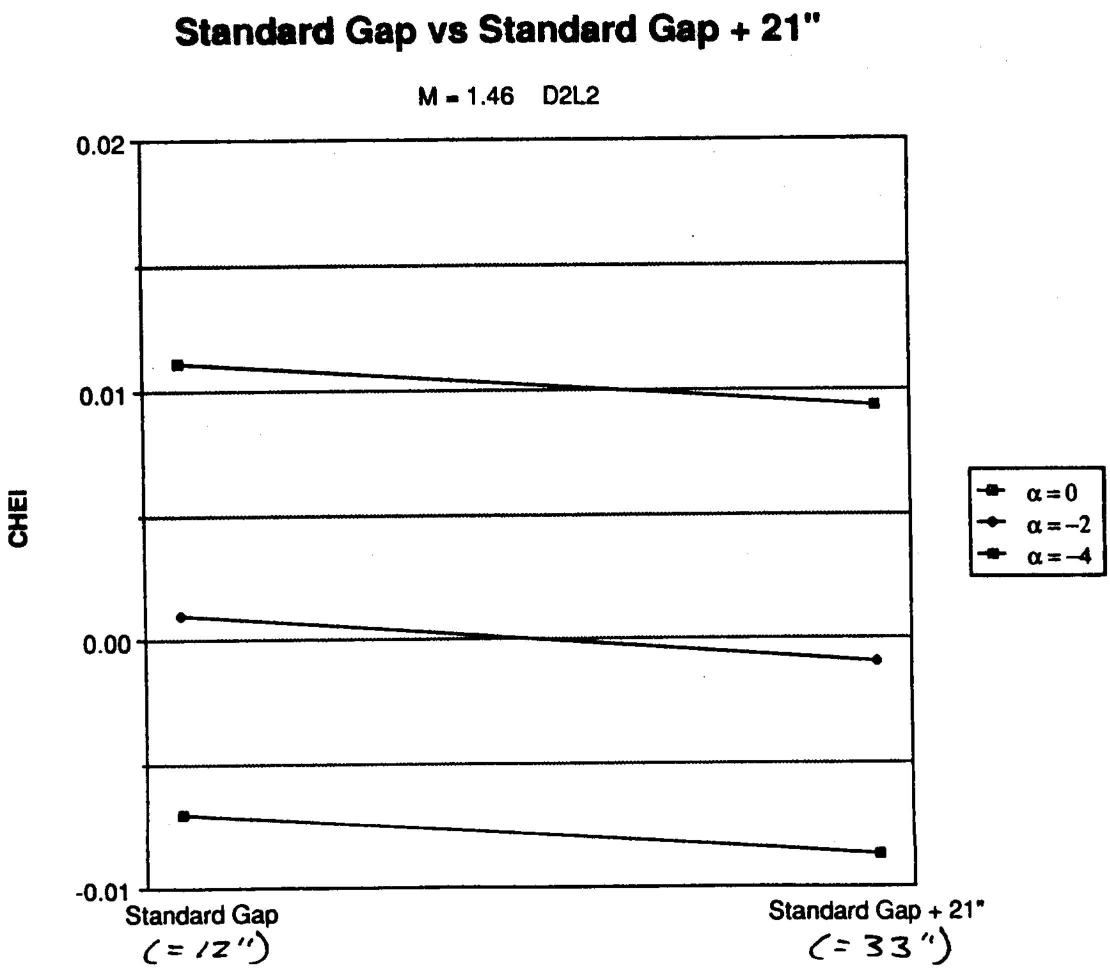

Fig. 6-31 CHEI vs GAP (D2L2)

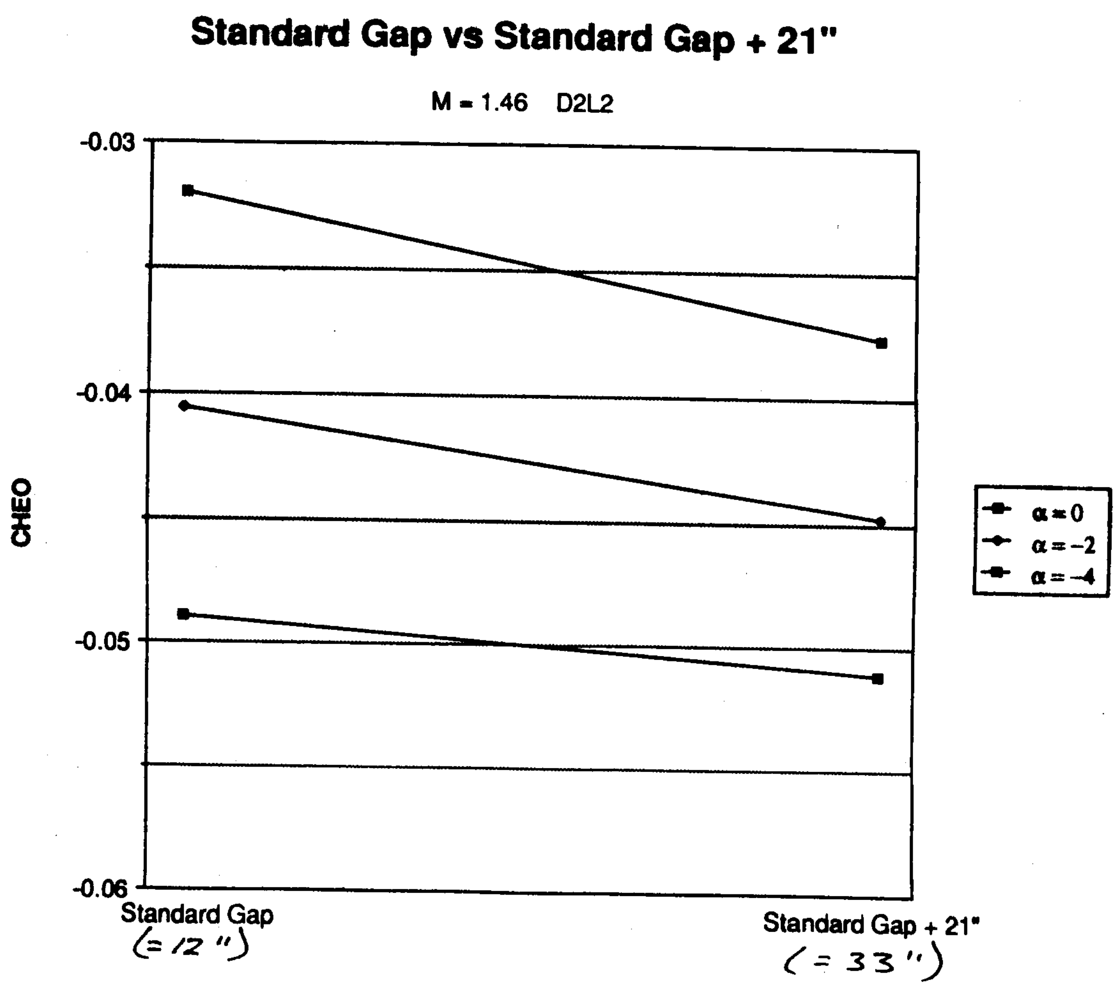

Fig. 6-32 CHEO vs GAP (D2L2)

6.2 AFT SKIRT EFFECTS SUMMARY

Data were also obtained from the wind tunnel test to determine the effects of aft skirts on aerodynamic coefficients. The two types of configurations tested, D1L1 and D2L2, can be found in Figs. 6-33 and 6-34. The test results can be found in Figs. 6-35 to 6-48 for D1L1 configurations, and in Figs. 6-49 to 6-58 for D2L2 configurations.

The conclusion from the analysis of the aft skirt effect is that the addition of the aft skirt had little effect on either total vehicle data or wind data. The addition of the skirt also had little effect when analyzing diameter and length effects.

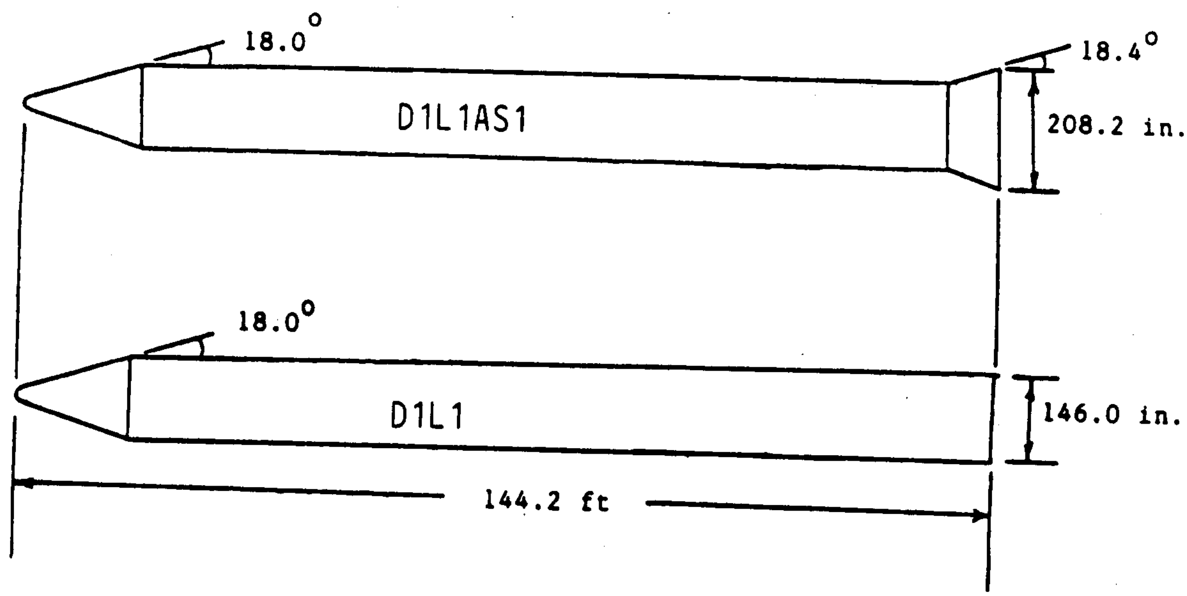

Fig. 6-33 Aft Skirt Configurations (D1L1)

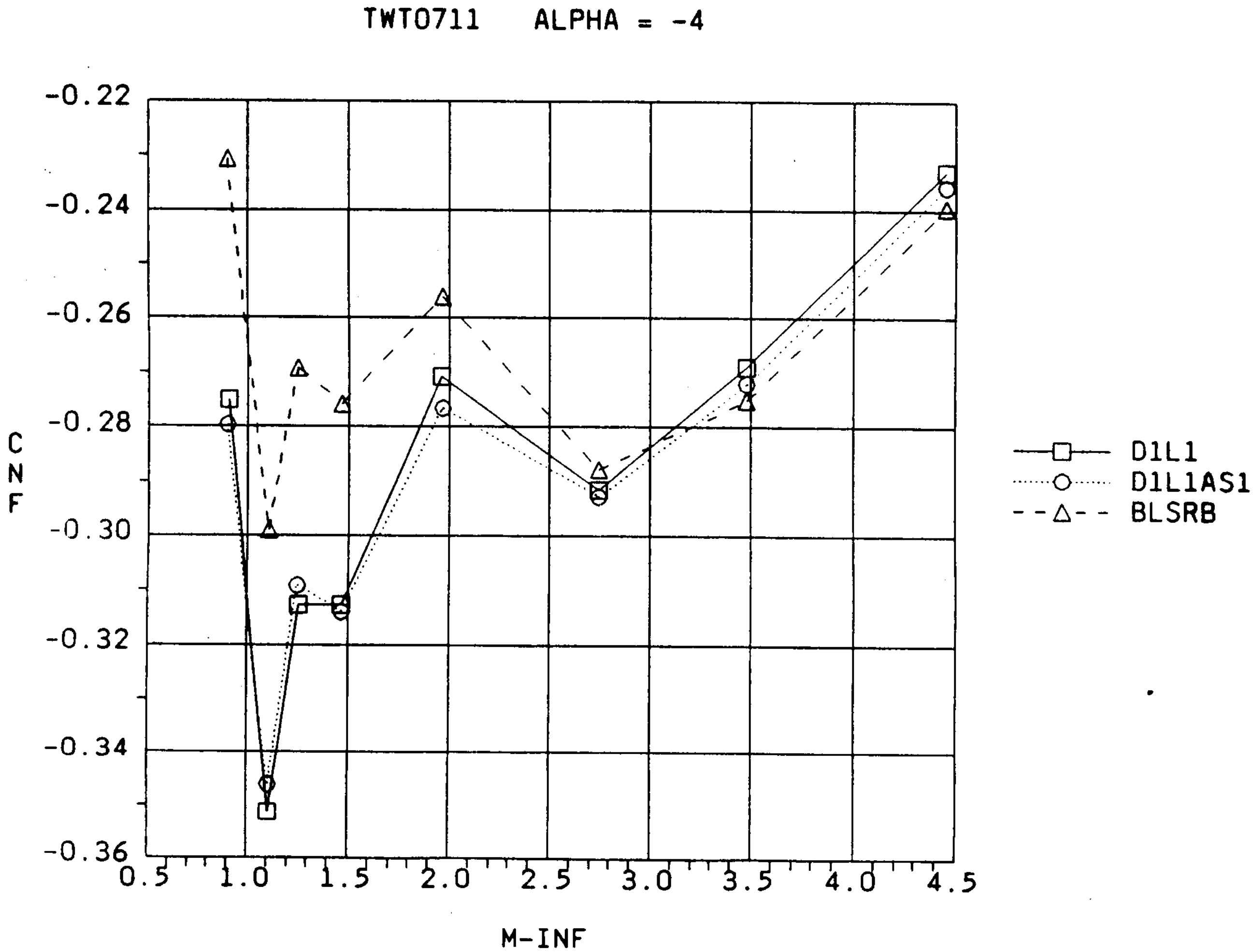

Fig. 6-35 C_{NF} vs Mach (D1L1)

PRECEDING PAGE BLANK NOT FILMED

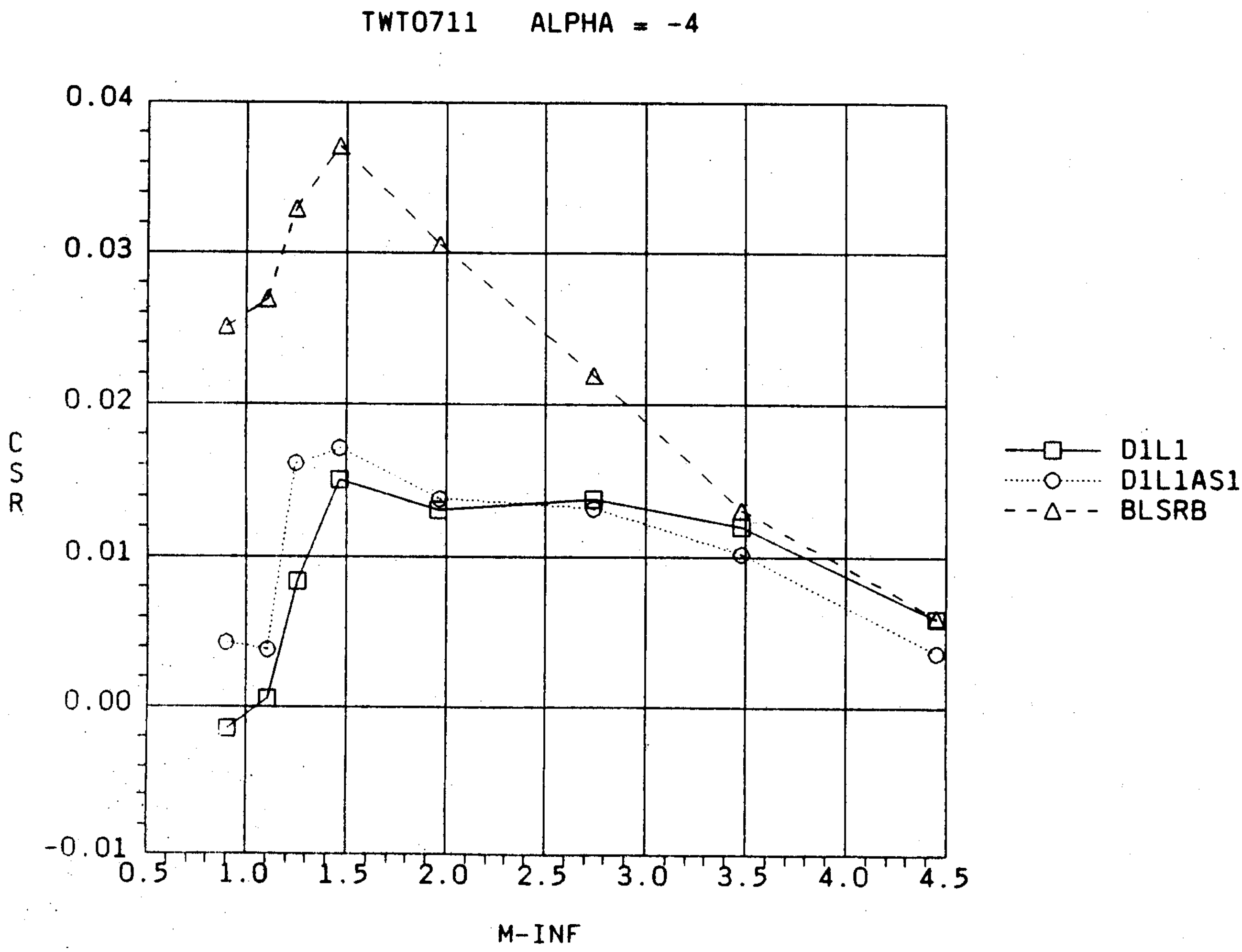

Fig. 6-36 C_{SR} vs Mach (D1L1)

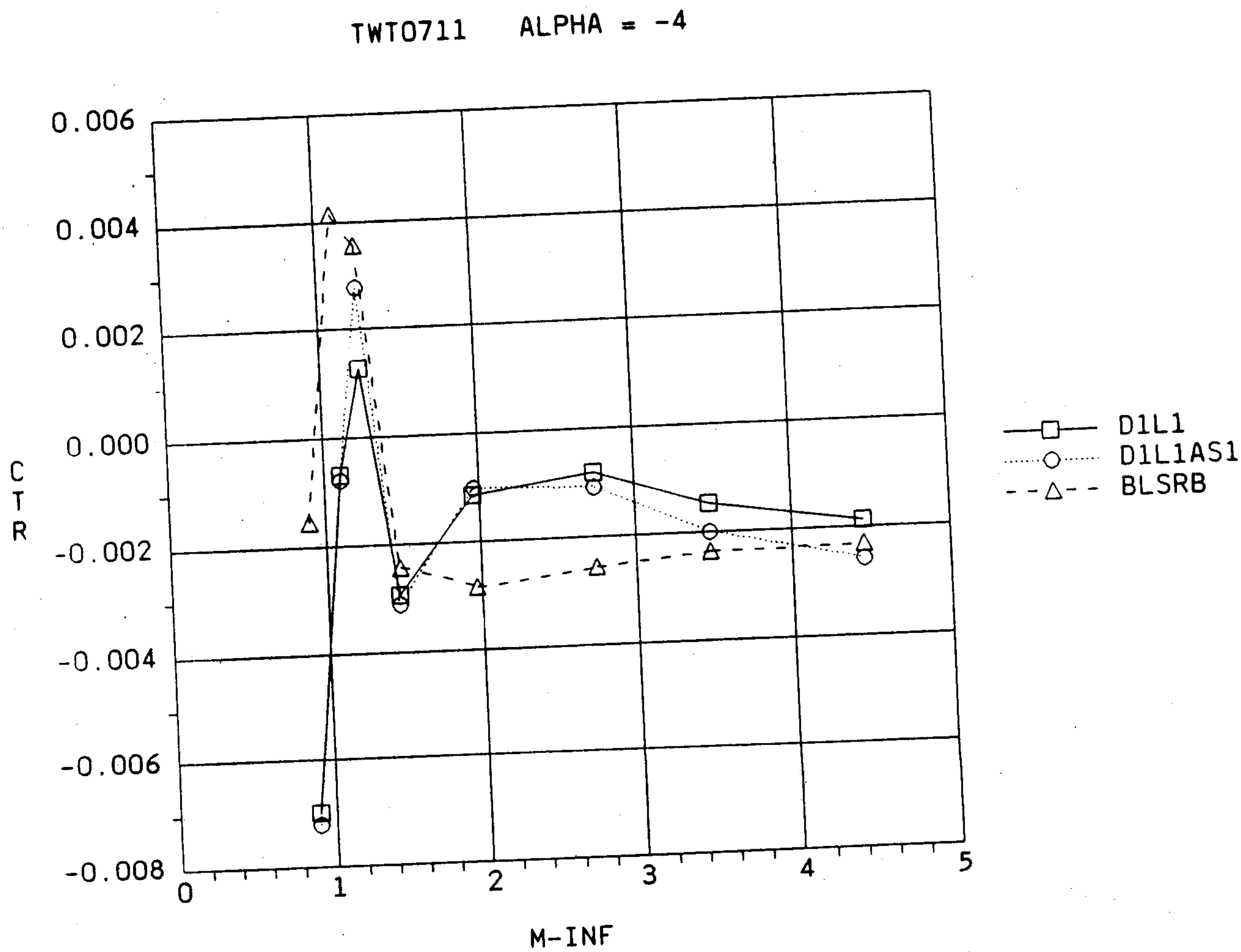

Fig. 6-37 C_{TR} vs Mach (D1L1)

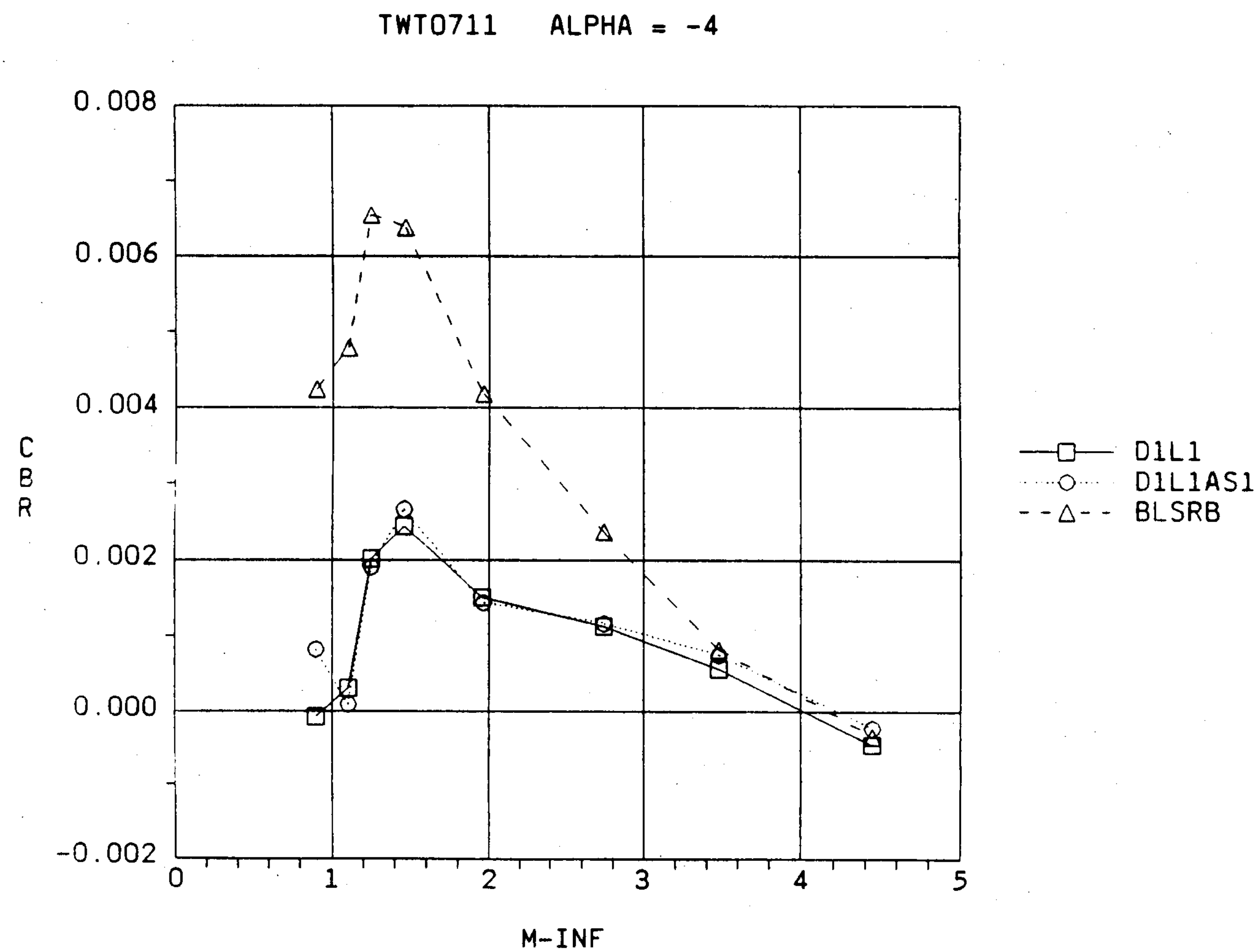

Fig. 6-38 C_{BR} vs Mach (D1L1)

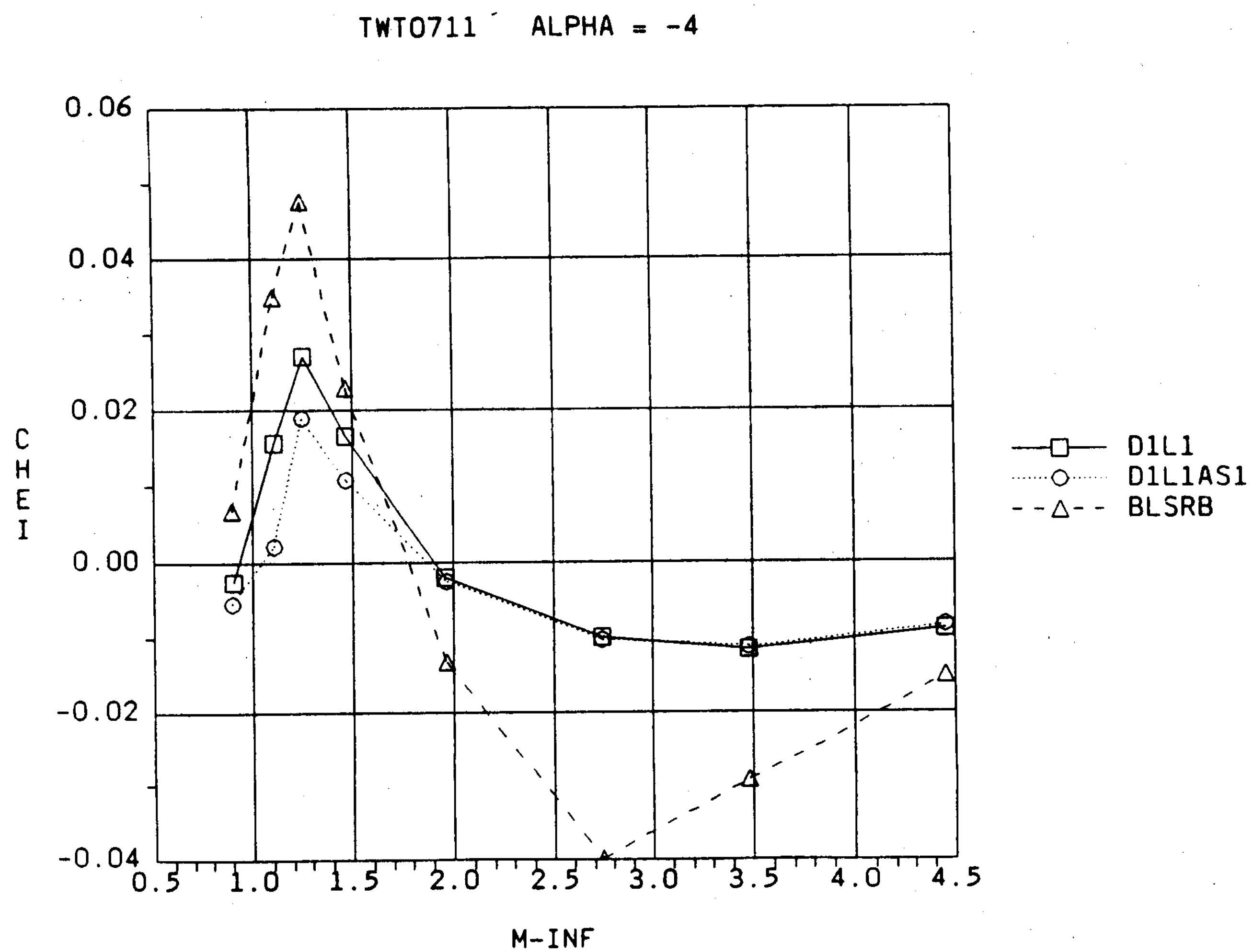

Fig. 6-39 CHEI vs Mach (D1L1)

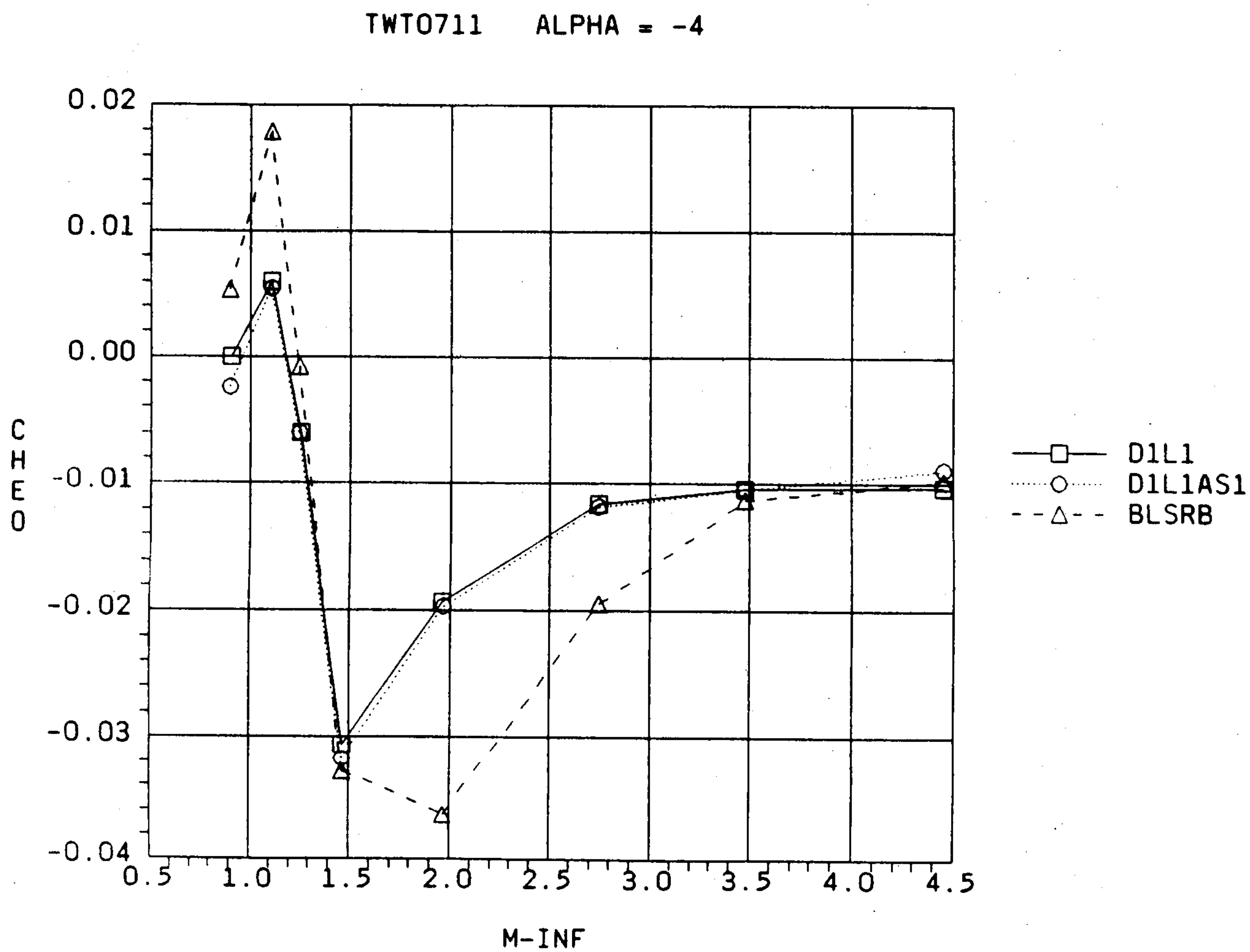

Fig. 6-40 CHEO vs Mach (D1L1)

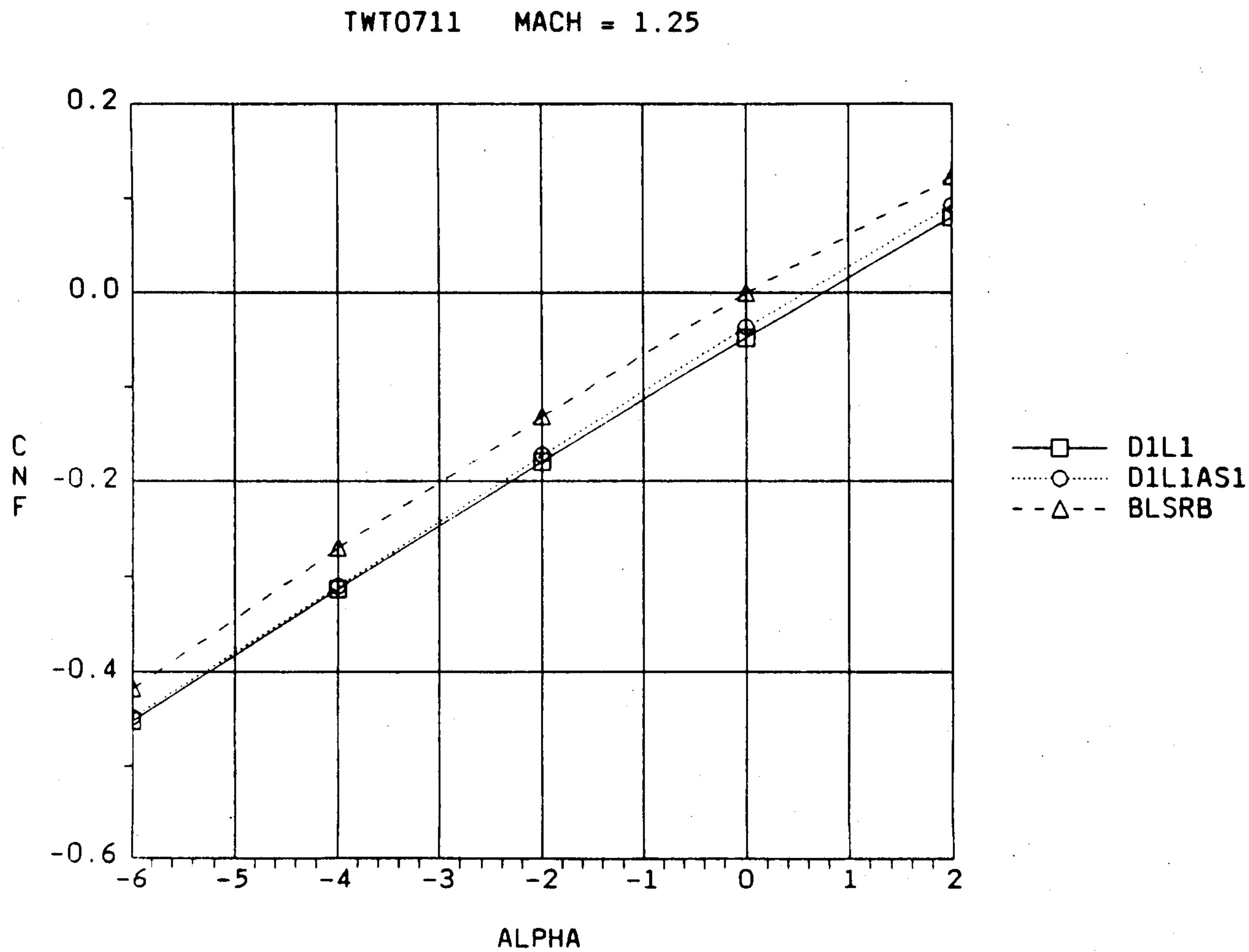

Fig. 6-41 C_{NF} vs α (D1L1, M = 1.25)

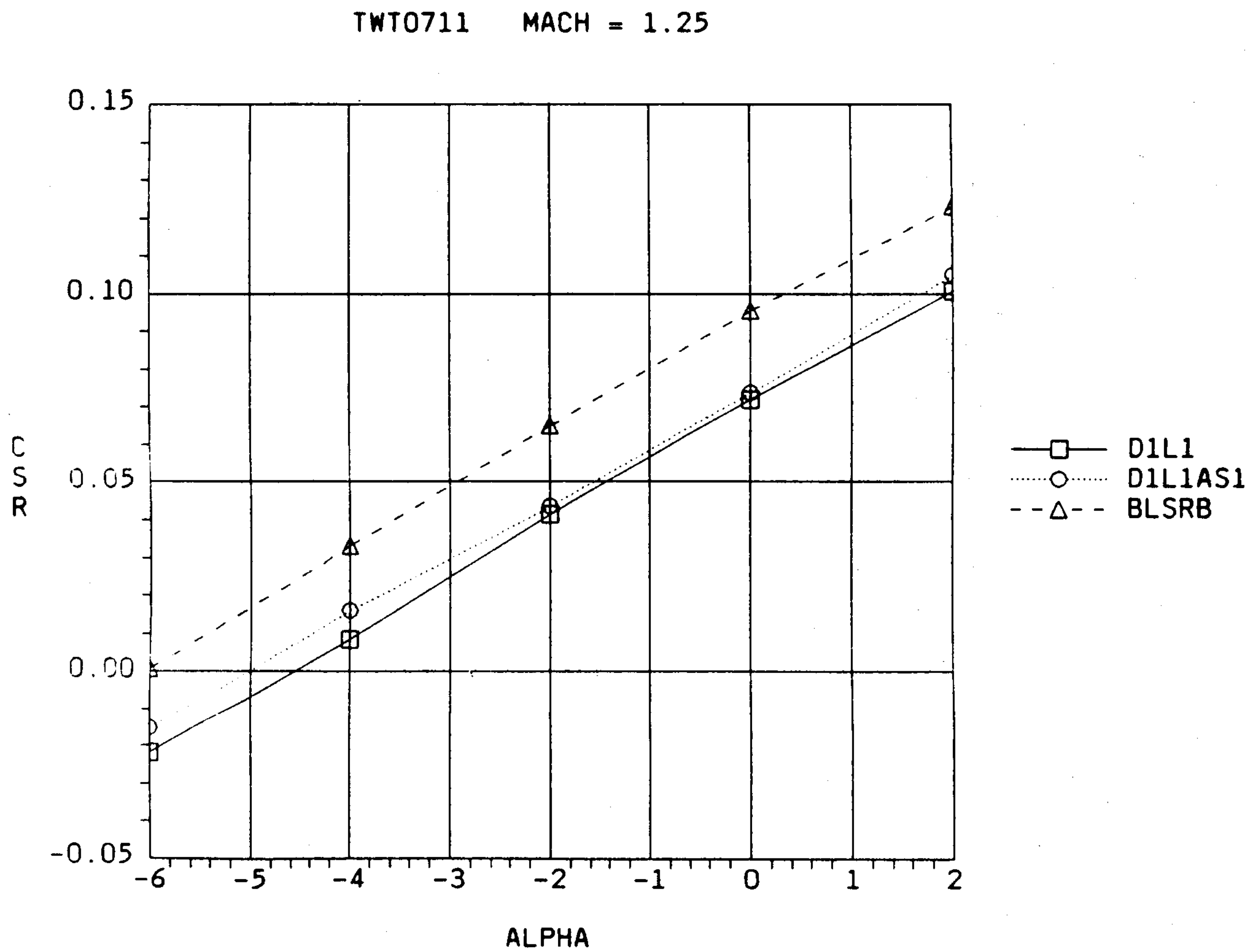

Fig. 6-42 C_{SR} vs α (D1L1, M = 1.25)

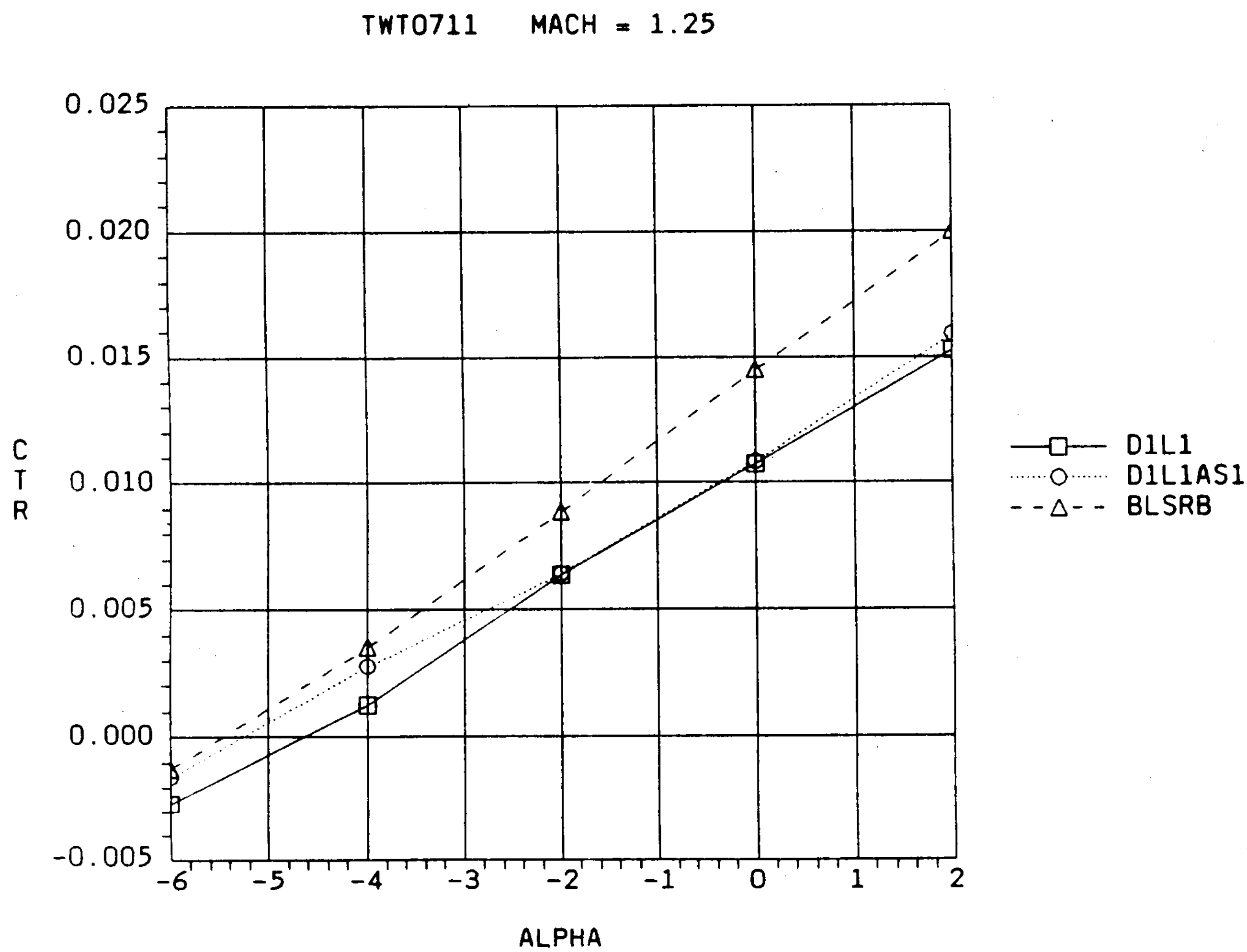

Fig. 6-43 C_{TR} vs α (D1L1, M = 1.25)

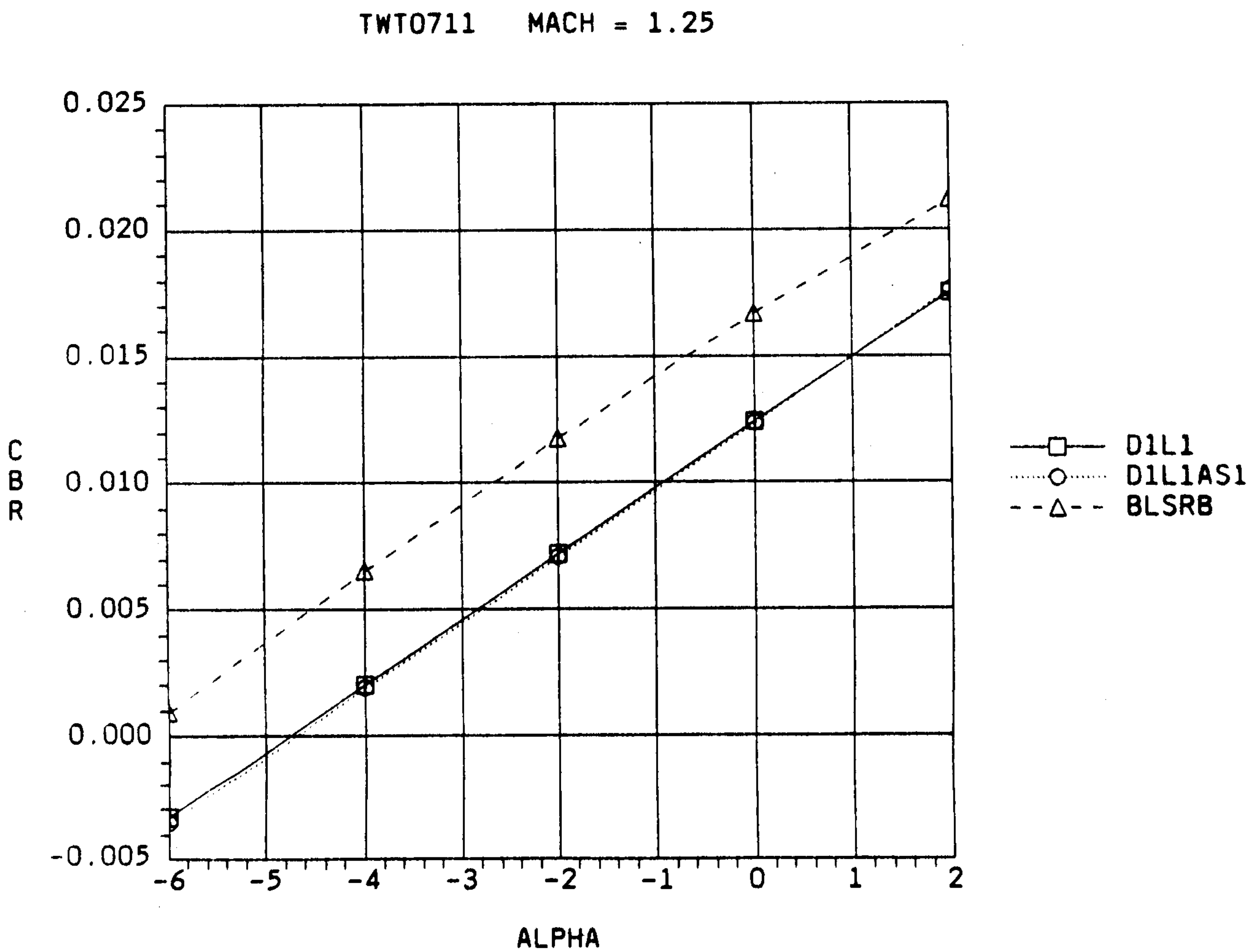

Fig. 6-44 C_{BR} vs α (D1L1, M = 1.25)

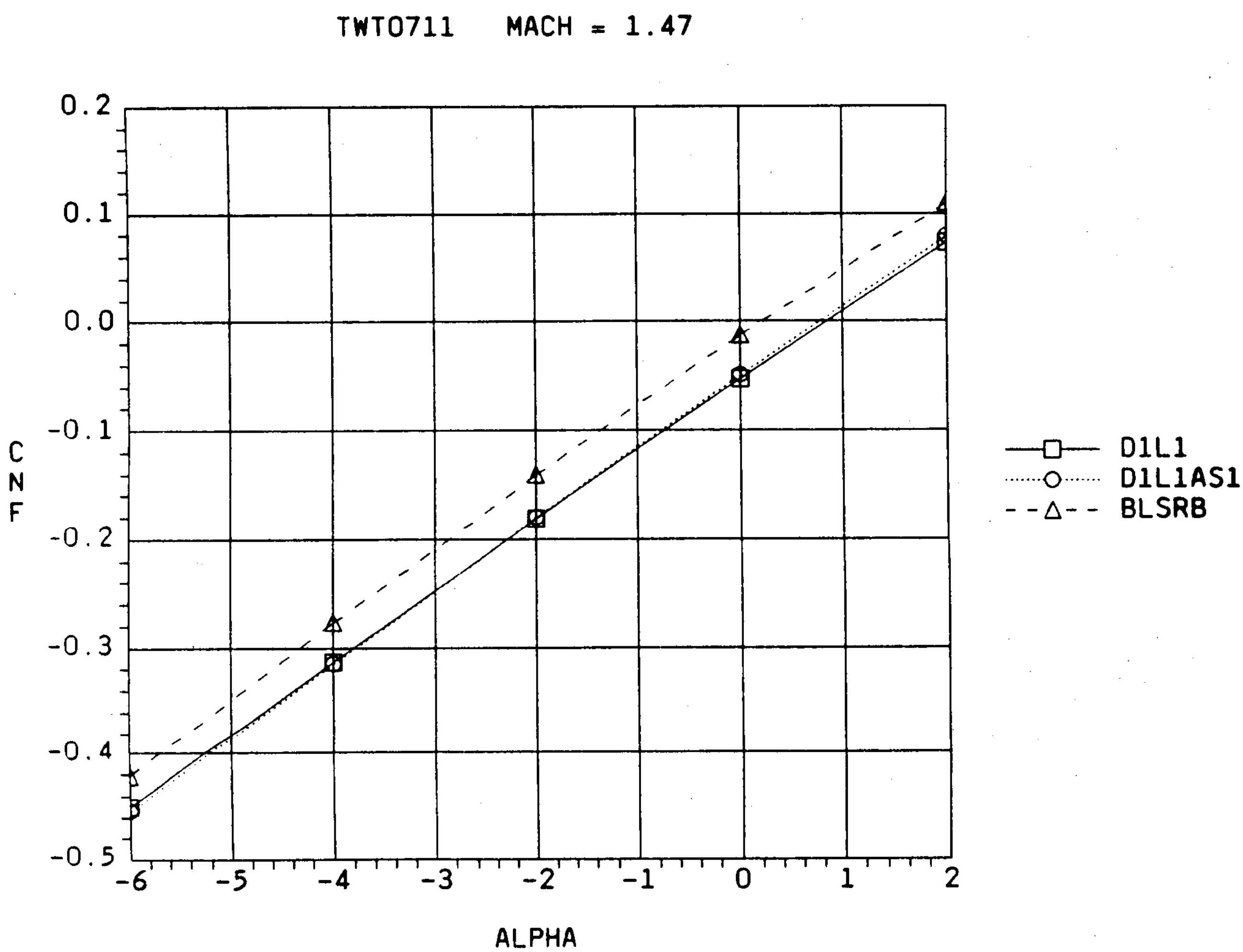

Fig. 6-45 C_{NF} vs α (D1L1, M = 1.47)

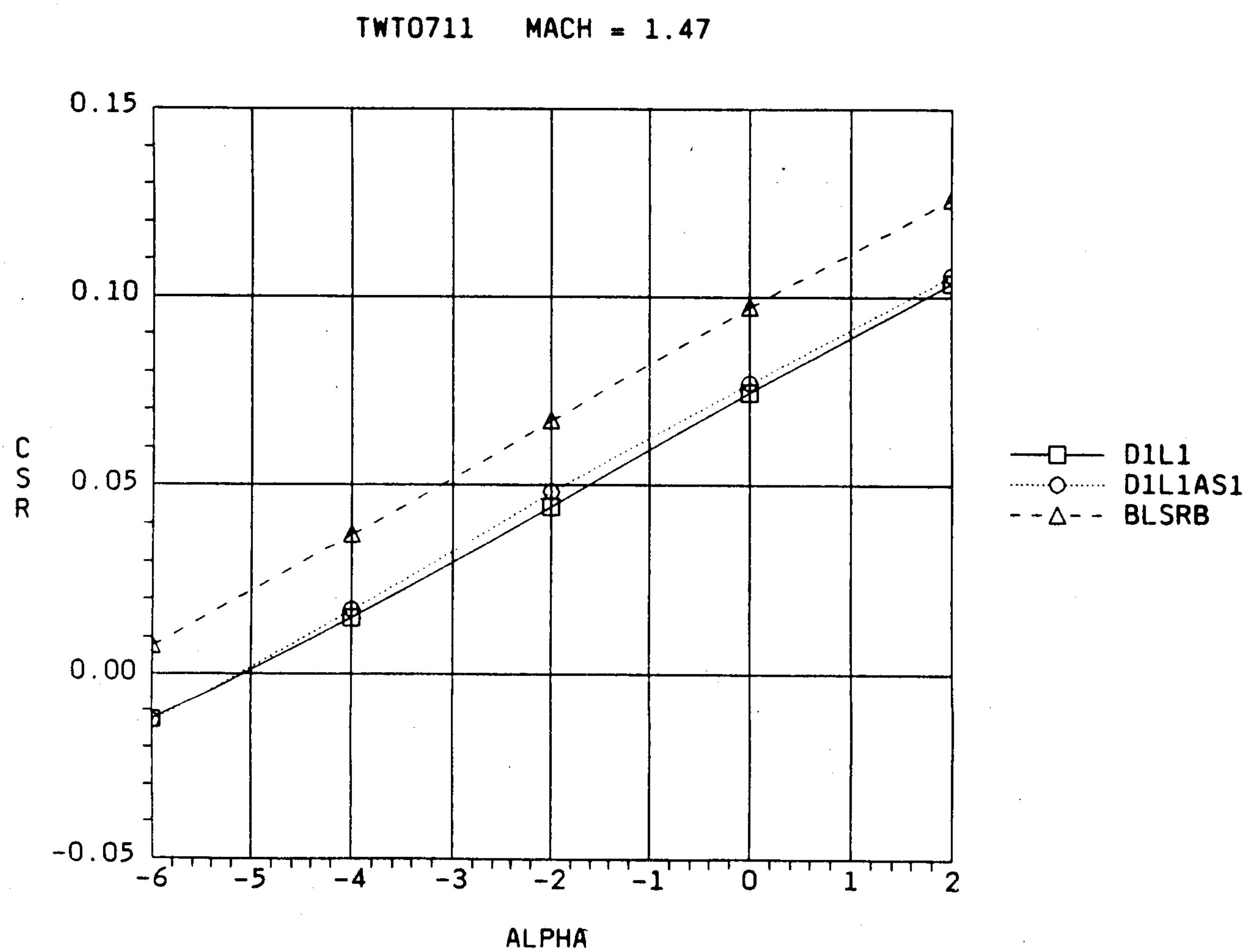

Fig. 6-46 C_{SR} vs α (D1L1, M = 1.47)

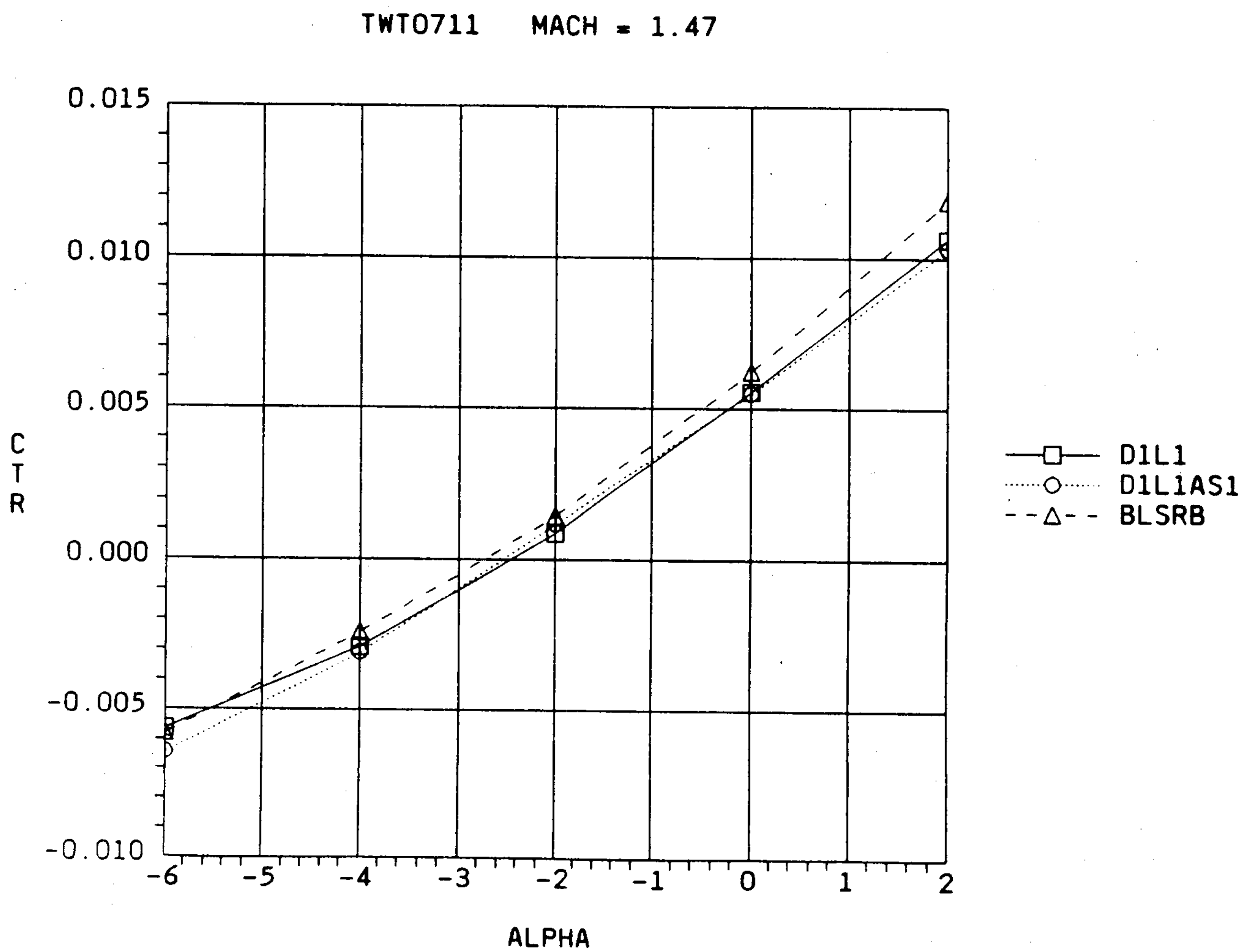

Fig. 6-47 C_{TR} vs α (D1L1, M = 1.47)

C-3

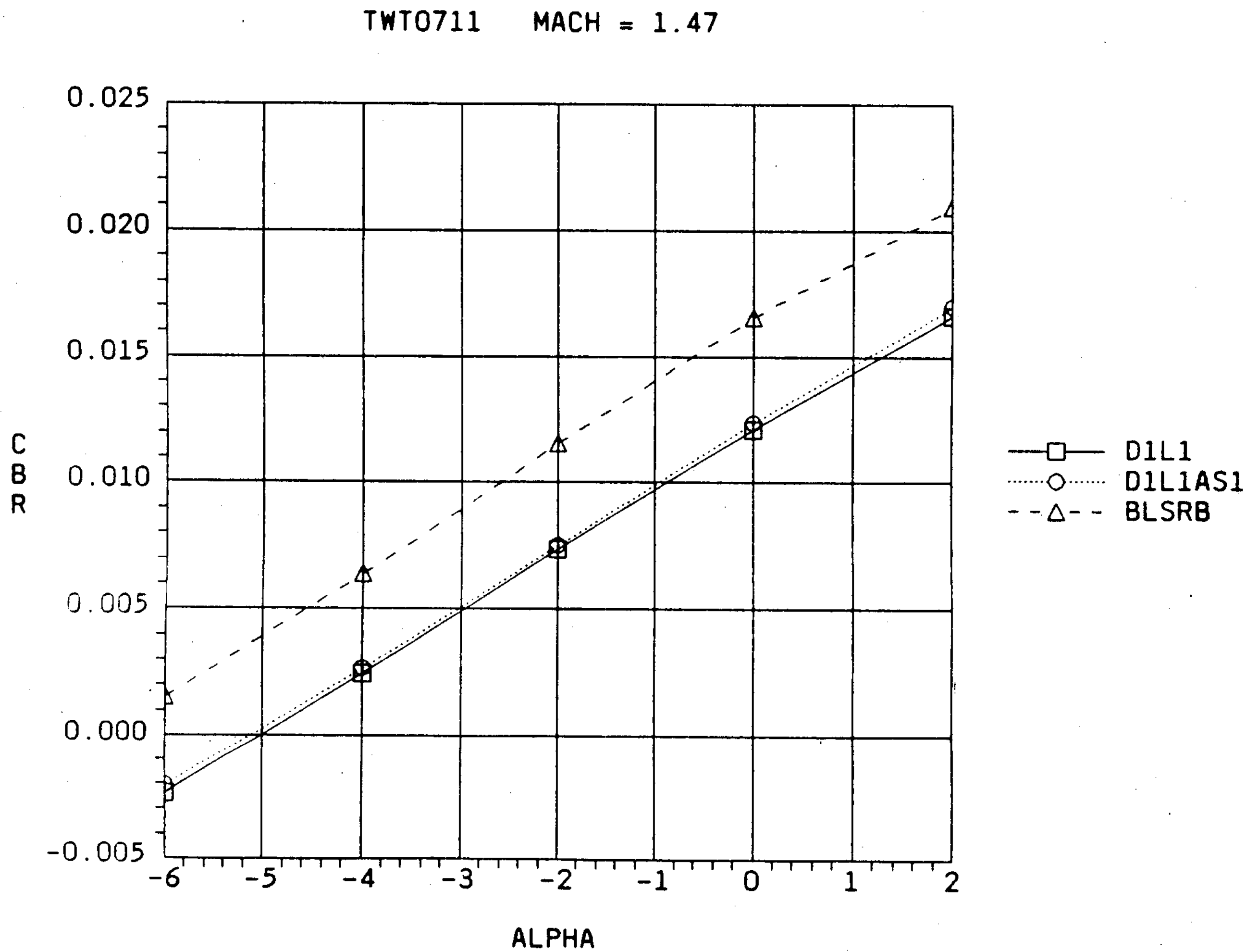

Fig. 6-48 C_{BR} vs α (D1L1, M = 1.47)

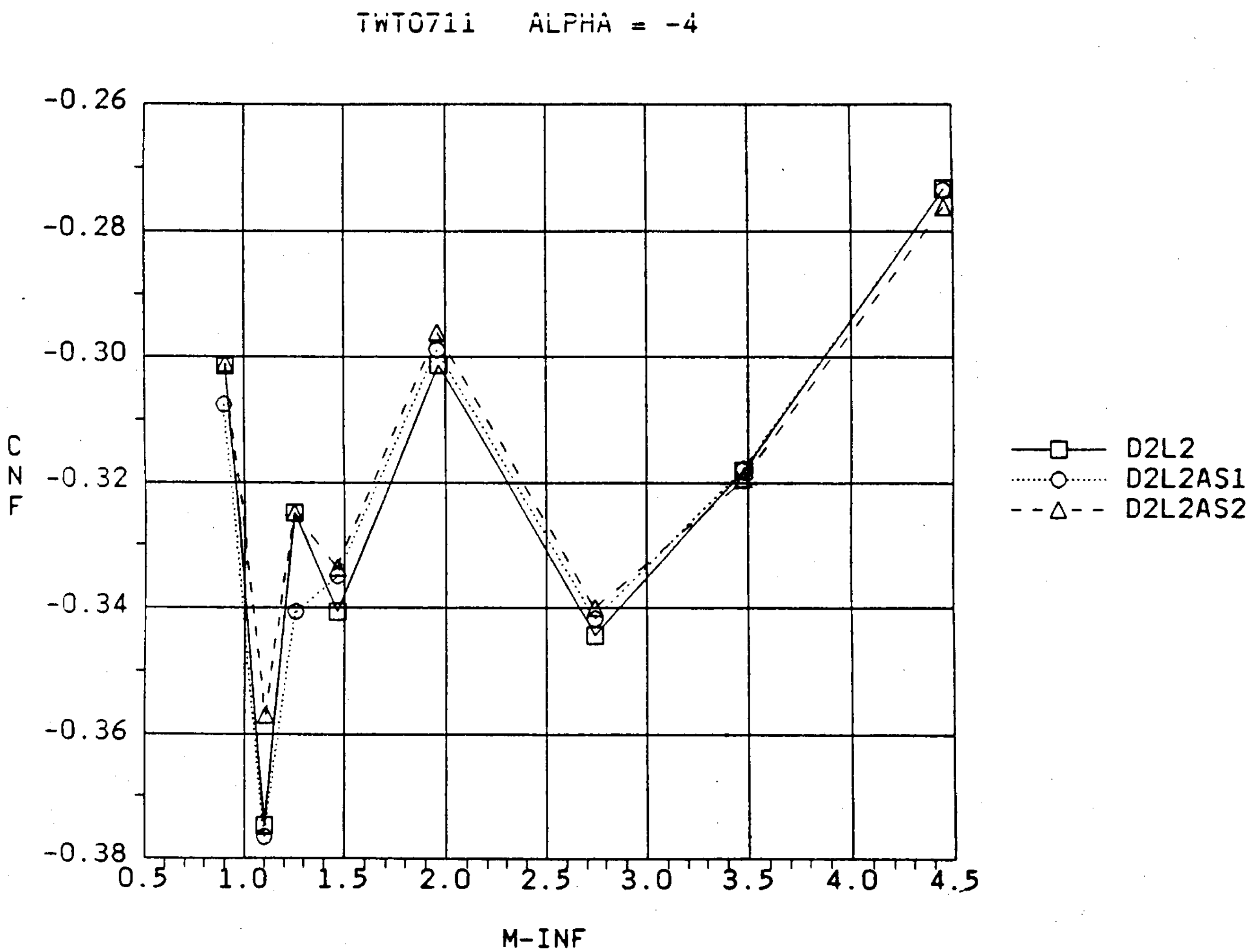

Fig. 6-49 C_{NF} vs Mach (D2L2)

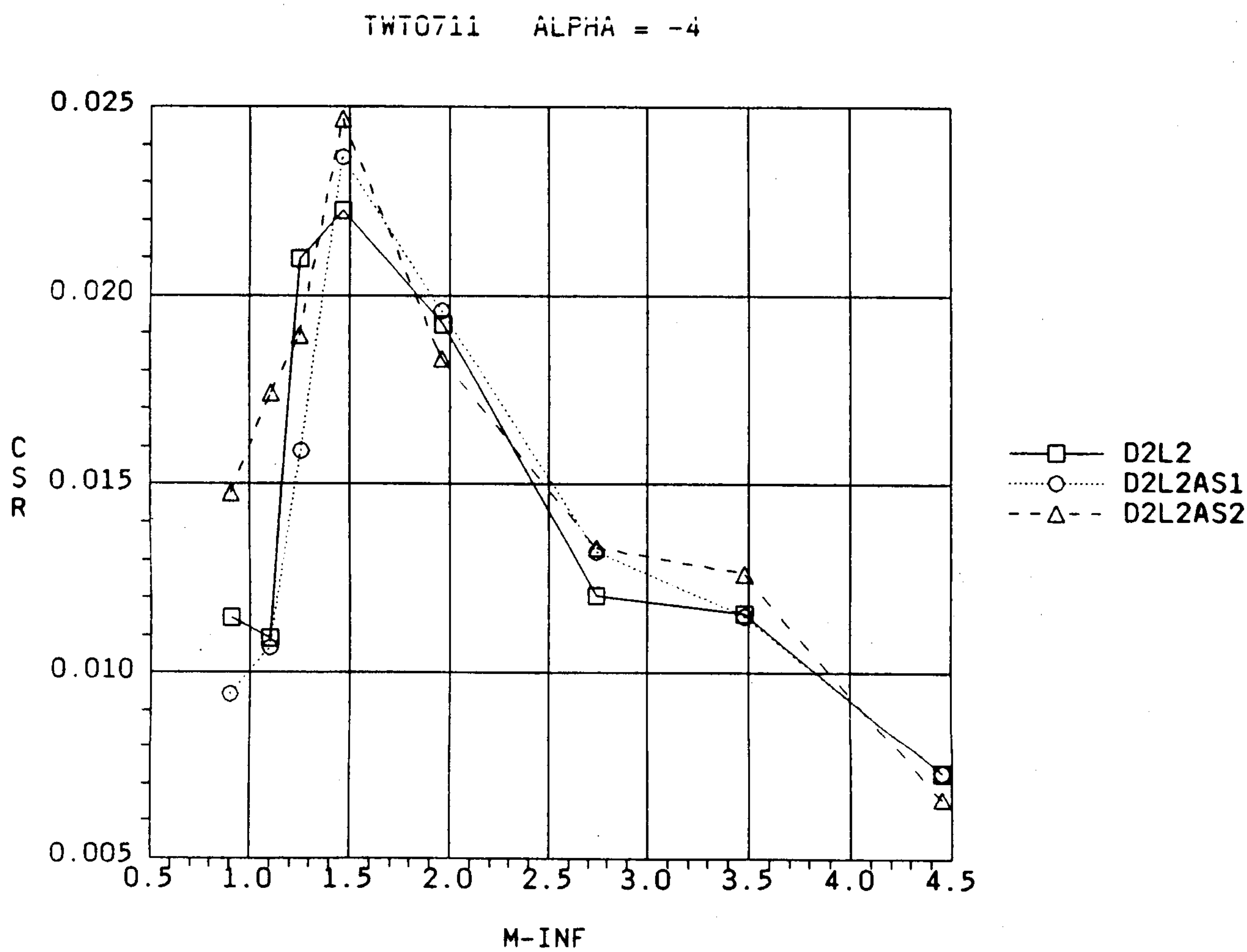

Fig. 6-50 C_{SR} vs Mach (D2L2)

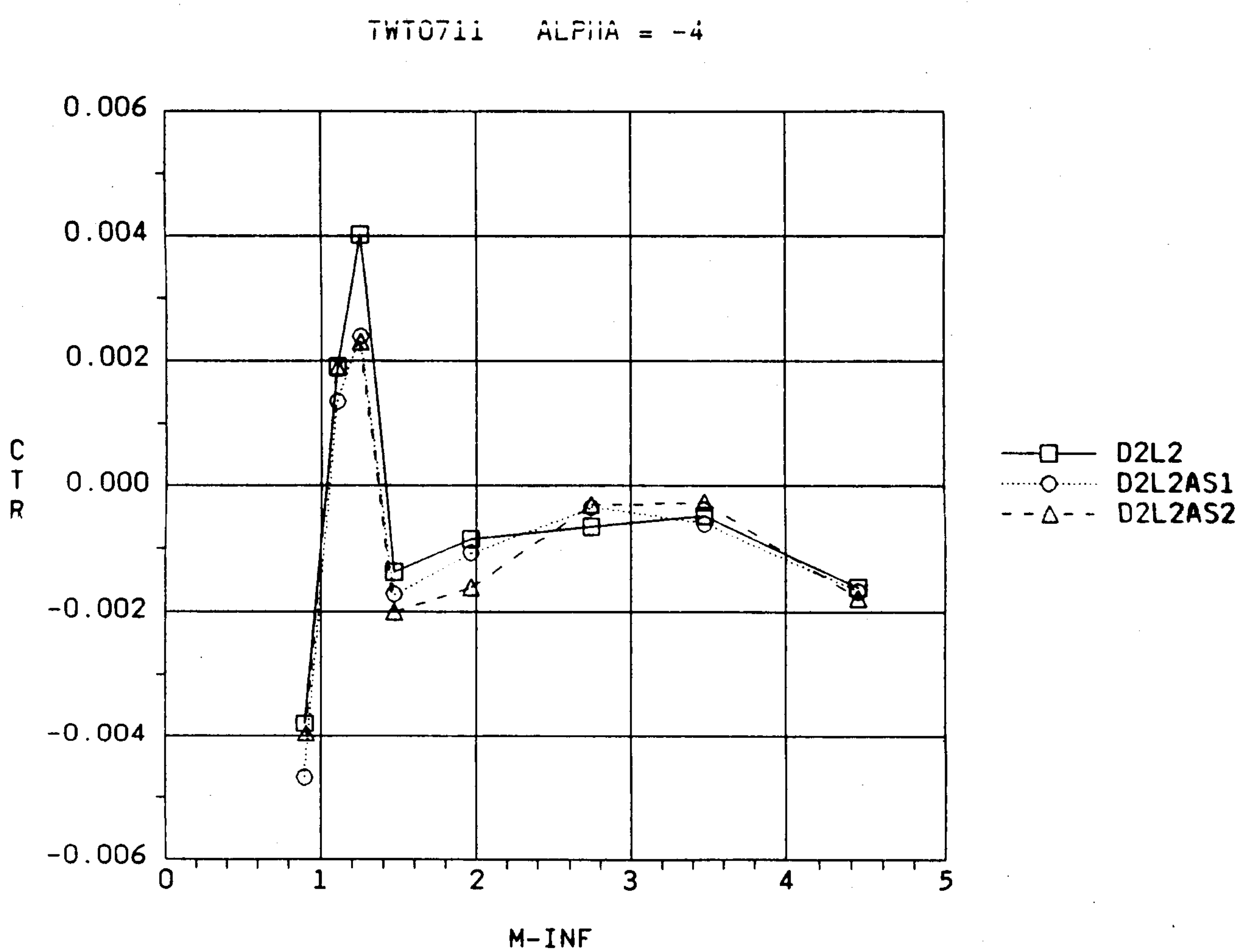

Fig. 6-51 C_{TR} vs Mach (D2L2)

ORIGINAL PAGE IS
OF POOR QUALITY

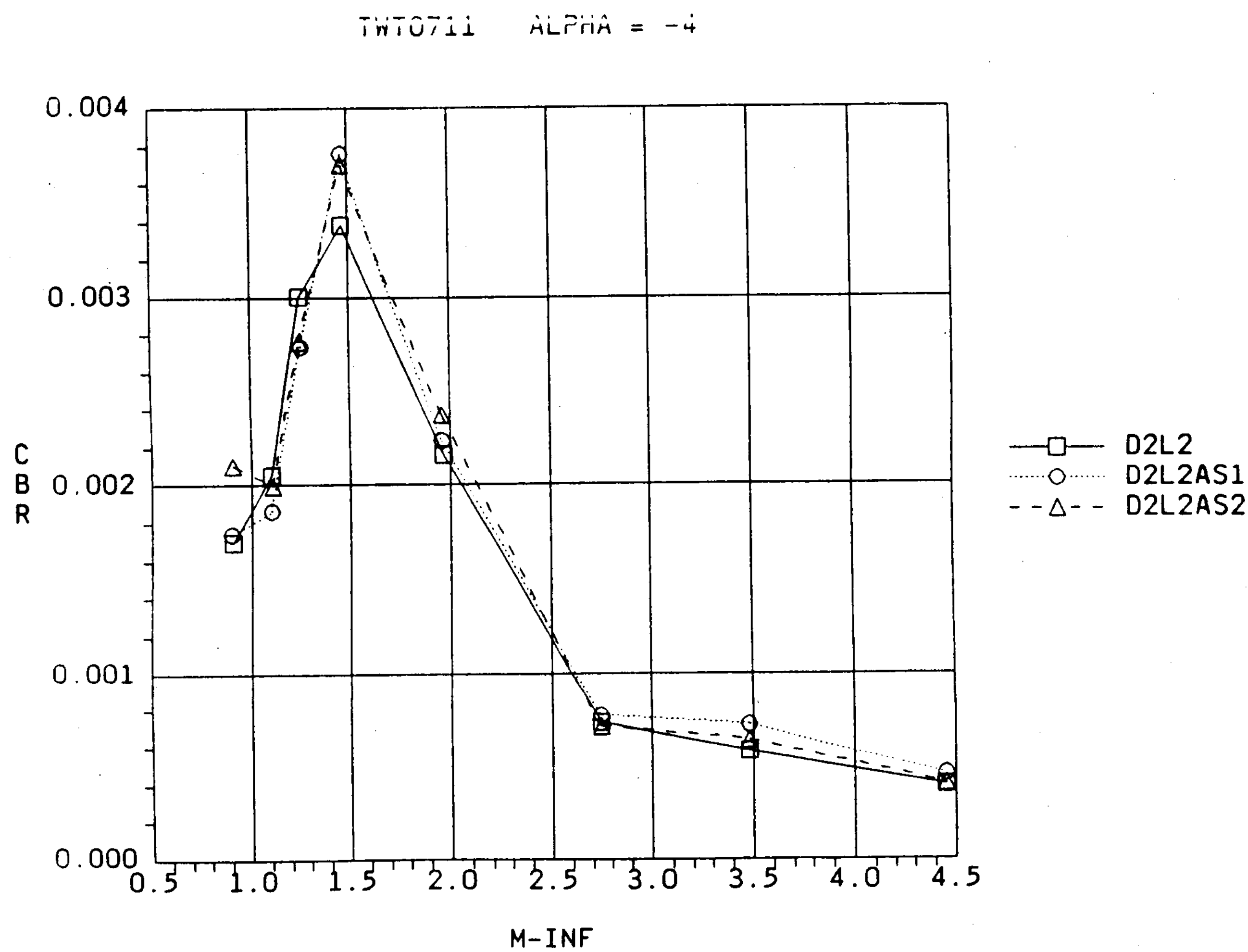

Fig. 6-52 C_{BR} vs Mach (D2L2)

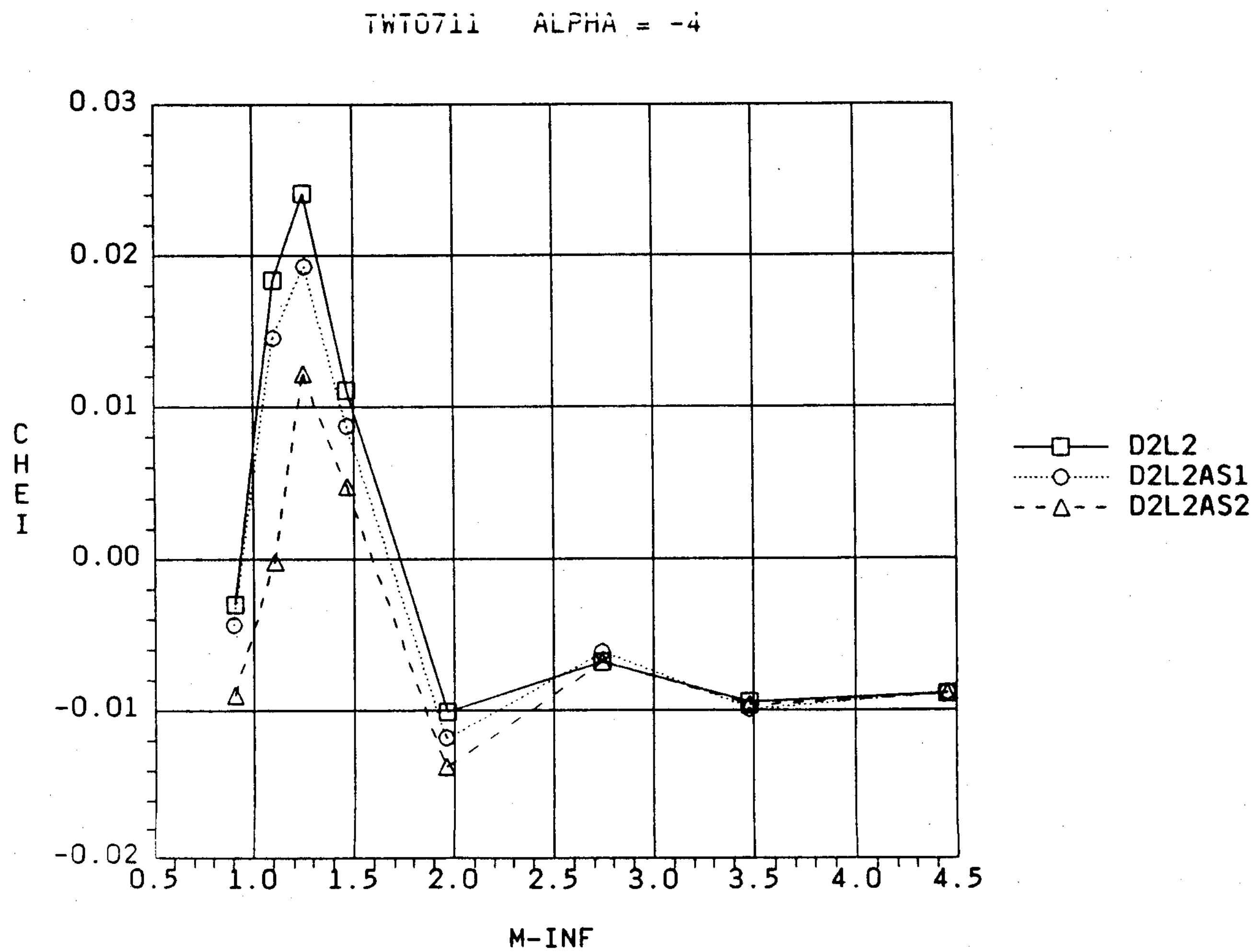

Fig. 6-53 CHEI vs Mach (D2L2)

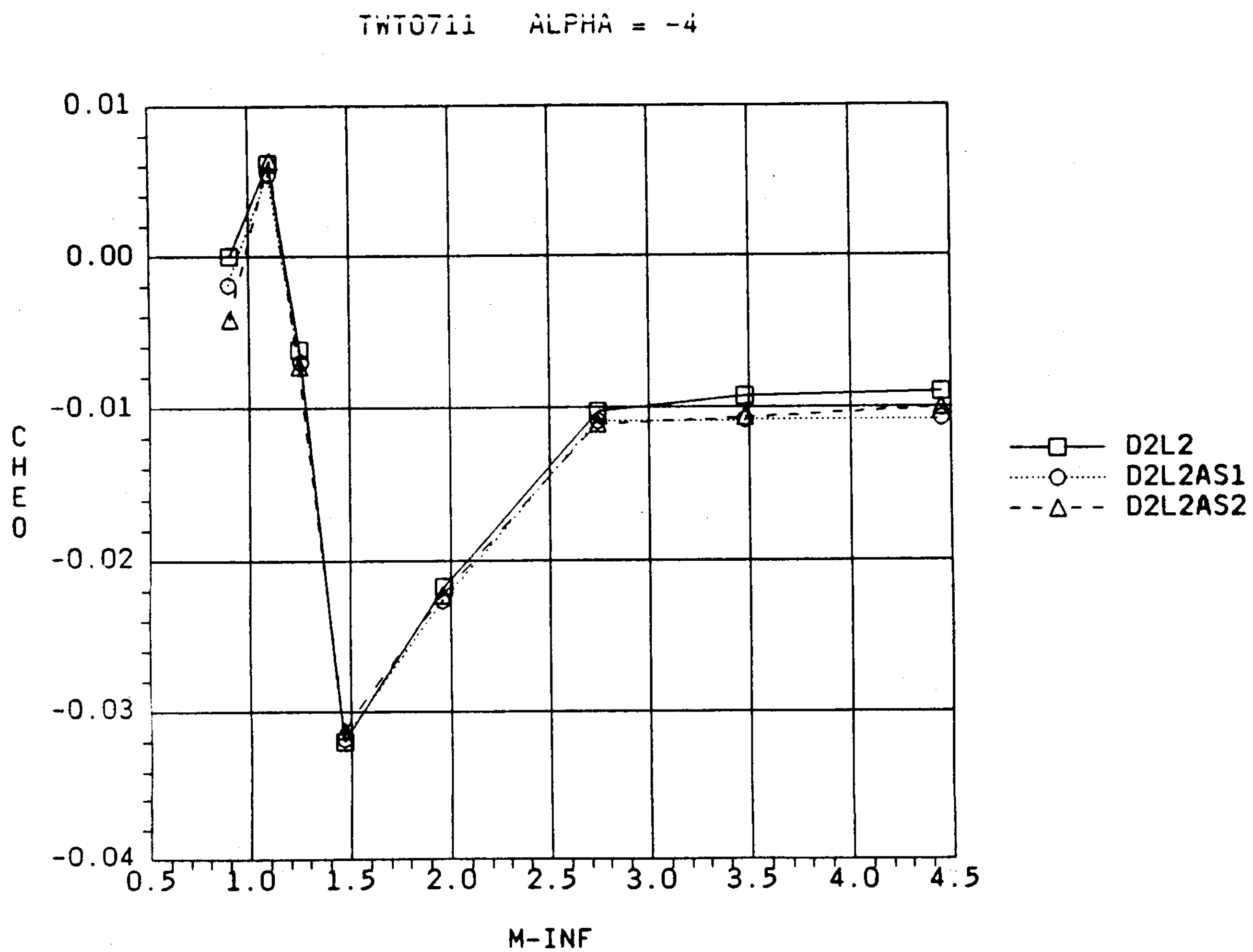

Fig. 6-54 CHEO vs Mach (D2L2)

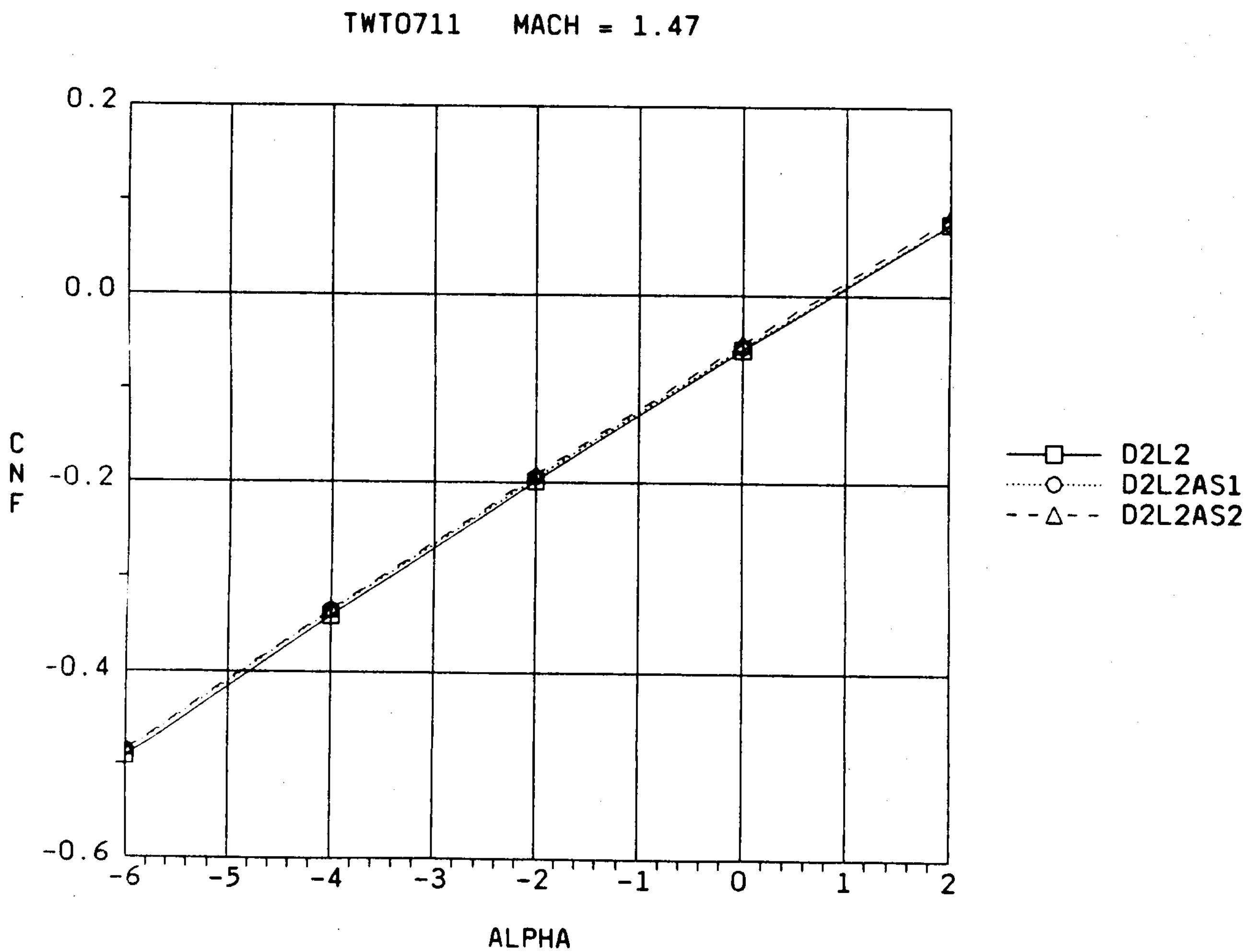

Fig. 6-55 C_{NF} vs α (D2L2, M = 1.47)

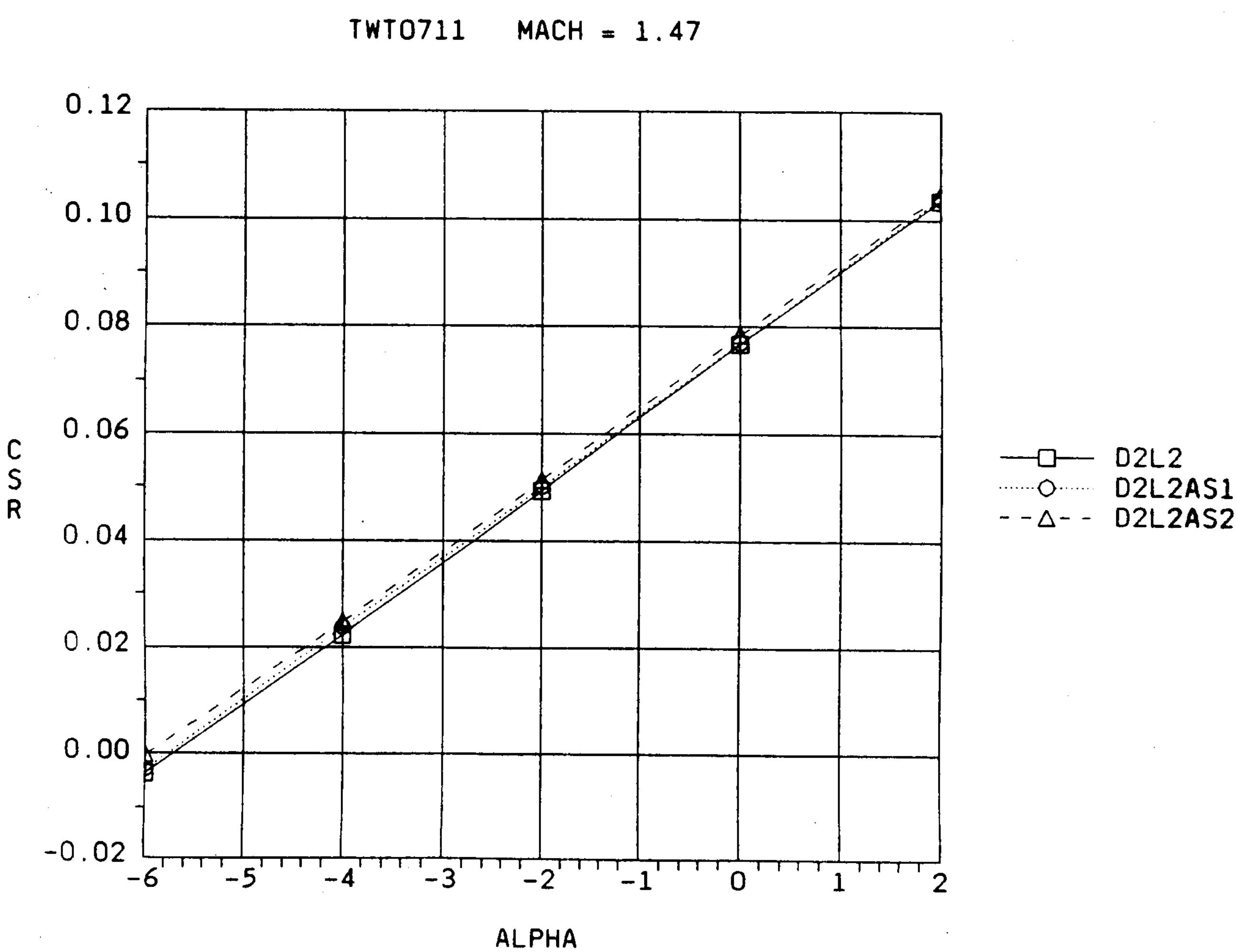

Fig. 6-56 C_{SR} vs α (D2L2, M = 1.47)

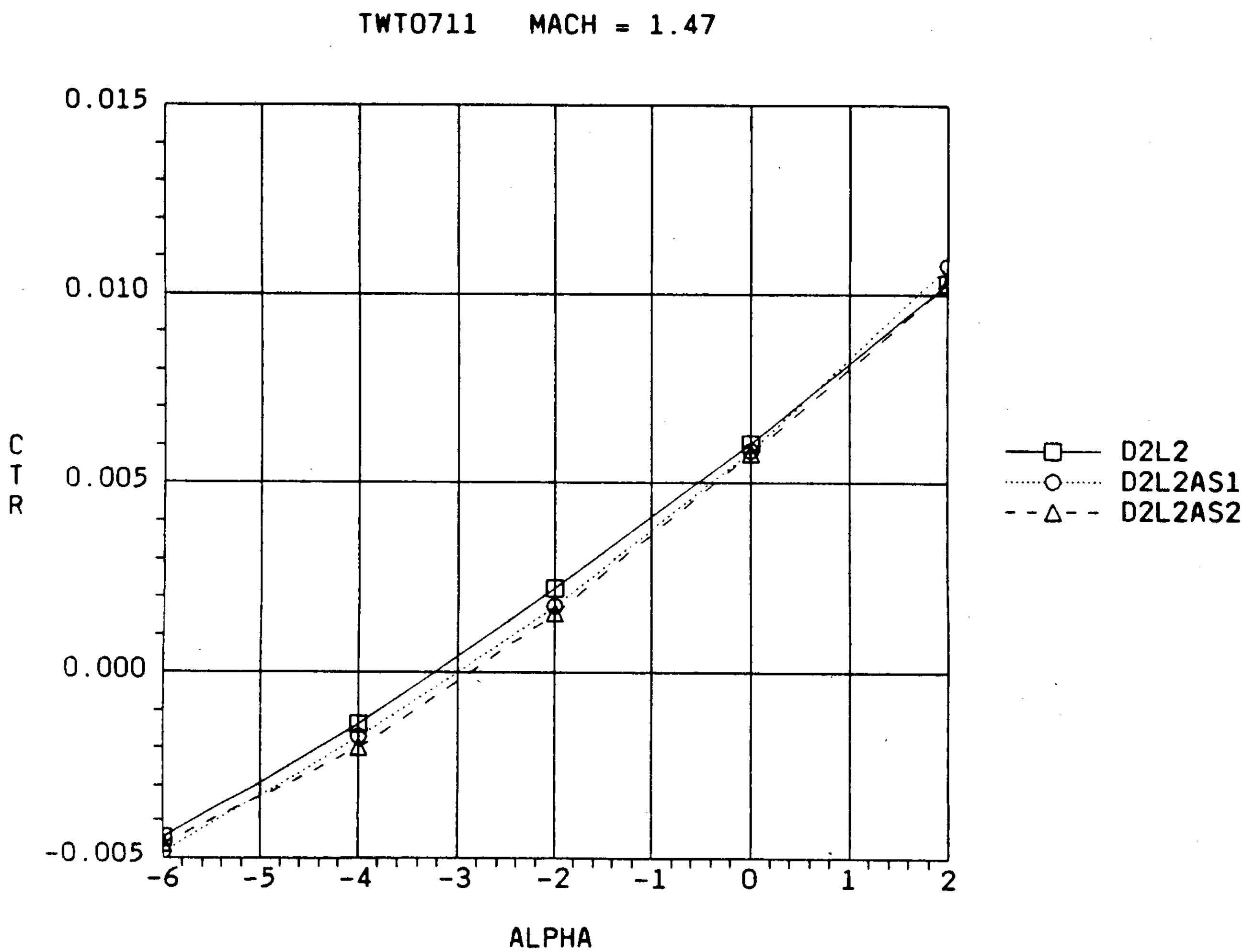

Fig. 6-57 C_{TR} vs α (D2L2, M = 1.47)

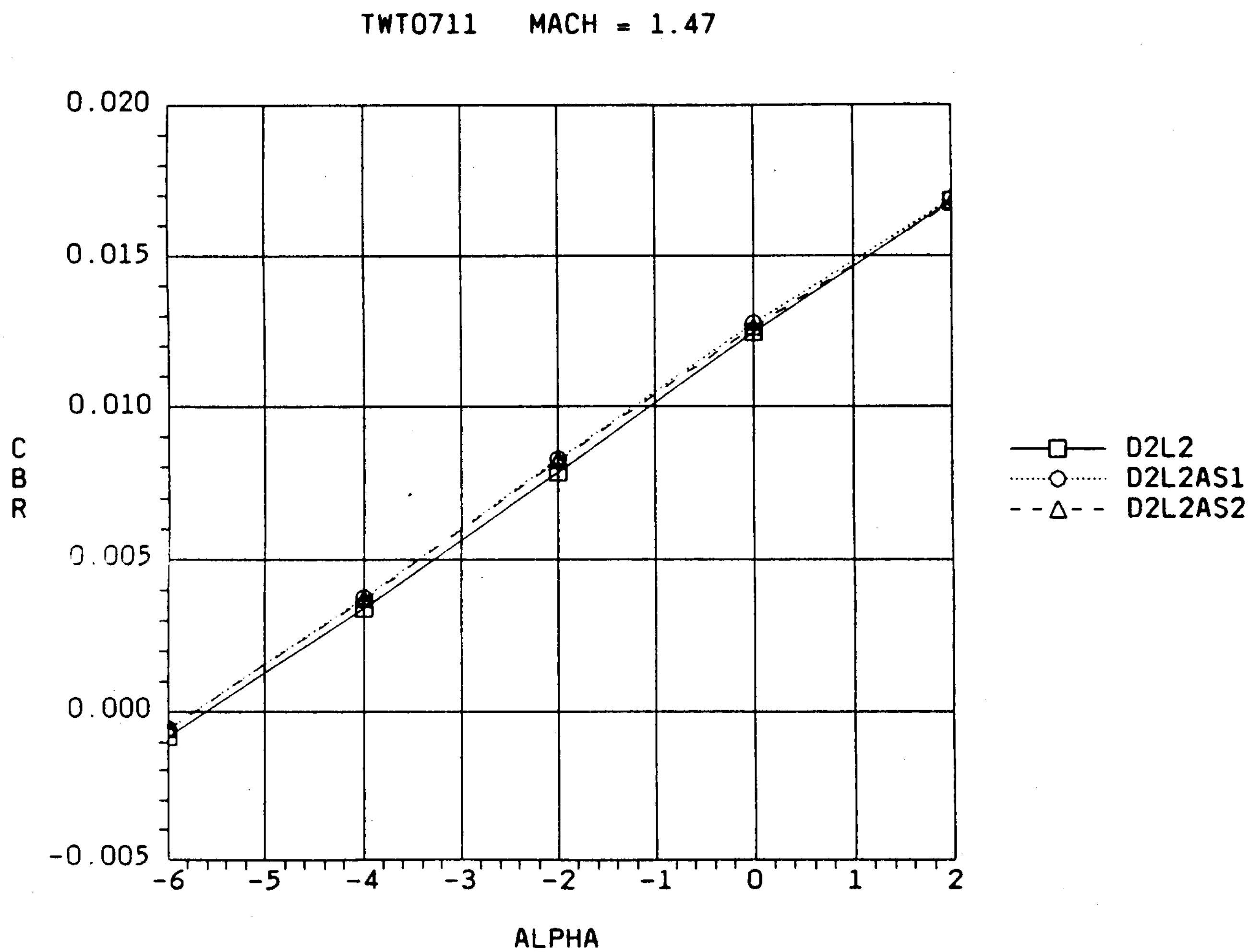

Fig. 6-58 C_{BR} vs α (D2L2, M = 1.47)

7. LRB BASE DRAG STUDY

As part of the effort in selecting a booster in the proposed LRB concept for the space shuttle program, Lockheed Missiles and Space Co. conducted a base drag study on a number of candidate boosters. At the root of the study was the development of a computer code which would calculate base drag based on the methods found in the Compendium of Flight Vehicle Base Pressure and Base Drag Prediction Techniques (Lockheed Missiles and Space Co.; August 1983. Once the code was operational it was used to obtain base drag estimates on two Martin Marietta and two General Dynamics LRB configurations. These results were compared with those found in an earlier base drag study, conducted by Lockheed. The final results were then selected, and included in the shuttle aerodynamic data base.

7.1 ORIGINAL BASE DRAG ESTIMATES

A study hereafter was conducted in late 1987 called the baseline study on base drag effects for a number of generic LRB configurations, having 1, 2, 3, 4, and 5 nozzles (see Fig. 7-1) The study used as its basis the same base drag compendium mentioned above. The results were calculated for an STS vehicle with SRB's (see Fig. 7-2) and with an average LRB, Fig. 7-3. The trajectory used in these calculations can be found in Figs. 7-4 to 7-6. Results for total base drag were calculated for each (see Figs. 7-7, 7-8, and Tables 7-1, 7-2). To obtain delta base drag values (Fig. 7.9 and Table 7-3), the SRB results were subtracted from the LRB results. These delta base drag values were the proposed results to be included in the shuttle aerodynamic data base.

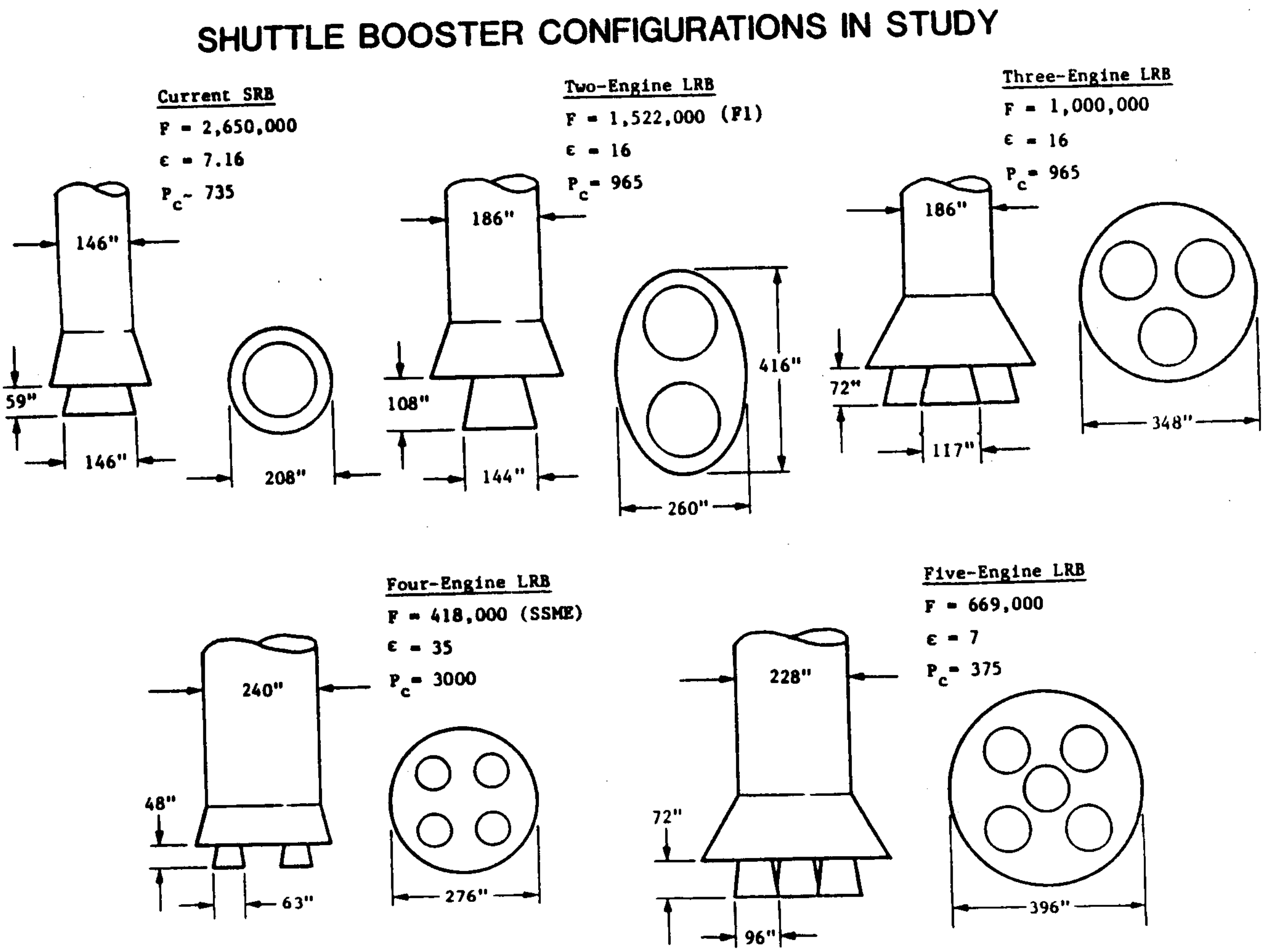

Fig. 7-1 Baseline Study LRB Configurations

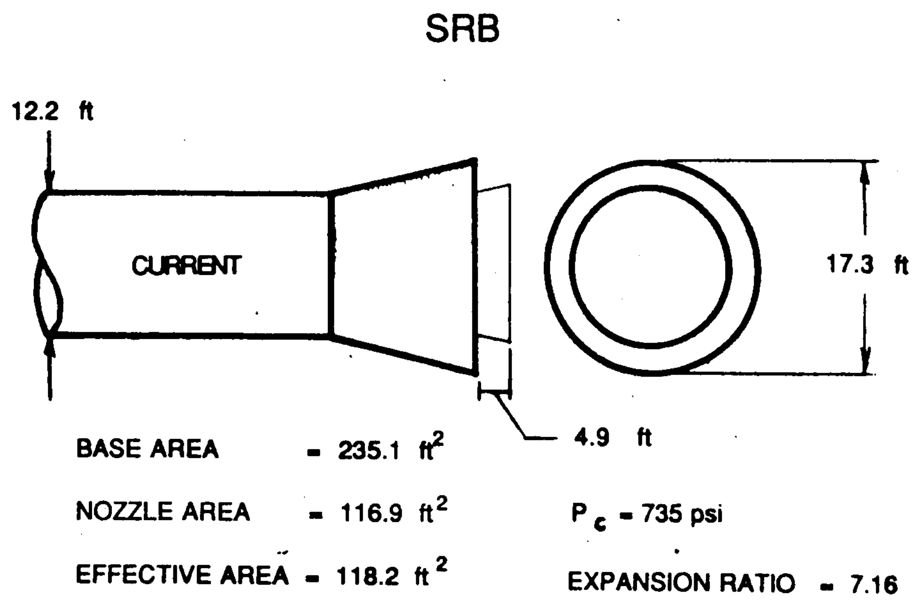

Fig. 7-2 Current SRB

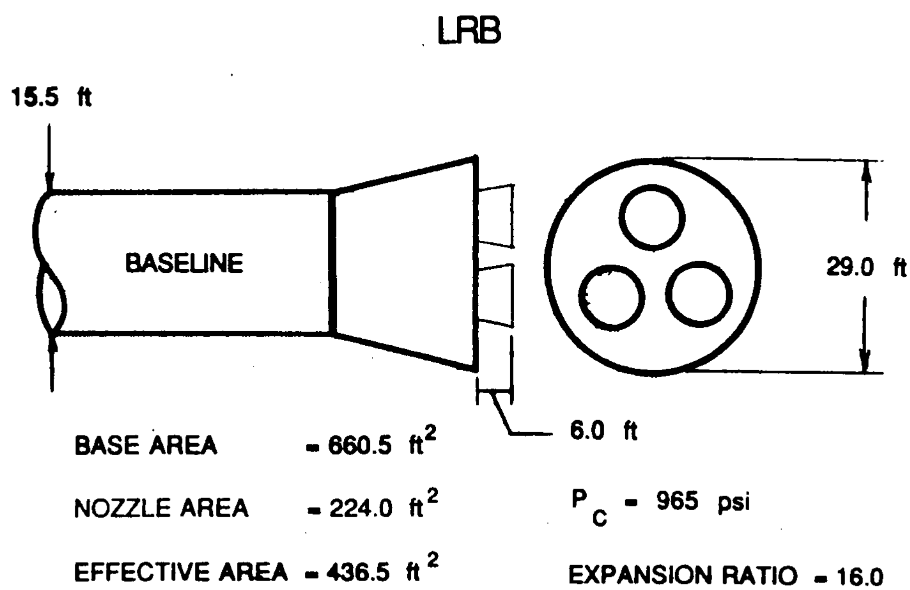

Fig. 7-3 Baseline Study LRB

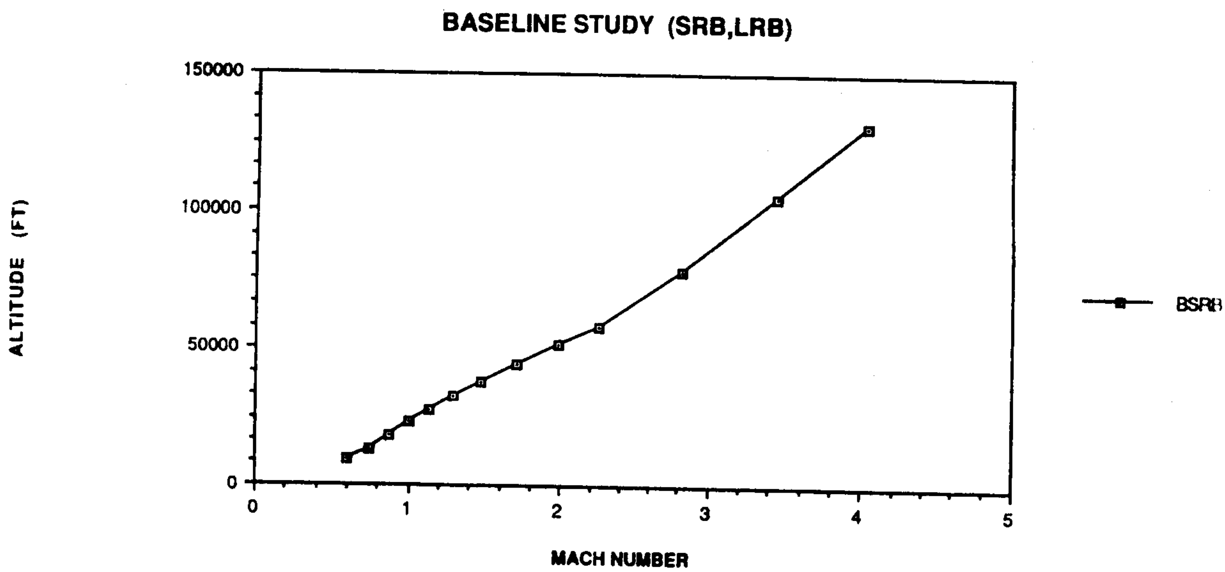

Fig. 7-4 Baseline Study Altitude vs Mach

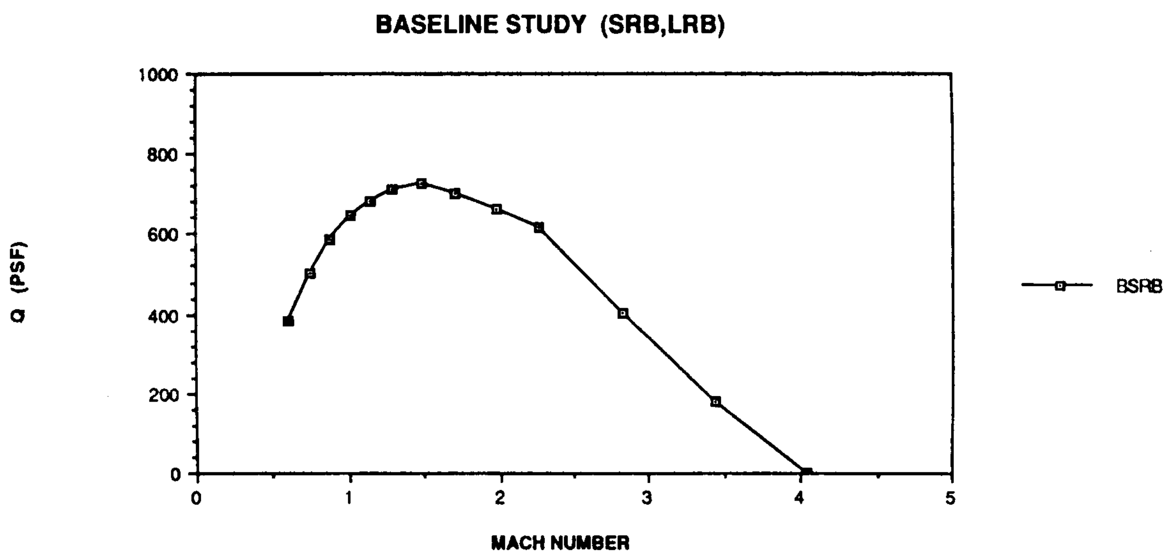

Fig. 7-5 Baseline Study Q vs Mach

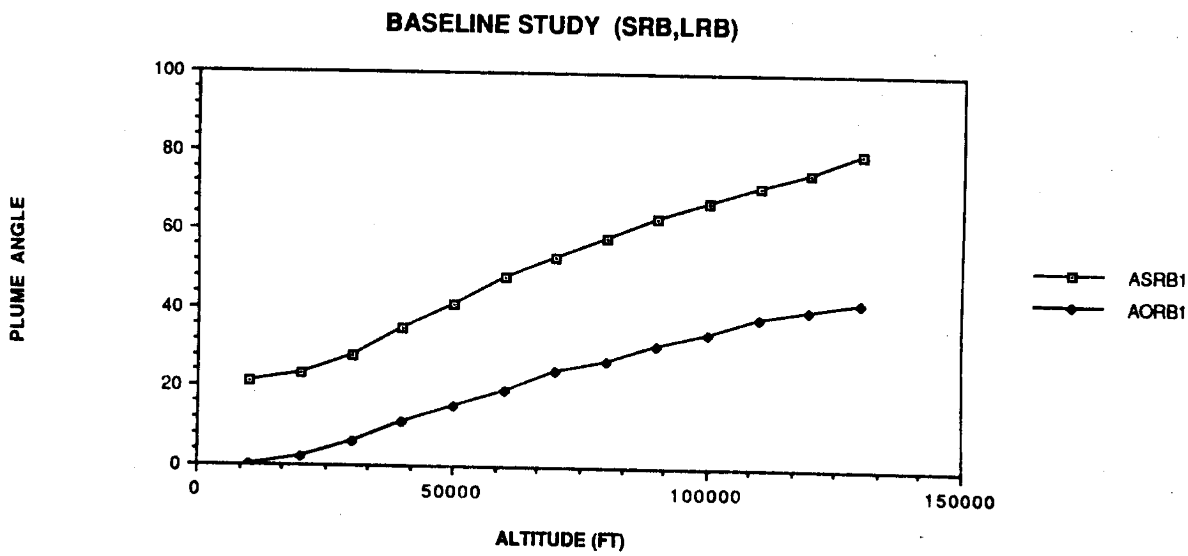

Fig. 7-6 Baseline Study Plume Angle vs Mach

Table 7-1 BASELINE CONCEPT (SRB)

BASELINE CONCEPT (SRB)

TOTAL BASE DRAG

MACH	ALT(ft)	Q(psf)	LV(lbs)	ORB(lbs)	2SRB(lbs)	ET(lbs)
0.60	9169.00	383.80	85508.00	20696.00	19973.00	44839.00
0.74	13188.39	503.84	97314.00	23465.90	20358.00	53491.00
0.87	17772.60	588.80	100753.00	24465.40	18761.10	57527.30
1.01	22832.80	644.33	106169.00	28484.40	17515.40	60169.20
1.14	27418.19	683.19	112520.00	32424.20	16575.20	63520.60
1.29	32386.86	711.47	69953.00	21842.33	5638.74	42472.41
1.48	37932.33	724.01	30910.00	14765.33	-3091.34	19236.06
1.71	44451.32	699.98	2197.00	8564.36	-8530.64	2163.47
1.98	51310.85	663.64	-19574.00	3390.80	-11330.00	-11635.05
2.26	58188.39	615.26	-35652.00	-535.40	-12541.40	-22575.80
2.82	78577.51	401.67	-39647.00	-2593.00	-10327.48	-26727.16
3.44	105414.84	176.63	-34905.00	-2050.50	-6368.16	-26487.22
4.03	130953.59	2.05	-30393.00	-1534.25	-2600.42	-26258.89

Table 7-2 BASELINE CONCEPT (LRB)

BASELINE CONCEPT (LRB)

TOTAL BASE DRAG

MACH	ALT(ft)	Q(psf)	LV(lbs)	ORB(lbs)	2LRB(lbs)	ET(lbs)
0.60	9169.00	383.80	136013.00	20696.00	70478.00	44839.00
0.74	13188.40	503.85	154065.30	23465.90	77108.40	53491.00
0.87	17772.00	558.80	159681.00	24633.00	77661.00	57527.00
1.01	22832.80	644.33	163921.41	28484.40	73288.40	62160.60
1.14	27418.20	683.19	167289.41	32424.20	66598.80	68288.00
1.29	32386.87	711.48	120595.48	21842.33	48409.20	50343.94
1.48	37932.34	724.01	77027.26	14765.33	30752.46	31557.46
1.71	44451.32	699.98	46252.27	8564.36	15576.88	22130.64
1.98	51310.85	663.64	21057.50	3390.80	1627.15	16028.55
2.26	58188.40	615.26	787.00	-535.40	-10060.40	11382.80
2.82	78577.52	401.68	-6680.68	-2593.00	-18194.00	14106.32
3.44	105414.84	176.64	-2712.06	-2050.50	-20240.00	19578.44
4.03	130953.59	2.05	1064.53	-1534.25	-22187.00	24785.78

Table 7-3 BASELINE CONCEPT (LRB)

BASELINE CONCEPT (LRB)

DELTA BASE DRAG

MACH	ALT(FT)	Q(psf)	LV(lbs)	ORB(lbs)	2RB(lbs)	ET(lbs)
0.60	9169.00	383.8	50505.00	0.00	50505.00	0.00
0.74	13188.39	503.8	56751.30	0.00	56750.40	0.00
0.87	17772.60	588.8	58928.00	0.00	58899.90	0.00
1.01	22832.80	644.3	57752.41	0.00	55773.00	1991.40
1.14	27418.19	683.2	54769.41	0.00	50023.60	4767.40
1.29	32386.86	711.5	50642.48	0.00	42770.46	7871.53
1.48	37932.33	724.0	46117.26	0.00	33843.80	12321.40
1.71	44451.32	700.0	44055.27	0.00	24107.52	19967.17
1.98	51310.85	663.6	40631.50	0.00	12957.15	27663.60
2.26	58188.39	615.3	36439.00	0.00	2481.00	33958.60
2.82	78577.51	401.7	32966.32	0.00	-7866.52	40833.48
3.44	105414.84	176.6	32192.94	0.00	-13871.84	46065.66
4.03	130953.59	2.0	31457.53	0.00	-19586.58	51044.67

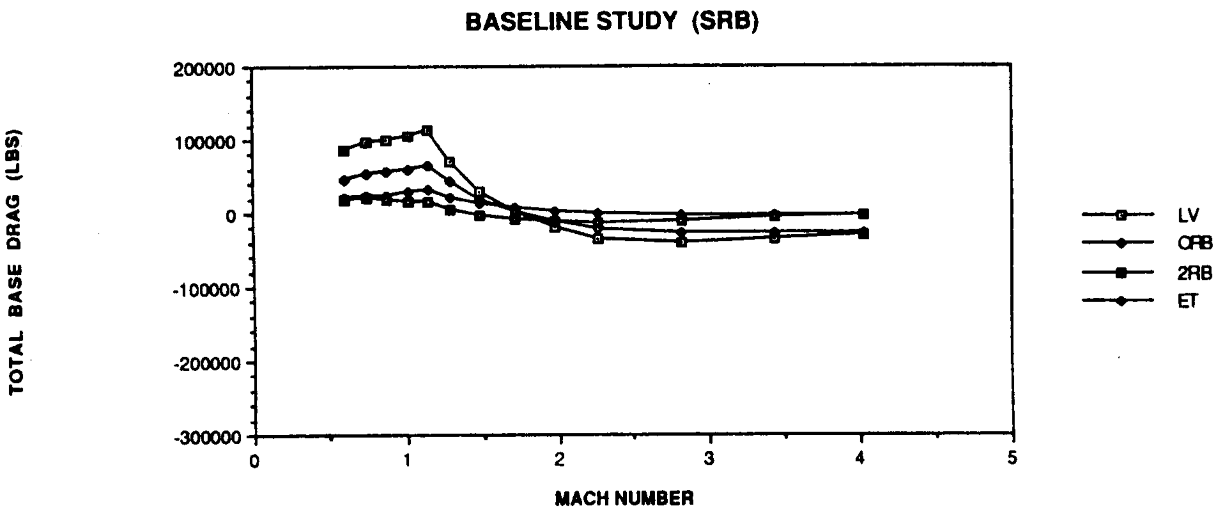

Fig. 7-7 Baseline Study SRB Total Base Drag

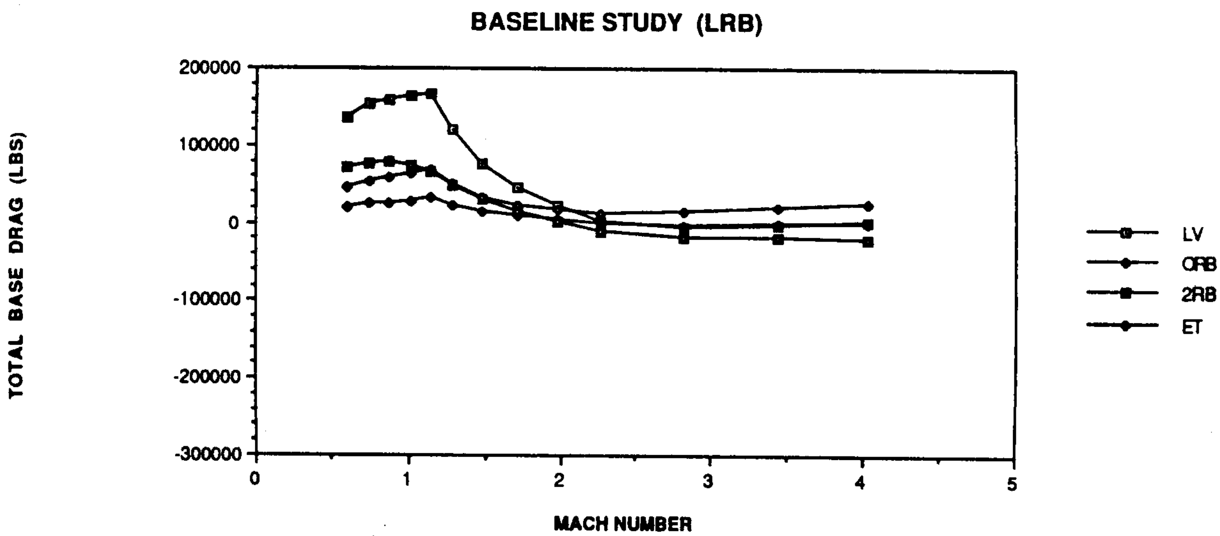

Fig. 7-8 Baseline Study LRB Total Base Drag

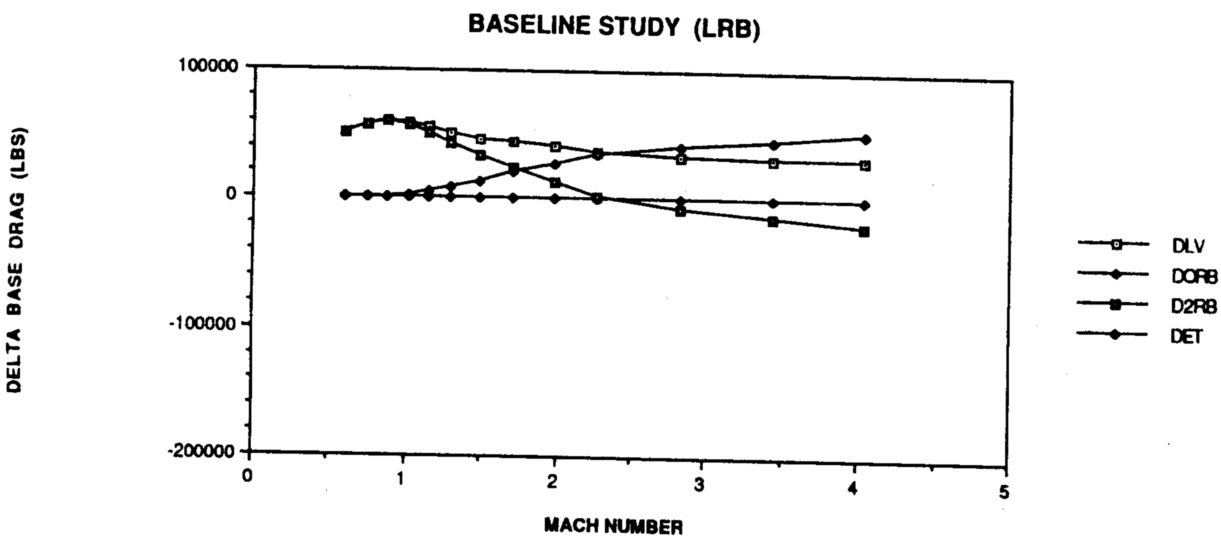

Fig. 7-9 Baseline Study LRB Delta Base Drag

7.2 BASE DRAG CALCULATION CODE

Prediction of base drag for a given configuration can be a tedious effort, considering all the variables associated with it. A faster means of calculation was needed. Using the methods found in the Compendium of Flight Vehicle Base Pressure and Base Drag Prediction Techniques, Lockheed developed a FORTRAN computer code. It takes into account all the trajectory and geometry effects found in the compendium, and obtains base drag predictions. See Fig. 7-10 for a flow diagram of the code and Fig. 7-11 for sample results.

7.3 STS FLIGHTS 2, 3, and 5

In order to obtain delta base drag values using the new prediction code, an STS vehicle with SRB's, on a typical STS trajectory, had to be found to submit from. This typical case was found by using an average of STS flights 2, 3, and 5. The typical trajectory used can be found in Figs. 7-12 to 7-14. The base drag results appear in Fig. 7-15 and Table 7-4.

7.4 MARTIN PUMP FED (LRB1)

The first LRB candidate configuration used in the base drag code was the Martin Pump Fed, shown in Fig. 7-16. The trajectory provided by Martin for this case can be found in Figs. 7-17 to 7-19. The base drag results obtained for this case can be found in Fig. 7-20 and Table 7-5. After subtracting these results with those from STS 2, 3, and 5 the delta base drag values are obtained (see Fig. 7-21 and Table 7-6). It is important to note the large value for delta base drag found in the Mach 2.0 - > 3.5 range.

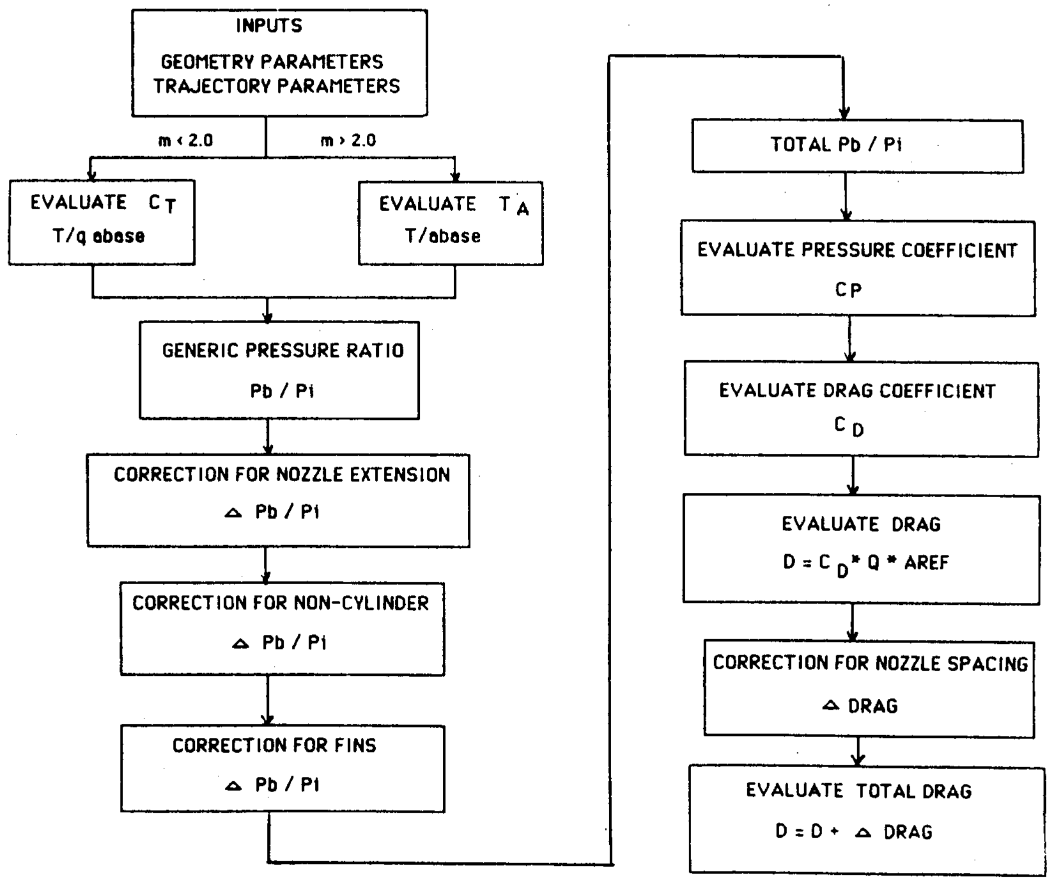

Fig. 7-10 Base Drag Calculation Code Flowchart

```
MACH                        2.820000
ALT             (FT)        76703.00
Q              (PSF)        382.0900
PRESS          (PSF)        70.13728
THRUST TOT      (LB)        5780105.
BOOSTER THRUST  (LB)        2162044.
ORB THRUST      (LB)        1456018.
T/A BOOSTER             6550.385
T/A ORB                 3356.921
T/A ET                  3415.838
PLUME ANGLE     (RB ORB)          63.61095        26.83385

UNCORRECTED     (RB ORB ET)   1.828659        1.178031        1.199655
NOZZLE EXT      (RB ORB ET)  -1.9599998E-02  1.0091913E-02  0.0000000E+00
NON CYLINDER    (RB ORB ET)  -0.1060880      0.0000000E+00  0.0000000E+00
FINS            (RB ORB ET)   0.0000000E+00 -2.1762000E-02  0.0000000E+00
TOTAL Pb/Pi     (RB ORB ET)   1.702971        1.166361        1.199655

CPB             (RB ORB ET)   0.1262819      2.9885069E-02  3.5866115E-02
CDB             (RB ORB ET)  -9.2637083E-03 -3.3462415E-03 -7.9770088E-03
DFB (wo/NS)     (RB ORB ET)  -19042.89       -3439.341       -8198.946
DFB (wo/NS)     (TOTAL)      -30681.18

NOZ SP Pb/Pi    (RB ORB ET)   8.000000       0.0000000E+00   2.611960
NOZ SP Pb       (RB ORB ET)   561.0982       0.0000000E+00   183.1957
NOZ SP DRAG     (RB ORB ET)  -16015.68       0.0000000E+00  -18248.94

DFB (w/NS)      (RB ORB ET)  -51074.26       -3439.341       -26447.89
DFB (w/NS)      (TOTAL)      -80961.48
```

Fig. 7-11 Base Drag Calculation Code Output

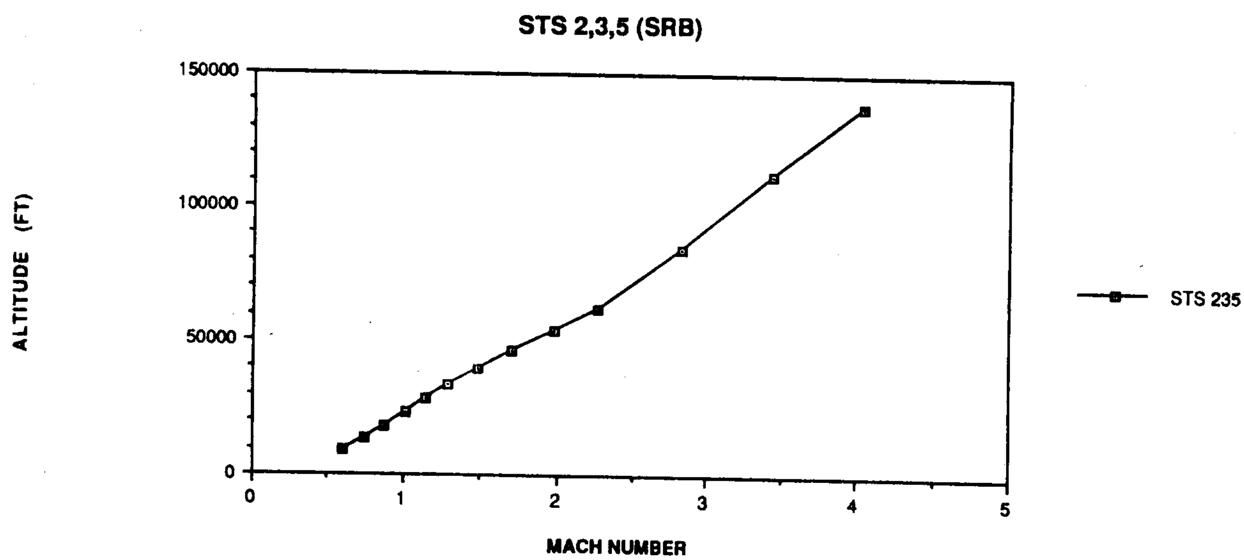

Fig. 7-12 STS 2, 3, 5, Altitude vs Mach

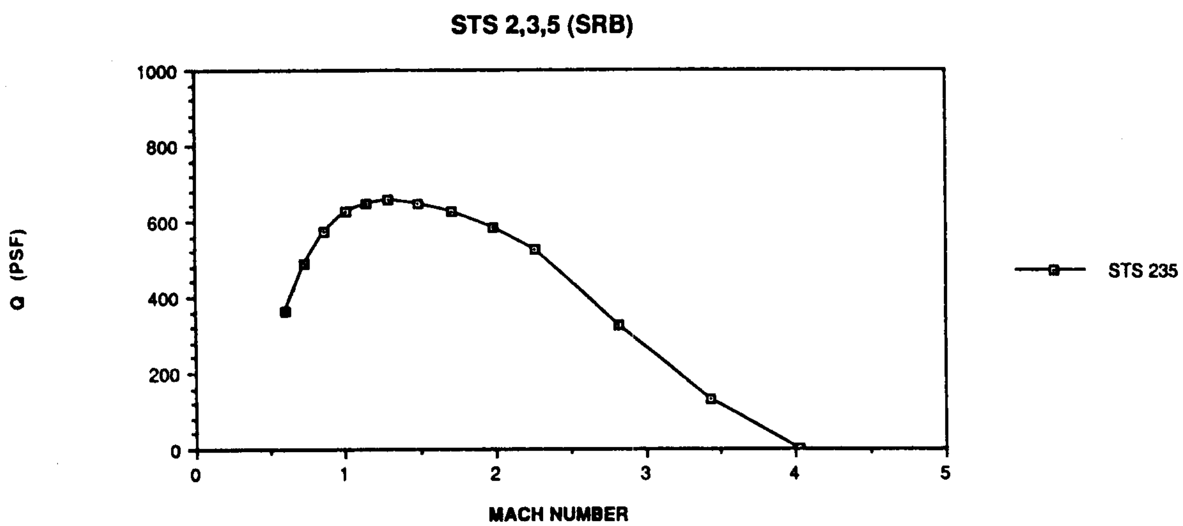

Fig. 7-13 STS 2, 3, 5 Q vs Mach

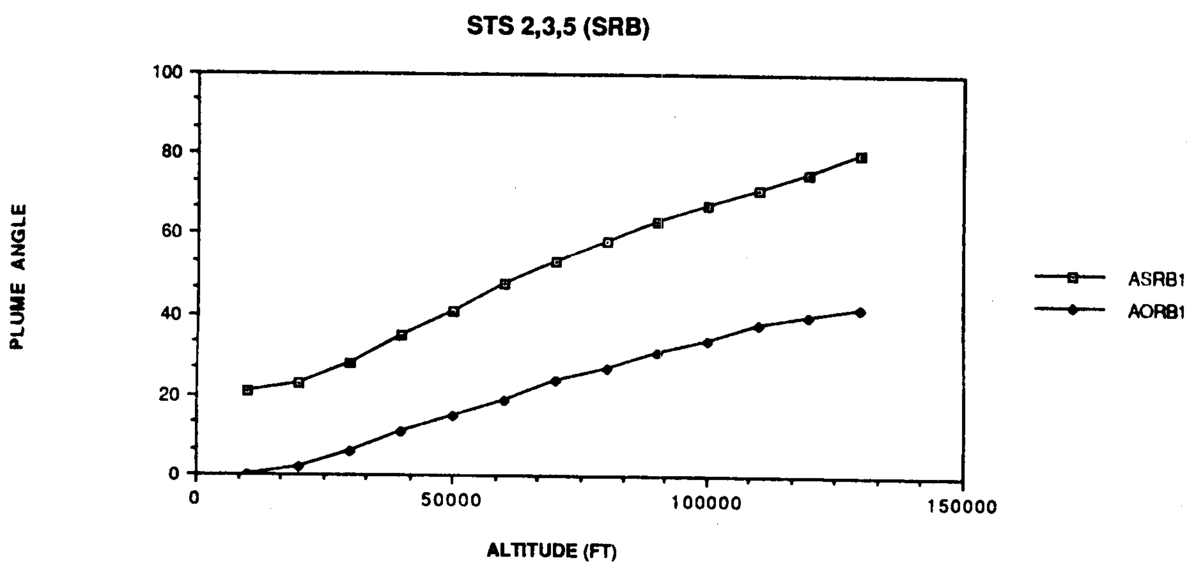

Fig. 7-14 STS 2, 3, 5 Plume Angle vs Mach

Table 7-4 STS 2, 3, 5, (SRB)

TOTAL BASE DRAG

MACH	ALT(FT)	Q(psf)	LV(lbs)	ORB(lbs)	2RB(lbs)	ET(lbs)
0.60	9065.00	383.79	82508.93	16917.90	20155.25	45435.77
0.74	13447.70	493.69	92581.52	18578.35	21273.24	52729.92
0.87	17979.00	576.15	97112.17	19921.74	21016.70	56173.72
1.01	23256.00	626.44	107046.77	22951.75	21263.98	62831.03
1.14	28248.40	648.84	105831.92	25638.99	17478.22	62714.70
1.29	33622.93	657.06	71643.03	17901.90	9384.42	44356.70
1.48	39848.53	648.33	30772.77	11223.04	-542.03	20091.76
1.71	46490.44	625.93	242.14	6507.47	-7259.87	994.54
1.98	53950.90	585.98	-21445.04	1472.69	-10187.36	-12730.37
2.26	61880.59	525.74	-35010.25	-2402.45	-11259.30	-21348.49
2.82	83994.19	323.72	-36647.77	-3974.51	-8090.34	-24582.91
3.44	111853.90	131.95	-31002.95	-3127.16	-4140.62	-23735.16
4.03	138365.56	2.05	-25631.26	-2320.82	-382.02	-22928.42

* AVERAGE VALUES FROM STS 2,3,5 FLIGHTS

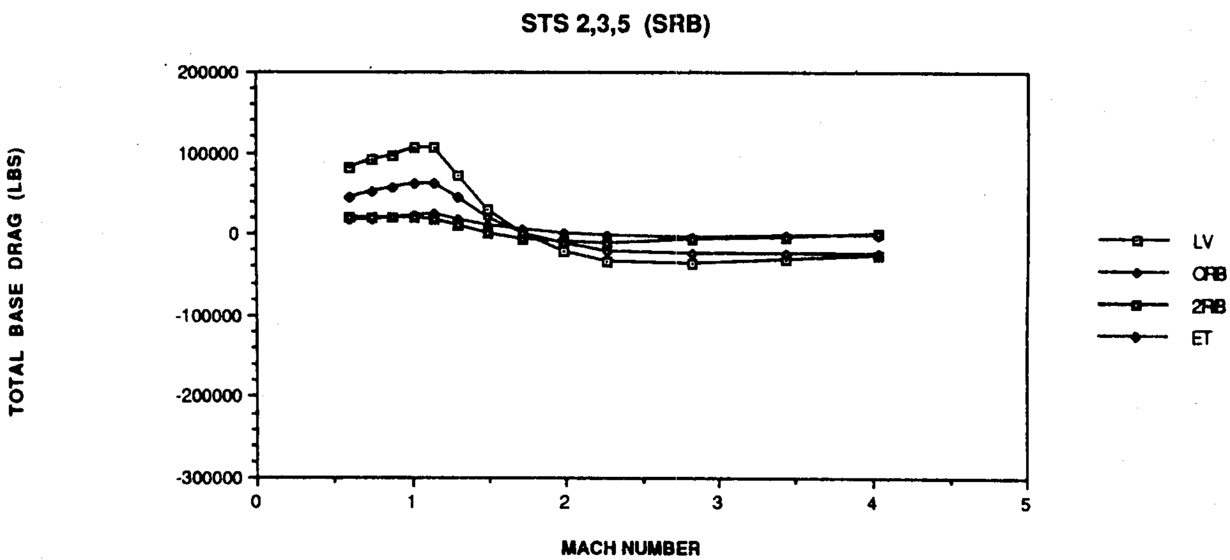

Fig. 7-15 STS 2, 3, 5 Total Base Drag

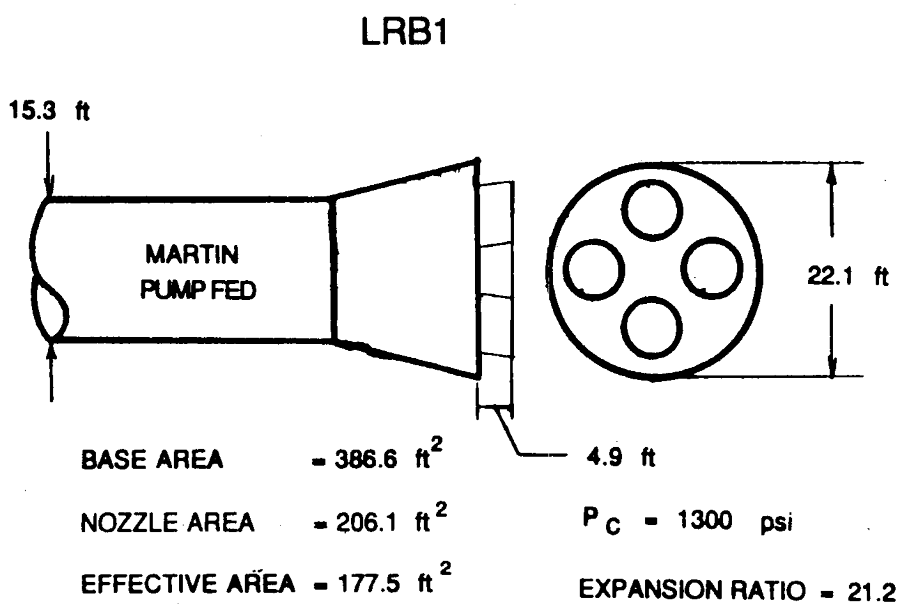

Fig. 7-16 LRB1 (Martin Pump Fed)

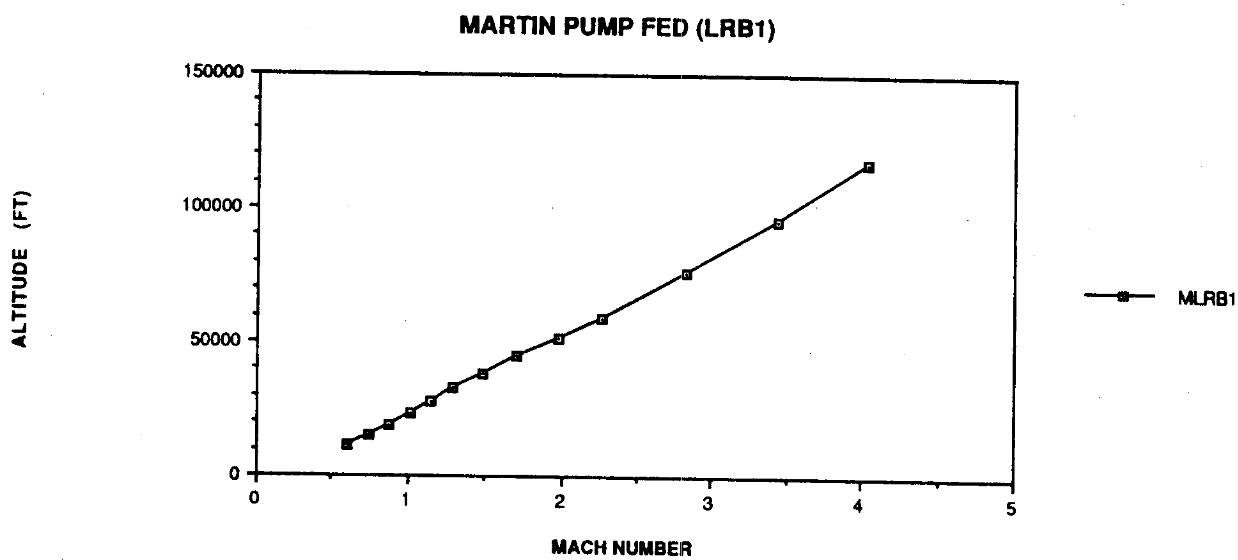

Fig. 7-17 LRB1 Altitude vs Mach

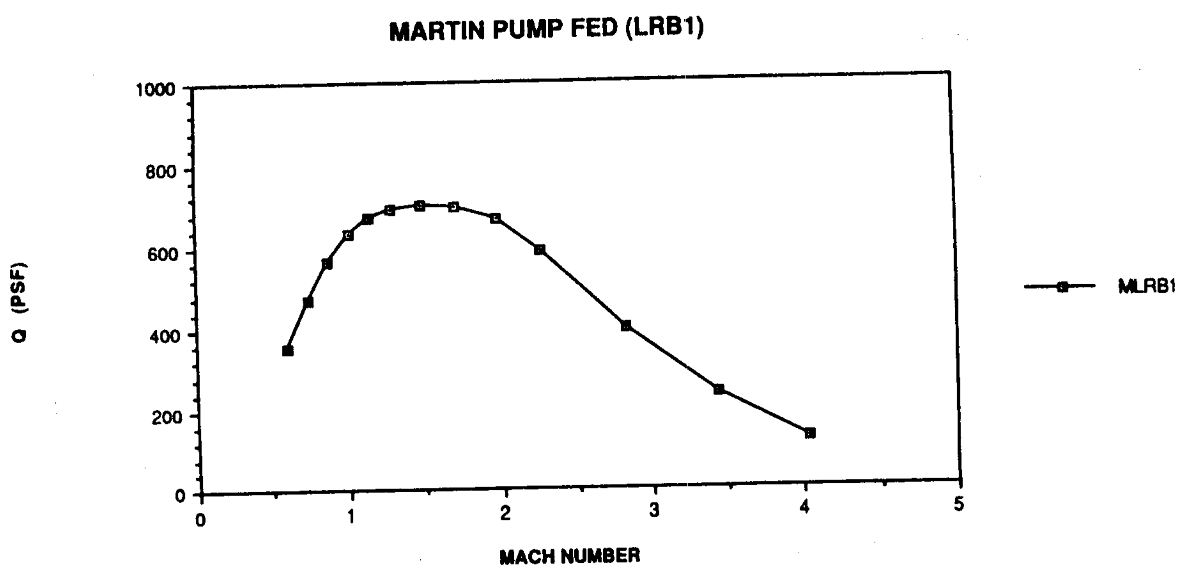

Fig. 7-18 LRB1 Q vs Mach

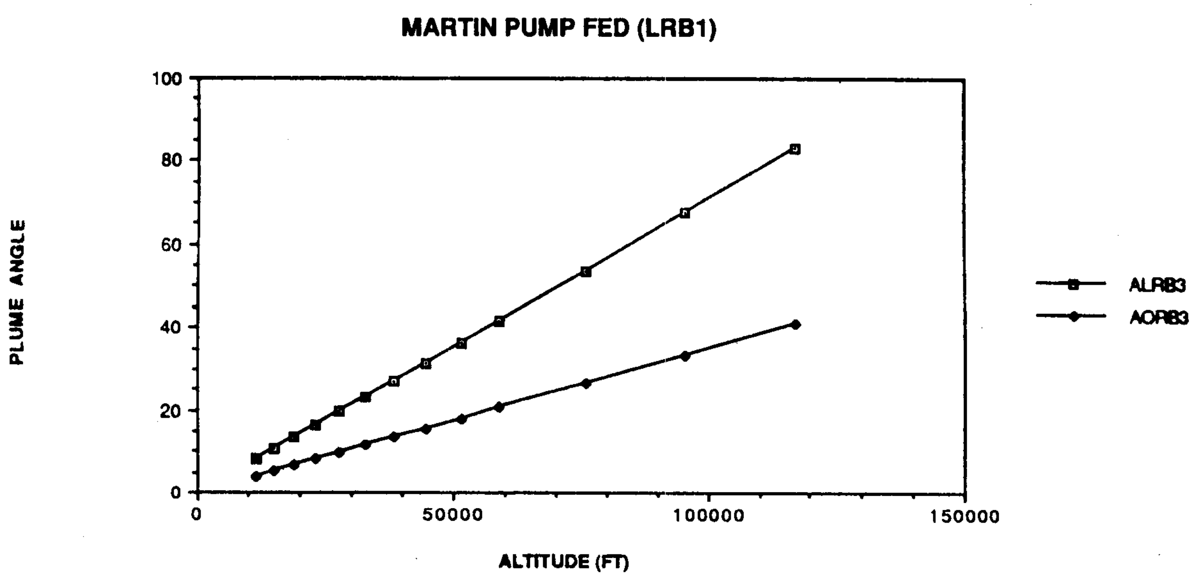

Fig. 7-19 LRB1 Plume Angle vs Mach

Table 7-5 MARTIN PUMP FED (LRB1)

TOTAL BASE DRAG

MACH	ALT(FT)	Q(psf)	LV(lbs)	ORB(lbs)	2RB(lbs)	ET(lbs)
0.60	11439.00	354.1	90121.27	22647.26	25439.72	42034.27
0.74	15188.00	470.9	97449.14	24769.23	27356.17	45323.73
0.87	18884.00	565.0	100679.61	26067.21	28357.47	46254.92
1.01	23056.00	635.9	126811.89	33016.43	34399.14	59396.33
1.14	27677.00	672.8	116658.11	30605.34	30472.93	55579.84
1.29	32728.00	692.0	91287.60	25161.46	20321.63	45804.51
1.48	38282.00	701.0	50612.79	16100.30	5776.70	28735.79
1.71	44439.00	697.6	36313.83	13497.04	-235.69	23052.48
1.98	51272.00	666.2	1891.44	8644.59	-18148.03	11394.88
2.26	58804.00	588.9	-38116.73	2935.08	-40194.39	-857.42
2.82	75818.00	399.1	-85398.99	-3402.95	-65108.59	-16887.46
3.44	95308.00	241.4	-64089.47	-3830.44	-38310.08	-21948.95
4.03	117102.00	128.1	-33940.29	-2794.35	-17728.64	-13417.30

Table 7-6 MARTIN PUMP FED (LRB1)

DELTA BASE DRAG

MACH	ALT(FT)	Q(psf)	LV(lbs)	ORB(lbs)	2RB(lbs)	ET(lbs)
0.60	9065.00	354.1	7612.34	5729.36	5284.47	-3401.50
0.74	13447.70	470.9	4867.62	6190.88	6082.93	-7406.19
0.87	17979.00	565.0	3567.44	6145.47	7340.77	-9918.80
1.01	23256.00	635.9	19765.12	10064.68	13135.16	-3434.70
1.14	28248.40	672.8	10826.19	4966.35	12994.71	-7134.86
1.29	33622.93	692.0	19644.57	7259.56	10937.21	1447.81
1.48	39848.53	701.0	19840.02	4877.26	6318.73	8644.03
1.71	46490.44	697.6	36071.69	6989.57	7024.18	22057.94
1.98	53950.90	666.2	23336.48	7171.90	-7960.67	24125.25
2.26	61880.59	588.9	-3106.48	5337.53	-28935.09	20491.07
2.82	83994.19	399.1	-48751.22	571.56	-57018.25	7695.45
3.44	111853.90	241.4	-33086.52	-703.28	-34169.46	1786.21
4.03	138365.56	128.1	-8309.03	-473.53	-17346.62	9511.12

* DELTA DRAG VALUES ARE BASED ON DELTA FROM STS FLIGHTS 2,3,5

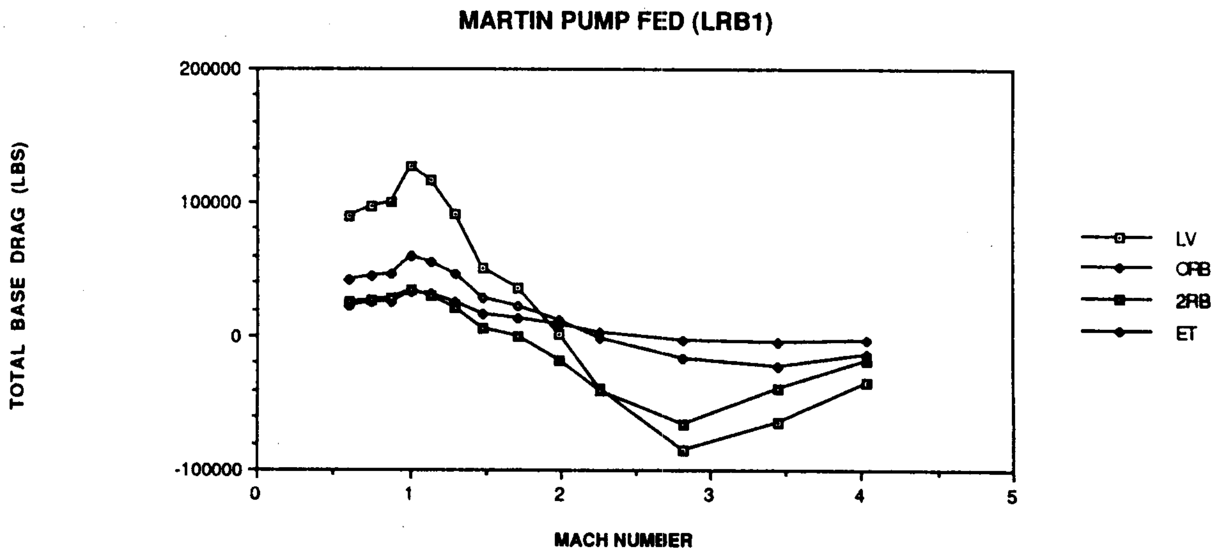

Fig. 7-20 LRB1 Total Base Drag

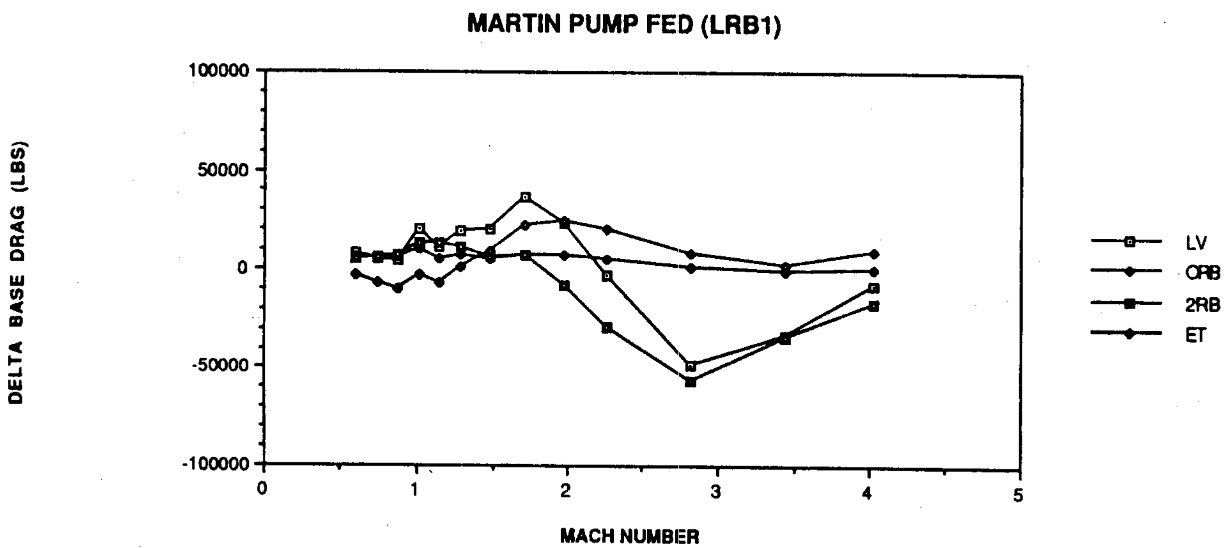

* DELTA DRAG VALUES ARE BASED ON DELTA FROM STS FLIGHTS 2,3,5

Fig. 7-21 LRB1 Delta Base Drag

7.5 MARTIN PRESSURE FED (LRB2)

The next LRB candidate configuration used in the base drag code was the Martin Pressure Fed, shown in Fig. 7-22. The trajectory provided by Martin for this case can be found in Figs. 7-23 to 7-25. The base drag results obtained for this case can be found in Fig. 7-26 and Table 7-7. After subtracting these results with those from STS 2, 3, and 5 the delta base drag values are obtained (see Fig. 7-27 and Table 7-8). It is important to note the large value for delta base drag found in the Mach 2.0 - > 3.0 range.

7.6 GENERAL DYNAMICS O2/H2 PUMP FED (LRB3)

The next LRB candidate configuration used in the base drag code was the General Dynamics O2/H2 Pump Fed, shown in Fig. 7-28. The trajectory provided by General Dynamics for this case can be found in Figs. 7-29 to 7-31. The base drag results obtained for this case can be found in Fig. 7-32 and Table 7-9. After subtracting these results with those from STS 2, 3, and 5 the delta base drag values are obtained (see Fig. 7-33 and Table 7-10). It is important to note the large value for delta base drag found in the Mach 1.5 - > 3.5 range.

7.7 GENERAL DYNAMICS O2/RP1 PUMP FED (LRB4)

The next LRB candidate configuration used in the base drag code was the General Dynamics Pump Fed shown in Fig. 7-34. The trajectory provided by Martin for this case can be found in Figs. 7-35 to 7-37. The base drag results obtained for this case can be found in Fig. 7-38 and Table 7-11. After subtracting these results with those from STS 2, 3, and 5 the delta base drag values are obtained (see Fig. 7-39 and Table 7-12. It is important to note the large value for delta base drag found in the Mach 2.0 - > 3.5 range.

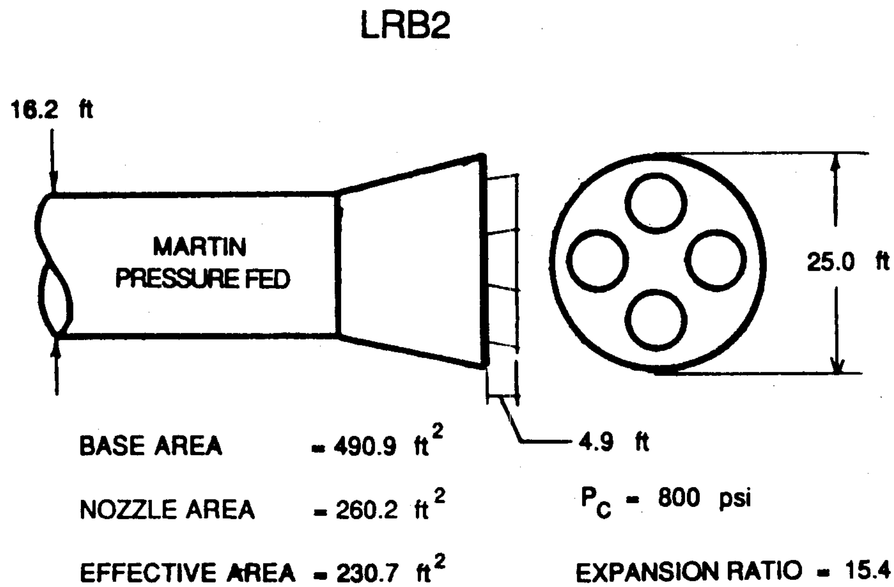

Fig. 7-22 LRB2 (Martin Pressure Fed)

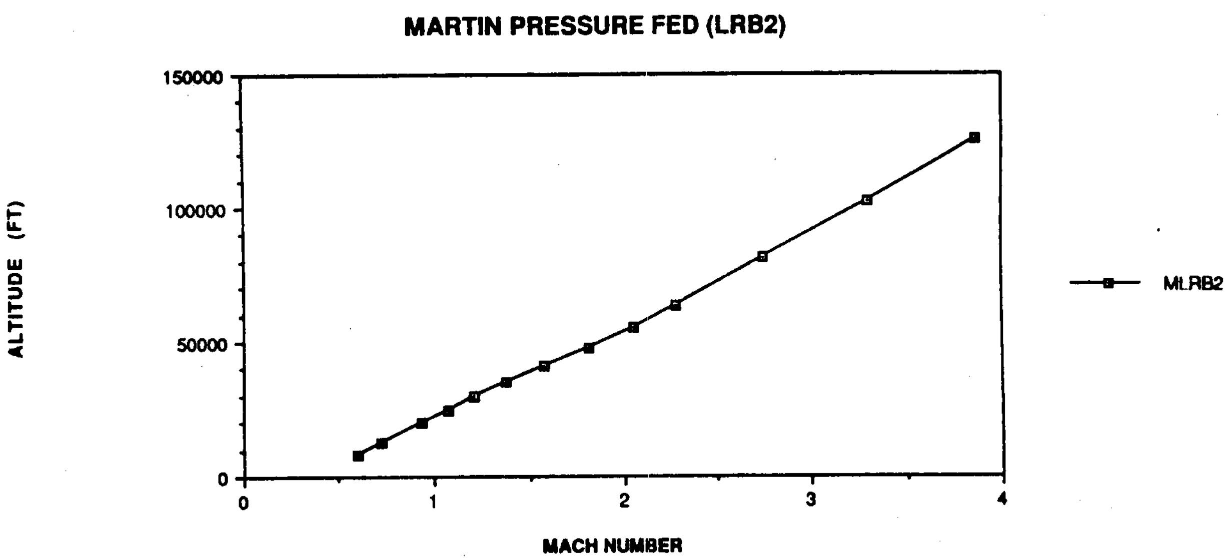

Fig. 7-23 LRB2 Altitude vs Mach

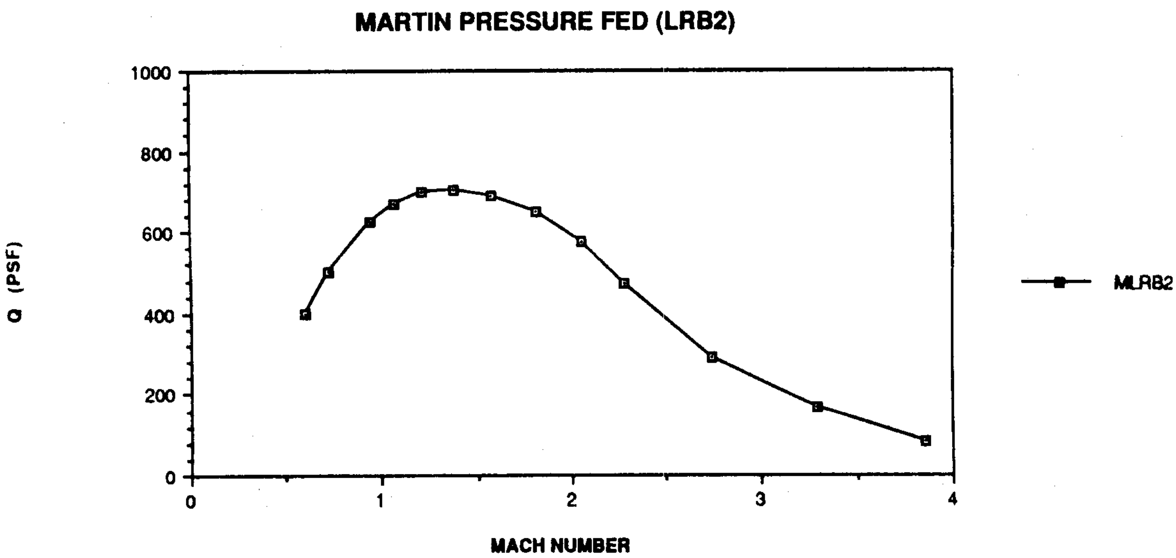

Fig. 7-24 LRB2 Q vs Mach

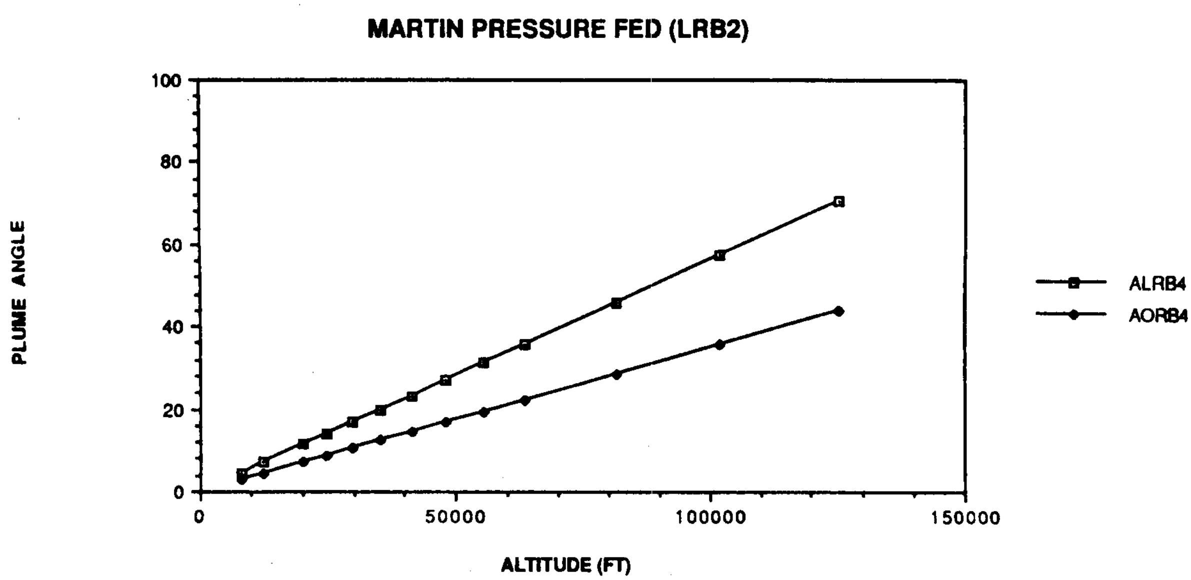

Fig. 7-25 LRB2 Plume Angle vs Mach

Table 7-7 MARTIN PRESSURE FED (LRB2)

TOTAL BASE DRAG

MACH	ALT(FT)	Q(psf)	LV(lbs)	ORB(lbs)	2RB(lbs)	ET(lbs)
0.60	8224.00	398.9	111153.84	25512.55	38288.93	47352.36
0.73	12404.00	503.9	115526.58	26845.83	39516.39	49164.35
0.94	20182.00	625.4	127219.05	30258.93	43060.29	53899.82
1.07	24713.00	671.0	138130.73	33027.53	45859.09	59244.11
1.21	29714.00	698.0	118996.87	29539.59	36713.43	52743.85
1.38	35229.00	706.1	79519.70	20898.54	21128.10	37493.05
1.57	41319.00	689.0	42197.63	14026.65	2531.22	25639.75
1.81	48042.00	652.5	16510.84	10483.26	-13790.10	19817.68
2.05	55422.00	576.2	-9962.88	5000.08	-24159.76	9196.80
2.28	63460.00	473.6	-49951.26	276.37	-49719.78	-507.85
2.75	81442.00	292.6	-69105.40	-3948.87	-55328.49	-9828.04
3.30	101970.00	165.5	-45803.08	-5598.42	-29895.52	-10309.15
3.86	125165.00	84.4	-27067.54	-2439.16	-15062.38	-9566.00

Table 7-8 MARTIN PRESSURE FED (LRB2)

DELTA BASE DRAG

MACH	ALT(FT)	Q(psf)	LV(lbs)	ORB(lbs)	2RB(lbs)	ET(lbs)
0.60	9065.00	398.9	28644.91	8594.65	18133.68	1916.59
0.73	13134.65	503.9	23664.53	8386.08	18323.01	-3044.56
0.94	20460.00	625.4	26567.23	8827.58	23086.47	-5346.82
1.07	25687.20	671.0	25395.14	8093.05	24272.83	-6970.72
1.21	30776.00	698.0	28257.98	7358.78	23106.31	-2207.09
1.38	36752.53	706.1	31916.80	7834.00	16607.88	7474.92
1.57	42516.68	689.0	24036.60	3979.94	6961.17	13095.48
1.81	49317.55	652.5	28352.84	6404.33	-4649.43	26597.95
2.05	55858.75	576.2	15436.35	4600.55	-13541.41	24377.21
2.28	62525.13	473.6	-14561.76	2846.27	-38554.68	21146.64
2.75	80848.75	292.6	-31820.31	121.31	-46792.22	14850.58
3.30	105563.00	165.5	-13525.49	-2279.92	-24863.03	13617.43
3.86	130726.59	84.4	111.50	113.99	-13597.38	13594.87

* DELTA DRAG VALUES ARE BASED ON DELTA FROM STS FLIGHTS 2,3,5

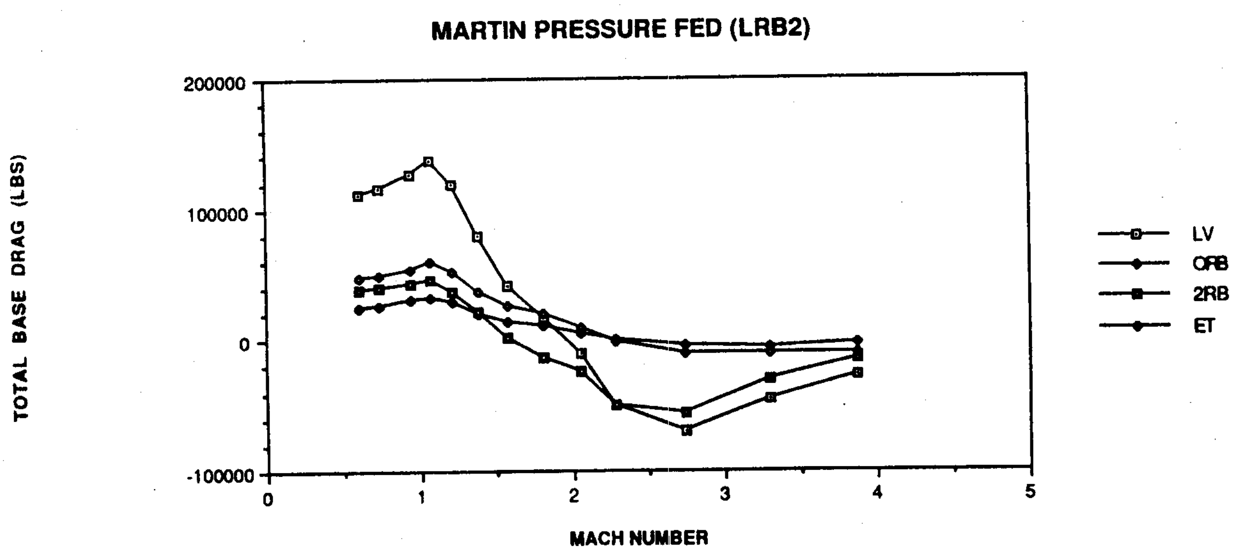

Fig. 7-26 LRB2 Total Base Drag

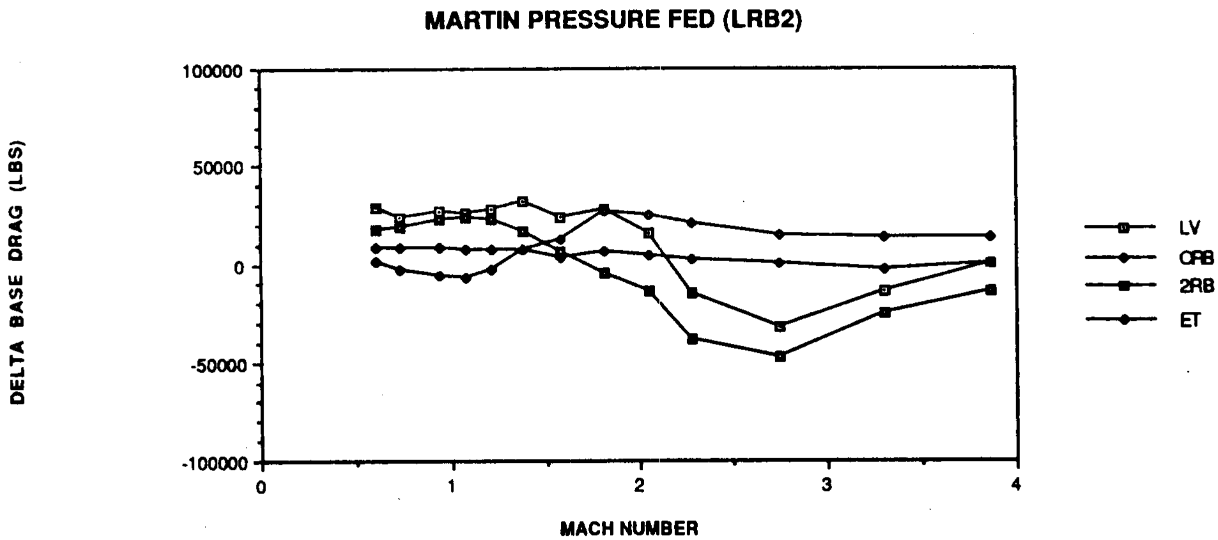

* DELTA DRAG VALUES ARE BASED ON DELTA FROM STS FLIGHTS 2,3,5

Fig. 7-27 LRB2 Delta Base Drag

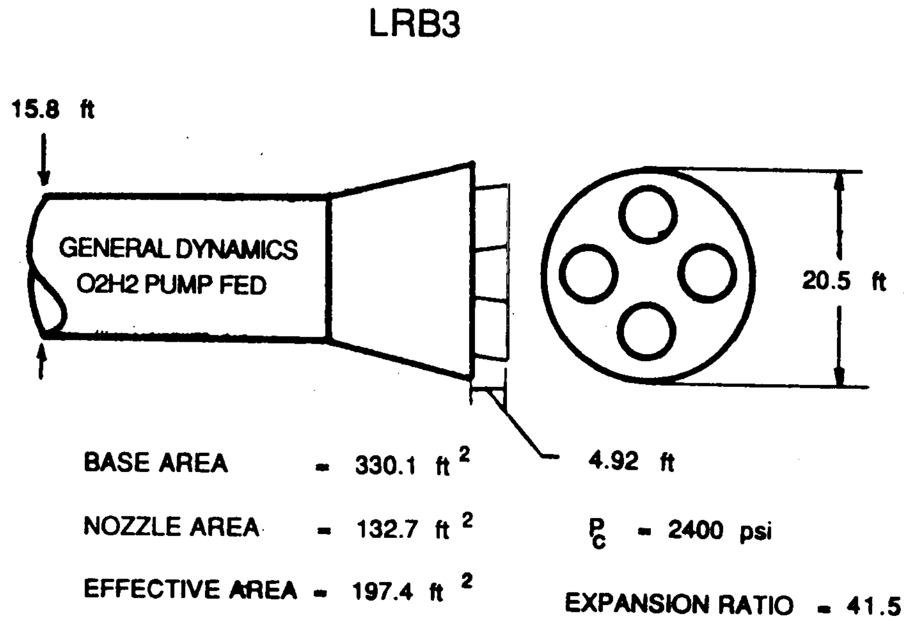

Fig. 7-28 LRB3 (General Dynamics O2H2 Pump Fed)

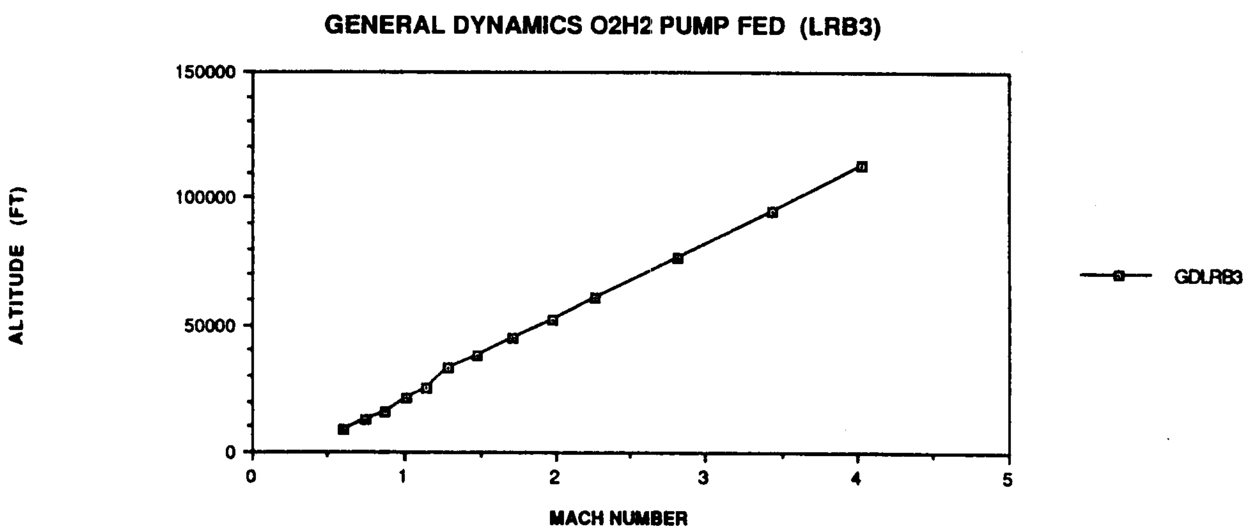

Fig. 7-29 LRB3 Altitude vs Mach

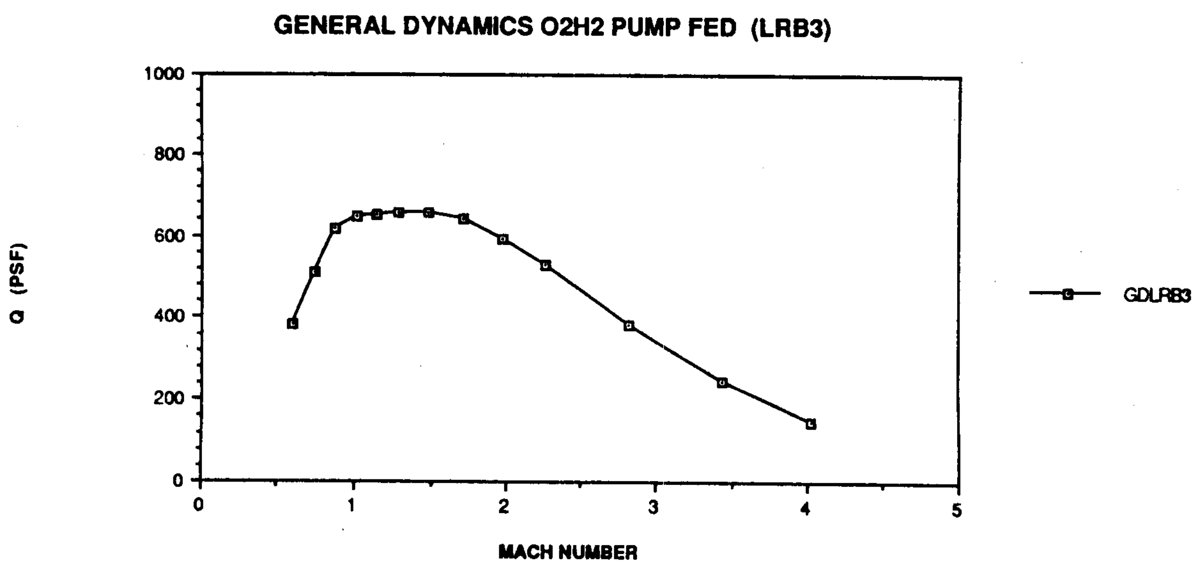

Fig. 7-30 LRB3 Q vs Mach

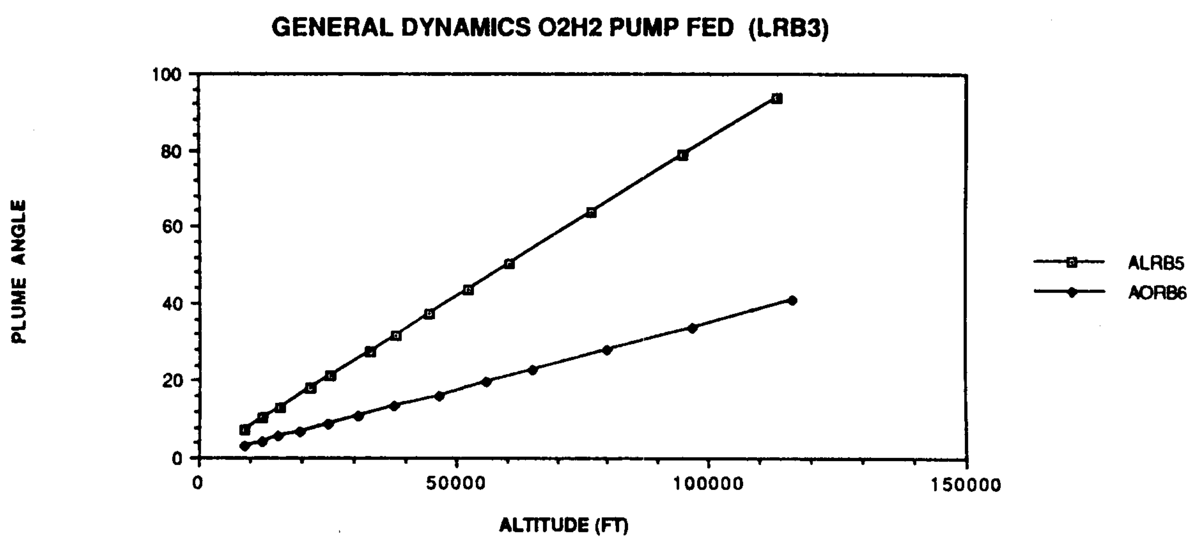

Fig. 7-31 LRB3 Plume Angle vs Mach

Table 7-9 GENERAL DYNAMICS O2H2 PUMP (LRB3)

TOTAL BASE DRAG

MACH	ALT(FT)	Q(psf)	LV(lbs)	ORB(lbs)	2RB(lbs)	ET(lbs)
0.60	8967.00	382.1	99706.46	24435.51	29917.63	45353.33
0.74	12248.00	511.6	108641.82	26912.14	32484.75	49244.93
0.87	15627.00	618.8	113187.52	28548.44	33981.34	50657.73
1.01	21627.00	648.6	135482.20	33748.65	39947.76	61785.79
1.14	25321.00	651.0	115992.51	29424.86	31099.15	55468.50
1.29	33079.00	637.1	72657.88	21992.71	7210.25	43454.92
1.48	38191.00	659.0	10533.36	13895.38	-26411.73	23049.71
1.71	44691.00	641.8	-22206.24	10495.01	-49562.45	16861.20
1.98	52458.00	594.8	-58799.78	6412.80	-72319.77	7107.20
2.26	60462.00	528.7	-85485.80	2142.89	-84820.01	-2808.68
2.82	76703.00	382.1	-80961.48	-3439.34	-51074.26	-26447.89
3.44	94896.00	245.1	-64203.41	-3781.56	-28020.01	-32401.84
4.03	113267.00	146.6	-35320.96	-2895.41	-15719.96	-16705.59

Table 7-10 GENERAL DYNAMICS 02H2 PUMP (LRB3)

DELTA BASE DRAG

MACH	ALT(FT)	Q(psf)	LV(lbs)	ORB(lbs)	2RB(lbs)	ET(lbs)
0.60	9065.00	382.1	17197.53	7517.61	9762.38	-82.44
0.74	13447.70	511.6	16060.30	8333.79	11211.51	-3484.99
0.87	17979.00	618.8	16075.35	8626.70	12964.64	-5515.99
1.01	23256.00	648.6	28435.43	10796.90	18683.78	-1045.24
1.14	28248.40	651.0	10160.59	3785.87	13620.93	-7246.20
1.29	33622.93	637.1	1014.85	4090.81	-2174.17	-901.78
1.48	39848.53	659.0	-20239.41	2672.34	-25869.70	2957.95
1.71	46490.44	641.8	-22448.38	3987.54	-42302.58	15866.66
1.98	53950.90	594.8	-37354.74	4940.11	-62132.41	19837.57
2.26	61880.59	528.7	-50475.55	4545.34	-73560.71	18539.81
2.82	83994.19	382.1	-44313.71	535.17	-42983.92	-1864.98
3.44	111853.90	245.1	-33200.46	-654.40	-23879.39	-8666.68
4.03	138365.56	146.6	-9689.70	-574.59	-15337.94	6222.83

* DELTA DRAG VALUES ARE BASED ON DELTA FROM STS FLIGHTS 2,3,5

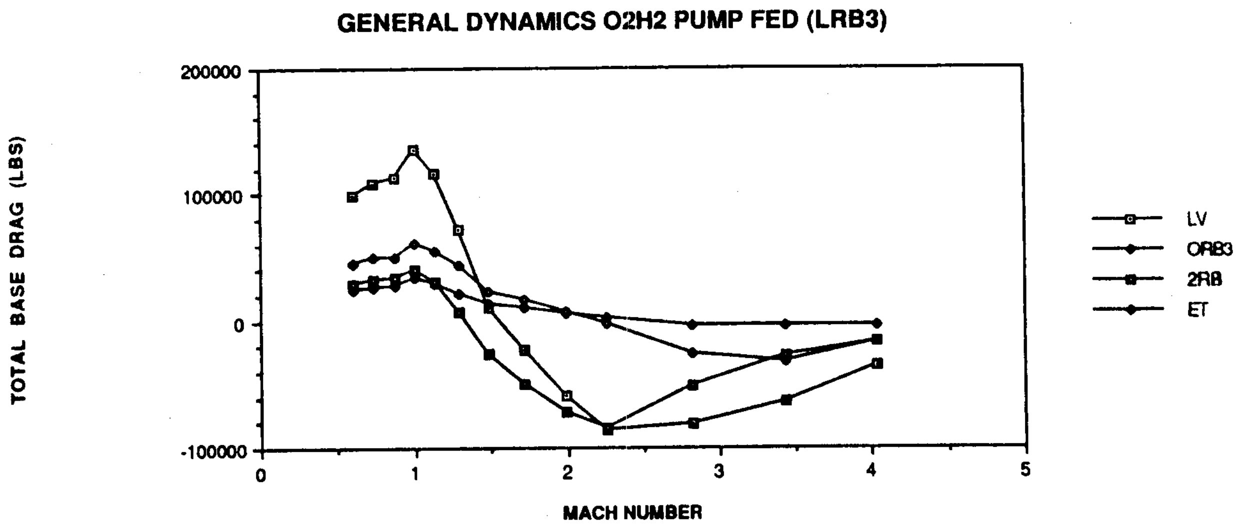

Fig. 7-32 LRB3 Total Base Drag

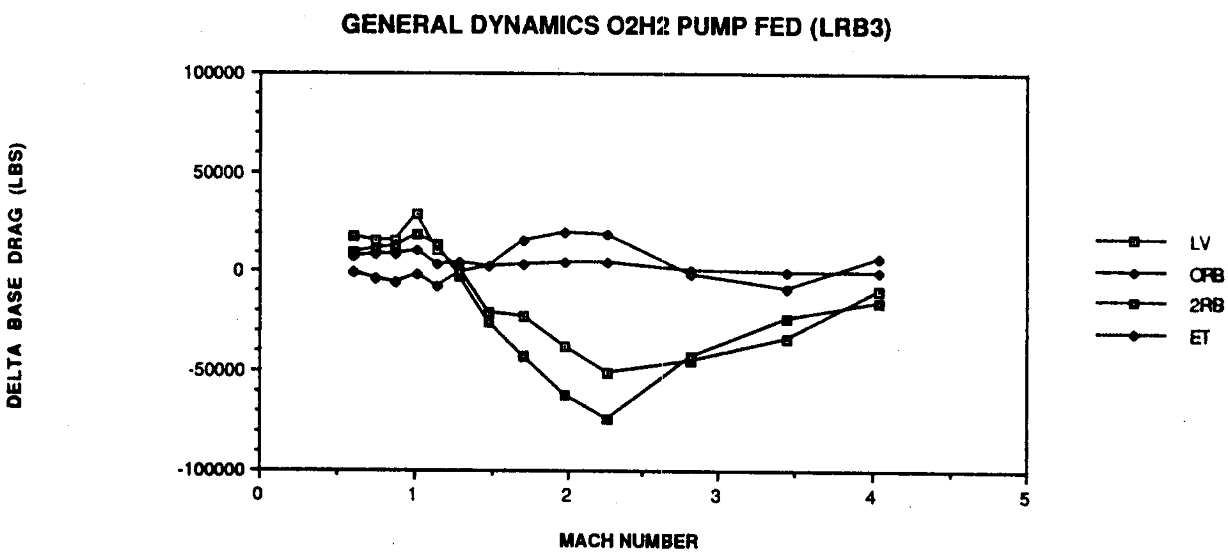

* DELTA DRAG VALUES ARE BASED ON DELTA FROM STS FLIGHTS 2,3,5

Fig. 7-33 LRB3 Delta Base Drag

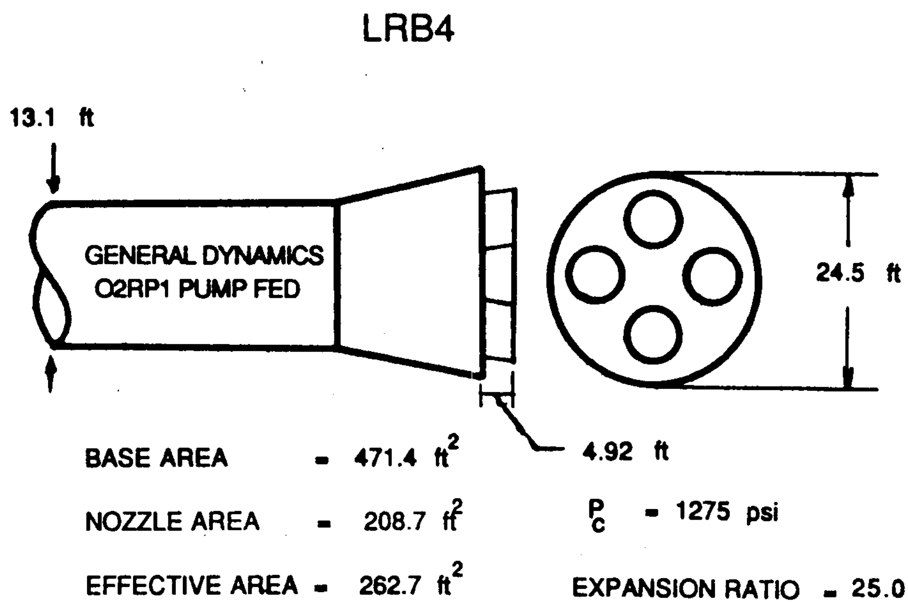

Fig. 7-34 LRB4 (General Dynamics O2RP1 Pump Fed)

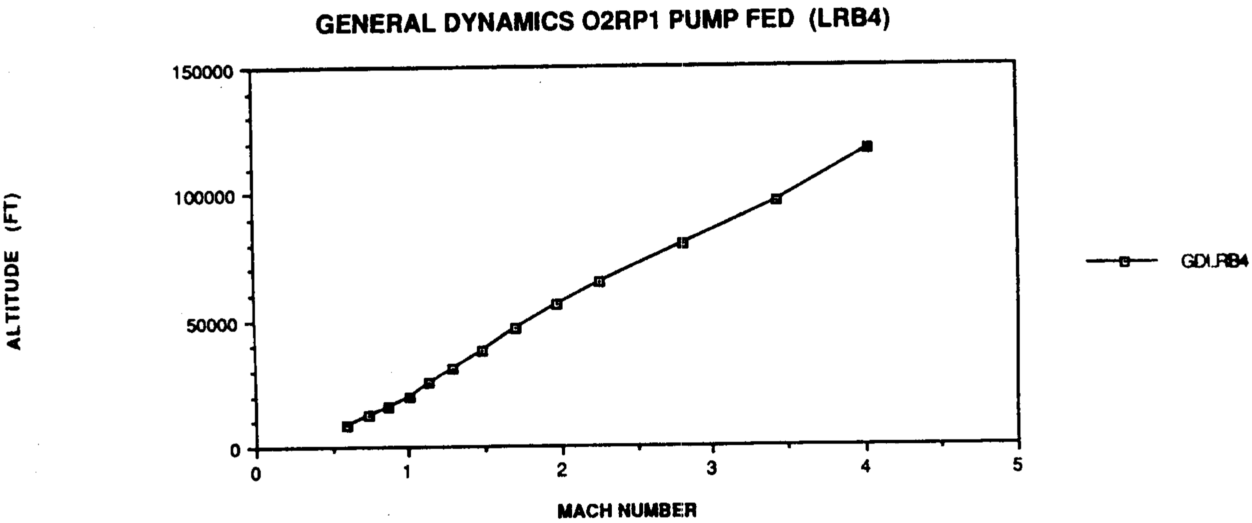

Fig. 7-35 LRB4 Altitude vs Mach

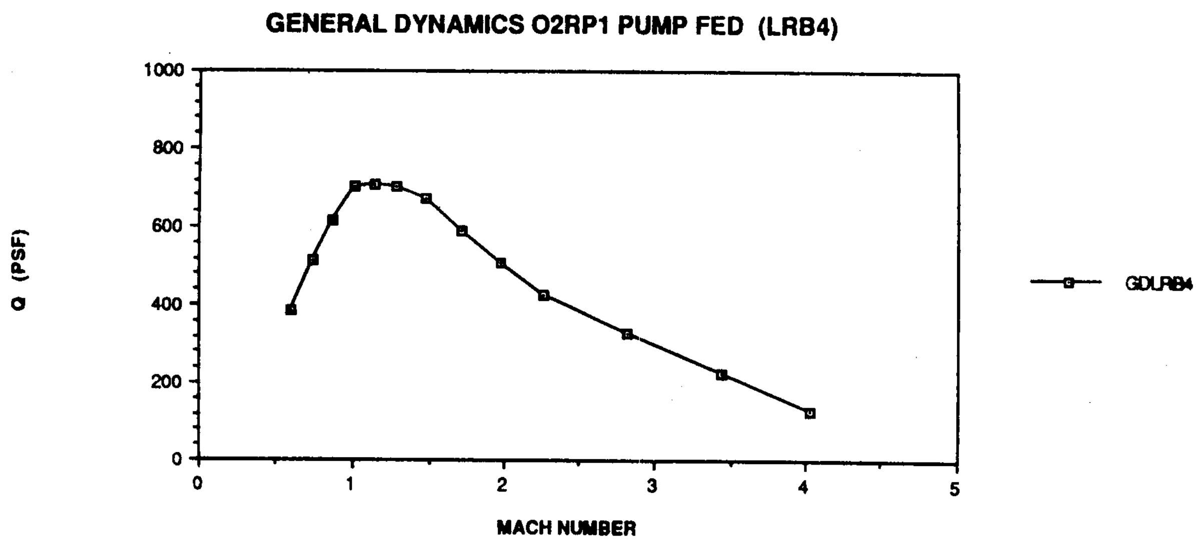

Fig. 7-36 LRB4 Q vs Mach

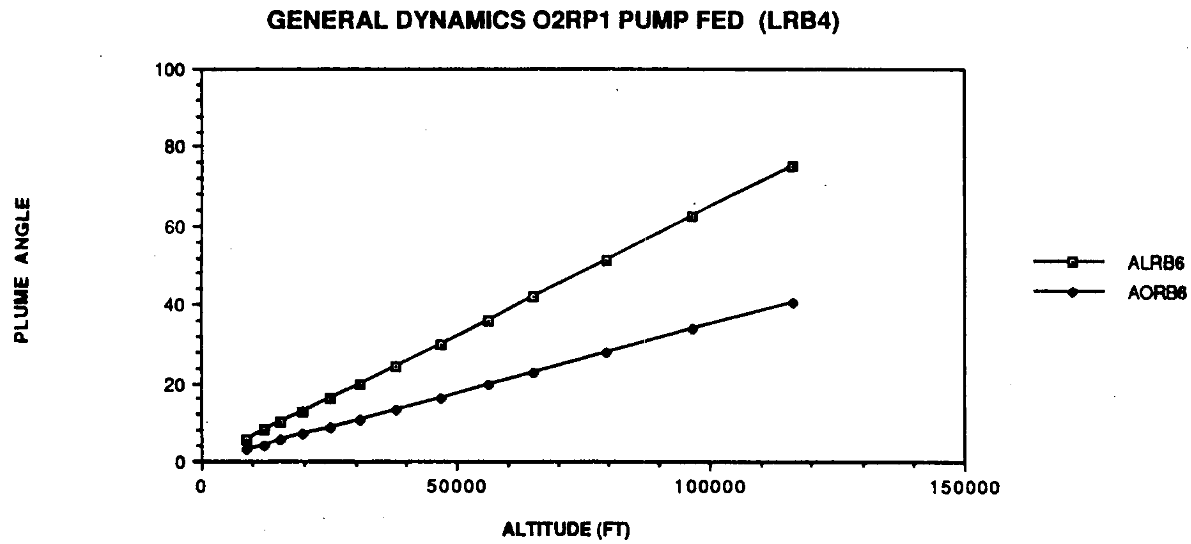

Fig. 7-37 LRB4 Plume Angle vs Mach

Table 7-11 GENERAL DYNAMICS O2RP1 PUMP FED (LRB4)

TOTAL BASE DRAG

MACH	ALT(FT)	Q(psf)	LV(lbs)	ORB(lbs)	2RB(lbs)	ET(lbs)
0.60	8825.00	384.2	111958.64	24570.46	41784.38	45603.80
0.74	12268.00	511.3	120945.38	26895.31	44835.93	49214.13
0.87	15612.00	617.2	125708.64	28476.93	46700.87	50530.83
1.01	19749.00	703.2	163307.53	36849.52	59631.35	66826.65
1.14	25233.00	707.0	143871.08	32579.33	51236.24	60055.51
1.29	30997.00	700.3	113054.79	25700.65	37776.69	49577.44
1.48	37812.00	670.9	48943.43	14535.58	3492.97	30914.87
1.71	46603.00	588.5	24445.61	7992.53	-3005.13	19458.21
1.98	55905.00	505.2	-18465.70	3344.40	-33081.82	11271.73
2.26	65080.00	425.0	-54432.28	-445.97	-57637.99	3651.69
2.82	79785.00	329.8	-73499.05	-3327.81	-55249.38	-14921.86
3.44	96629.00	226.9	-47778.41	-2166.37	-31608.99	-14003.06
4.03	116507.00	129.2	-31993.45	-1015.14	-18291.99	-12686.32

Table 7-12 GENERAL DYNAMICS 02RP1 PUMP FED (LRB4)

DELTA BASE DRAG

MACH	ALT(FT)	Q(psf)	LV(lbs)	ORB(lbs)	2RB(lbs)	ET(lbs)
0.60	9065.00	384.2	29449.71	7652.56	21629.13	168.03
0.74	13447.70	511.3	28363.86	8316.96	23562.69	-3515.79
0.87	17979.00	617.2	28596.47	8555.19	25684.17	-5642.89
1.01	23256.00	703.2	56260.76	13897.77	38367.37	3995.62
1.14	28248.40	707.0	38039.16	6940.34	33758.02	-2659.19
1.29	33622.93	700.3	41411.76	7798.75	28392.27	5220.74
1.48	39848.53	670.9	18170.66	3312.54	4035.00	10823.11
1.71	46490.44	588.5	24203.47	1485.06	4254.74	18463.67
1.98	53950.90	505.2	2979.34	1871.71	-22894.46	24002.10
2.26	61880.59	425.0	-19422.03	1956.48	-46378.69	25000.18
2.82	83994.19	329.8	-36851.28	646.70	-47159.04	9661.05
3.44	111853.90	226.9	-16775.46	960.79	-27468.37	9732.10
4.03	138365.56	129.2	-6362.19	1305.68	-17909.97	10242.10

* DELTA DRAG VALUES ARE BASED ON DELTA FROM STS FLIGHTS 2,3,5

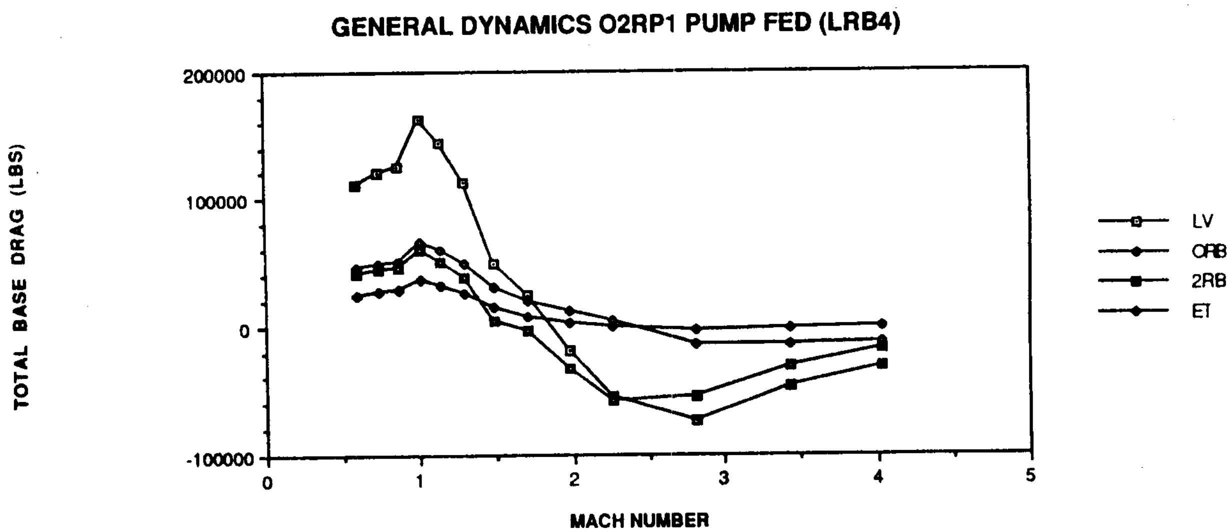

Fig. 7-38 LRB4 Total Base Drag

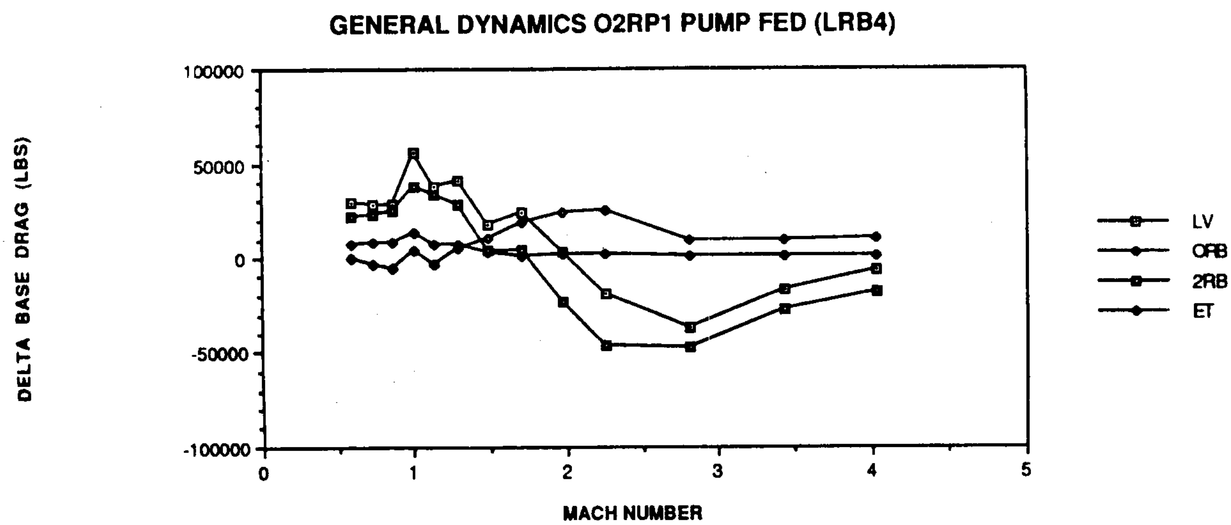

* DELTA DRAG VALUES ARE BASED ON DELTA FROM STS FLIGHTS 2,3,5

Fig. 7-39 LRB4 Delta Base Drag

7.8 CONCEPT COMPARISON/CONCLUSION

The next step was to choose which of the base drag values to use in the shuttle aerodynamic data base. The baseline study provided average values for a set of LRB configurations, and the LRB base drag study a different set of values for each specific configuration. If the base drag values have little variance from one configuration to another and are a small percentage of the total launch vehicle base drag, the baseline study results will be sufficient. If the opposite case is true the values from the LRB base drag study should be used. Shown in Figs. 7-40 to 7-43 are a comparison of total base drag from both studies. In Fig. 7-42 the same 100,000 lb variation occurs in booster base drag. In Fig. 7-43 up to 40,000 lb variation is found when comparing ET base drag.

When comparing the results from both studies a large variation can be seen from one configuration to another and the difference is a significant part of the total base drag. It is for this reason that Lockheed recommends using the results from the new LRB base drag study.

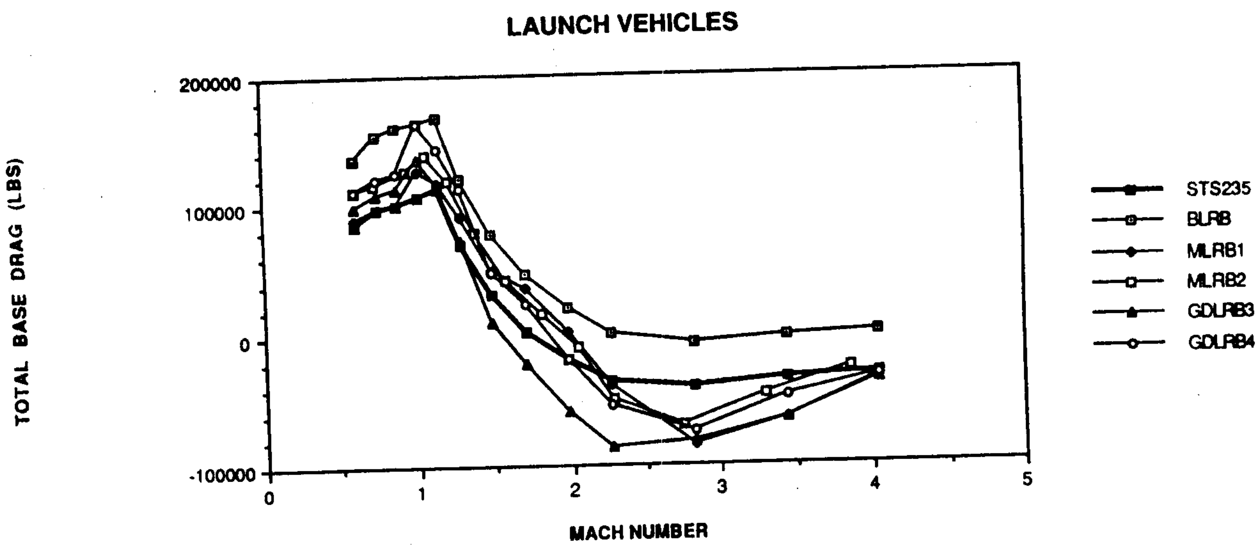

Fig. 7-40 Launch Vehicle Total Base Drag

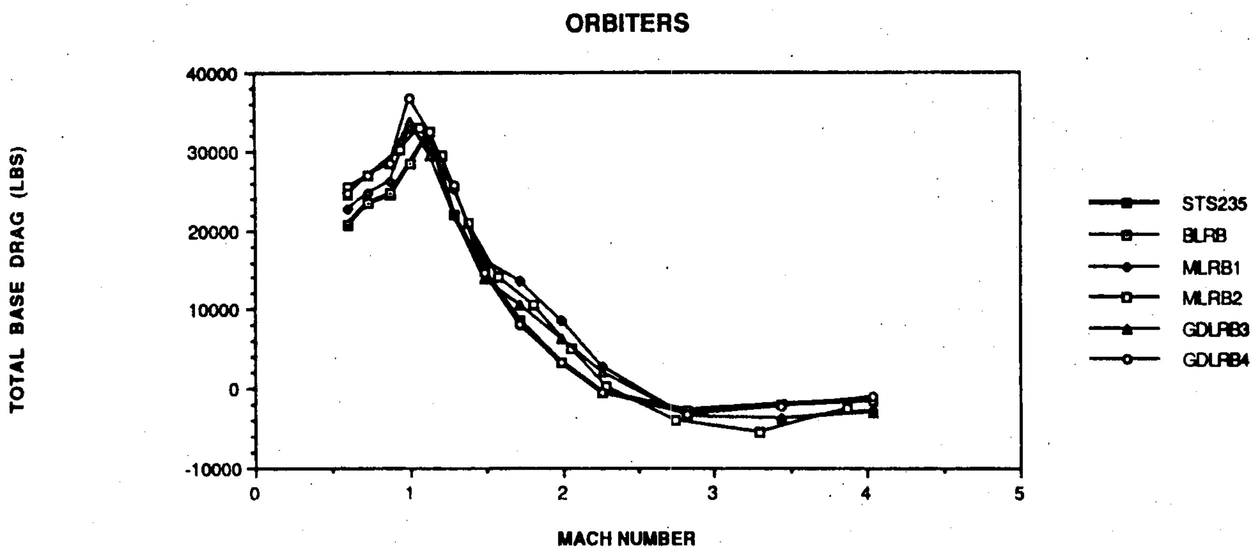

Fig. 7 41 Orbiter Base Total Base Drag

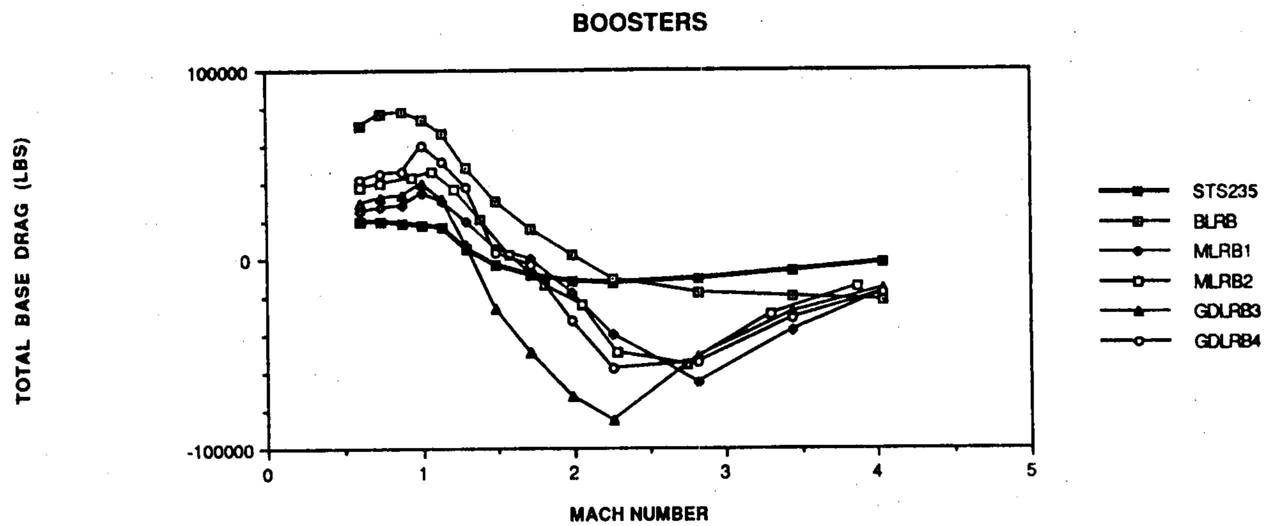

Fig. 7-42 Booster Total Base Drag

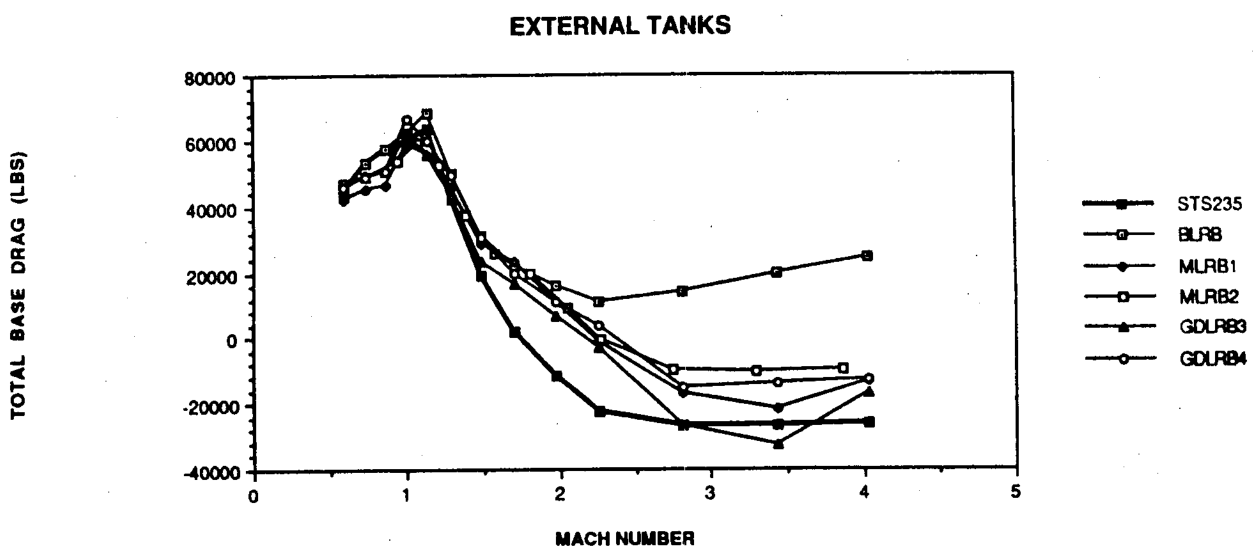

Fig. 7-43 External Tank Total Base Drag

8. SUMMARY

Phase I and Phase II of wind tunnel tests comprise a number of LRB configurations varying in length and diameter, with and without protuberances and aft skirts and varying ET-LRB gap width.

Conclusions drawn from these tests, with regard to varying length/diameter, included the following Longitudinal Trends:

- CAF increased with both length and diameter.
- CNF was relatively unaffected by changes in length, but a more negative CNF was produced by an increase in diameter.
- CMF was relatively unaffected by changes in diameter, but CMF decreases with an increase in length.
- The aerodynamic center moves forward with an increase in both length and diameter.
- Wing loading coefficients CSR, CRB, CTR, and elevon coefficients CHEI, and CHEO were relatively unchanged by increase in length but were all increased by increase in diameter.

Conclusions drawn from the tests, with regard to varying length/diameter, included the following lateral/directional trends:

- |CYβ| increases with increase in diameter. Length has little effect on |ΔCYβ| below $M = 1.05$, |CYβ| decreases with increase in length for $1.05 < M < 1.80$, and increases with increase n length for $M > 1.80$.
- |CYMβ| increases with increase in diameter, and |ΔCYMF| decreases with increase in length.
- |CRMβ| decreases with increase in diameter, and is relatively unaffected by increase in length.
- |ΔCSR| generally increases with increases in diameter (for all β), and has little length effect.

- $|\Delta CTR|$ for $1.80 < M < 3.48$, an increase in diameter produces a decrease in $|\Delta CTR|$ (for all β); for all other M an increase in diameter shows an increase in CTR. Length effects on CTR are small.

- ΔCHEI generally increases with increase in diameter except for $1.8 < M < 2.5$ where ΔCHEI decreases. Length has little effect.

- ΔCHEO generally increases with increase in diameter except for $1.8 < M < 2.5$ where ΔCHEO decreases. Length has little effect.

Analysis of SRB protuberances showed that they had a major effect on both wing loads and SSLV normal force coefficient. The test first recommended modification of certain protuberances. It was later decided that since proposed LRB configurations did not have these protuberances, the coefficients should be removed for the LRB data base.

Conclusions drawn from the tests, with regard to varying gap width, included the following trends:

- CAF increases as gap width increases for transonic and supersonic Mach numbers.

- CNF increases as gap width increases in the transonic range (for negative alpha).

- CMF decreases as gap width increases in the transonic range (for negative alpha).

- Effects of gap width on CSR vary with configuration.

- CBR increases as gap width increases.

- CTR, CHEI, CHEO decreases as gap width increases.

Conclusions drawn from these tests, with regard to aft skirt variation, showed that, with the exception of a slight increase in CAF, the aft skirt had little effect on either wing or total vehicle data.

Finally, on the subject of base drag/plume effects it was concluded that the effects were significant. It was recommended that each specific LRB configuration's base drag be calculated before adding to the LRB data base.

Appendix A

BASE DRAG CALCULATION CODE USERS GUIDE

BASE DRAG CALCULATION CODE USERS GUIDE

A-1 INTRODUCTION

The Base Drag calculation code, BASE4, is based on the methods found in the Compendium of Flight Vehicle Base Pressure and Base Drag Prediction Techniques, (Lockheed Missiles and Space Co., 1983). Sections 2 and 3 of this document give a detailed background of base drag theory, which the code follows. The remainder of this appendix will deal only with issues involved in running the BASE4 Code, and assumes the user has some knowledge of the parameters involved. If any questions arises the reader should refer to the above document for more detail.

A-2 CODE ALGORITHM

BASE4 is presently set up to handle a SSLV, with the Orbiter, external tank and a user selected pair of boosters. The boosters can vary in size, configuration, and thrust profile. The user supplies the booster geometry, thrust profile, and trajectory. Among the factors the code takes into account during calculation are corrections for nozzle extension, non-cylindrical shape, addition of fins, and nozzle spacing. A flow chart for BASE4 can be found in Fig. A-1. A program listing can be found at the end of this section.

A-3 PARAMETERS

A list of parameters used in the BASE4 code can be found in Table A.1. All units in the code assumed to be in the English system except where noted otherwise. Those parameters in Table A-1 noted with an asterisk "*" are inputs supplied by the user, those with a "**" are tabular inputs supplied by the user. Figures A-2 and A-3 depict these input parameters and their usage.

A-4 PROGRAM INPUT/OUTPUT

All I/O in BASE4 is handled via files. For input the user creates and specifies the input file, which the code prompts for, and the code generates five ouput files. The following describes these I/O files:

Filename	Format
xxxxx.INP	User supplied input file, See Fig. 1-4 for a sample input case.
BASE4.OUT	Tabular listing of Mach, Altitude, Q, Total Base Drag, Orbiter Base Drag, Booster Base Drag, and External Tank Base Drag at each of the specified trajectory points. See Fig. A-5 for a sample case.
BASE4.TRACE	Listing of the calculation of base drag at each of the specified trajectory points. See Fig. A-5 for a sample case.
BASE4.TRAJ	Tabular listing of Mach, Altitude, and Dynamic Pressure. See Fig. A-7 for a sample case.
BASE4.THRUST	Tabular listing of Mach, Alttitude, Orbiter Thrust, Single Booster Thrust, and Total Thrust, at each of the specified trajectory points. See Fig. A-8 for a sample Case.
BASE4.PLUME	Tabular listing of Mach, Altitude, Orbiter Plume Angle and Booster Plume Angle at each of the specified trajectory points. See Fig. A-9 for a sample case.

ORIGINAL PAGE IS
OF POOR QUALITY

TABLE A.1 LIST OF PARAMETERS

	Parameter	Description
	ABET	External Tank Base Area
	ABLRB	Booster Base Area
	ABORB	Orbiter Base Area
	ACYLRB	Booster Cylindrical Section Base Area
	AEFET	External Tank Effective Base Area
	AEFLRB	Booster Effective Base Area
	AEFORB	Orbiter Effective Base Area
	AELRB	Booster Nozzle Exit Area
	AEORB	Orbiter Nozzle Exit Area
*	AFLRB	Area Multipling Factor (used with 3,4,5 nozzles)
	ALT	Altitude
	ALTI(N)	Altitude Table (used in conjunction with, PPI(N), Ambiant Pressure Table)
	ANET	External Tank Nozzle Spacing Effective Area
	ANLRB	Booster Nozzle Spacing Effective Area
	ANORB	Orbiter Nozzle Spacing Effective Area
	CDBET	External Tank Base Drag Coefficient
	CDBLRB	Booster Base Drag Coefficient
	CDBORB	Orbiter Base Drag Coefficient
	CPBET	External Tank Base Pressure Coefficient
	CPBLRB	Booster Base Pressure Coefficient
	CPBORB	Orbiter Base Pressure Coefficient
	CTET	External Tank Thrust Coefficient
	CTLRB	Booster Thrust Coefficient
	CTORB	Orbiter Thrust Coefficient
	DBET	External Tank Base Diameter
*	DBLRB	Booster Base Diameter
	DBORB	Orbiter Base Diameter
*	DCYLRB	Booster Cylindrical Section Base Diameter
*	DELRB	Booster Nozzle Exit Diameter
	DEORB	Orbiter Nozzle Exit Diameter
	DFBET	External Tank Total Base Drag
	DFBLRB	Booster Total Base Drag
	DFBORB	Orbiter Tank Total Base Drag
	DFNET	External Tank Nozzle Spacing Effect Base Drag
	DFNLRB	Booster Nozzle Spacing Effect Base Drag
	DFNORB	Orbiter Tank Nozzle Spacing Effect Base Drag
	DFTOT	Total Vehicle Base Drag
	DJET	External Tank Plume Angle (used for nozzle effect on ET)
	DJLRB	Booster Plume Angle
	DJORB	Orbiter Plume Angle
	DXJLRB	Booster Nozzle Extension Fator
	DXJORB	Orbiter Nozzle Extension Fator
*	EEET	External Tank Nozzle Expansion Ratio (used for nozzle effect on ET)
*	EELRB	Booster Nozzle Expansion Ratio
	EEORB	Orbiter Nozzle Expansion Ratio
*	INLRB	Number of Booster Nozzles
	INORB	Number of Orbiter Nozzles
*	KØET	External Tank Nozzle Constant (used for nozzle effect on ET)
*	KØLRB	Booster Nozzle Constant
	KØORB	Orbiter Tank Nozzle Constant
	MACH	Mach Number

* - USER INPUT
** - USER TABULAR INPUT

Table A-1 LIST OF PARAMETERS

TABLE A.1 LIST OF PARAMETERS (cont.)

	PBETT	External Tank (Total Base Pressure / Ambiant Pressure)
	PBLRBT	Booster (Total Base Pressure / Ambiant Pressure)
	PBORBT	Orbiter (Total Base Pressure / Ambiant Pressure)
	PBTORB	Orbiter Tail (Base Pressure / Ambiant Pressure)
	PBWORB	Orbiter Wing (Base Pressure / Ambiant Pressure)
*	PCET	External Tank Chamber Pressure (used for nozzle effect on ET)
*	PCLRB	Booster Chamber Pressure
	PCORB	Orbiter Tank Chamber Pressure
	PP	Ambiant Pressure
	PPI(N)	Ambiant Pressure Table (used in conjunction with, ALT(I), Altitude Table)
	PRLRB	Non-Cylindrical Area Ratio
**	Q	Dynamic Pressure
	SREF	Orbiter Reference Area
	TAAET	External Tank (Thrust/Area)(used for nozzle effect on ET)
	TAALRB	Booster (Thrust/Area)
	TAAORB	Orbiter (Thrust/Area)
	TCT	Orbiter Tail Thickness
	TCW	Orbiter Wing Thickness
**	THLRB	Booster Thrust (one booster)
	THORB	Orbiter Thrust
**	THTOT	Total Thrust
*	XJLRB	Booster Nozzle Extension
	XJORB	Orbiter Nozzle Extension
	XSDLRB	Booster Nozzle Spacing Ratio
	XSDORB	Orbiter Nozzle Spacing Ratio
*	XSLRB	Booster Nozzle Spacing
	XSORB	Orbiter Nozzle Spacing

* - USER INPUT
** - USER TABULAR INPUT

Table A-1 LIST OF PARAMETERS (Continued)

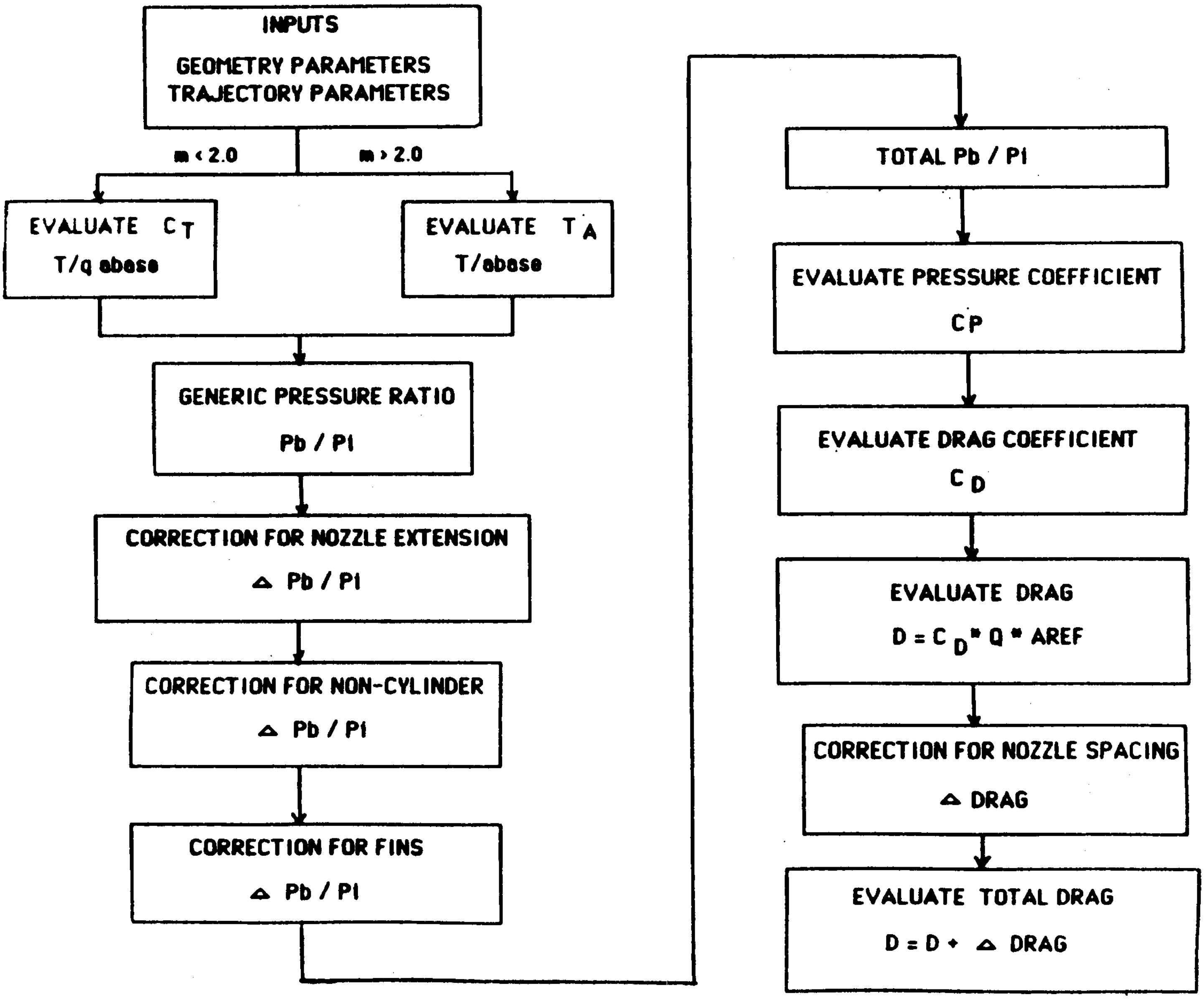

Fig. A-1 BASE4 Flowchart

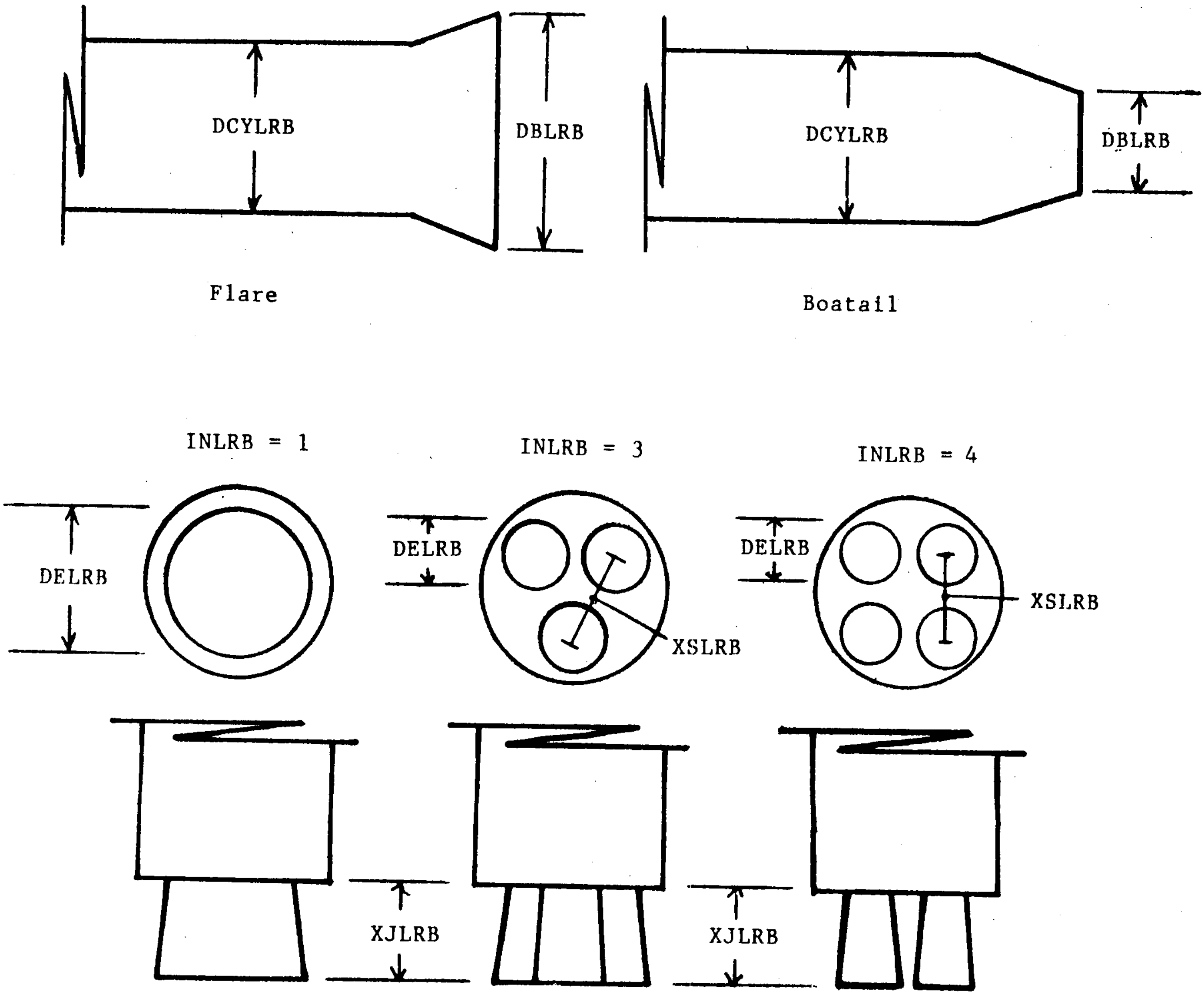

Fig. A-2 Geometric Inputs

INPUTS FOR MOTOR CHARACTERISTICS

EELRB - Nozzle Expansion Ratio

PCLRB - Motor Chamber Pressure

KOLRB - Motor Constant

(All three are inputs which determine the Booster's plume angle effects at each given altitude in the trajectory)

$$Dj = KO * (alt) * (Pc)^{0.8} * (EE)^{-0.5}$$

The inputs **EEET**, **PCET** and **KOET**, are the similar inputs for the plume effects on the External Tank. These Values in general use the same EE, Pc and KO as the Booster.

AFLRB - Base Area Multiplying Factor

For 1 Nozzle - AFLRB = 1.0
For 2 Nozzles - AFLRB = 0.333
For 3 Nozzles - AFLRB = 0.333
FOR 4 Nozzles - AFLRB = 0.333

(This quantity accounts for the CP distribution that occurs in the inner area between multi-nozzle set-ups)

TABULAR TRAJECTORY INPUTS

Trajectory inputs should be in the following form:

Mach(1)	**Altitude(1)**	**Q(1)**	**THTOT(1)**	**THLRB(1)**
.	.	.	.	.
.	.	.	.	.
.	.	.	.	.
Mach(n)	**Altitude(n)**	**Q(n)**	**THTOT(n)**	**THLRB(n)**

THTOT is the total mated vehicle thrust
THLRB is the thrust of one booster

Fig. A-3 Motor Characteristics and Trajectory Inputs

```
* INPUT FILE FOR BASE4
*
* VEHICLE - SSLV
*
** GEOMETRIC PARAMETERS
*
 1              INLRB
 17.3           DBLRB
 12.2           DELRB
 15.3           DCYLRB
 4.9            XJLRB
 0.0            XSLRB
 0.0001713      KOLRB
 7.16           EELRB
 105840.        PCLRB
 0.0001713      KOET
 7.16           EEET
 105840.        PCET
 1.0            AFLRB
*
** TRAJECTORY PARAMETERS
*
** MACH, ALTITUDE, Q, TOTAL-THRUST, BOOSTER-THRUST
*
0.60       9065.00000     383.79999    6437333.00000    2607000.00000
0.74      13447.70020     493.69998    6039033.00000    2474000.00000
0.87      17979.00000     576.15002    5786666.00000    2369633.00000
1.01      23256.00195     626.44000    5569533.00000     956333.18750
1.14      28248.40039     648.84003    5605800.50000    2283133.50000
1.29      33622.93359     657.06665    5926244.50000    2369200.00000
1.48      39848.53516     648.33997    6219244.50000    2461622.50000
1.71      46490.44141     625.93597    6416799.50000    2522293.25000
1.98      53950.90234     585.98499    6494199.50000    2554483.00000
2.26      61880.59766     525.74005    6473133.00000    2538999.75000
2.82      83994.19531     323.72403    5825667.00000    2211053.50000
3.44     111853.90625     131.95799    5030000.00000    1810740.00000
[illegible].03     138365.56250       2.05000    4272832.50000    1429796.37500
```

Fig. A-4 Sample Input File

XXXXXXXX XXXXXXXX (XXX)

TOTAL BASE DRAG

MACH	ALT(FT)	Q(psF)	LV(lbs)	ORB(lbs)	2RB(lbs)	ET(lbs)
0.60	9065.00	383.8	88103.11	24546.79	17996.44	45559.88
0.74	13447.70	493.7	92256.71	25968.50	18769.99	47518.21
0.87	17979.00	576.2	92559.63	26581.64	18810.24	47167.74
1.01	23256.00	626.4	106989.99	26947.87	22794.83	57247.29
1.14	28248.40	648.8	95184.19	31010.86	13959.38	50213.95
1.29	33622.93	657.1	66081.19	25314.08	4729.38	36037.72
1.48	39848.54	648.3	24157.26	14983.85	-5636.19	14809.60
1.71	46490.44	625.9	4889.39	10445.44	-11735.59	6179.54
1.98	53950.90	586.0	-18516.41	6899.03	-16862.33	-8553.11
2.26	61880.60	525.7	-35989.62	2291.34	-16975.81	-21305.15
2.82	83994.20	323.7	-39757.47	-3714.92	-13536.17	-22506.38
3.[illegible]4	111853.91	132.0	-26571.28	-3002.27	-6822.41	-16746.60
4.	138365.56	2.0	-3863.47	-58.35	-144.85	-3660.27

Fig. A-5 Sample BASE4.OUT File

ABLRB	235.0618	ABORB	433.7361	ABET	598.2849
AELRB	116.8987	AEORB	132.5359	AEFET	1502.145
AEFLRB	118.1631	AEFORB	301.2002	AEET	350.6960
ACYLRB	183.8539	L1ORB	17.50000	DEET	21.13102
ARLRB	1.278525	L2ORB	17.50000	ANET	299.1425
L1LRB	12.20000	L3ORB	15.15544	XSDET	1.975768
L2LRB	12.20000	ANORB	7.4203491E-02		
ANLRB	31.94133	XSDORB	1.333333		
XSDLRB	0.0000000E+00				

****
****

MACH		0.6000000		
ALT	(FT)	9065.000		
Q	(PSF)	383.8000		
PRESS	(PSF)	1535.280		
THRUST TOT	(LB)	6437333.		
BOOSTER THRUST	(LB)	2607000.		
ORB THRUST	(LB)	1223333.		
CTBOOSTER		28.89708		
CTORB		7.348761		
CTET		11.16578		
PLUME ANGLE	(RB ORB)	6.072794	3.171308	
UNCORRECTED	(RB ORB ET)	0.9500000	0.9500000	0.9500000
NOZZLE EXT	(RB ORB ET)	0.0000000E+00	0.0000000E+00	0.0000000E+00
NON CYLINDER	(RB ORB ET)	0.0000000E+00	0.0000000E+00	0.0000000E+00
FINS	(RB ORB ET)	0.0000000E+00	-3.5100002E-03	0.0000000E+00
TOTAL Pb/Pi	(RB ORB ET)	0.9500000	0.9464900	0.9500000
CPB	(RB ORB ET)	-0.1984127	-0.2123413	-0.1984127
CDB	(RB ORB ET)	8.7156398E-03	2.3775930E-02	4.4129126E-02
DFB (wo/NS)	(RB ORB ET)	17996.44	24546.79	45559.88
DFB (wo/NS)	(TOTAL)	88103.11		
NOZ SP Pb/Pi	(RB ORB ET)	0.0000000E+00	0.0000000E+00	0.0000000E+00
NOZ SP Pb	(RB ORB ET)	0.0000000E+00	0.0000000E+00	0.0000000E+00
NOZ SP DRAG	(RB ORB ET)	0.0000000E+00	0.0000000E+00	0.0000000E+00
DFB (w/NS)	(RB ORB ET)	17996.44	24546.79	45559.88
DFB (w/NS)	(TOTAL)	88103.11		

****

.
.

MACH (n) .

DFB (n) . . . .

MACH	ALTITUDE (FT)	Q (PSF)
0.6000000	9065.000	383.8000
0.7400000	13447.70	493.7000
0.8700000	17979.00	576.1500
1.010000	23256.00	626.4400
1.140000	28248.40	648.8400
1.290000	33622.93	657.0667
1.480000	39848.54	648.3400
1.710000	46490.44	625.9360
1.980000	53950.90	585.9850
2.260000	61880.60	525.7401
2.820000	83994.20	323.7240
3.440000	111853.9	131.9580
4.030000	138365.6	2.050000

Fig. A-7 Sample BASE4.TRAJ file

MACH	ALTITUDE (FT)	ORBITER (LBS)	BOOSTER (LBS)	TOTAL (LBS)
0.6000000	9065.000	1223333.	2607000.	6437333.
0.7400000	13447.70	1091033.	2474000.	6039033.
0.8700000	17979.00	1047400.	2369633.	5786666.
1.010000	23256.00	3656867.	956333.2	5569533.
1.140000	28248.40	1039534.	2283134.	5605801.
1.290000	33622.93	1187845.	2369200.	5926245.
1.480000	39848.54	1296000.	2461623.	6219245.
1.710000	46490.44	1372213.	2522293.	6416800.
1.980000	53950.90	1385234.	2554483.	6494200.
2.260000	61880.60	1395134.	2539000.	6473133.
2.820000	83994.20	1403560.	2211054.	5825667.
3.440000	111853.9	1408520.	1810740.	5030000.
4.030000	138365.6	1413240.	1429796.	4272833.

Fig. A-8 Sample BASE4.THRUST File

MACH	ALTITUDE (FT)	ORB ANGLE (DEG)	RB ANGLE (DEG)
0.6000000	9065.000	3.171308	6.072794
0.7400000	13447.70	4.704556	9.008839
0.8700000	17979.00	6.289790	12.04443
1.010000	23256.00	8.135902	15.57958
1.140000	28248.40	9.882447	18.92407
1.290000	33622.93	11.76268	22.52456
1.480000	39848.54	13.94065	26.69519
1.710000	46490.44	16.26426	31.14472
1.980000	53950.90	18.87423	36.14260
2.260000	61880.60	21.64837	41.45484
2.820000	83994.20	29.38461	56.26911
3.440000	111853.9	39.13108	74.93279
4.030000	138365.6	48.40594	92.69341

Fig. A-9 Sample BASE4.PLUME File

BASE4 PROGRAM LISTING

```
C*********************************************************************
C
C       CALULATION OF BASE PRESSURE FOR SSLV w/LRB
C
C       WRITTEN BY:  Richard Reheuser
C
C               AT:  Lockheed Missiles and Space Co.
C                    4800 Bradford Drive
C                    Huntsville, Alabama  35807
C
C               PH:  (205)722-4238
C
C*********************************************************************
C
        INTEGER INLRB,INORB,IWORB,ITORB,IEL,ILRB
        REAL SREF,MACH,ALT,Q,PI,THTOT,THLRB,THORB,THET,
     .       PP,PP1,PPI(21),ALTI(21),
     .       DBLRB,DELRB,DCYLRB,XJLRB,DXJLRB,LRB,
     .       K0LRB,KLRB,EELRB,DJLRB,PCLRB,XSDLRB,
     .       ANLRB,L1LRB,L2LRB,
     .       DBORB,DEORB,XJORB,DXJORB,XSORB,TCW,TCT,
     .       K0ORB,KORB,EEORB,DJORB,PCORB,XSDORB,
     .       ANORB,L1ORB,L2ORB,L3ORB,
     .       DBET,DEET,XSET,XSDET,ANET,K0ET,KET,EEET,
     .       DJET,PCET,
     .       ABLRB,AELRB,AEFLRB,ACYLRB,AFLRB,PRLRB,PLRB1,
     .       PLRB2,CTLRB,TAALRB,CPBLRB,CDBLRB,DFBLRB,
     .       ABORB,AEORB,AEFORB,PBWORB,PBTORB,CTORB,TAAORB,
     .       CPBORB,CDBORB,DFBORB,
     .       ABET,AEFET,CTET,TAAET,CPBET,CDBET,DFBET,
     .       PBLRB1,PBLRB2,PBLRB3,PBLRB4,PBLRBA,PBLRB5,PBLRBT,
     .       PBORB1,PBORB2,PBORB3,PBORB4,PBORBA,PBORB5,PBORBT,
     .       PBET1,PBET2,PBET3,PBET4,PBETA,PBET5,PBETT,
     .       DFBLRB1,DFBORB1,DFBET1,DFTOT1,PBLRB4A,PBORB4A,PBET4A,
     .       DFNLRB,DFNORB,DFNET
        CHARACTER*1  LINE
        CHARACTER*20 FNAME1,FNAME2,FNAME3,FNAME4,FNAME5,FNAME6
C
        DATA SREF,PI /2690.,3.141592654/
C
        DATA ALTI /     0., 10000., 20000., 30000., 40000.,
     .             50000., 60000., 70000., 80000., 90000.,
     .            100000.,110000.,120000.,130000.,140000.,
     .            150000.,160000.,170000.,180000.,190000.,
     .            200000./
C
        DATA PPI/1.10325E+3,6.96946E+2,4.66006E+2,3.01486E+2,1.88230E+2,
     .          1.16641E+2,7.23120E+1,4.48767E+1,2.80154E+1,1.76096E+1,
     .          1.11428E+1,7.10413    ,4.59717    ,3.02101    ,2.01393    ,
     .          1.36070    ,9.29799E-1,6.36667E-1,4.39927E-1,2.94703E-1,
     .          1.97960E-1/
        DATA INORB,IWORB,ITORB /3,2,1/
C
        DATA PBLRB1,PBLRB2,PBLRB3 /0.0,0.0,0.0/
        DATA PBLRB4,PBLRB5,PBLRBT /0.0,0.0,0.0/
C
        DATA PBORB1,PBORB2,PBORB3 /0.0,0.0,0.0/
        DATA PBORB4,PBORB5,PBORBT /0.0,0.0,0.0/
```

Fig. A-10 BASE4 PROGRAM LISTING

```
      DATA DBORB,DEORB,AFORB /23.5,7.5,.333/
      DATA KØORB,EEORB,PCORB /.0000963,77.5,427680./
      DATA XJORB,XSORB /9.2,10.0/
      DATA TCW,TCT /.06,.06/
C
      DATA PBET1,PBET2,PBET3 /0.0,0.0,0.0/
      DATA PBET4,PBET5,PBETT /0.0,0.0,0.0/
      DATA DBET,XSET,AFET /27.6,41.75,.333/
C
      DATA FNAME2 /'BASE4.TRACE'/
      DATA FNAME3 /'BASE4.OUT'/
      DATA FNAME4 /'BASE4.PLUME'/
      DATA FNAME5 /'BASE4.TRAJ'/
      DATA FNAME6 /'BASE4.THRUST'/
C
      WRITE(6,*)
 5    WRITE(5,1000)
      READ(5,1001,ERR=5) FNAME1
      WRITE(6,*)
C
      OPEN(19,FILE=FNAME1,STATUS='OLD')
      OPEN(20,FILE=FNAME2,STATUS='NEW')
      OPEN(21,FILE=FNAME3,STATUS='NEW')
      OPEN(22,FILE=FNAME4,STATUS='NEW')
      OPEN(23,FILE=FNAME5,STATUS='NEW')
      OPEN(24,FILE=FNAME6,STATUS='NEW')
C
      READ(19,1001,ERR=998) LINE
      READ(19,1001,ERR=998) LINE
      READ(19,1001,ERR=998) LINE
      READ(19,1001,ERR=998) LINE
      READ(19,1001,ERR=998) LINE
      READ(19,1001,ERR=998) LINE
      READ(19,*,ERR=998) INLRB
      READ(19,*,ERR=998) DBLRB
      READ(19,*,ERR=998) DELRB
      READ(19,*,ERR=998) DCYLRB
      READ(19,*,ERR=998) XJLRB
      READ(19,*,ERR=998) XSLRB
      READ(19,*,ERR=998) KØLRB
      READ(19,*,ERR=998) EELRB
      READ(19,*,ERR=998) PCLRB
      READ(19,*,ERR=998) KØET
      READ(19,*,ERR=998) EEET
      READ(19,*,ERR=998) PCET
      READ(19,*,ERR=998) AFLRB
      READ(19,1001,ERR=998) LINE
      READ(19,1001,ERR=998) LINE
      READ(19,1001,ERR=998) LINE
      READ(19,1001,ERR=998) LINE
      READ(19,1001,ERR=998) LINE
C
C     LRB CALCULATIONS
C
      ABLRB  = PI * (DBLRB/2.0)**2
      AELRB  = (PI * (DELRB/2.0)**2) * FLOAT(INLRB)
      AEFLRB = ABLRB - AELRB
      ACYLRB = PI * (DCYLRB/2.0)**2
      ARLRB = ABLRB/ACYLRB
      L1LRB = XSLRB + DELRB                ! NOTE - L1 AND L2 ARE SET UP HERE FOR
      L2LRB = XSLRB + DELRB                ! A 4 NOZZLE CONFIGURATION, THIS SHOULD
```

Fig. A-10 BASE4 PROGRAM LISTING (Continued)

```
      ANLRB = L1LRB * L2LRB - AELRB          ! BE CHANGED FOR A 2, 3, OR 5 SETUP
      XSDLRB = XSLRB/DELRB
C
C     ORB CALCULATIONS
C
      ABORB  = PI * (DBORB/2.0)**2
      AEORB  = (PI * (DEORB/2.0)**2) * FLOAT(INORB)
      AEFORB = ABORB - AEORB
      L1ORB  = XSORB + DEORB
      L2ORB  = XSORB + DEORB
      L3ORB  = SQRT(L1ORB**2 - (L2ORB/2.0)**2)
      ANORB  = 0.5 * L2ORB * L3ORB - AEORB
      XSDORB = XSORB/DEORB
C
      ABET  = PI * (DBET/2.0)**2
      AEFET = ABET + ABORB + 2*(ABLRB)
      AEET  = 3.0 * AELRB
      DEET  = 2.0 * SQRT(AEET/PI)
      ANET  = 0.5 * ABET
      XSDET = XSET/DEET
C
      WRITE(20,*)
      WRITE(20,2006) ABLRB,ABORB,ABET
      WRITE(20,2007) AELRB,AEORB,AEET
      WRITE(20,2008) AEFLRB,AEFORB,AEFET
      WRITE(20,2009) ACYLRB,L1ORB,DEET
      WRITE(20,2010) ARLRB,L2ORB,ANET
      WRITE(20,2011) L1LRB,L3ORB,XSDET
      WRITE(20,2012) L2LRB,ANORB
      WRITE(20,2013) ANLRB,XSDORB
      WRITE(20,2014) XSDLRB
C
      WRITE(20,*)
      WRITE(20,*)'*********************************************'
      WRITE(20,*)'*********************************************'
      WRITE(20,*)
      WRITE(21,2000)
      WRITE(21,2001)
      WRITE(21,*)
      WRITE(21,2002)
      WRITE(21,*)
      WRITE(21,2003)
      WRITE(21,2004)
      WRITE(22,*)'     MACH          ALTITUDE        ORB ANGLE         ',
     .           ' RB ANGLE'
      WRITE(22,*)'                     (FT)            (DEG)           ',
     .           '  (DEG)'
      WRITE(22,*)
      WRITE(23,*)'     MACH          ALTITUDE          Q'
      WRITE(23,*)'                     (FT)           (PSF)'
      WRITE(23,*)
      WRITE(24,*)'     MACH          ALTITUDE        ORBITER           ',
     .           'BOOSTER          TOTAL'
      WRITE(24,*)'                     (FT)            (LBS)           ',
     .           ' (LBS)           (LBS)'
      WRITE(24,*)
C
C     BEGIN TRAJECTORY LOOP
C
 100  READ(19,*,ERR=998,END=999,IOSTAT=IER) MACH,ALT,Q,THTOT,THLRB
C
```

Fig. A-10 BASE4 PROGRAM LISTING (Continued)

```
      THORB = THTOT - 2.Ø*THLRB
      THET  = THTOT
      CTLRB = THLRB/(Q*ABLRB)
      CTORB = THORB/(Q*ABORB)
      CTET  = THET/(Q*AEFET)
C
      TAALRB = THLRB/ABLRB
      TAAORB = THORB/ABORB
      TAAET  = THET/AEFET
C
C     UNCORRECTED BASE PRESSURE RATIO - (ALL M; ALL ELEMENTS)
C
        IF(MACH.LT.1.8) THEN
         CALL EXTCT(MACH,CTLRB,PBLRB1A)
         CALL EXTCT(MACH,CTORB,PBORB1A)
         CALL EXTCT(MACH,CTET,PBET1A)
         PBLRB1 = PBLRB1A
         PBORB1 = PBORB1A
         PBET1  = PBET1A
        ENDIF
C
        IF(MACH.GE.1.8.AND.MACH.LE.2.2) THEN
         CALL EXTCT(MACH,CTLRB,PBLRB1A)
         CALL EXTCT(MACH,CTORB,PBORB1A)
         CALL EXTCT(MACH,CTET,PBET1A)
         CALL EXTCA(ALT,TAALRB,PBLRB1B)
         CALL EXTCA(ALT,TAAORB,PBORB1B)
         CALL EXTCA(ALT,TAAET,PBET1B)
         PBLRB1 = (PBLRB1A + PBLRB1B)/2.Ø
         PBORB1 = (PBORB1A + PBORB1B)/2.Ø
         PBET1  = (PBET1A  + PBET1B )/2.Ø
        ENDIF
C
        IF(MACH.GT.2.2) THEN
         CALL EXTCA(ALT,TAALRB,PBLRB1B)
         CALL EXTCA(ALT,TAAORB,PBORB1B)
         CALL EXTCA(ALT,TAAET,PBET1B)
         PBLRB1 = PBLRB1B
         PBORB1 = PBORB1B
         PBET1  = PBET1B
        ENDIF
C
C     CORRECTION FOR NOZZLE EXTENSION - (ALL M; LRB,ORB)
C
      DXJLRB = ABS(XJLRB/DBLRB - Ø.34)
      CALL EXTDXJ(MACH,DXJLRB,PBLRB2)
      IF(XJLRB/DBLRB.LT.Ø.34) PBLRB2 = -PBLRB2
      DXJORB = ABS(XJORB/DBORB - Ø.34)
      CALL EXTDXJ(MACH,DXJORB,PBORB2)
      IF(XJORB/DBORB.LT.Ø.34) PBORB2 = -PBORB2
C
C     CORRECTION FOR NON-CYLINDRICAL - (1.5Ø .GE. M .LE. 3.5; LRB)
C
      IF(MACH.LT.1.Ø) THEN
       PLRB1  = Ø.Ø
       PLRB2  = Ø.Ø
       PBLRB3 = Ø.Ø
      ENDIF
      IF(MACH.GE.1.Ø.AND.MACH.LT.1.5) THEN
       CALL EXTCYL(ARLRB,MACH,PRLRB)
       PLRB1 = PBLRB1 + PBLRB2 + PBLRB3
```

Fig. A-10 BASE4 PROGRAM LISTING (Continued)

```
       PLRB2 = PLRB1/PRLRB
       PBLRB3 = PLRB2 - PLRB1
       PBLRB3 = PBLRB3 * ((2.0 * MACH) - 2.0)
      ENDIF
      IF(MACH.GE.1.5.AND.MACH.LT.3.5) THEN
       CALL EXTCYL(ARLRB,MACH,PRLRB)
       PLRB1 = PBLRB1 + PBLRB2 + PBLRB3
       PLRB2 = PLRB1/PRLRB
       PBLRB3 = PLRB2 - PLRB1
      ENDIF
      IF(MACH.GE.3.5.AND.MACH.LT.4.0) THEN
       CALL EXTCYL(ARLRB,MACH,PRLRB)
       PLRB1 = PBLRB1 + PBLRB2 + PBLRB3
       PLRB2 = PLRB1/PRLRB
       PBLRB3 = PLRB2 - PLRB1
       PBLRB3 = PBLRB3 * ((-2.0 * MACH) + 8.0)
      ENDIF
      IF(MACH.GE.4.0) THEN
       PLRB1  = 0.0
       PLRB2  = 0.0
       PBLRB3 = 0.0
      ENDIF
C
C     CORRECTIONS FOR FINS - (ALL M; ORB)
C
      CALL EXTFIN(MACH,PBWORB)
      CALL EXTFIN(MACH,PBTORB)
      PBWORB = PBWORB * (TCW/0.1) * (IWORB/4.0)
      PBTORB = PBTORB * (TCT/0.1) * (ITORB/4.0)
      PBORB5 = PBWORB + PBTORB
C
C     TOTAL ALL Pb/Pi
C
      PBLRBT = PBLRB1 + PBLRB2 + PBLRB3 + PBLRB5
      PBORBT = PBORB1 + PBORB2 + PBORB3 + PBORB5
      PBETT  = PBET1  + PBET2  + PBET3  + PBET5
C
C     BASE PRESSURE COEFF
C
      CPBLRB   = (PBLRBT - 1.0)/(0.7 * MACH**2)
      CPBORB   = (PBORBT - 1.0)/(0.7 * MACH**2)
      CPBET    = (PBETT  - 1.0)/(0.7 * MACH**2)
C
C     BASE DRAG COEFF
C
      CDBLRB = -(CPBLRB * AEFLRB/SREF)
      CDBORB = -(CPBORB * AEFORB/SREF)
      CDBET  = -(CPBET  *   ABET/SREF)
C
C     CORRECTION FOR NOZZLE SPACING - (ALL M; LRB,ORB,ET)
C
       DJLRB = K0LRB * (ALT/1000.) * (PCLRB)**0.8 * (EELRB)**(-0.5)
       DJORB = K0ORB * (ALT/1000.) * (PCORB)**0.8 * (EEORB)**(-0.5)
       DJET =  K0ET  * (ALT/1000.) * (PCET)**0.8  * (EEET)**(-0.5)
C
       WRITE(22,*) MACH,ALT,DJORB,DJLRB
       WRITE(23,*) MACH,ALT,Q
       WRITE(24,*) MACH,ALT,THORB,THLRB,THTOT
C
       IF(XSDLRB.GT.0.0) THEN
        CALL EXTXS1(DJLRB,XSDLRB,PBLRB4)
```

Fig. A-10 BASE4 PROGRAM LISTING (Continued)

```
          ENDIF
C
          IF(XSDORB.GT.0.0) THEN
           CALL EXTXS2(DJORB,XSDORB,PBORB4)
          ENDIF
C
          IF(XSDET.GT.0.0) THEN
           CALL EXTXS2(DJET,XSDET,PBET4)
          ENDIF
C
C        NOZZLE SPACING EFFECT DRAG
C
         CALL ATP(ALT,ALTI,PPI,21,PP)
         PP1 = PP * 2.089
C
         PBLRB4A = PBLRB4 * PP1
         PBORB4A = PBORB4 * PP1
         PBET4A  = PBET4  * PP1
C
         DFNLRB = -PBLRB4A * AFLRB * ANLRB
         DFNORB = -PBORB4A * AFORB * ANORB
         DFNET  = -PBET4A  * AFET  * ANET
C
C        BASE DRAG
C
         DFBLRB1 = 2.0 * CDBLRB*Q*SREF
         DFBORB1 = CDBORB*Q*SREF
         DFBET1  = CDBET*Q*SREF
         DFBTOT1 = DFBLRB1 + DFBORB1 + DFBET1
C
         DFBLRB  = DFBLRB1 + 2.0 *DFNLRB
         DFBORB  = DFBORB1 + DFNORB
         DFBET   = DFBET1  + DFNET
         DFBTOT  = DFBLRB + DFBORB + DFBET
C
         WRITE(20,*)
         WRITE(20,*)' MACH                        ',MACH
         WRITE(20,*)' ALT                 (FT)   ',ALT
         WRITE(20,*)' Q                  (PSF)   ',Q
         WRITE(20,*)' PRESS              (PSF)   ',PP1
         WRITE(20,*)' THRUST TOT          (LB)   ',THTOT
         WRITE(20,*)' BOOSTER THRUST      (LB)   ',THLRB
         WRITE(20,*)' ORB THRUST          (LB)   ',THORB
         IF(MACH.LT.2.0) THEN
          WRITE(20,*)' CTBOOSTER          ',CTLRB
          WRITE(20,*)' CTORB              ',CTORB
          WRITE(20,*)' CTET               ',CTET
         ENDIF
         IF(MACH.GE.2.0) THEN
          WRITE(20,*)' T/A BOOSTER        ',TAALRB
          WRITE(20,*)' T/A ORB            ',TAAORB
          WRITE(20,*)' T/A ET             ',TAAET
         ENDIF
         WRITE(20,*)' PLUME ANGLE    (RB ORB)       ',DJLRB,DJORB
         WRITE(20,*)
         WRITE(20,*)' UNCORRECTED    (RB ORB ET)  ',PBLRB1,PBORB1,PBET1
         WRITE(20,*)' NOZZLE EXT     (RB ORB ET)  ',PBLRB2,PBORB2,PBET2
         WRITE(20,*)' NON CYLINDER   (RB ORB ET)  ',PBLRB3,PBORB3,PBET3
         WRITE(20,*)' FINS           (RB ORB ET)  ',PBLRB5,PBORB5,PBET5
         WRITE(20,*)' TOTAL Pb/Pi    (RB ORB ET)  ',PBLRBT,PBORBT,PBETT
         WRITE(20,*)
```

Fig. A-10 BASE4 PROGRAM LISTING

```
      WRITE(20,*)' CPB           (RB ORB ET) ',CPBLRB,CPBORB,CPBET
      WRITE(20,*)' CDB           (RB ORB ET) ',CDBLRB,CDBORB,CDBET
      WRITE(20,*)' DFB (wo/NS)   (RB ORB ET) ',DFBLRB1,DFBORB1,DFBET1
      WRITE(20,*)' DFB (wo/NS)   (TOTAL)     ',DFBTOT1
      WRITE(20,*)
      WRITE(20,*)' NOZ SP Pb/Pi  (RB ORB ET) ',PBLRB4,PBORB4,PBET4
      WRITE(20,*)' NOZ SP Pb     (RB ORB ET) ',PBLRB4A,PBORB4A,PBET4A
      WRITE(20,*)' NOZ SP DRAG   (RB ORB ET) ',DFNLRB,DFNORB,DFNET
      WRITE(20,*)
      WRITE(20,*)' DFB (w/NS)    (RB ORB ET) ',DFBLRB,DFBORB,DFBET
      WRITE(20,*)' DFB (w/NS)    (TOTAL)     ',DFBTOT
      WRITE(20,*)
      WRITE(20,*)'*******************************************'
      WRITE(20,*)
      WRITE(21,2005) MACH,ALT,Q,DFBTOT,DFBORB,DFBLRB,DFBET
      GO TO 100
C
C
 1000 FORMAT(' ENTER INPUT FILE NAME --> ',$)
 1001 FORMAT(A)
 1002 FORMAT(' ENTER BOOSTER TYPE ',/,
     .       ' 1-SRB 2-MLRB1 3-MLRB2 4-GDLRB3 5-GDLRB4 --> ',$)
 2000 FORMAT(2(/))
 2001 FORMAT(26X,8('X'),1X,8('X'),2X,'(XXX)')
 2002 FORMAT(30X,'TOTAL BASE DRAG')
 2003 FORMAT(5X,'MACH      ALT(FT)    Q(psf)     LV(lbs)    ',
     .       '  ORB(lbs)     2RB(lbs)     ET(lbs)')
 2004 FORMAT(3X,74('-'))
 2005 FORMAT(5X,F4.2,2X,F10.2,2X,F6.1,2X,F10.2,2X,F10.2,2X,
     .       F10.2,2X,F10.2)
 2006 FORMAT(T2 ,'ABLRB ',T13,F11.5,T28,'ABORB ',T38,F11.5,
     .       T53,'ABET  ',T63,F11.5)
 2007 FORMAT(T2 ,'AELRB ',T13,F11.5,T28,'AEORB ',T38,F11.5,
     .       T53,'AEET  ',T63,F11.5)
 2008 FORMAT(T2 ,'AEFLRB',T13,F11.5,T28,'AEFORB',T38,F11.5,
     .       T53,'AEFET ',T63,F11.5)
 2009 FORMAT(T2 ,'ACYLRB',T13,F11.5,T28,'L1ORB ',T38,F11.5,
     .       T53,'DEET  ',T63,F11.5)
 2010 FORMAT(T2 ,'ARLRB ',T13,F11.5,T28,'L2ORB ',T38,F11.5,
     .       T53,'ANET  ',T63,F11.5)
 2011 FORMAT(T2 ,'L1LRB ',T13,F11.5,T28,'L3ORB ',T38,F11.5,
     .       T53,'XSDET ',T63,F11.5)
 2012 FORMAT(T2 ,'L2LRB ',T13,F11.5,T28,'ANORB ',T38,F11.5)
 2013 FORMAT(T2 ,'ANLRB ',T13,F11.5,T28,'XSDORB',T38,F11.5)
 2014 FORMAT(T2 ,'XSDLRB',T13,F11.5)
C
 998  WRITE(6,*) ALT,MACH,Q,THTOT,THLRB
      WRITE(6,*)' READ ERROR ',IER
 999  END
C
C****************************************************************
C
       SUBROUTINE EXTCT(MACH,CTHRUST,PBB7)
C
C      EXTRAPOLATE Pb/Pi vs M and CT PB(M,CT)
C
       REAL M(9),CT(7),PB(9,7),MACH,CTHRUST,PERM,PERCT,
     .      PBB1,PBB2,PBB3,PBB4,PBB5,PBB6,PBB7
C
       DATA M  /0.00,0.60,0.90,1.00,1.10,1.25,1.50,1.75,2.00/
       DATA CT / 0.0, 5.0,10.0,15.0,20.0,25.0,30.0/
```

Fig. A-10 BASE4 PROGRAM LISTING (Continued)

```
C
        DATA PB /0.9500,0.9500,0.9250,0.8800,0.8600,0.8000,0.7400,
     .          0.6000,0.4600,
     .          0.9500,0.9500,0.9250,0.8900,0.8800,0.8750,0.9100,
     .          0.8900,0.8700,
     .          0.9500,0.9500,0.9250,0.9000,0.8950,0.9250,1.0400,
     .          1.1000,1.1600,
     .          0.9500,0.9500,0.9250,0.9150,0.9100,0.9500,1.0700,
     .          1.1900,1.3100,
     .          0.9500,0.9500,0.9250,0.9250,0.9200,0.9700,1.1000,
     .          1.2400,1.3800,
     .          0.9500,0.9500,0.9250,0.9400,0.9400,0.9850,1.1300,
     .          1.2900,1.4500,
     .          0.9500,0.9500,0.9250,0.9500,0.9500,0.9850,1.1500,
     .          1.3200,1.4900/
C
      DO I=2,9
       IF(M(I).GT.MACH) THEN
        IM = I
        GO TO 20
       ENDIF
       IF(I.EQ.9) IM = 9
      ENDDO
C
 20   DO J=2,7
       IF(CT(J).GT.CTHRUST) THEN
        ICT = J
        GO TO 30
       ENDIF
       IF(J.EQ.7) ICT = J
      ENDDO
C
 30   PERM  = (M(IM)-MACH)/(M(IM)-M(IM-1))
      PERCT = (CT(ICT)-CTHRUST)/(CT(ICT)-CT(ICT-1))
      PBB1 = PB(IM-1,ICT-1)
      PBB2 = PB(IM,ICT-1)
      PBB3 = PB(IM-1,ICT)
      PBB4 = PB(IM,ICT)
      PBB5 = PBB2 - (PBB2 - PBB1)*PERM
      PBB6 = PBB4 - (PBB4 - PBB3)*PERM
      PBB7 = PBB6 - (PBB6 - PBB5)*PERCT
C
      RETURN
      END
C
C*********************************************************************
C
       SUBROUTINE EXTCA(ALT,TAAA,PBB7)
C
C      EXTRAPOLATE Pb/Pi vs C/A and ALT PB(TAA,H)
C
       REAL TAA(6),H(14),PB(6,14),ALT,TAAA,PERTAA,PERH,
     .      PBB1,PBB2,PBB3,PBB4,PBB5,PBB6,PBB7
C
     . DATA TAA /3000.,3500,4000.,5000.,6000.,10000./
       DATA H /     0.0, 10000.0, 20000.0, 30000.0, 40000.0, 50000.0,
     .         60000.0, 70000.0, 80000.0, 90000.0,100000.0,110000.0,
     .         120000.0,130000.0/
C
       DATA PB /0.50,0.55,0.60,0.73,0.78,0.88,
     .          0.58,0.65,0.70,0.80,0.90,0.98,
```

Fig. A-10 BASE4 PROGRAM LISTING (Continued)

```
     .           0.63,0.70,0.78,0.90,1.00,1.08,
     .           0.70,0.76,0.85,1.00,1.10,1.20,
     .           0.78,0.85,0.93,1.11,1.23,1.30,
     .           0.85,0.93,1.00,1.20,1.33,1.40,
     .           0.90,0.98,1.13,1.33,1.45,1.50,
     .           0.98,1.13,1.30,1.55,1.66,1.73,
     .           1.08,1.28,1.50,1.80,1.90,1.95,
     .           1.18,1.43,1.70,2.03,2.25,2.20,
     .           1.30,1.60,1.93,2.30,2.45,2.48,
     .           1.43,1.80,2.18,2.60,2.75,2.85,
     .           1.55,2.00,2.45,2.95,3.20,3.35,
     .           1.58,2.30,2.85,3.45,3.85,4.10/
C
      DO I=2,6
       IF(TAA(I).GT.TAAA) THEN
        ICA = I
        GO TO 20
       ENDIF
       IF(I.EQ.6) ICA = I
      ENDDO
C
 20   DO J=2,14
       IF(H(J).GT.ALT) THEN
        IH = J
        GO TO 30
       ENDIF
       IF(J.EQ.14) IH = J
      ENDDO
C
 30   PERTAA  = (TAA(ICA)-TAAA)/(TAA(ICA)-TAA(ICA-1))
      PERH    = (H(IH)-ALT)/(H(IH)-H(IH-1))
      PBB1 = PB(ICA-1,IH-1)
      PBB2 = PB(ICA,IH-1)
      PBB3 = PB(ICA-1,IH)
      PBB4 = PB(ICA,IH)
      PBB5 = PBB2 - (PBB2 - PBB1)*PERTAA
      PBB6 = PBB4 - (PBB4 - PBB3)*PERTAA
      PBB7 = PBB6 - (PBB6 - PBB5)*PERH
C
      RETURN
      END
C
C**********************************************************************
C
      SUBROUTINE EXTDXJ(MACH,DELXJ,DPBB7)
C
C     EXTRAPOLATE DPb/Pi vs M and DXJ DPB(M,DXJ)
C
      REAL M(18),DXJ(11),DPB(18,11),MACH,DELXJ,PERM,PERXJ,
     .     DPBB1,DPBB2,DPBB3,DPBB4,DPBB5,DPBB6,DPBB7
C
      DATA M   /0.0,0.4,0.8,1.2,1.6,2.0,2.4,2.8,3.2,3.6,4.0,4.4,
     .           4.8,5.2,5.6,6.0,6.4,6.8/
      DATA DXJ / 0.0,0.1,0.2,0.3,0.4,0.5,0.6,0.7,0.8,0.9,1.0/
C
      DATA DPB /0.000,0.000,0.000,0.000,0.000,0.000,0.000,
     .           0.000,0.000,0.000,0.000,0.000,0.000,0.000,
     .           0.000,0.000,0.000,0.000,
     .           0.000,0.000,0.000,0.007,0.024,0.032,0.028,
     .           0.020,0.012,0.007,0.003,0.000,0.000,0.000,
     .           0.000,0.000,0.000,0.000,
```

Fig. A-10 BASE4 PROGRAM LISTING (Continued)

```
     .               Ø.000,Ø.005,Ø.006,Ø.016,Ø.048,Ø.062,Ø.056,
     .               Ø.046,Ø.032,Ø.024,Ø.016,Ø.008,Ø.002,Ø.000,
     .               Ø.000,Ø.000,Ø.000,Ø.000,
     .               Ø.010,Ø.012,Ø.014,Ø.032,Ø.080,Ø.094,Ø.086,
     .               Ø.072,Ø.056,Ø.040,Ø.030,Ø.018,Ø.006,Ø.000,
     .               Ø.000,Ø.000,Ø.000,Ø.000,
     .               Ø.020,Ø.022,Ø.024,Ø.053,Ø.116,Ø.132,Ø.120,
     .               Ø.100,Ø.080,Ø.063,Ø.046,Ø.028,Ø.012,Ø.003,
     .               Ø.000,Ø.000,Ø.000,Ø.000,
     .               Ø.029,Ø.031,Ø.038,Ø.077,Ø.156,Ø.168,Ø.150,
     .               Ø.128,Ø.104,Ø.083,Ø.062,Ø.040,Ø.022,Ø.008,
     .               Ø.000,Ø.000,Ø.000,Ø.000,
     .               Ø.039,Ø.040,Ø.052,Ø.103,Ø.188,Ø.204,Ø.184,
     .               Ø.156,Ø.129,Ø.104,Ø.078,Ø.054,Ø.034,Ø.015,
     .               Ø.002,Ø.000,Ø.000,Ø.000,
     .               Ø.047,Ø.050,Ø.066,Ø.125,Ø.224,Ø.240,Ø.216,
     .               Ø.184,Ø.153,Ø.125,Ø.095,Ø.068,Ø.044,Ø.024,
     .               Ø.009,Ø.000,Ø.000,Ø.000,
     .               Ø.056,Ø.060,Ø.080,Ø.153,Ø.264,Ø.276,Ø.244,
     .               Ø.212,Ø.179,Ø.147,Ø.114,Ø.084,Ø.056,Ø.032,
     .               Ø.015,Ø.003,Ø.000,Ø.000,
     .               Ø.065,Ø.070,Ø.102,Ø.184,Ø.300,Ø.316,Ø.276,
     .               Ø.240,Ø.203,Ø.161,Ø.130,Ø.098,Ø.066,Ø.041,
     .               Ø.023,Ø.007,Ø.000,Ø.000,
     .               Ø.077,Ø.081,Ø.130,Ø.213,Ø.336,Ø.348,Ø.308,
     .               Ø.268,Ø.229,Ø.187,Ø.146,Ø.110,Ø.076,Ø.049,
     .               Ø.030,Ø.013,Ø.000,Ø.000/
C
      DO I=2,18
       IF(M(I).GT.MACH) THEN
        IM = I
        GO TO 2Ø
       ENDIF
       IF(I.EQ.18) IM = 18
      ENDDO
C
 2Ø   DO J=2,11
       IF(DXJ(J).GT.DELXJ) THEN
        IXJ = J
        GO TO 3Ø
       ENDIF
       IF(J.EQ.11) IXJ = J
      ENDDO
C
 3Ø   PERM  = (M(IM)-MACH)/(M(IM)-M(IM-1))
      PERXJ = (DXJ(IXJ)-DELXJ)/(DXJ(IXJ)-DXJ(IXJ-1))
      DPBB1 = DPB(IM-1,IXJ-1)
      DPBB2 = DPB(IM,IXJ-1)
      DPBB3 = DPB(IM-1,IXJ)
      DPBB4 = DPB(IM,IXJ)
      DPBB5 = DPBB2 - (DPBB2 - DPBB1)*PERM
      DPBB6 = DPBB4 - (DPBB4 - DPBB3)*PERM
      DPBB7 = DPBB6 - (DPBB6 - DPBB5)*PERXJ
C
      RETURN
      END
C
C*********************************************************************
C
       SUBROUTINE EXTCYL(AR,MACH,PR)
C
```

Fig. A-10 BASE4 PROGRAM LISTING (Continued)

```
C        EXTRAPOLATE Pressure Ratio of NON-CYL vs
C         Mach and Base Area Ratio  PR = f(M,AR)
C
         REAL M(7),S(7),AR,MACH,PR
C
         DATA M  /0.00,1.50,1.75,2.00,2.50,3.50,30.00/
         DATA S  /.000,.000,.050,.140,.105,.080,.080/
C
        DO I=2,7
         IF(M(I).GT.MACH) THEN
          IM = I
          GO TO 20
         ENDIF
         IF(I.EQ.7) IM = 7
        ENDDO
C
 20     PERM  = (M(IM)-MACH)/(M(IM)-M(IM-1))
        SLOPE = S(IM) - (S(IM) - S(IM-1))*PERM
        PR = SLOPE * (AR - 1.0) + 1.0
C
        RETURN
        END
C
C**********************************************************************
C
         SUBROUTINE EXTXS1(DJ,XSDD,PBB7)
C
C        EXTRAPOLATE Pb/Pi vs DJ and XSD PB(PL,XSD)
C
C        ********* FOUR NOZZLE CONFIGURATION *********
C
         REAL PL(10),XSD(4),PB(10,4),DJ,XSDD,PERPL,PERXSD,
     .        PBB1,PBB2,PBB3,PBB4,PBB5,PBB6,PBB7
C
         DATA PL /0.0,10.0,20.0,30.0,40.0,50.0,60.0,70.0,80.0,90.0/
         DATA XSD/1.00,1.22,1.35,1.48/
C
         DATA PB / 0.0, 0.3, 2.0, 7.0,12.0,17.0,22.0,27.0,32.0,37.0,
     .             0.0, 0.0, 0.0, 1.0, 4.8, 9.5,14.5,19.5,24.5,29.5,
     .             0.0, 0.0, 0.0, 0.0, 1.0, 5.0,10.3,15.3,20.3,25.3,
     .             0.0, 0.0, 0.0, 0.0, 0.2, 1.6, 5.5,10.5,15.5,20.5/
C
        DO I=2,10
         IF(PL(I).GT.DJ) THEN
          IPL = I
          GO TO 20
         ENDIF
         IF(I.EQ.10) IPL = 10
        ENDDO
C
 20     DO J=2,4
         IF(XSD(J).GT.XSDD) THEN
          IXSD = J
          GO TO 30
         ENDIF
         IF(J.EQ.4) IXSD = J
        ENDDO
C
 30     PERPL  = (PL(IPL)-DJ)/(PL(IPL)-PL(IPL-1))
        PERXSD = (XSD(IXSD)-XSDD)/(XSD(IXSD)-XSD(IXSD-1))
        PBB1 = PB(IPL-1,IXSD-1)
```

Fig. A-10 BASE4 PROGRAM LISTING (Continued)

```
      PBB2 = PB(IPL,IXSD-1)
      PBB3 = PB(IPL-1,IXSD)
      PBB4 = PB(IPL,IXSD)
      PBB5 = PBB2 - (PBB2 - PBB1)*PERPL
      PBB6 = PBB4 - (PBB4 - PBB3)*PERPL
      PBB7 = PBB6 - (PBB6 - PBB5)*PERXSD
      IF(PBB7.LT.0.0) PBB7 = 0.0
      IF(PBB7.GT.8.0) PBB7 = 8.0
C
      RETURN
      END
C
C***********************************************************************
C
       SUBROUTINE EXTXS2(DJ,XSDD,PBB7)
C
C      EXTRAPOLATE Pb/Pi vs DJ and XSD PB(PL,XSD)
C
C      ********* THREE NOZZLE CONFIGURATION *********
C
       REAL PL(10),XSD(3),PB(10,3),DJ,XSDD,PERPL,PERXSD,
     .      PBB1,PBB2,PBB3,PBB4,PBB5,PBB6,PBB7
C
       DATA PL /0.0,10.0,20.0,30.0,40.0,50.0,60.0,70.0,80.0,90.0/
       DATA XSD/1.00,1.22,3.00/
C
       DATA PB / 0.0, 0.0, 0.0, 0.0, 0.3, 1.1, 3.5, 8.5,13.5,18.5,
     .           0.0, 0.0, 0.0, 0.0, 0.1, 0.5, 1.8, 6.0,11.0,16.0,
     .           0.0, 0.0, 0.0, 0.0, 0.0, 0.1, 0.4, 3.0, 7.8,12.8/
C
      DO I=2,10
       IF(PL(I).GT.DJ) THEN
        IPL = I
        GO TO 20
       ENDIF
       IF(I.EQ.10) IPL = 10
      ENDDO
C
 20   DO J=2,3
       IF(XSD(J).GT.XSDD) THEN
        IXSD = J
        GO TO 30
       ENDIF
       IF(J.EQ.3) IXSD = J
      ENDDO
C
 30   PERPL  = (PL(IPL)-DJ)/(PL(IPL)-PL(IPL-1))
      PERXSD = (XSD(IXSD)-XSDD)/(XSD(IXSD)-XSD(IXSD-1))
      PBB1 = PB(IPL-1,IXSD-1)
      PBB2 = PB(IPL,IXSD-1)
      PBB3 = PB(IPL-1,IXSD)
      PBB4 = PB(IPL,IXSD)
      PBB5 = PBB2 - (PBB2 - PBB1)*PERPL
      PBB6 = PBB4 - (PBB4 - PBB3)*PERPL
      PBB7 = PBB6 - (PBB6 - PBB5)*PERXSD
      IF(PBB7.LT.0.0) PBB7 = 0.0
      IF(PBB7.GT.8.0) PBB7 = 8.0
C
      RETURN
      END
C
```

Fig. A-10 BASE4 PROGRAM LISTING (Continued)

C-4

```
C************************************************************************
C
        SUBROUTINE EXTFIN(MACH,PBB3)
C
C       EXTRAPOLATE Pb/Pi for Fins vs M PB(M)
C
        REAL M(9),PB(9),MACH,PBB1,PBB2,PBB3
C
        DATA M  / 0.00,0.50,0.75,1.00,1.25,1.50,2.00,3.00,30.00/
        DATA PB / 0.000,-0.005,-0.012,-0.030,-0.044,-0.049,
     .          -0.050,-0.048,-0.048/
C
       DO I=2,9
        IF(M(I).GT.MACH) THEN
         IM = I
         GO TO 20
        ENDIF
        IF(I.EQ.9) IM = 9
       ENDDO
C
 20    PERM  = (M(IM)-MACH)/(M(IM)-M(IM-1))
       PBB1 = PB(IM-1)
       PBB2 = PB(IM)
       PBB3 = PBB2 - (PBB2 - PBB1)*PERM
C
       RETURN
       END
C
C***********************************************************************
C
       SUBROUTINE ATP(ALT,ALTI,PPI,N,PP)
       DIMENSION ALTI(21),PPI(21)
C
       DO 10 I=2,N
        IF(ALT.LE.ALTI(I)) GO TO 20
   10  CONTINUE
       I=N
C
   20  PCT=(ALT-ALTI(I-1))/(ALTI(I)-ALTI(I-1))
       PP=PPI(I-1)+PCT*(PPI(I)-PPI(I-1))
       RETURN
       END
```

Fig. A-10 BASE4 PROGRAM LISTING (Concluded)